Role of Endocytosis in Regulating Cancer Cell Migration

Thesis submitted as requirement for the degree of Doctor of Philosophy

School of Biological Sciences

Bandar F. Alharbi

April 2019

Declaration

I confirm that this is my own work and the use of all material from other sources has been properly and fully acknowledged.

Signature:

Date: 26/04/2019

Table of contents

Acknowledgment

When I arrived in UK in 2011as a scholarship student who carried the trust of his country, university and family to complete the stage of English Language, Masters and Ph.D. Despite the circumstances surrounding me, I never thought I will be completing those stages without a break between them. This achievement would not have been completed without the help and support I received throughout my career.

I would like to express my humble appreciation and give my special gratitude to my supervisor Assoc. proof. Dr. Phil Dash who provided me with constant encouragement, support, guidance, very unusual kindness and friendship. He always welcoming me into his office even when I can see he is busy. It is a real pleasure to work and communicate with such a respectful, truthful and open-minded person. I also wanted to thank Dr Mike for the advice he provided at lab meeting as I completed my research project.

I would like to thank my lab colleagues for their assistance during my work in the lab. I particularly want to thank my previous lab members Dr. Dhurgham Al-Fahad, Dr. Kelsey Huang, Dr. Shirley Keeton, Dr. Khatab Mawlood and current lab member Salem Alharthi for our exchanges of knowledge and skills, which helped enrich the experience. I would also like to thank the laboratory staff for their kindness and help.

I would like to thank my family mother and father for their encouragement throughout my entire life. Special thanks to my wife, daughter and son for being beside me through these years. I would not have finished this project without their love, great support and understanding.

Finally, a very special thanks goes out to the University of Hail for their financial sponsorship and support.

Abstract

Cell migration is significant in many physiological and pathophysiological processes, including wound healing, angiogenesis, embryonic development, vascular remodelling and inflammation. Migration is a necessary component of the metastatic cascade as cancer cells have the ability to detach from the primary site, migrate into the blood or lymphatic system and travel to a distant location. Emerging evidence suggests that endocytosis may regulate the migration of tumour cells, but the contribution of different endocytotic pathways have not been addressed in detail. Thus, our aim was to determine the link between endocytosis pathways with cell migration.

Focal adhesions are necessary in many physiological and pathophysiological processes including cell survival, morphology, proliferation and cell migration. They are not only structural elements that provide the stability of the cells through its connection to ECM, they also can regulate internal and external signalling to trigger various cellular responses. Several studies have hypothesised that vesicles such as endosomes might interact with focal adhesions or be implicated in their turnover. Therefore, our aim was to examine the possible link between focal adhesions and the early endosomal compartment, including the influence of clathrin and dynamin pathways on focal adhesion dynamics as well as identifying signalling pathways affecting endocytotic regulation of cell migration and focal adhesion turnover.

Cell migration using wound-healing assay and time-lapse microscopy on a variety of surfaces demonstrated that both micropinocytosis and caveolae pathways had no effect on cell migration. However, dynamin and clathrin dependent endocytosis pathways significantly decreased cell migration and impaired early endosome trafficking. Inhibition of dynamin or clathrin pathways, decreased the expression of EEA1 and numbers of endosomes containing EEA1, while leading to the enlargement of endosomes. Additionally, dynamin and clatherin dependent pathways significantly increase the number of paxillin and vinculin containing focal adhesions. In addition, both pathways significantly decreased focal adhesion turnover time.

Another main finding is that endosomes associate with focal adhesion internalization. Immunocytochemical analysis and live cell imaging revealed that both early endosome markers Rab5 and EEA1 colocalized with focal adhesion proteins. This data was further supported by cell fractionation, and showed that Vinculin, Paxillin, Zyxin, FAK and Talin were found in the same fractions that endosomes were found in. Co-immunoprecipitation was performed to

confirm the association between endosomes and focal adhesions, and the results showed that vinculin was found to coimmunoprecipitate with Rab5 and EEA1.

Finally, we identified that nitric oxide may be a positive regulator of cell migration and focal adhesion turnover and that relies on early endosome trafficking. Our results show that a significant decrease in migration speed in MDA-MB-231 cells when the total NO synthesis or inducible NO synthase (iNOS) were inhabited. In addition, these treatment cause a significant decrease in focal adhesion turnover time. Importantly, these treatments resulted in a significant increase in endosomes containing EEA1 size and simultaneously decreased its number. This observation was further confirmed by immunocytochemistry results where EEA1 was found to moderately co-localize with eNOS or iNOS, and S-nitrosylated compared to non-modified control proteins like H2B or ubiquitin. This result was further confirmed by bioinformatics analysis using the GPS-SNO algorithm where EEA1 was predicted to be S-nitrosylated at four cysteine residues - Cys-46, Cys-255, Cys-894 and Cys-1102, with a high confidence score.

Taken together, our present study provides supporting evidence for the claim that endocytosis plays a crucial role in the migration of cancer cells. Moreover, it is suggested that there is a link between focal adhesions and early endosome markers, which indicates that the early-endosome compartment is involved in focal adhesion turnover.

Table of abbreviations:

ABPs	Actin binding proteins
ADF	Actin depolymerizing factor
ADP	Adenosine diphosphate
AKT	Serine/threonine-specific protein kinase
Amiloride	5-N-Ethyl-N-isopropyl
ANOVA	Analysis of variance
Ap	Adaptor protein complexes
APPL1	Adaptor protein phosphotyrsine interacting with PH domain and Leucine Zipper 1
ARF6	ADP-ribosylation factor 6
Arp2/3 complex	Actin-related protein-2/3
ATP	Adenosine triphosphate
BSA	Bovine serum albumin
CALM	Clathrin assemble lymphoid myeloid leukaemia protein
Cdc42	Cell division control protein 42 homolog
cGMP	Cyclic guanosine monophosphate
CHC1	Clathrin Heavy Chain 1
CLIC/GEEC	Clathrin-independent endocytic pathway
CME	Clathrin-mediated endocytosis

CORVET	Class C core vacuole/endosome tethering factor
CQ	Chloroquine
CSF-1	Macrophage colony-stimulating factor-1
CtBP1/BARS	C-terminal-binding protein-1/brefel-
DAPI	4′,6-diamidino-2-phenylindole
DMEM	Dulbecco's Modified Eagle's Medium
DMF	Dimethylformamide
DMSO	Dimethyl Sulphoxide
DNA	Deoxyribonucleic acid
ECL	Enhanced chemiluminescence
ECM	Extra Cellular Matrix
EDTA	Ethylenediaminetetraacetic acid
EEA1	Early Endosome Antigen 1
EGFR	Epidermal growth factor receptor
EMT	Epithelial-to-mesenchymal transitions
eNOS	Endothelial nitric oxide synthase
EPS15	Epidermal growth factor receptor substrate 15
ESCRT	Endosomal sorting complex required for transport
FAK	Focal adhesion kinase
FAs	Focal adhesions
FBS	Feotal bovine serum

FCHo1/2	Fer/Cip4 homology domain-only proteins 1 and 2
FcR	Fc-receptors
FERM domain	4.1 protein ezrin radixin moesin
FILM	Fluorescence lifetime imaging microscopy
FR	Folate receptor
FYN	Proto-oncogene tyrosine-protein kinase
G1	G domain
GBD	GTPase-binding domain
GEFs	Guanine nucleotide exchange factors
GFP	Green fluorescence protein
GrK	TGFα-like ligand of the Egfr
GSNOR	S-nitrosoglutathione reductase
HEK293	Human Embryonic Kidney cells
HSC70	Heat shock cognate 70
iNOS	Inducible nitric oxide synthase
KD	kinase domain
KSP1	kinesin spindle protein
LAMP1	Lysosomal associated membrane protein 1
LD motifs	Leucine aspartate-rich
LIMP II	Late endosomal/lysosomal membrane proteins
LIR	LC3-interacting region

L-NAME	Nω-Nitro-L-arginine methyl ester hydrochloride
Low glucose MEM	Low glucose Minimum Essential Medium
MAPs	Microtubule-binding proteins
MMPs	Matrix metalloproteinase proteins
MMTS	Methyl methanethiosulphonate
MVBs	Multivesicular bodies
MβCD	Methyl beta cyclodextrin
nNOS	Neural oxide synthase
NO	Nitric oxide
NOS	Nitric oxide synthase
N-WASP	Neuronal Wiskott–Aldrich Syndrome protein
PAGE	Polyacrylamide gel electrophoresis
Pak1	P21-Activated kinase
PBS	Phosphate Buffered Saline
PDGF	Platelet-derived growth factor
PDK1	3-phosphoinositide-dependent protein kinase-1
PI3K	Phosphatidylinositol 3-kinase
PIC	Protease Inhibitors Cocktail
PIP3	Phosphatidylinositol 3,4,5-triphosphate

Pitstop2	N-[5-(4-Bromobenzylidene)-4-oxo-4,5-dihydro-1, thiazol-2-yl]naphthalene-1-sulfonamide
PKG	Protein kinase G
PKN3	anti-protein kinase N3
PLC	Phospholipase C
PTB	Phosphotyrosine-binding domains
PtdIns(4,5)P2	Phosphatidylinositol-4,5-bisphosphate
PTK2	Protein tyrosine kinases 2
PTP-PEST	Protein tyrosine phosphatase, non-receptor type 12
PVR	Proliferative vitreoretinopathy
Rab5	Ras-related protein Rab-5
RAC1	Ras-related C3 botulinum toxin substrate 1
RIPA buffer	Radioimmunoprecipitation assay buffer
ROI	Region of interest
SDS	Sodium dodecyl sulphate
SE	Standard error
Ser/Thr	serine/threonine
SNARE	Soluble N-ethylmaleimide-sensitive factor activating protein receptor
S-NO	S-nitrosylation
Src	Proto-oncogene tyrosine-protein kinase
TBST	Tris-Buffered Saline Tween

TEMED	Tetramethylenediamine
TGFβR	Transforming Growth Factor Beta Receptor
TGN	Trans-Golgi network
TNF	Tumour necrosis factor receptors
VCA domain	Verprolin, cofilin, acidic
VEGF	Vascular endothelial growth factor
WB	Western blot

Chapter 1: Introduction

1 Cancer

Cancer is not just one disease but a complex of diseases that affects both males and females of all ages. It is a disease of uncontrolled cell proliferation where normal cells begin to proliferate and acquire additional capabilities which may eventually progresses into a systemic disease that can be lethal. According to a 2018 world health organization (WHO) report, cancer is one of the leading causes of death in the world, and 9.6 million people died as a result of cancer in 2018 (Bray et al., 2018). Breast cancer is the second leading cause of death after lung cancer and skin cancer is the fifth (Bray et al., 2018).

There are more than 200 different types of cancer, and the disease can originate from different types of tissues. Origination of cancer can be due to alterations on chromosomes or from genetic mutations (Schuh and Dreau, 2018). This alteration allows some cellular function to reprogram the proliferation system, which makes cancer treatment complex (Cheng et al., 2008). The complexity of cancer led Hanahan and Weinberg to hypothesise several acquired function (hallmarks) (Hanahan and Weinberg, 2011). Theses hallmarks cause cells to behave abnormally (Figure 1.1). Some cancer cells have the ability to proliferate and secrete their own growth factor (autocrine agent) as a result of mutation in the regulatory proteins such as Ras family (Miller and Miller, 2012). Others have mutation in the growth factor receptors such as epidermal growth factor receptor (EGFR) and is active even in the absence of its ligands or autocrine agent. It also evades growth suppressor genes such as p53 protein and RB (retinoblastoma) and disables them (Junttila and Evan, 2009). In addition, some cancers have the ability to evade cell death by disabling the apoptotic pathways either by down regulation or through the stimulation of pro-apoptotic proteins (Debatin, 2004).

Unlike cancer cells, normal cells under the control of telomerase stop cell division when it proceeds to its limit. Cancer cells enable the replicative immortality through activation of the telomerase

enzymes, and that increases telomere length of chromosomes causing the cells to divide (Blasco, 2005). It also has the ability to survive by inducing the formation of blood vessels to supply growth requirements such as nutrients as well as the consumption of energy sources, such as glucose through the production of ATP (DeBerardinis et al., 2008). These markers lead to the metastasis of cancer cells by migrating to and invading organs locally and throughout the body (Hanahan and Weinberg, 2011; 2000).

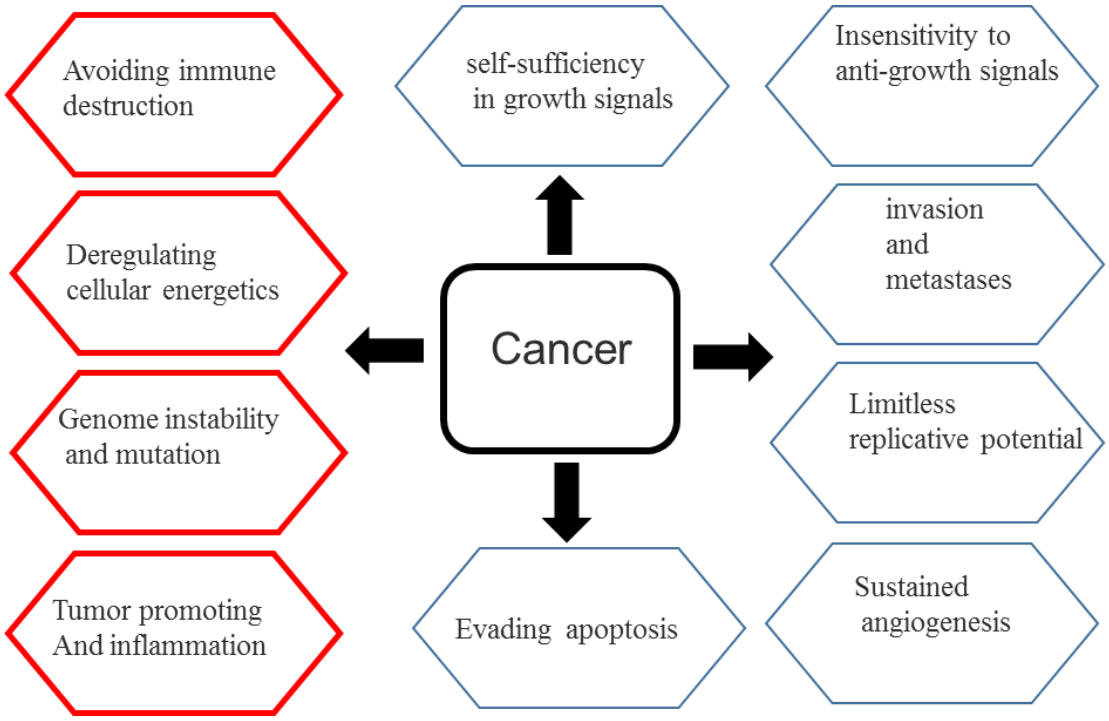

Figure 1. 1 Hallmarks of cancer

In this figure, the 10 hallmarks of cancer are illustrated. Six hallmarks that proposed in 2000 are highlighted in blue (Hanahan and Weinberg, 2000). Where the new emerged markers that proposed in 2011 highlighted in red (Hanahan and Weinberg, 2011). Modified from (Hanahan and Weinberg, 2011)

2 Metastasis

Metastasis refers to the ability of cancer cells to spread from primary sites to distant locations and is considered to be the primary cause of mortality in most cancer patients (Seyfried and Huysentruyt, 2013) (DeVita et al., 1975). In order for Cancer cells to detach from the primary location and to metastasise, they go through many distinct steps called the metastatic cascade (Samatov et al., 2013b) (Brooks, 1996). During this cascade event, cancer cells lose the adherent junction that makes them closely connected through the process called EMT (epithelial-mesenchymal transition) (Chambers et al., 2002). The epithelial-mesenchymal transition (EMT) process occurs in wound healing, organ fibrosis, and the onset of cancer progression metastasis (Gonzalez and Medici, 2014) (Thiery, 2002). Primarily, epithelial, and mesenchymal cells differ in phenotype and function. Epithelial cells are closely connected to each other via tight junctions, gap junctions, and adherent junctions. They also have apico-basal polarity—polarization of the actin cytoskeleton—and are bound by a basal lamina at their basal surface. Mesenchymal cells, on the other hand, lack polarization, have a spindle-shaped morphology, and interact via focal points (Gonzalez and Medici, 2014). Epithelial cells convey high levels of E-cadherin, while mesenchymal cells convey N-cadherin, fibronectin, and vimentin (Moreno-Bueno et al., 2008).

Losing the adherent junctions allow cancer cells to detach from neighbouring cells in the original site of the tumour. Successful detachments cause cancer cells to migrate and secrete protease enzymes such as metalloproteinase that lead to the degradation of cancer cells and the invasion of the extracellular matrix such as basement membranes (Artym et al., 2006). It then penetrates the blood vessels and interact with platelets to survive in the blood circulation system (Schlesinger, 2018). After this step, metastasised cells colonise and breakdown the basement membrane of distal organ in a process called extravasation, as shown in Figure 1.2 (Kawauchi, 2012; Gonzalez and Medici, 2014) (Samatov et al., 2013a).

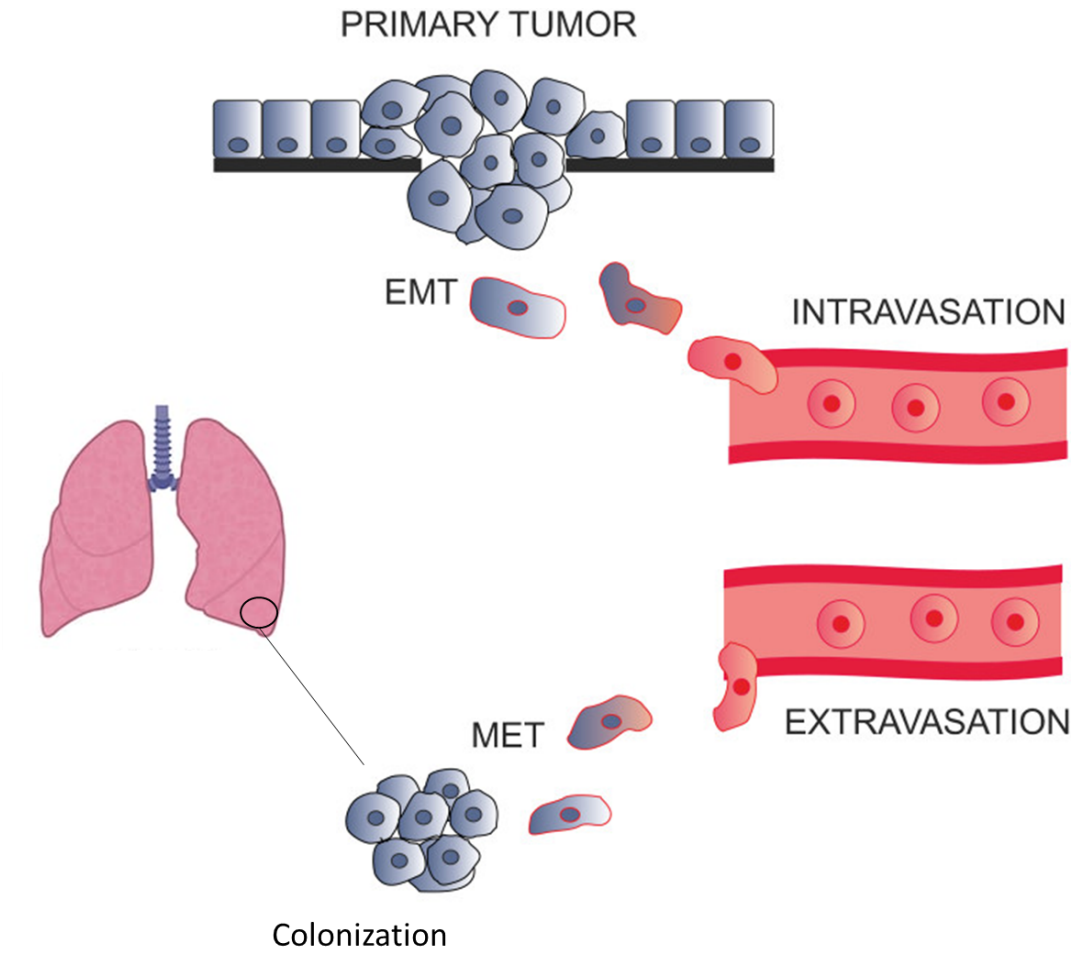

Figure 1.2. This figure represents a multi-step proses of the metastatic cascade include primary tumour invasion, intravasation, extraversion and colonization. Abbreviations: Epithelial-mesenchymal transition (EMT). Mesenchymal-epithelial transition (MET). Modified from (Samatov et al., 2013a)

The metastatic cascade is therefore dependent on the cell migration process which results in multiple changes to the cancer cells that interacts with basement membranes (Joyce and Pollard, 2009). Therefore, strengthening the knowledge of cell migration will help uncover the metastasis of cancer cells.

3 Cell migration:

Cell migration plays a critical role in the maintenance of multicellular organisms. It is an essential process because it is involved in many biological and physiological process, such as the formation of blood vessels (angiogenesis), during embryonic and organ development (Kurosaka and Kashina, 2008), wound healing when the epithelial cells migrate to the edge of the wounds (Li et al., 2015a) and immune response such as the migration of the white blood cells to the site of infected cells (Madri and Graesser, 2000).

There are three basic steps associated with the movement of such cells: 1) extending a plasma-membrane protrusion at the leading edge, 2) cell body movement and 3) cell-trailing detachment (Figure1.3) (Ananthakrishnan and Ehrlicher, 2007). The first step in epithelial cell migration involves the extending plasma-membrane protrusion at the leading edge, and the direction of cell is not restricted. For example, cells can move over and between each other and even invade the extracellular matrix. Epithelial cells use their cytoskeletons in order for four different types of protrusion to be extended. These protrusions are driven by actin polymerization and can be lamellipodia, filopodia, membrane blebs and invadopodia. Each of these structures has its own features, regulating cell migration in specific ways. Lamellipodia was originally identified in 1970 by Michael Abercrombie (Abercrombie et al., 1970). It is characterised by extending a thin sheet through ECM in vivo and pulling cells through the tissue (Friedl and Gilmour, 2009). Filopodia are actin-containing spikes that explore cell environments. They are essential for guiding cells towards chemoattractants and facilitating adhesion to the extracellular matrix (Gupton and Gertler, 2007). Membrane blebs are spherical membrane protrusions that guide cell migration during the development stage (Charras and Paluch, 2008). Finally, invadopodia are usually found in invasive cancer cells. Their structures degrade the extra matrix and allow epithelial cells to invade blood vessels (Buccione et al., 2009).

Once the cell establishes polarity via actin polymerization to produce lamellipodia at the leading edge, cells need to form new adhesion proteins called focal adhesions to specific extracellular matrix components. This attachment allows the actin network which is associated with myosin fibres to generate force. This force resulting in translocation of the rest of the cell body foreword. This process is followed by the detachment of the trailing edges of the cell (back of the cell) and the process of movement is repeated.

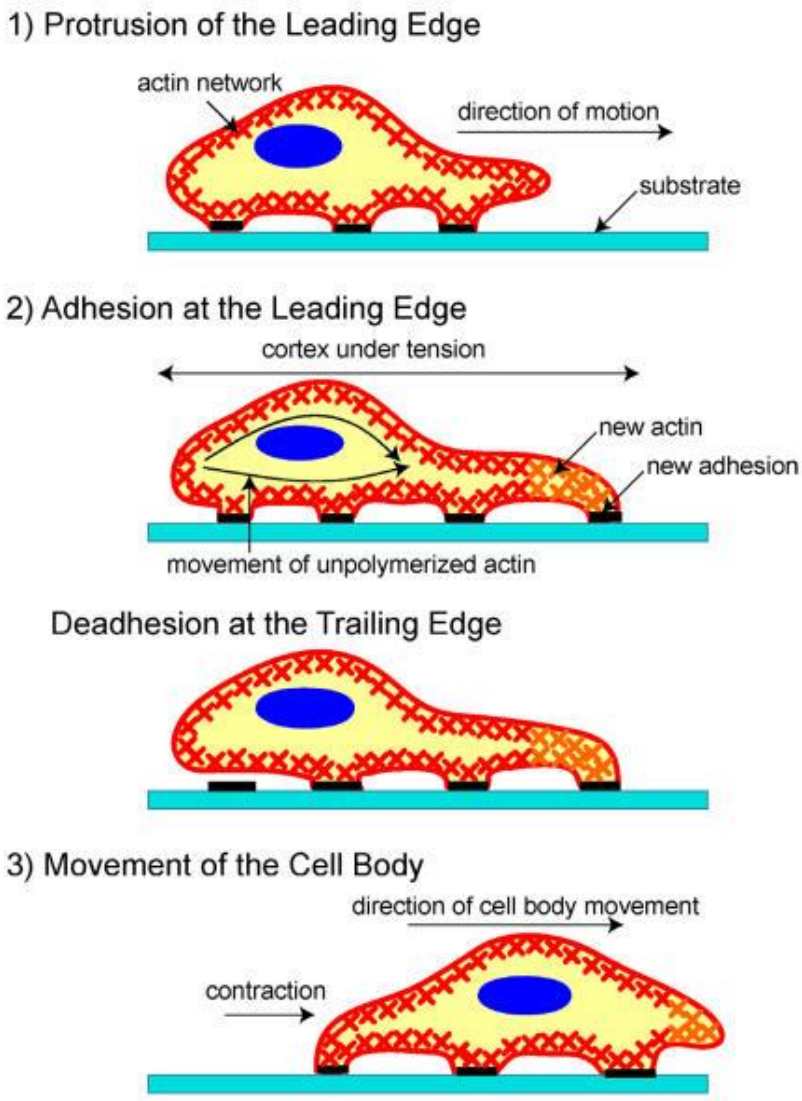

Figure 1. 3. Three stages of cell migration.

Once the cells determine its direction, they extend the protrusion via actin polymerization and thereby forming a lamellipodia structure. Cells then form an adhesive molecule at the leading edge and remove the adhesions formed in the cell rear. Removal of adhesions generate contraction force that causes the whole cell body to move forward. Finally, cells will cycle through these steps during the migration. Taken from (Ananthakrishnan and Ehrlicher, 2007).

One of the key players in these process are cytoskeleton proteins, which regulate polarization and protrusion during migration, and adhesion proteins, which mediate the dynamic formation of adhesion, attachments of adhesion and detachments at the trailing edges (Ridley, 2011).

3.1 The cytoskeleton

The cytoskeleton is a cytoplasmic network which not only plays an important role in cell movement, such as the extension of lamellipodia and control of the polymerization and depolymerisation into actin fibers, but also participates in maintaining cell morphology and certain mechanical strength (Pollard and Borisy, 2003). This network is found in most eukaryotic cells and is composed of three types—microfilaments, intermediate filaments and microtubules (Fuchs and Karakesisoglou, 2001).

Actin is a structural component of microfilaments, and there are three types of actin—α, β and γ. Among them, the β-actin isoform is a major and abundant conserved protein in eukaryotic cells (Rayment et al., 1993). In the cytoplasm, actin exists in two forms, monoactin (G-actin) and actin fibers (F-actin). Monoactin is an individual actin that has a pointed end and a barbed end and consists of 375 to 377 amino acid residues, with a molecular mass of 43-kDa (Dominguez and Holmes, 2011). During actin polymerization, G-actin aggregates into short monomers (three G-actin) called trimers (Percipalle, 2013). Once the trimer is formed, the elongation process proceeds by adding G actin at the barbed end (+), forming filaments (F actin). This cycle is a ATP-based process, as G-actin associates with the barbed end in the ATP state and disassociates at the pointed end (-) when G actin is released in an ADP-bound state (Figure 1.4) (Percipalle, 2013). This dynamic mechanism of gaining and losing individual actin monomers is called the treadmilling process (Bugyi and Carlier, 2010).

The association and disassociation of individual actin monomer G actin at both ends is regulated by several actin binding proteins (ABPs), such as ADF/Cofilin and profilin (Paavilainen et al., 2004). ADF/Cofilin binds to the ADP-bound actin and enhances the rate of dissociation of G actin from pointed end (Figure 1.4) (Bamburg and Bernstein, 2010). Profilin reverses the effect of cofilin by mediating the exchange of bound ADP to ATP resulting in loading ATP bound to the barbed ends (Kardos et al., 2009). In this way, ADF/Cofilin and profilin control the assembly and disassembly of monomer G actin during the treadmilling process.

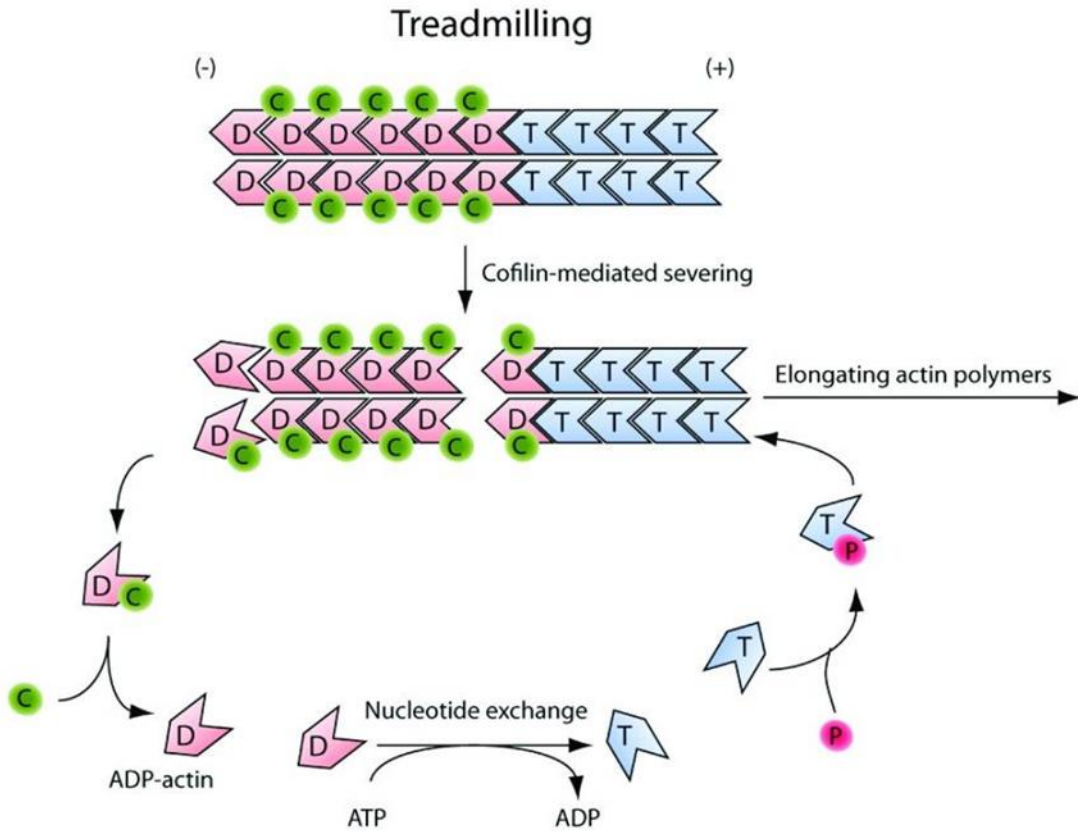

Figure 1.4. Schematic diagram of actin polymerization and depolymerisation by treadmilling.

This figure illustrates the treadmilling process in which the G actin at the barbed end (+) and released at pointed end (-). Cofilin enhances the rate of dissociation of G actin from the pointed end (+). D = ADP-actin, T= ATP actin, C= cofilin P= profilin. Taken from (Percipalle, 2013).

Other actin binding proteins (ABPs) such as Formin facilitates the nucleation process in which three G-actin joins to form a trimer. This accelerates the length of filaments at the barbed end and allows polymerization to proceed rapidly (Evangelista et al., 2003).

The Arp2/3 complex and the N-WASP (neuronal Wiskott–Aldrich Syndrome protein) actin binding proteins control the branch of actin filaments that occur extensively at the leading edge of migrating cells (Swaney and Li, 2016). The Arp2/3 complex consists of seven subunits ArpC1, ArpC2, ArpC3, ArpC4, ArpC5; of these seven subunits, Arp2 and Arp3 are required for remodelling the cytoskeleton (Borths and Welch, 2002). Structurally, Arp2 and Arp3 are similar to actin monomer (G-actin), which

together become similar to trimer (Machesky and Gould, 1999). This Arp2/Arp3 complex binds near to the barbed end of the microfilaments and facilitates the formation of a new actin branch. The formation of branching actin via Arp2/3 complex is stimulated via N-WASP in a process that requires small GTPases (Cdc42 : cell division control protein 42 homolog) (Carlier et al., 1999). For example, N-WASP on its C-terminal side contains the acidic domain (A domain) which interacts with the Arp2/3 complex. The C-terminal also contains the VCA domain which binds the G actin and which is also required for nucleation activity. On the other site, the NH2-terminal of N-WASP particularly WASP homology 1 (WH1) interacts with phosphatidylinositol-4,5-bisphosphate (PtdIns(4,5)P2). The WH1 domain is followed by the GTPase-binding domain (GBD), which includes the Cdc42/Rac interactive binding (CRIB) domain (Kurisu and Takenawa, 2009). Therefore, the binding of active Cdc42 with phosphatidylinositol-4,5-bisphosphate (PtdIns(4,5)P2) to the NH2 terminal of N-WASP directly enhances its ability to activate Arp2/3, and thus promotes the growth of actin fibers that are required for cell migration as well as lamellipodia formation morphology (Higgs and Pollard, 2000; Nakagawa et al., 2001).

3.2 Integrin:

Integrins are a class of important cell adhesion molecules that provide attachments between the cell and the surrounding extracellular matrix. They are transmembrane proteins with long extracellular domains which each contain a ligand binding region and a short intracellular domain. These domains allow the integrins to connect the extracellular matrix to cytoskeletal linker proteins within a cell and mediates bidirectional signal transmission between intracellular and extracellular regions to trigger several intracellular pathways. For example, they mediate cell adhesion, cell differentiation, cell migration, cell growth and proliferation (Schwartz and Assoian, 2001); (Hood and Cheresh, 2002).

Structurally, integrins are composed of α and β transmembrane glycoproteins subunits (18 α, 8 β), which can assemble into 24 alpha beta heterodimers, and most of them can have specific functions depending on the specific ECM ligands such as collagen, laminin, fibronectin and glycine (Figure 1.5) (Kumar, 1998); (Humphries et al., 2006). The α-chain consists of four to five extracellular domains, and the bindings to their ligands depends on cations such as Mg^{2+} and Ca^{2+} (Lee et al., 1995). The cytoplasmic tail of the β subunit is short and contains NPXY and NxxY motifs. Due to the lack of enzyme activity in the integrin itself, focal adhesions play an important role in the process of transferring extracellular stimuli from the cytoplasmic tail of the integrin to the cells (Legate and Fässler, 2009). This leads to integrins on the cell membrane clustering and allows epithelial cells to generate force by actin that influences cell migration.

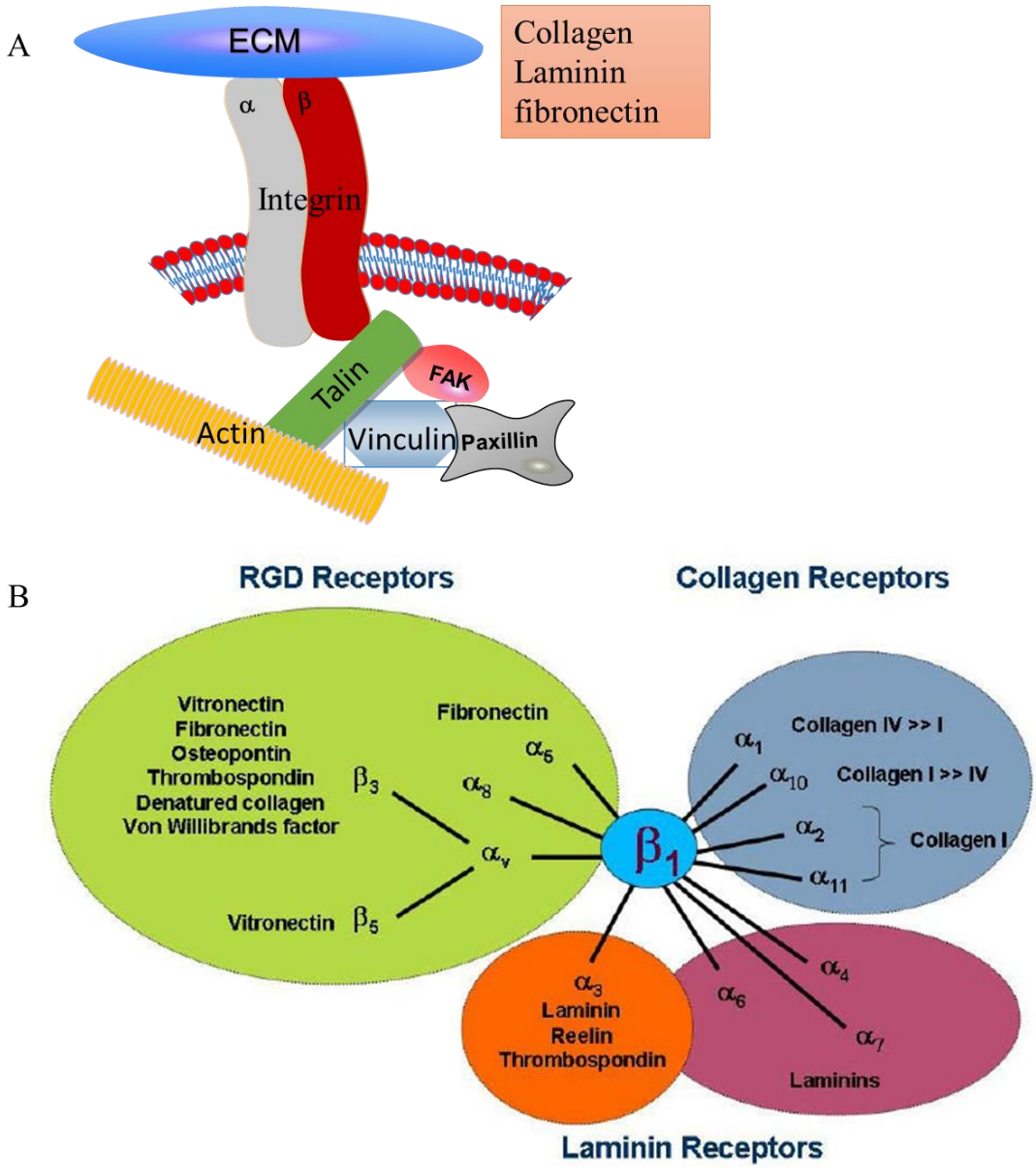

Figure 1. 5: The integrin family of matrix receptors.

A) Structure of integrin adhesions. Integrin composed α (grey) and β (red) transmembrane glycoproteins subunits, bind talin which connect focal adhesion proteins and actin. b) The integrin subunits and their EXM receptors. Figure 1.4 B taken from (Lal et al., 2007)

3.3 Focal adhesions formation and turnover:

3.3.1 Focal adhesions formation

As described earlier, focal-adhesion proteins allow epithelial cells to interact with their outside environments through integrin. Focal adhesions can be divided into the following sub-classes: nascent adhesions, focal complex and focal adhesions (Parsons et al., 2010). A nascent focal adhesion has a short life, as it can either turn over or grow into larger focal complexes. Focal complexes are larger than nascent focal adhesions. As the migration cycle continues, focal complexes transforms into larger sizes of approximately 3 to 10 μm long (Figure1.6 B) (Zimerman et al., 2004).

More than 150 focal-adhesion proteins have been identified. Using 3D super-resolution fluorescence microscopy, Kanchanawong et. al determined the relative 3D organization of focal adhesions and mapped three main functional regions close to the membrane where integrin cytoplasmic tails appear. They have identified an integrin signalling region in close proximity with the plasma membrane where talin and Paxillin bind to the integrin cytoplasmic tail. Above this, an intermediate force transducing region, which links structure focal adhesion such as vinculin. Furthest from the membrane, an actin-filament regulatory layer containing zyxin and α-actinin, which is crosslinking the actin to bundle actin filaments. This is where the forces are generated to move the cell forwarded (Figure 1.6 A) (Kanchanawong et al., 2010).

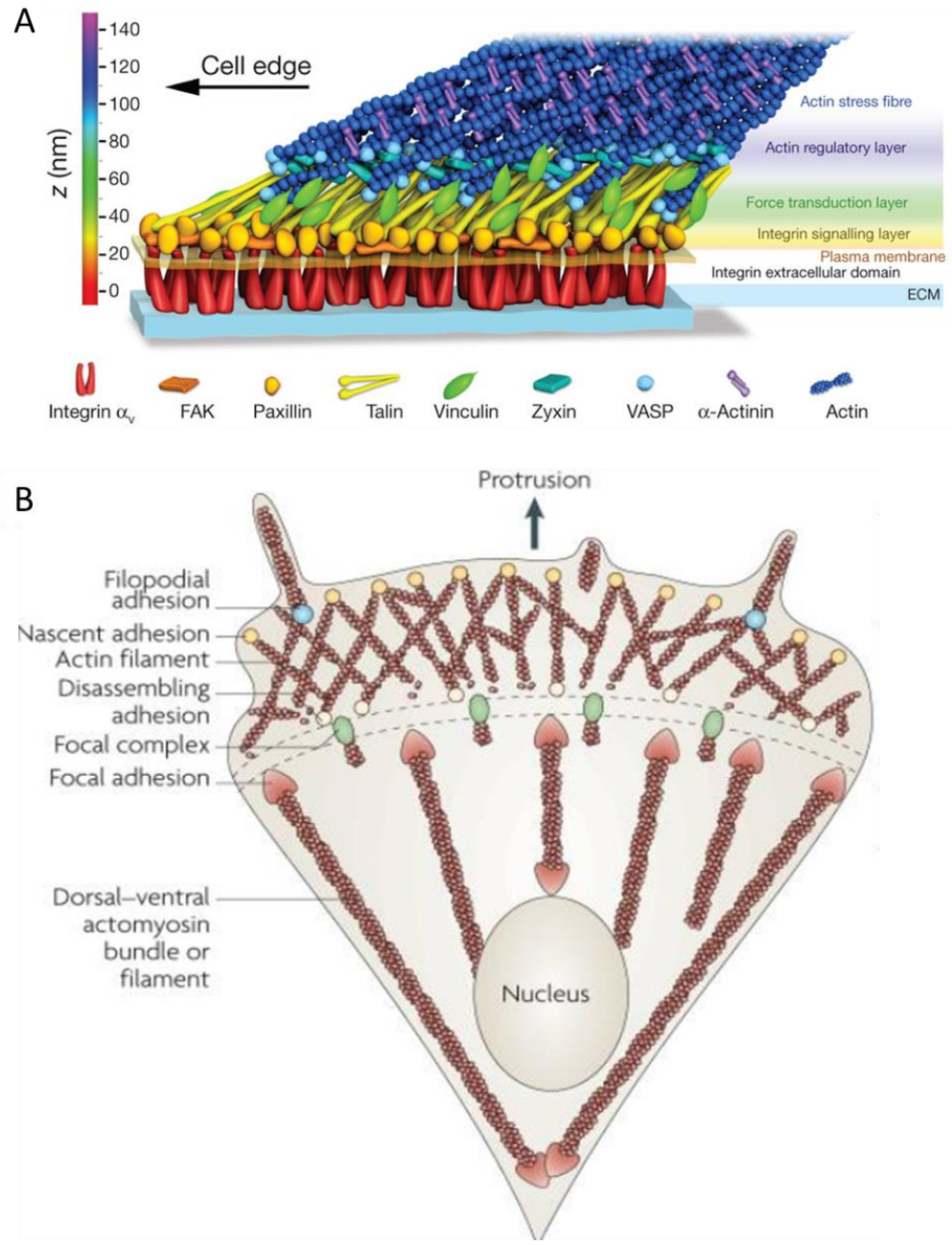

Figure 1. 6 Focal adhesions.

A) The architecture of the connection between focal-adhesion molecules and integrin. Taken from (Kanchanawong et al., 2010). B) Illustrate focal adhesions sub-classes: nascent adhesions, focal complex and focal adhesions. Taken from (Zimerman et al., 2004)

In order for focal adhesion to form and for cells to continue migrating, three important categories of focal adhesion proteins have to be recruited. These categories are structural proteins (Talin), which interact with the cytoplasmic tail of integrin, adaptors or scaffolding proteins (vinculin and paxillin), which link the structural protein with actin and enzymes (FAK), which transmit the signal to actin or other cellular compartments and also regulate FA assembly and disassembly (Geiger et al., 2009).

Once the integrin binds to the extracellular matrix ligands (fibronectin, vitronectin or collagen), talin is the first cytoskeletal protein that binds the NPXY motifs of the cytoplasmic tail of the β subunit through its N-terminal protein band 4.1 -ezrin-radixin-moesin (FERM) domain. The carboxy-terminal rod domain of the talin has a site for vinculin binding (Martin et al., 2002). The binding between vinculin and talin results in the regulation of the formation of focal adhesions and recruiting FAK (Humphries et al., 2007).

Focal adhesion kinase (FAK) or Protein tyrosine kinases 2 (PTK2) is a cytoplasmic tyrosine kinase with a molecular weight of 125kDa. Focal adhesion kinase is expressed in all species and consists of three main domains: the FERM domain at the N-terminal, the kinase domain (KD) and the C-terminal FAT domain which targets focal adhesion proteins such as paxillin (Parsons, 2003).

When talin bind to integrin, FAK auto-phosphorylation at Tyr397 occurs (Moser et al., 2009) (Sieg et al., 2000). In turn, FAK recruit SH2 domain containing molecules such as Src and Fyn (Schaller et al., 1994b). These molecules further phosphorylate the FAK Y576 and Y577 sites, which are located in the KD region and which determine the maximum activation of FAK. The activated FAK/Src complex causes the FAT region of FAK to interact with focal adhesions paxillin (Parsons et al., 2000).

Auto-phosphorylation of FAK at Tyr397, can also activate kinases, phosphatases and other functional proteins, including phosphatidylinositol 3-kinase (PI3K) and phospholipase C (PLC). The activated

PI3K produces PIP3, which promotes recruitment and activation of AKT to the membrane and regulates downstream proteins (Wang and Basson, 2011).

Paxillin is an adaptor protein that contains 559 amino acids with a molecular weight of 65KDa. It binds structural proteins such as vinculin and enzymes such as FAK and Src proteins. Structurally, there are five LD motifs (leucine aspartate-rich) at the amino terminus, and a number of domains such as SH2 and SH3. The main function of these domains is to facilitate the interaction between focal adhesion proteins, including vinculin and FAK (Brown and Turner, 2004b). The C-terminal of the protein is composed of four LIM domains which are binding sites for the protein tyrosine phosphatase PTP-PEST (Cote et al., 1999).

Zyxin is an adhesion protein with a molecular weight of 82 kDa. It can be distinguished from paxillin as it has three LIM domains at the C-terminal. Whereas, in the N-terminal, zyxin contains proline-rich domains and proline-rich motifs which mediate the interactions with the many proteins that contain SH3 domains, including vinculin and VASP (Wang and Gilmore, 2003).

3.3.2 Focal adhesion turnover

Many cells attached to the ECM are forming large and more stable focal adhesions. These FAs do not turnover due to the fact that these cells are not motile. However, in cancer cells, the majority of focal adhesion can be turned over, allowing the cancer cells to detach and migrate. Therefore, rapid focal adhesion turnover is critical for cancer cell motility.

There are many important factors that have been suggested as playing an important role in focal adhesion turnover. Those factors include calpain and microtubules. Calpain 2 also called m-Calpain is a family of calcium dependent that plays an important role in cell migration by proteolysis of several focal adhesions include talin, vinculin, paxillin and FAK (Franco et al., 2004; Chan et al., 2010; Cortesio et al., 2011; Serrano and Devine, 2004). Research which involved using a timelapse

microscope to track the duration time of GFP-Talin disassembly discovered that the knock down of calpain prevented focal adhesion disassembly (Franco et al., 2004).

Microtubules play an important role in maintaining cell morphology, structure, material transport, cell movement, cell differentiation and cell division. Microtubules are composed of tubulin and microtubule associated proteins (MAPs). Tubulin is a family of proteins with many members, the most common members of which are α-tubulin and β-tubulin. Microtubule-binding proteins stabilise the microtubules by binding the tubulin subunits that make up microtubules. It also organises the microtubules into bundles and mediates its interaction with other proteins (de Forges et al., 2012)

Microtubules have been shown to play an important role in cell directions as it undergoes changes to direct the cell movements and is associated with focal adhesions (Rinnerthaler et al., 1988); (Nobes and Hall, 1999). For example, individual microtubules grow toward the ventral cell surfaces and the growth phase switches to the shortening phase (Kaverina et al., 1998). The growth and the shortening phase occur seven times higher at focal adhesions site than elsewhere in the cytoplasm (Efimov et al., 2008)

4 Endocytosis

Endocytosis is initiated when the cell takes up molecules from the extracellular medium or from the plasma membrane into the cytoplasm forming vesicles. These molecules (cargo), progress through different intracellular compartments and can be recycled back to the cell surface or are subjected to lysosomal degradation (Mellman, 1996).

4.1 Endocytosis pathways

A number of endocytosis modes have been demonstrated to be involved in the uptake of particles. Key among these are the phagocytosis and pinocytosis pathways (Doherty and McMahon, 2009). Phagocytosis internalizes large molecules and predominantly occurs in macrophages and dentric cells that have the ability to clear most of the foreign materials and pathogens. In phagocytosis, foreign materials, such as bacteria, yeast and cellular debris, are recognised by the phagocyte. The recognition depends on the cell surface protein of the phagocyte such as complement receptors, Fc-receptors (FcR), scavenger receptors and pathogen-specific receptors (Toll-like receptors)(Rosales and Uribe-Querol, 2017) .

In contrast, pinocytosis is the most common form of endocytosis, and it can occur in all types of cells (Doherty and McMahon, 2009). According to differences in morphology, size, cargo and characteristic proteins of vesicles formed by endocytosis, pinocytosis can be classified into the following pathways—clathrin-dependent endocytosis, caveolae-dependent endocytosis, macropinocytosis and clathrin- and caveolae- independent endocytosis (Figure 1.7) (Table 1.1) (Sigismund et al., 2012) (Canton and Battaglia, 2012).

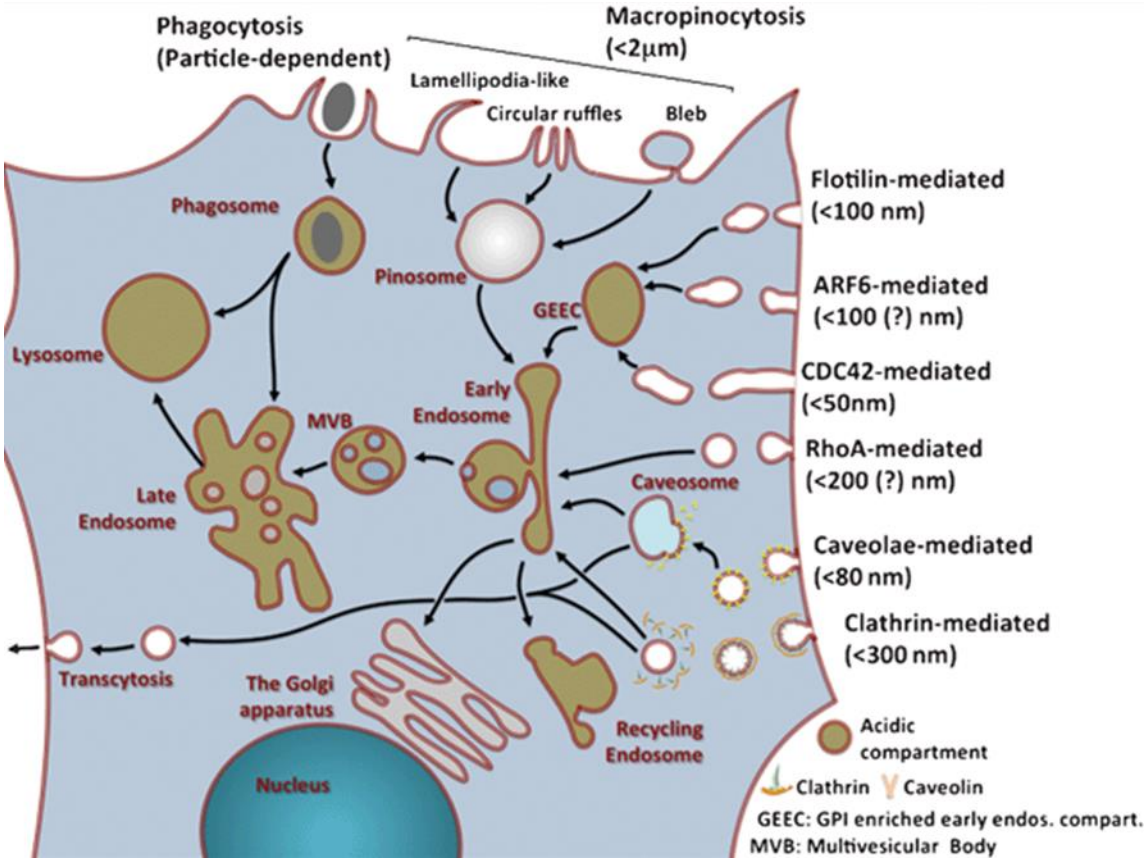

Figure 1.7. This figure demonstrates multiple endocytosis pathways. Taken from (Canton and Battaglia, 2012).

Table 1. 1 demonstrates the morphological features and molecular markers for each pathway. Taken from (Sigismund et al., 2012)

Pathway	Morphology and Size	Coat or Coat-like	Dynamin Dependence	Small GTPase Involved	Internalized Cargoes
Phagocytosis	Cargo-shaped >500 nm	None	No	RAC1/RHOA/CDC42 depending on type	Pathogens, apoptotic cells, FcRs
Macro-pinocytosis	Ruffled 0.2–10 μm	None	In some cases (575)	RAC1, CDCD42 , ARF6 , RAB5	RTKs, fluids, bacteria
Clathrin-mediated	Vesicular 150–200 nm	Clathrin	Yes	RAB5	RTKs , GPCR, TFR, LDLR, toxins , bacteria , viruses
Caveolae-mediated	Flask-shaped 50–120 nm	Caveolin 1 and 2	Yes	Not clear	GPI-linked proteins , CTxB , SV40 , TGF-βR , IGF-1R

Pathway	Morphology and Size	Coat or Coat-like	Dynamin Dependence	Small GTPase Involved	Internalized Cargoes
CLIC/GEEC	Tubular	None	No	CDC42, ARF1	Fluids, bulk membrane, GPI-linked proteins
IL-2Rβ	Vesicular 50–100 nm	None	Yes	RHOA, RAC1	IL-2Rβ (424), γc-cytokine receptor
Arf6-dependent	Tubular	None	None as yet	ARF6	MHC I-II , CD59 (551), CD55, GLUT1 , AchR
Flotillin-dependent	Vesicular	Flotillin 1 and 2	No	None	CTxB, CD59, proteoglycans , DAT, EAAT2

4.1.1 Clathrin-mediated endocytosis:

Clathrin-mediated endocytosis (CME) is one of the most well understood pathways that presents in all eukaryotic cells and plays a major role in cellular entry. It can occur either constitutively or in response to certain stimuli. The mechanism starts when the plasma membrane receptor such as transmembrane, transferrin and low-density lipoprotein receptors accumulate at the plasma membrane. This accumulation leads to recruitment of the intracellular proteins such as adaptor protein complex (Traub, 2009a).

There are at least three different adaptor protein complexes (Ap) which are involved in the formation of vesicles and can specifically select different sorting signals. It is known that the adaptor protein AP-1 mainly mediates the sorting and transportation of cargo from the trans-Golgi network (TGN) to endosomes; AP-2 is responsible for endocytosis of cell surface receptors; AP-3 localized to TGN and endosomes is involved in lysosomes and degradation (Collins et al., 2002). The AP-2 adaptor coordinates clathrin nucleation at sites on the plasma membrane and help to wrap the non-particles by the polymerization of clathrin (Collins et al., 2002).

Structurally, clathrin is a protein complex composed of three heavy chain proteins with a relative molecular mass of approximately 190KDa and three light chain proteins with a relative molecular mass of approximately 25KDa (Pearse, 1975) . These proteins are closely associated with each other's forming three arm structure termed a clathrin triskelion. As triskelions assemble, they tend to form a spherical clathrin lattice structure known as Cage (Figure 1.8) (Schmid and McMahon, 2007).

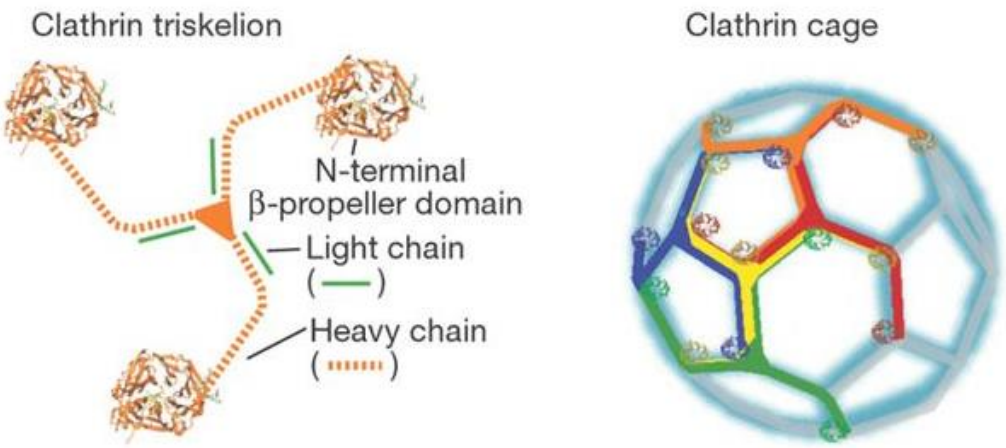

Figure 1. 8 Clathrin structures. Taken from (Schmid and McMahon, 2007).

The formation of clathrin cage requires a number of adaptor proteins and scaffold proteins. Adaptor protein such as AP2, clathrin assemble lymphoid myeloid leukaemia protein (CALM) and epsins, that are involved in the interaction between the plasma membrane lipid, particularly phosphoinositides (PIPs) and cargo (Cocucci et al., 2012). Whereas, scaffold proteins such as clathrin and EPS15 (epidermal growth factor receptor substrate 15), bind the clathrin adaptors to cluster the coat components (Traub, 2009b).

The clathrin-dependent endocytosis is a multi-step process (Kaksonen and Roux, 2018). Initiation of coat pit is an early step and occurs before the clathrin coating is formed. It is initiated when Eps l5 (EGFR pathway sub-strate-15), protein contain a membrane-binding F-BAR domain such as FCHo1/2 (Fer/Cip4 homology domain-only proteins 1 and 2) bind to the plasma membrane (Henne et al., 2010). These proteins are collected in the core of the coated pit, and adaptor proteins AP-2 are recruited through the binding sites of multiple adaptor protein 2 (AP-2) on Eps l5. This binding recruits clathrin and allows them to assemble into hexagonal and pentagonal lattices to form clathrin coated pits (cage) (Kaksonen and Roux, 2018). Another adaptor involved in the clathrin recruitment process is assembly protein 180 (AP180). This adaptor protein has an assembly protein activity, which can help clathrin to form around the coated pit (Figure 1.9) (Ford et al., 2001).

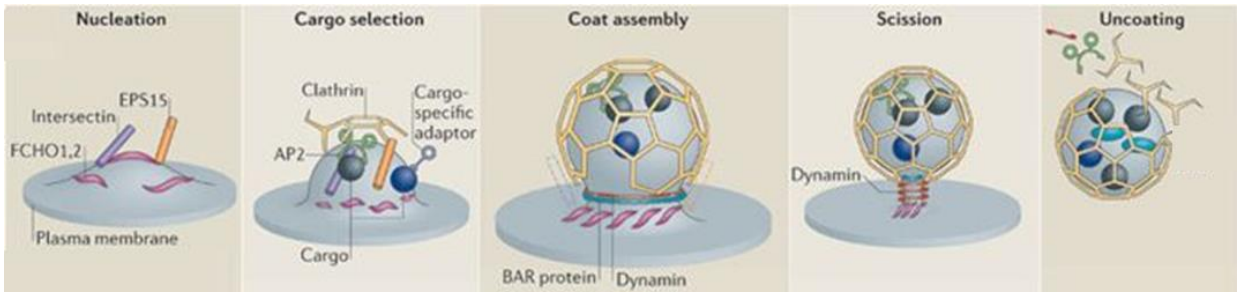

Figure 1.9 Overview of the five steps involved in clathrin-mediated endocytosis

Nucleation: it is the first step of clathrin-coated pit initiation, where the FCH domain only (FCHO) proteins bind to phosphatidylinositol-4,5-bisphosphate (PtdIns(4,5)P2. This binding recruit adaptor protein 2 (AP2) which bind to the μ-subunit and σ-subunit of the cytoplasmic tail of the receptors (cargo selection step). AP 2 then recruits clathrin to assemble around the nascent pit at the intracellular surface of the plasma membrane. BAR domain-containing proteins is then recruit dynamin at the neck of the clathrin coat pit and upon GTP hydrolysis The clathrin vesicles detaches from the plasma membrane. The vesicle loses its clathrin by the ATPase heat shock cognate 70 (HSC70), leaving the naked transport vesicle for fusion. Taken from (McMahon and Boucrot, 2011).

Once the clathrin vesicles are formed, dynamin is then recruited. Dynamin is an important regulatory protein that has been identified as being responsible for mediating the membrane fission and release of clathrin coated pits (Antonny et al., 2016). Dynamin is 100 KDa and consists of five domains (GTPase hydrolysis domain, Middlil domain, PH domain and GTPase effector domain) and has been identified as a high-molecular-weight GTPase as it shares a high sequence number on its C-terminal GTPases (300 amino acid) that distinguishes it from other members of the GTPase family, such as Ras (Ferguson and De Camilli, 2012) Initial characterisation revealed that dynamin localizes at the neck of budding vesicles, forming a helix, and acts as a GTPase switch. This switch mediates 'pinch' activity, resulting in vesicle scission from the membrane (Sweitzer and Hinshaw, 1998). The pinches activity is stimulated when the lipid binds to dynamin at the PH domain and the lipid bilayer undergoes conformational change in a GTP-hydrolysis manner, which in turn drives the neck constriction and scission (Stowell et al., 1999).

Once the clathrin-coated vesicle is released from the plasma membrane, the heat shock cognate 70 (HSC70) protein binds to the C-terminal of clathrin heavy chains (Sousa and Lafer, 2015) (Barouch

et al., 1994). This binding induces the clathrin disassembly, leaving the naked transport vesicle for fusion with early endosomes in pH of approximately 6.0. The pH falls further to around pH 5, where the early endosomes mature to late endosomes followed by lysosome degradation (Figure 1.12) (McMahon and Boucrot, 2011, Kaksonen and Roux, 2018).

4.1.2 Caveolae-dependent endocytosis

Caveolae were first defined in the 1950s using electron microscopy as a flask-shaped structure (approximately 50–100 nm in diameter) composed of cholesterol (Palade, 1953). It is involved in the regulation of a range of important cellular activities such as lipid metabolism, transmembrane signalling and endocytosis of certain toxins or pathogens. Caveolin is the main protein that induces the formation and stability of the caveolae (Nabi and Le, 2003).

Three caveolins have been identified: caveolin1, caveolin2 and caveolin3. Caveolin1 and caveolin2 are present in most non-muscle cells, except the neuron, while caveolin 3 is muscle specific (Way and Parton, 1995). Caveolin1 is present on the plasma membrane and is composed of the N-terminal domain (101 amino acid), caveolin scaffolding domain (CSD: 33 amino acid sequence) and the C-terminal domain (44 amino acid sequence). Both its carboxyl and amino termini face the cytoplasm (Figure 1.10) (Parton and Collins, 2016).

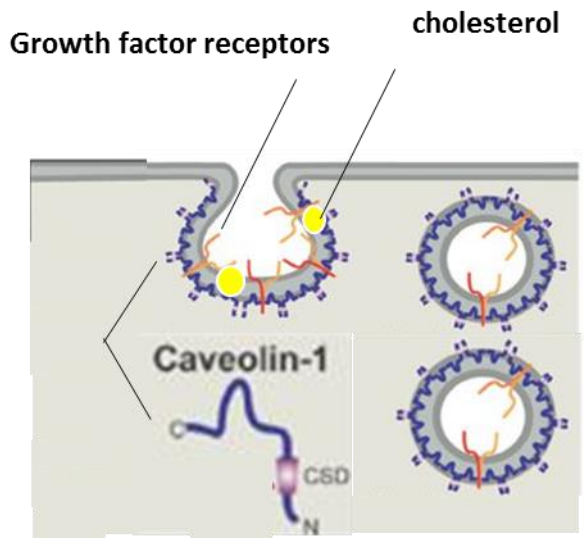

Figure 1. 10 Schematic representation of Caveolae endocytosis and Caveolin1 structure. CSD: caveolin scaffolding domain. Modified from (Baker and Tuan, 2013)

During endocytosis, pathogens interact with the receptor on the plasma membrane to induce the formation of lipid rafts. These caveolae are also driven by dynamin, which induces the pinching off of the caveolar vesicle followed by fusion to a caveosome which is a specific endosomal compartment with a neutral internal pH (Nabi and Le, 2003). These vesicles do not travel through the lysosome system and many pathogens, such as simian virus 40 follow this pathway to avoid lysosome degradation (Kiss and Botos, 2009). Consequently, targeting caveolae-dependent endocytosis may prove beneficial for improving therapeutic effects.

4.1.3 Macropinocytosis

Macropinocytosis is the third endocytic pathway and can take place in many types of cell. It is derived from membrane folds (ruffles) that extend out of the actin-rich plasma membrane and form vesicles called macropinosomes. Macropinosomes have an irregular shape, and its size is approximately 0.2 to 10 μm in diameter, which is larger than other pinocytosis vesicles (Figure1.11) (Swanson and Watts, 1995).

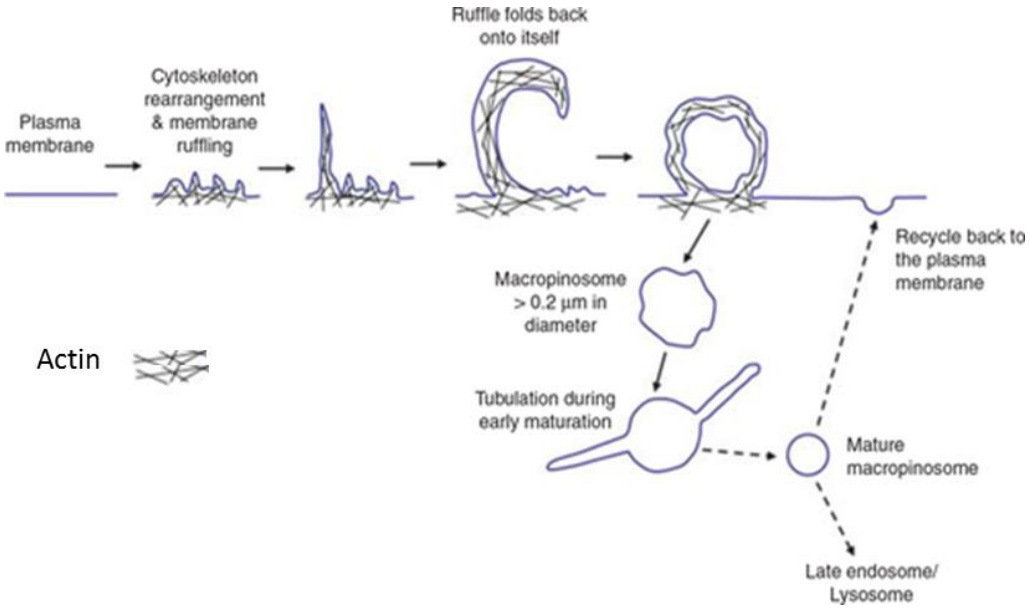

Figure 1. 2 Schematic representation of micropinocytosis pathway. Taken from (Lim and Gleeson, 2011)

The formation of macropinosomes normally occur upon external stimulation from growth factors such as epidermal growth factor (EGF), platelet-derived growth factor (PDGF) and macrophage colony-stimulating factor-1 (CSF-1). These factors activate multiple signalling pathways such as RAC1 (Ras-related C3 botulinum toxin substrate 1) (Bar-Sagi et al., 1987). These signalling pathways with the help of actin induce the formation of membrane ruffles and the traffic of macropinosomes.

The breakage and cleavage of macropinosomes can occur without the aid of dynamin. It relies on actin dynamics (Sigismund et al., 2012). It can occur through extensive folding and protrusion of the plasma membrane mediated by phosphoinositide 3-kinase (PI3K) and phospholipase C (PLC)

interaction (Bar-Sagi et al., 1987). Therefore, drugs that disrupt the actin cytoskeleton can inhibit this process(Dutta and Donaldson, 2012) (Rauchenberger et al., 1997).

Alternatively, it can occur via mechanisms that require the involvement of CtBP1/BARS (C-terminal-binding protein-1/brefel-dinA-ADP ribosylated substrate) (Bonazzi et al., 2005). Studies have shown that upon EGF receptor engagement, the CtBP1/BARS migrates and accumulates around the macropinosomes. p21-Activated kinase (Pak1) phosphorylates CtBP1/BARS on a specific serine. This phosphorylation promotes the membrane fission (Liberali et al., 2008).

4.1.4 Non Clathrin- and caveolae independent endocytosis

Clathrin- and caveolae-independent endocytosis is the fourth endocytic pathway, and it can be distinguished by its dependency on cholesterol, and it requires specific lipid compositions such as lipid rafts (Damm et al., 2005). Lipid rafts (also called lipid microdomains) are highly dense membrane domains that are rich in molecules, including cholesterol and phospholipids, such as phosphatidylcholine (Simons and Sampaio, 2011).

A common feature of these pathways is the involvement of rho protein family members such as CDC42 and ARF6 (ADP-ribosylation factor 6) (Sabharanjak et al., 2002). Once the extracellular ligand accumulates and binds to the protein receptor on the lipid rafts. The lipid raft region form large tubular which then detaches from the cell membrane depending on actin polymerisation and the curvature of the membrane (Gallop et al., 2013). The investigation into these pathways has recently strengthened, but more work is needed due to the lack of understanding of their mechanisms.

4.2 Endosomes

Endosomes are vesicles coated by envelopes which are responsible for transporting endocytic particles to the lysosomes for degradation or back to the plasma membrane for recycling. They also play a role in regulating signal transduction (Murphy et al., 2009). For example, they prevent the generation of excessive signals by regulating the number of receptors on the plasma membrane through degradation or recycling pathways. Therefore, defects in endocytosis can lead to abnormal transport of ligand receptors such as EGFR, causing degradation or accumulation, resulting in the development of cancer in humans (Tomas et al., 2014). The early endosome compartment is the first compartment that labels the incoming cargo and fluid and transports it to the correct destination (Maxfield and McGraw, 2004, Helenius et al., 1983). The lumen of the early endosome is slightly acidic, usually ranging between pH 6.3 to 6.8 and takes cargo molecules from different internalization routes including the clathrin pathway, Caveolae pathway, micropinocytosis pathway and ARF6-dependent pathway (Mayor and Pagano, 2007).

Structurally, early endosomes are composed of big vesicular structures and many tabulated membranes. The vesicular structures are generally 700nm in diameter, while the tabulated membranes range from 50 to 60 nm in diameter. Differences in this structure can determine the destination of internalized cargo. For example, thin tubular extension is responsible for recycling the receptor directly from early endosomes or indirectly via recycling compartments, which contain a large number of tubular structures with the molecular marker Rab11, whereas vesicles serve as sites for fusion with late endosome compartments (Mellman, 1996). Early endosomes can be distinguished from other compartments according to the time at which internalized cargo reach them (10 minutes) and the different molecular markers such as Rab5A (Ras-related protein Rab-5A) (Figure 1.12) (Maxfield and McGraw, 2004).

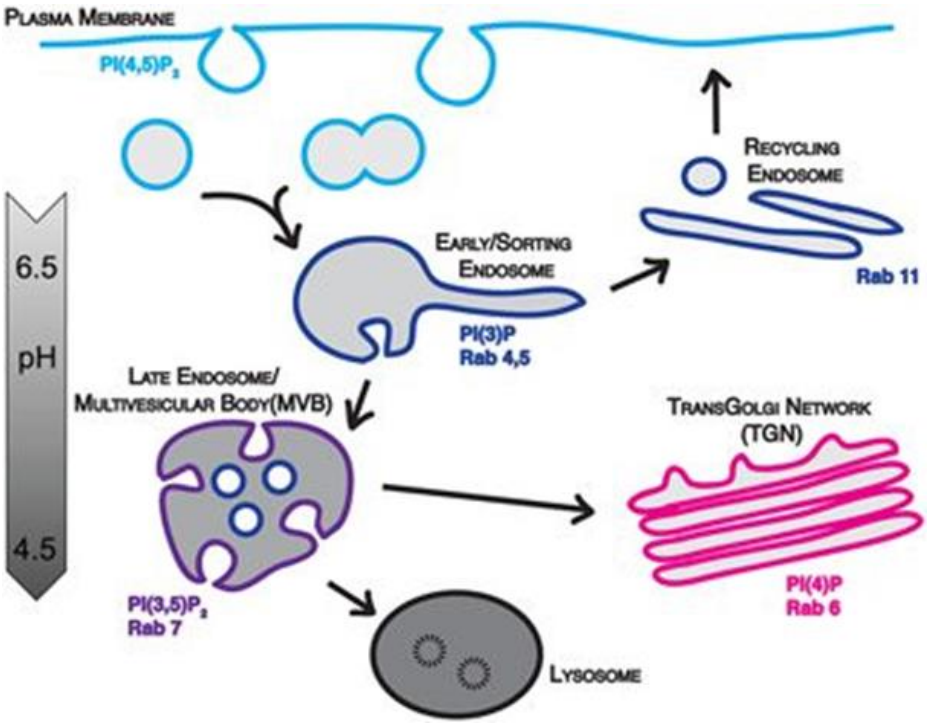

Figure 1. 3 overview of endosomal trafficking.

Internalised endosomes undergo homotypic fusion to form vesicular and tubular early endosomes. The tubular endosomes are recycled back to the cell membrane by Rab4. The vesicular endosomes can be fused with multivesicular bodies/ late endosomes to the lysosome by Rab7 or to trans-Golgi network by Rab6. Taken from (Elkin et al., 2016)

Rab5A protein is a member of Rab family, which belongs to small GTP binding protein. It has three isomers—Rab5A, Rab5B and Rab5C. Rab5A is one of the key proteins that cycle between Rab-GTP-bound (active) and Rab-GDP-bound (inactive) by GTP/GDP exchange factors: guanine nucleotide exchange factors (GEFs) (Schwartz et al., 2007) .

Rab5a is composed of 215 amino acid residues with a molecular weight of 23 kDa. It characterized by a G domain (G1 to G5) figure 1.13 (Zhu et al., 2004) (Lachance et al., 2014). Switch 1 and Switch 2 regions, which are part of the conserved element of G2 and G3, play an important role in exchanging inactive GDP to active GTP. Amino acid Ser/Thr in switch regions bind to the gamma phosphate of GTP, which results in conformational change within the protein structure (localized change of the amino acid) as the Rab5 protein switches from GDP to GTP structure (Lee et al., 2009). This change

allows the effector protein to recognise the GTP structure and regulates the fusion of uncoated clathrin vesicles with early endosomes and mediates intraluminal vesicle formation (Zhu et al., 2004).

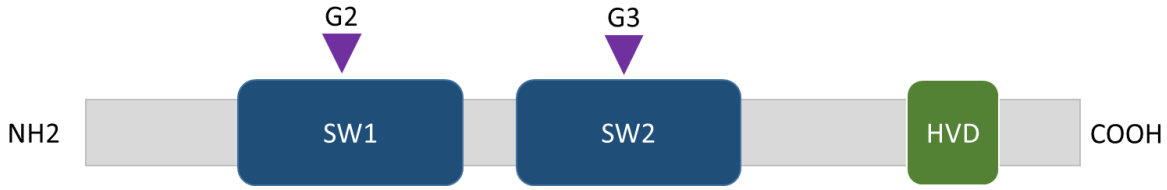

Figure 1. 4 Molecular structure of Rab5a. G domain (grey) contains molecular switch I (Sw l), molecular switch II (Sw2) and a hypervariable domain (HVD). Modified from (Zhu et al., 2004).

Rab5a GTP alone is not sufficient to regulate the trafficking and membrane fusion of the endosome but requires other effectors that can bind lipid of the endosomes membrane and Rab5a. The early endosomal autoantigen 1 (EEA1) is one of Rab5A effector that is specifically located on early endosomes and regulates vesicle membrane fusion (Jovic et al., 2010).

Structurally, EEA1 protein consists of three regions—the N-terminal region FYVE domain, which bind Phosphatidylinositol 3,4,5-triphosphate (PI3P), C-terminal region C2H2 zinc finger domain binds active Rab5 GTP- and central region of 1,200 residues which has coiled-coil structure (two alpha helices)(Rubino et al., 2000) (Dumas et al., 2001). This large coiled-coil structure extends the length to capture and tether the upcoming Rab5 positive vesicle via its C-terminal. the long coiled coil then collapses to bring the vesicles closer to the early endosome compartments as shown in Figure 1.14 (Dumas et al., 2001, Das and Lambright, 2016, Murray et al., 2016).

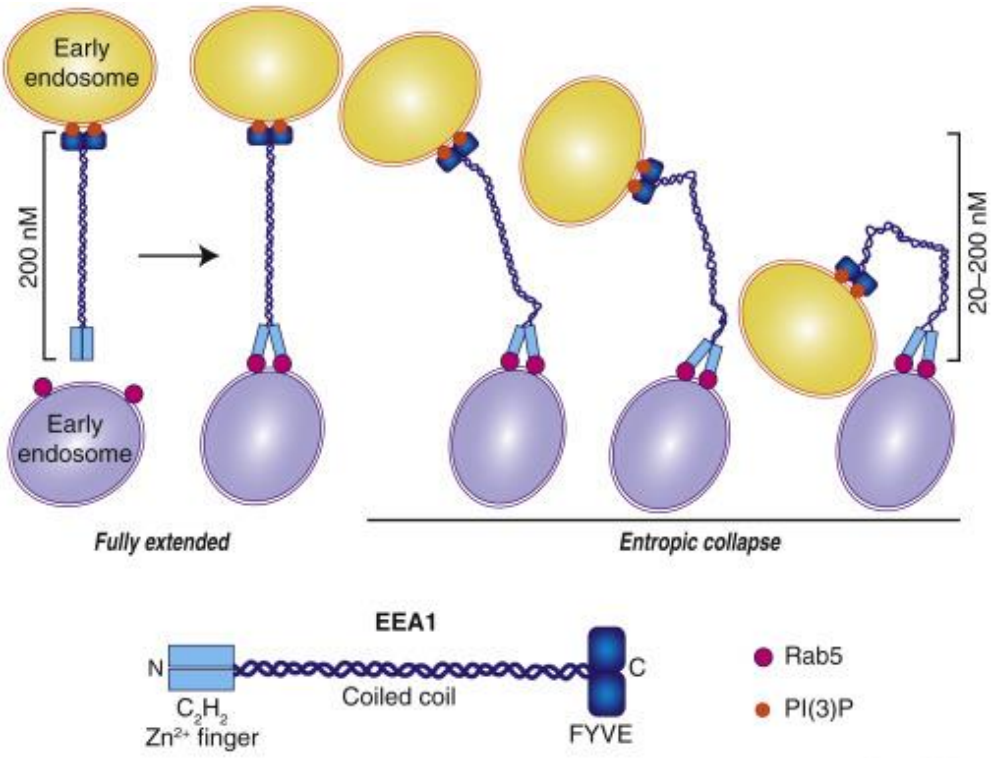

Figure 1. 5. Endosome tethering

Early endosome antigen 1 protein with a diameter of 200 nm collapsed by binding phosphatidylinositol 3-phosphate (PI3P) at its C-terminal region FYVE domain and Rab5 at its C-terminal C2H2 zinc finger. Taken from (Das and Lambright, 2016)

Late endosomes, also known as multivesicular bodies (MVBs), are usually spherical or tubular with a large number of intraluminal vesicles labelled with Rab7, Rab9 and LAMP1 (Lysosomal associated membrane protein 1) (Luzio et al., 2000). The maturation of late endosomes require Rab5 conversion in which early endosomes lose Rab5A and acquire Rab7A (Somsel Rodman and Wandinger-Ness, 2000). This occurs when ubiquitinated receptors recruit the endosomal sorting complex required for transport (ESCRT) machinery that induces inward budding into the endosomal lumen. The luminal pH gradually decreases from 6.5 to 5 under the action of V-ATPase on the membrane (Bishop and Woodman, 2000). The membrane fusion also regulates by replacing the class C core vacuole/endosome tethering factor (CORVET) by the late endosome (Solinger and Spang, 2013). The late endosomes are then fused with lysosomes for degradation (Huotari and Helenius).

4.3 The role of endocytosis in cell migration:

The plasma membrane is the physical barrier whose features defend the cytoplasmic content of the cell by separating it from the external environment. At the same time, it works as a communications interface allowing cells to receive or sense signals from the external environment or from its neighbouring cells. These signals are activated when the membrane receptors bind to their specific ligands and the signal is transmitted across the plasma membrane inside the cell. Once these receptors have bound the ligands and transmitted the signal through the cell membrane, the cell undergoes physiological and behavioural changes.

One key feature of endocytosis are the internalizing plasma membrane proteins, especially the surface receptors and ligands. Endocytosis of these receptors and ligands modifies the shape and dynamics of the plasma membrane. Endocytosis also controls the intracellular signalling because endocytosis has the ability to translocate membrane receptors to the nucleus or between endocytosis compartments and thereby sustain the signal by recycling membrane receptors or terminating the signal by degrading membrane receptors through lysosomal activity. Therefore, endocytosis plays an important role in regulating cell signalling (Di Fiore and von Zastrow, 2014).

Emerging evidence suggests that endocytosis can contribute to cell migration steps both indirectly and directly in many ways (Maritzen et al., 2015). These steps can be subdivided into three stages—response to external signal(s), assembly or disassembly of adhesions (cell-cell adhesion or cell to ECM) and protrusions that are mediated by cytoskeleton polarization at the leading edge (Maritzen et al., 2015).

In the first step of cell migration, endocytosis pathways mediate the internalization and trafficking of exogenous signals such as chemokines and growth factors as they play an important role in cell movement (Luker et al., 2010). A good example of this is the directional migration of border cells from the anterior end of the egg to the posterior end of the oocyte during ovarian developments of

Drosophila. Multiple growth factors receptors (PVR and EGFR) were found to be secreted from border cells where as its ligands (PVF1 and GrK) expressed by the oocyte (Duchek et al., 2001). Interestingly, endocytotic events regulate the localization of these receptors. Inhibiting these receptors affects endocytic mechanisms leading to the defective migration of border cells (Mateus et al., 2011).

Moreover, endocytosis can initiate the signalling cascade and control the activity of signalling by controlling the quantity and quality of surface receptors (Platta and Stenmark, 2011, Di Fiore and von Zastrow, 2014). The Wnt signalling pathway, which plays a main role in the progression of a tumour to an invasive or metastatic state by disrupting tight junctions in epithelial cell-cell contact through a process called cadherin switching. Hanaki and colleagues showed that endocytosis can modulate Wnt signalling and contribute to a decrease in tumour spread by inhibiting the protein Wnt5a (Hanaki et al., 2012). These observations suggest an important role of endocytosis pathways as they can work as attenuators of signalling and any defect in endocytic mechanisms can affect many cellular processes, such as cell adhesion, proliferation and survival (Mosesson et al., 2008).

In addition to signalling, endocytosis mediates cell-cell adhesion (E.Cadherin) trafficking and degradation through the lysosomal pathways, thereby maintaining cell-cell communication. Inhibiting the function of endocytosis may lead to the development of epithelial-to-mesenchymal transitions (EMT) (Sato et al., 2011). The phenomenon of EMT is implicated in many processes and diseases such as cancer cell metastasis (Baum et al., 2008). Because multiple pathways are implicated in both signalling and cell-cell adhesion, more information is still needed to distinguish the function and mechanisms of each endocytotic pathway.

Endocytosis also mediates the trafficking and recycling of integrins that have been implicated in many processes, including morphology, proliferation and invasion. Some studies have provided evidence that endocytosis translocates integrin subtypes from early endosomes to recycling endosomes, thus facilitating the migration speed (Bridgewater et al., 2012). Another study has indicated a new

trafficking route for integrins through the degradation pathway (Dozynkiewicz et al., 2012). However, data is still needed to determine whether integrins are recycled from late endosomes or targeted for degradation and which endocytosis pathways are involved.

Aside from its function in mediating signalling and membrane trafficking, endocytosis has been implicated in the cytoskeleton network organisation and actin assembly. Actin polarization mediates the formation of lamellipodia and protrusion during cell migration steps. In yeast, for example, the ARP2/3 complex are major components that facilitate actin assembly. It has been discovered that these complexes are recruited at the late stage of clathrin pathways by endocytotic adaptors. In addition to that, eps15 amphiphysin proteins that are associated with clathrin endocytosis adaptors are also found to bind to the actin cytoskeleton directly. Mutations of the clathrin pathway, either dynamin or its endocytotic adaptors, affect the function of these complexes and delays the time that actin needs to polymerize new filaments. Similar to yeast, mutations of dynamin1 in mammalian cells (Hela cells) disrupt the actin fibres. Nevertheless, other clathrin independent pathways have also been implicated in cytoskeleton organisation (Coppolino et al., 2001);(Castellano et al., 2001); (May et al., 2000) (Basquin et al., 2015)

These observations suggest that actin may participate in endocytotic actions. Actomyosin contractility may facilitate the invagination of the plasma membrane while actin polymerization may provide force at the neck of the vesicles to facilitate membrane fusion and detachment (Qualmann et al., 2000). For example, in yeast, disruption of the cytoskeleton through either mutation or chemical inhibitors completely blocks endocytosis. In contrast, in mammalian systems, understanding the role of actin in endocytosis is lacking and needs to be better defined. For example, intracellular actin inhibitors cytochalasin D, latrunculin A and jasplakinolide displayed no effect on the endocytosis of transferrin in two different cell lines A321 CHO (Miya Fujimoto et al., 2000). However, other studies have demonstrated that the inhibition of actin function partially inhibits the endocytosis (Lamaze et al.,

1997). In addition, depletion of myosin 1E inhibits transferrin endocytosis and increases the average lifetime of clathrin coated vesicles (Cheng et al., 2012).

Recently, endocytosis has been shown to play an important role in focal adhesion disassembly. Ezratty et al. (2009) have shown, however, that endocytosis plays a crucial role in focal-adhesion disassembly by demonstrating the relationship between the endocytosis of integrin and microtubules and the mediation of focal-adhesion disassembly through the clatherin pathway, which has implications for epithelial polarisation. Similarly, other studies have shown that integrin endocytosis can mediate focal adhesion disassembly in response to PDK1 (Gagliardi et al., 2015). These findings may indicate that the interaction of integrin with ECM and focal adhesion may not be sufficient to induce its clustering and may require the activity of other mechanisms such as endocytosis.

Emerging evidence suggests that endocytosis is implicated in focal adhesion disassembly by controlling the expression of calpain (Mendoza et al., 2018) This study showed that calpain co-localized, co-immunoprecipitated with early endosomes markers (EEA1 and Rab5) as well as accumulated at endosomes fraction. In addition, the knock down of rab5 decreased the expression of calpain and prevented focal adhesion disassembly (Mendoza et al., 2018).

Overall, all these observations regarding signalling, internalizing adhesions, cytoskeleton organisation and focal adhesion disassembly indicate a role for endocytosis in cell migration and possibly FA turnover. However, the exact mechanisms need to be elucidated. In addition, there is a lack of knowledge regarding the relationship between each endocytosis pathway and cell migration. As a result, there exists a need for the mechanisms of endocytosis to be examined so that the methods in which cell migration mediates the metastasis of cancer cells can be better understood.

5 Aims of project

The aim of this project is to accomplish an in *vitro* investigation of the role of endocytosis in regulating cell migration and focal adhesions. We aim to understand the role of endocytosis pathways on endocytosis (ligand uptake and endosome markers) and cell migration by using four endocytosis pathways inhibitors—dynamin pathway inhibitors (Dynasore), Clathrin pathways inhibitors (Pitstop2), Caveolae pathways inhibitor (Filipin III) and Micropinocytosis pathways inhibitor (Amiloride), and three different cancer cell types that originate from different histological organs: MDA-MB-231 breast cancer cell line, SK-MEL-28 melanoma cell line and HT1080 fibrosarcoma cancer. Furthermore, we intend to identify the role of early endosome proteins in directing cell migration.

In addition, in this project we also aim to study the impact of endocytosis inhibition on focal adhesion dynamics (number, size and turnover), and to clarify the association between early endosome portions and focal adhesion. Finally, this project also aims to identify signalling pathways affecting endocytic regulation of cell migration and focal adhesion turnover and to study the role of nitric oxide in cell migration, endocytosis and focal adhesion turnover.

Chapter 2: Materials and Methods

2.1 Materials and Reagents:

2.1.1 Tissue Culture:

Table 2. 1: All materials and reagents listed below were used for Tissue culture:

Tissue Culture	Source
Collagen	BD Bioscience
DMSO (Dimethyl Sulphoxide)	Sigma Aldrich
Dulbecco's Modified Eagle's Medium (DMEM)	Gibco
Dulbecco's Phosphate Buffered Saline (PBS)	Gibco
Fetal Bovine Serum (FBS)	Gibco
Gelatine	Sigma Aldrich
Low glucose MEM (Minimum Essential Medium)	Gibco
L-Glutamine	Gibco
Penicillin /Streptomycin	Gibco
Trypsin /EDTA 0.05%	Gibco

Table 2. 2 Cell lines:

Cell Line	Source
MDA-MB-231 (Human Invasive Breast Cancer Cell Line)	ATCC
HT1080(HumanFibrosarcoma Cell Line)	ATCC
SK-MEL-28 (Melanoma Cell Lines)	ATCC

2.1.2 Inhibitors

Table 2. 3 All inhibitors listed below were used for endocytosis:

Inhibitors	Source
Amiloride (5-(N-Ethyl-N-isopropyl) Stock: 33.36 mM in DMSO Working concentration: 50 µM	Sigma
Dynasore Stock: 80mM in DMSO Working concentration: 20 µM and 80 µM	Selleckchem
Filipin III from Streptomyces filipinensis Stock: 1.5 mM in DMSO Working concentration: 16 µM	SigmaAldrich
Pitstop2 (N-[5-(4-Bromobenzylidene)-4-oxo-4,5-dihydro-1,3-thiazol-2-yl]naphthalene-1-sulfonamide) Stock: 8 mM in DMSO Working concentration: 25 µM	Abcam

Table 2. 4 All inhibitors listed below were used for nitric oxide:

Inhibitors	Source
L-NAME (Nω-Nitro-L-arginine methyl ester hydrochloride) Stock: 100 mM in PBS Working concentration: 5mM	Abcam
1400W (dihydrochloride iNOS inhibitor) Stock: 19.291 mM in PBS Working concentration: 2mM	Tocris Bioscience
Nitric Oxide Donors (PAPA/NO; NOC-15; 1-(3-aminopropyl)-2-hydroxy-3-oxo-1-propyltriazan PAPA NONOate Stock: 10mM in PBS Worked concentration: 50 µM	Santa Cruz

2.1.3 Antibodies:

Table 2. 5 All antibodies that listed below were used for endocytosis, focal adhesions, nitric oxide and other experiments

Antibodies	Source
Anti-APPL1 Rabbit Working concentration: 1:200 IHC, 1:50 IP and 1:1000 WB	Abcam
Anti-EEA1 Mouse Working concentration: 1:200 IHC, 1:50 IP and 1:1000 WB	Cell signalling
Anti-EEA1 Rabbit Working concentration: 1:200 IHC, 1:50 IP and 1:1000 WB	Cell Signalling
Anti-Clathrin Heavy Chain Rabbit Working concentration: 1:200 IHC, 1:50 IP and 1:1000 WB	Abcam
Anti-Rab5 Rabbit Working concentration: 1:200 IHC, 1:50 IP and 1:1000 WB	Abcam
Anti-LAMP1 Rabbit Working concentration: 1:200 IHC, 1:50 IP and 1:1000 WB	Cell Signalling

Antibodies	Source
Anti-Vinculin Mouse Working concentration: 1:100 IHC, 1:50 IP and 1:1000 WB	Abcam
Anti-Vinculin Rabbit Working concentration: 1:100 IHC, 1:50 IP and 1:1000 WB	Abcam
Anti-Talin1 Rabbit Working concentration: 1:200 IHC, 1:50 IP and 1:1000 WB	Abcam
Anti-Paxillin Mouse Working concentration: 1:100 IHC, 1:50 IP and 1:1000 WB	Abcam
Anti-Paxillin Rabbit Working concentration: 1:100 IHC, 1:50 IP and 1:1000 WB	Abcam
Anti-FAK Mouse Working concentration: 1:200 IHC, 1:50 IP and 1:1000 WB	Abcam
Anti-Actin Mouse Working concentration: 1:100 IHC, 1:50 IP and 1:1000 WB	Abcam
Anti-GAPDH Rabbit Working concentration: 1:100 IHC, 1:50 IP and 1:1000 WB	Sigma
Anti-H2B Mouse Working concentration: 1:100 IHC, 1:50 IP and 1:1000 WB	Abcam
Anti-ubiquitin Mouse Working concentration: 1:100 IHC, 1:50 IP and 1:1000 WB	Sigma

Antibodies	Source
Anti-IgG Rabbit Working concentration: 1:1000 WB	Sigma
Anti-Mouse Alexa Flour 488 Goat Working concentration: 1:100 /1500 IHC	Cell Signalling
Anti-Rabbit Alexa Flour 488 Goat Working concentration: 1:100 /1500 IHC	Cell Signalling
Anti-Mouse Alexa Flour 546 Goat Working concentration: 1:100 /1500 IHC	Cell Signalling
Anti-Rabbit Alexa Flour 546 Goat Working concentration: 1:100 /1500 IHC	Cell Signalling
Anti-Rabbit Alexa Flour 647 Goat Working concentration: 1:100 /1500 IHC	Cell Signalling
Anti-Mouse Alexa Flour 647 Goat Working concentration: 1:100 /1500 IHC	Cell Signalling
Anti-eNOS Rabbit Working concentration: 1:100 IHC, 1:50 IP and 1:1000 WB	Cell Signalling
Anti-NOS2 Mouse Working concentration: 1:100 IHC, 1:50 IP and 1:1000 WB	Santa Cruz

2.1.4 Ligands:

Table 2. 6 All ligands s that listed below were used for endocytosis uptake:

Ligand	Source
Transferrin From Human Serum, Alexa Fluor® 546 Conjugate	Thermo Fisher
Dextran, Fluorescein, 10,000 MW, Anionic, Lysine Fixable (Fluoro-Emerald)	Thermo Fisher

2.1.5 Plasmids:

Table 2. 7 All plasmids that listed below were used for transfection:

plasmid	Source
mCHerry-Zyxin	Phil Dash Lab
GFP-Paxillin	Phil Dash Lab

2.1.6 Reagents:

Table 2. 8 Biochemical reagents:

Items	Company
Acetone	Sigma Aldrich
Acrylamide	Sigma Aldrich
Agarose	Sigma Aldrich
Ammonium perusulphate	Sigma Aldrich
Ampicillin	Sigma Aldrich
Bovine serum albumin	Thermo Fisher
Bromophenol Blue	Sigma Aldrich
Clarity Western ECL Substrate	Thermo Scientific
DAPI Vectashield	Vector Laboratories
DMF (Dimethylformamide)	Sigma Aldrich
EDTA	Sigma Aldrich
Glycine	Sigma Aldrich
Goat Serum	Thermo Fisher
Glycerol	Sigma Aldrich
Hybond ECL Nitrocellulose Nembrane	Sigam Aldrich
Hepes	Sigma Aldrich
Isopropanol	Sigma Aldrich
Kanamycin	Sigma Aldrich
Luria Bertani Agar and Broth	Sigma Aldrich
Maxprep Kit	Qiagen
Medical X-Ray Film	Fuji
Mercury(II) Chloride	Sigma Aldrich

Items	Company
Protein A/G Agarose	Thermo Scientific
Precision Plus Protein Dual Colour Standards	Thermo Fisher
Paraformaldehyde	Sigma Aldrich
Phosphate Buffered Saline (PBS) Tablets	Thermo Scientific
Protease Inhibitors Cocktail (PIC)	Calbiochem
Percoll	VWr
RIPA Lysis Buffer	Thermo Fisher
Streptavidin Agarose from Streptomyces Avidinii	Sigma Aldrich
Sodium Chloride	Sigma Aldrich
Sodium Dodecyl sulphate	Sigma Aldrich
Sodium Fluoride	Sigma Aldrich
Skimmed Milk Powder	Sigma Aldrich
Sucrose	Sigma Aldrich
Tris-Base	Sigma Aldrich
Tris-HCL	Sigma Aldrich
Tween	Sigma Aldrich
TEMED (Tetramethylenediamine)	Sigma Aldrich
Triton 100X	Sigma Aldrich
TurboFect Transfection Reagent	Thermo Scientific

2.1.7 Solutions Preparations:

2.1.7.1 Western blot solution preparation:

- 10% SDS (w/v): 50g of SDS (Sodium dodecyl sulphate) in 450ml of ddH2O.

- Tris –Glycine electrophoresis (5x): 25mM Tris base: 15.1g (w/w), 250 mM Glycine: 94g (w/w), 0.1% SDS: 50ml of 10% SDS and all Diluted in 950ml distilled water. pH adjusted to 8.3.

- Tris –Glycine electrophoresis (1x): 5X (v/v) Tris –Glycine electrophoresis: 200 ml in 800ml ddH2O.

- Transfer Buffer: 39mM Glycine: 2.5g (w/w), 48mM Tris Base: 2.93g (w/w), Methanol (200ml) and all diluted in 800ml distilled water.

- 10x Tris Buffer Saline (TBS): 80g (w/w) Sodium Chloride, 2g (w/w) Potassium Chloride, 30g (w/w) Tris Base and all diluted in 1000 ml distilled water. pH adjusted to 7.4

- Tris Buffer Saline Tween (TBST): 10x TBS (100mL), 0.1% of Tween 20 (Sigma): 1 ml (v/v) and all diluted in 900 ml distilled water.

2.1.7.2 Acrylamide gel preparation

2.1.7.2.1 Solution for preparing 10% resolving Gels:

- 7.9 ml H2O
- 6.7 ml 30% Acrylamide mix
- 5 ml 1.5 M Tris
- 0.2 ml 10% SDS
- 0.2 ml 10% (w/v) Ammonium Persulfate
- 8µL TEMED (Tetramethylenediamine)

2.1.7.2.2 Solution for preparing 5% Stacking Gels:

- 5.5 ml H2O
- 1.3 ml 30% Acrylamide mix
- 1 ml 1.0 M Tris
- 0.08 ml 10% SDS
- 0.08 ml 10% (w/v) Ammonium Persulfate
- 8µL ml TEMED (Tetramethylenediamine)

2.2Methods:

2.2.1 Cell Culture:

2.2.1.1 Cell Thawing and Freezing:

Vials which contain cell lines were removed from liquid nitrogen and gently thawed with agitation in a 37˚C water bath for approximately 2 minutes. As soon as the cells were thawed, the vial was removed from the water bath and decontaminated by spraying with 70% ethanol. Cells were subsequently transferred to a T25 Flask and diluted with 5 ml of DMEM (10% FBS, 1% Penicillin/streptomycin). Flasks were then incubated at 37˚C, 5% CO_2 incubators for a week with medium renewal every 2 - 3 days.

Once cells reached 80% confluency, media was discarded and cells washed twice with PBS. In order to freeze cells for long term storage, cells were then incubated with 2ml 0.05 % Trypsin (trypsin-EDTA) for 2-3 minutes in a 37˚C, 5% CO_2 incubator. Trypsin was inactivated by addition of 3 ml fresh media and the suspension mix transferred to a falcon tube. The mixture was centrifuged at 1000 rcf (Eppendorf 5810) for 10 minutes. The supernatant was removed and the cell pellet resuspend in FBS with 10% DMSO (1ml DMSO in 9 ml FBS). Cells were then aliquoted into several cryo vials, transferred into a Mr Frosty containing 100% isopropyl alcohol and cooled to -80 ˚C for 24h. Finally, cryo vials were then transferred to liquid nitrogen for long term storage.

2.2.1.2 Cell growth:

MDA-MB-231 human breast cancer, HT1080 Human Fibrosarcoma and SK-MEL-28 Melanoma Cell lines were used. These cells were grown in Dulbecco's modified Eagle's medium (DMEM) containing 10% of foetal bovine serum (FBS), 1% v/v penicillin/streptomycin (10,000 units/ml penicillin, 10,000 µg/ml streptomycin, Gibco). Cells were cultured in T75 flasks and incubated at 37°C in 95% air and 5% CO_2. The media was changed every 48 hours. Once the cells reached 80% confluency, the growth medium was discarded and the cells were washed in 5 mL phosphate-buffered saline (PBS), and

incubated with 2.5 mL of 1x trypsin (0.05% trypsin-EDTA) for 6 min at 37°C. After incubation, 5mL of DMEM was added to the cells in order to inactivate the trypsin. Twenty microliters of the cell suspension was counted using the 1/400mm^2 haemocytometer. The following equation was used to determine cell concentration per millilitre:

(Number of cells counted /number of squares) X 10^4 X dilution factor = number of cells per ml.

Cell were seeded at 1:4 or 1:6; 0.4 -0.6 ml of cell suspension was added with 18 ml of fresh media into a new flask. Cells were incubated at 37°C in 95% air and 5% CO_2 for a week until 80% confluence with medium renewal every 2 - 3 days.

2.2.2 Cell growth on coverslips or differencent extracellular matrixes (ECM):

Glass coverslips were transferred into a 12 well plate and sterilized in 100% methanol for 1 hour in the culture hood. The methanol was aspirated and plate was dried. Then, 2 ml of DMEM was added to sterile glass coverslips and cells were plated at a density of 2×10^4 in 12 well plates containing 2ml for 24h.

For ECM experiments, once the plate was dried, the glass coverslips or 35mm ibidi dish (microscopy dish) were coated with 0.2% w/v gelatine for 30 min and left to dry up to 2 hours. Then, 2 ml of DMEM was added to glass coverslips coated with gelatine and the cells were plated at 2×10^4 in 12 well plates containing 2ml for 24h.

In the case of Collagen, 100µL of 10x DMEM (Gibco, Thermo Fisher Scientific) was mixed with 512µL/ml (v/v) of chilled rat tail type 1 collagen (4.41 mg/ml stock concentration). 15 to 20 µL of 1M NAOH was added to the mixture (pH normalized to 7.0) until the mixture colour changed to pink. Culture media was then added to the mixture to give the final concentration of 2mg/ml collagen. These steps were carried out on ice in a sterilized culture hood and special attention was paid to mix these

ingredients well while avoiding bubble formation. Then, the collagen mixture was added to sterile glass coverslips to a 12 well plate or 35mm ibidi dish (microscopy dish).

2.2.3 Wound Healing:

Cells were plated in six-well plates at 2×10^5 cell/cm^2 and incubated for 48 hours. Once the cells reached 100% confluency, cells were then treated with four endocytosis inhibitors or appropriate vehicle control (DMSO) at varying concentrations and incubation times. Then a wound/scratch was made using a 200 µL pipette tip and the media was then removed and replaced with 1 ml fresh media. Imaging of wound healing was performed by time lapse microscopy (Nikon Eclipse TiE) using a 10X objective with image capture occurring at 0, 18, and 24 hours. A minimum of three images per well were taken.

2.2.3.1 Wound Healing analysis:

Wound healing images were analysed using the ImageJ software. The wounded area for wound healing assay was manually drawn around the cell membrane at the initial time and end time points and measured using the following equation:

Percentage of wound area = (the average area at 0 time point / the average area at end time point) X 100

2.2.4 Cell Tracking:

Cells were plated on plastic or different surfaces (0.2% gelatine or 2mg/ml collagen) in a 12 well plate and incubated overnight. When the plate reached 30% confluence, cells were treated and placed in the heated stage of a time-lapse microscope supplied with 5 % CO_2. Cell migration were observed over 24 hours with images captured every 15 minutes for a period of 24 hours using Nikon Eclipse TE200 running NIS elements software a Nikon DXM1200 camera at 10 x objective. ImageJ software MtrackJ tool was used to calculate the total distance of individual cells. The speed were represented as the total distance moved divided by time in hours. If any inhibitors or treatments were required, each inhibitor was added to at least four wells. A minimum of 10 cells for each well were tracked.

2.3 Plasmid Transfection and live cell imaging:

2.3.1 LB media and agar preparation:

LB media was prepared by diluting 25g of LB broth into 1000 mL deionized water in an Erlenmeyer flask. Whereas, the LB agar was prepared by mixing 500 ml of LB media with 7.5 g agar in a different Erlenmeyer flask. Both flasks then were covered with aluminium foil and autoclaved. Once the autoclave process was complete, each flask was mixed with 50 µg/mL of Kanamycin. LB agar was poured in a sterile culture plates (5-10 mL for each plate) and sealed with parafilm. Finally, both agar plate and LB media were stored at 4 °C until use.

2.3.2 Plasmid Preparation:

One loop touch of *E.coli* culture, containing an inserted DNA plasmid construct (mCherry Rab5, GFP Paxillin or mCherry -Zyxine from Addgene), was added to 5 mL Luria-Bertani (LB) medium, containing 50 µg/ml of Kanamycin, and incubated in a shaking incubator at 37°C overnight. 10 µL of bacterial culture was transferred on to a Kanamycin-resistant LB agar culture plate and incubated for 16 hours at 37°C. One colony was picked and mixed with 5ml LB media in tube, and placed in a shaking incubator at 285 rpm 37°C for 10 hours . 1mL of the mixture was transferred into 100 mL LB media in a conical flask, which was covered with aluminium foil and placed in a shaking incubator at 285 rpm 37°C for 10 hours. The growth LB media was transferred into two 50 ml plastic tubes and centrifuged for 20 minutes at 6000 rcf at 4°C. The supernatant was removed and the plasmid DNA was isolated using HiSpeed Plasmid Maxi Kit reagents (Qiagen), according to the manufacture's instructions.

The bacteria pellet was re-suspend in 10mL buffer P1 and mixed with 10 ml buffer P2 and incubated at room temperature for 5 minutes. Once the incubation completed, pellet was mixed with 10 ml of buffer P3, poured into the barrel of the QIAfilter Cartridge and incubated for 10 minutes at room temperature. Later, Hispeed max were equilibrated with 10 ml of buffer QBT. The cap of the QIAfilter

Cartridge was removed and the cell lysate was filtered and passed through the cartridge into the equilibrated tip. Hispeed tips were washed with 60 mL buffer QC, and the DNA was eluted with 15 mL buffer QF, precipitated with 10.5ml isopropanol and incubated for 5 minutes. Once the eluate-isopropanol mixture was filtered through a QIAprecipitator using syring with constant pressure, the DNA contained in the QIAprecipitator was washed with 2 ml 70% ethanol. After QIAprecipitator was dried, the DNA was finally eluted with 1 ml buffer TE into a 1.5 ml collection tube. The plasmid concentration was measured using Nanodrop spectrophotometer 2000 (Thermo Scientific, Labtech International) at 260 nm and 280 nm absorbance. Once the blank (1 µl of buffer TE) was calibrated, samples (1 µl of DNA) was measured as ng/mL.

2.3.3 Plasmid Transfection:

Cells were plated on a 35 mm ibidi dish at 10000 cells/mm^2. In an Eppendorf tube, 3 µg of plasmid (3.5 µl mCherry Rab5 [857 µg/ml] , 7.1 µL GFP paxillin [420 µg/ml] and 5.8 µL mCherry - Zyxin [510 µg/ml] were diluted in 100 µL of serum-free media. The Eppendorf tube's contents was then mixed with 3 µL of TurboFect™ Transfection Reagent (Thermo Scientific) and incubated for 15 minutes. The mixture was added to the dish and the cells then incubated overnight (≥16 hours) and Live-cell confocal imaging was performed at 37◦ C in 5% CO_2.

2.3.4 Cell light Early Endosomes-GFP transfection:

Cells were seeded in a 35mm ibidi dish at density of 10000 cells/mm^2 and allowed to adhere overnight. Cell light Early Endosomes-GFP reagent **(**BacMam 2.0) was added to result in a final concentration of 30 particles per cells according to the following equation:

Volume of Cell light Reagent (mL) = number of cells × desired PPC/ 1 × 10^8 Cell light particles/mL

The cells then incubated overnight (≥16 hours) and Live-cell confocal imaging (Nikon A1R confocal microscope) was performed at 37◦ C in 5% CO_2.

2.3.5 Live cell imaging:

After cells were transfected and incubated overnight, the growth medium was discarded and replaced with media containing the inhibitors depending on the experiments. A 35 mm ibidi dish was placed in the heated stage of confocal microscope (Nikon A1R confocal microscope supplied with 5 % CO_2).

To measure focal adhesion turnover, the low power excitation laser beam of 586nm and resonant scanning (to prevent bleaching and generate the necessary speed for real-time imaging of living cells) were used. The image was then monitored by taking images every 5 seconds for 10 minutes. Using ImageJ, the average life time of Zyxin was concluded by counting the time period of focal adhesion in the turnover movie (from appearance and disappearance).

In case of live co-localization, MDA-MB-231 cells were co-transfected with both mCherry-Rab5 and GFP-Paxillin or mCherry-Zyxin and GFP-Rab5. Then, both 586nm and 488nm laser channels with resonant scanning were monitored by taking images every 5 seconds for 5 minutes. Using ImageJ, a minimum of five frames of each minute (25 frames) were used to calculate the number of endosomes or focal adhesions, and the average was taken for each movie. The number of co-localizations (based on Spearman's correlation analyses) were monitored on each movie.

2.4 Immunocytochemistry:

Cells were plated in 6 well plates and allowed to attach to glass coverslips overnight. The growth medium was discarded and replaced with media containing the inhibitors depending on the experiments. Thereafter, the cells washed in PBS (phosphate buffered saline) (life technologies) and fixed for 15 min in 4% paraformaldehyde in PBS at room temperature. The cells were washed and permeabilised with PBS containing 0.5% Triton X-100 for 10 minutes. After three PBS washes, cells were blocked with PBS containing 10% goat serum for 30 min at room temperature. Cells were then incubated for 60 min at room temperature with the primary antibody which was diluted to 1:100 in PBS containing 2% goat serum. After three 5-min PBS washes, the cells were transferred into light-

protected chambers and incubated for 30–60 min at room temperature with secondary antibodies (Alexa fluor) diluted in PBS to 1:200. The coverslips were then washed and mounted on glass slides with DAPI vectashield.

2.4.1 Focal adhesion and endosomes analysis:

Once the cells were seeded on cover slips, they were immunostained as described in section 2.2.5 and subsequently cells were subjected to Nikon A1R confocal microscopy for focal adhesions and endosomes count, size determination and co-localization analysis. To analyse number and size of focal adhesions and endosomes, the fixed cells images were captured digitally using a 100X oil-immersion objective lens and Nikon confocal system software. All confocal images were taken at a resolution of 1024 × 1024 pixels. The image was moved to the level until the endosomes and focal adhesion appeared and the sequential imaging were used to prevent crosstalk between each channel. Images were then analysed using ImageJ software to calculate the mean number and size of both focal adhesions and endosomes. Firstly, Subtract Background was applied to the image with sliding paraboloid option and rolling ball (50 pixels). Then, the CLAHE (Contrast Limited Adaptive Histogram Equalization) command was run to enhance the local contrast of the image (values: block size=19, Histogram bins=256, Maximum slope=6, no mask and fast). The mathematical exponential (EXP) were applied to further minimize the background. After the brightness & contrast were adjusted, threshold was then applied to a binary image with two pixel values, 255 (white) and 0 (black) to ensure only focal adhesion or endosomes 'dots' were selected. Finally, the analyse particles command were applied to count and measure endosomes or focal adhesion according to these parameters as follows: size = 0.5-infinity and circularity = 0.00–0.99.

2.4.2 Co-localization analysis

To analyse co-localization, the fixed cells imaging were captured digitally using a 100X oil-immersion objective lens and Nikon confocal system software. All confocal images were taken at a resolution of 1024 × 1024 pixels and 400Hz and with GALVANO mode. Using ImageJ, the Alexa Fluor 488, 546 channels were split and the focal adhesion or endosomes ‘were manually selected with a ROI and analysed with Coloc2 pluginas follow:

The sperman rank correlation value was recorded.

2.5 Transferrin or Dextran uptake:

Cell lines were plated in 6 well plates and allowed to attach to glass coverslips overnight. Subsequently, when the plate became 70% confluent, full media was replaced with serum free media and incubated for 3 hours at 37°C in 95% air and 5% CO_2. Later, the media was replaced with DMSO control or inhibitors at varying concentration and incubation time at 37°C in 95% air and 5% CO_2. Upon completion of the incubation times, the media was replaced with serum free media containing 20mg/ml Transferrin conjugate or 500µg/ml of dextran conjugate for 30 minutes at 37°C in 95% air and 5% CO_2. Later, the cells were washed twice with chilled PBS, incubated with PBS containing 0.5% Triton X-100 for 10 minutes. After three PBS washes, cells were fixed with 4% paraformaldehyde in PBS and immunostained for focal adhesion Paxillin to be able to determine the cell surfaces and edges. After the Confocal images were captured at a resolution of 1024 × 1024 pixels, Z stacks (multible slice) were scanned from the top to the bottom of the slide in order to determine the uptake of transferrin. The brightness & contrast were then adjusted using ImageJ.

Finally, 3D object counter was applied and the following values were used in the size filter space: 0.1 MIN and 200 Max.

In order to analyse the transferrin uptake via measuring the fluorescence intensity, the image was moved to the level where both transferrin and paxillin focal adhesion appeared. Then, Alexa Fluor 546 channels and laser power were adjusted as the following values: HV: 64, Offset: 0 and Alexa Fluor 546nm: 6.35 for all the experiments. Using ImageJ, the region of interest was selected around the cell and the relative intensity of transferrin were quantified and subtracted from the average background fluorescence (region where no fluorescence was detected).

In order to analyse the number and size of endosomes containing dextran, the image was moved to the level until the dextran and paxillin focal adhesion appeared and the sequential imaging were used to prevent crosstalk between each channel and analysed as described in section 2.2.5.1.

2.6 Western blot:

2.6.1 Lysate preparation:

After incubation of the cell culture, the media was discarded from the T75 flask and the cells were washed twice with 5 mL chilled PBS in order to remove any dead cells. Subsequently, cells were scraped in PBS using a rubber policeman and centrifuged at 4^{o} C at 1500 rcf for 15 minutes. The pellets were then mixed with RIPA buffer (25 mM Tris HCl pH 7.6, 150 mM NaCl, 1% v/v NP-40, 1% v/v sodium deoxycholate, 0.1% v/v SDS, Thermo Fisher Scientific) containing protein inhibitor cocktail (PIC: to release cell membrane) (1:100) and passed 21 times through 19 gauge needle to shear DNA, then incubated on ice for 30 min. After 30 minute incubation, the cell lysate was transferred to sterile 1.5 ml eppendorf tube and further centrifuged at 13,000 rcf for 15 minutes. Then, the supernatants were transferred to a new eppendorf tube and kept at -20ºC until required.

2.6.2 Bradford assay:

Bradford protein assay was performed to measure the concentration of total protein in cell lysates based on an absorbance of the dye Coomassie Brilliant Blue G-250.

The Bradford assay was performed using 96 well plate format. In the first three columns, 195 µL of blank Bradford reagent was added. Whereas, in column two and three 5 µL of a range of ascending concentrations of bovine serum albumin in the following series :25 µg/ml, 125 µg/ml, 250 µg/ml, 500 µg/ml, 750 µg/ml, 1000 µg/ml, 1500 µg/ml and 2000 µg/ml were added to produce a standard curve. In the remaining wells, 5 µl of cell lysate combined with 195 µL of Bradford reagent were added. After the plate was shaken for a few minutes, the plate was placed on microplate reader to read absorbance at a wavelength of 540 nm and to obtain the concentration of protein for each well in µg/ml.

2.6.3 Protein separations:

Once Bradford assay was performed, sample lysates were diluted in 5X SDS loading buffer: 312.5 mM Tris base, 10% v/v SDS, 50% v/v glycerol (25 µL per 100 µL cell lysate) and β-mercaptoethanol (5 µL per 100 µL cell lysate). This mixture was then boiled for 5 minutes at 95^{o} C to denature proteins. SDS and reducing agent (β-mercaptoethanol) are used to reduce disulphide bonds causing proteins unfold into linear polypeptide chains. The protein and sample buffer mix were loaded into each well of an SDS gel (5% stacking gel and 10 % or 12 % resolving gel) to separate the proteins based on their molecular weight. The gel was run at a constant voltage of 150V for 1 h at room temperature.

2.6.4 Protein transfer and incubation:

Once the protein separation was complete, the SDS gel was transferred to transfer buffer for 20 minutes. An appropriate size of PVDF (polyvinylidene difluoride) membrane (transfer membrane was activated by incubation in methanol for 30 seconds and then washed in destilled water), and six filter papers, after been submerged in transfer buffer, and the gel were placed on the semi-dry transfer machine as illustrated in the figure 2.1. Once all bubbles were removed from SDS- gel containing filters and membrane, an electrical current was applied to transfer the SDS- gel at 250V, 0.05A for 1.5 hours.

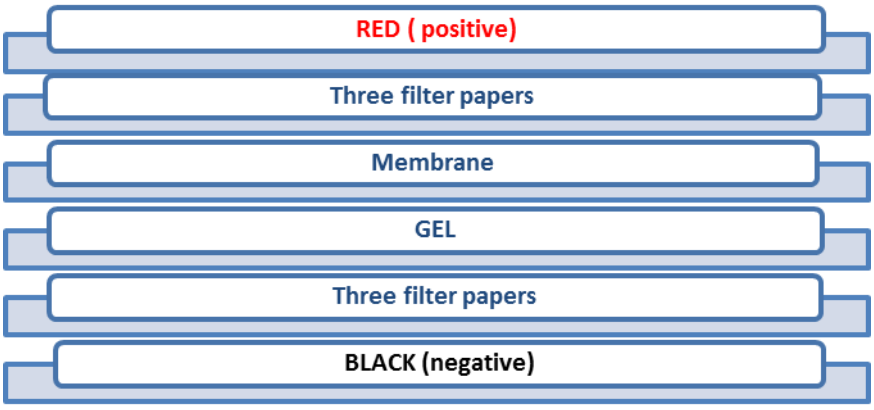

Figure 2. 1 : Illustration of the gel-blotting sandwich procedure

After the transfer was completed, the PVDF membrane was incubated in blocking solution (5% of dry milk dissolved in Tris-Buffered Saline Tween (TBST)) for one hour at room temperature. After blocking nonspecific binding sites, the membranes were washed three times in TBST for 10 min (10 minute each time) and incubated with primary antibody diluted in 5% of dry milk or BSA dissolved in TBST (1:1000) for overnight at 4^{o}C with agitation. Then, the membranes were washed three times in TBST for 10 min (10 minute each time) and incubated with HRP-conjugated antibody diluted in 1% of dry milk (1:2500) for 1 hour at room temperature with agitation. Once the secondary antibody incubation was complete, membranes were washed three times with TBST (10 minute each time). An ECL solution (western blotting detection reagents) was prepared, added to the membrane, and incubated for 5 min. Finally, the membrane was exposed to X-ray films, and the films recorded in a LAS 4000 mini machine and the image taken using Image Quant TL software.

2.6.5 Quantify western blot bands:

After bands were visualized on the membrane, the relative intensity of each protein band was quantified and corrected with their relevant loading control (β-actin total) using Image Quant LAS4000min (GE Healthcare). Finally, the results were expressed as mean ± standard error (SE) from at least three independent experiments.

2.7 Statistical analysis:

Data obtained by Image software were statistically analysed by GraphPad prism 5 software (GraphPad software, San Diego, CA). Two-tailed unpaired student's t test were used to test two variables and one-way analysis of variance (ANOVA) for three or more variables. Tukey's post hoc were conducted to compare treatment with each other and Dunnett's post-hoc test were used to compare each treatment to a single control (DMSO). Two-way-ANOVA with Bonferroni post-hoc test were used in starvation experiments where the cells subjected to two variances (time and distance). All results were obtained

from at least three independent experiments in triplicate (n=3). A value of p-value ≤ 0.05 was considered statistically significant.

Chapter 3: Identifying role(s) for endocytosis in cell migration

3.1 Introduction

In this chapter, three different cell lines originating from different tissues were used to establish a better understanding of endocytosis in cell migration and also confirm the effect(s) of endocytosis inhibitors in endocytosis and cell migration.

Inhibitors of endocytosis pathways including Dynamin pathways inhibitors (Dynasore), clathrin pathways inhibitors (Pitstop2), caveolae pathways inhibitor (Filipin III) and micropinocytosis pathways inhibitor (Amiloride) have been the main focus in this chapter (Figure3.1). The first part of this Chapter is focused on examining the effects of endocytosis inhibitors on ligand uptake. Transferrin and Dextran were the two ligands used in these experiments.

The second part of this Chapter is focused on the effect of these inhibitors on the endocytosis compartments.

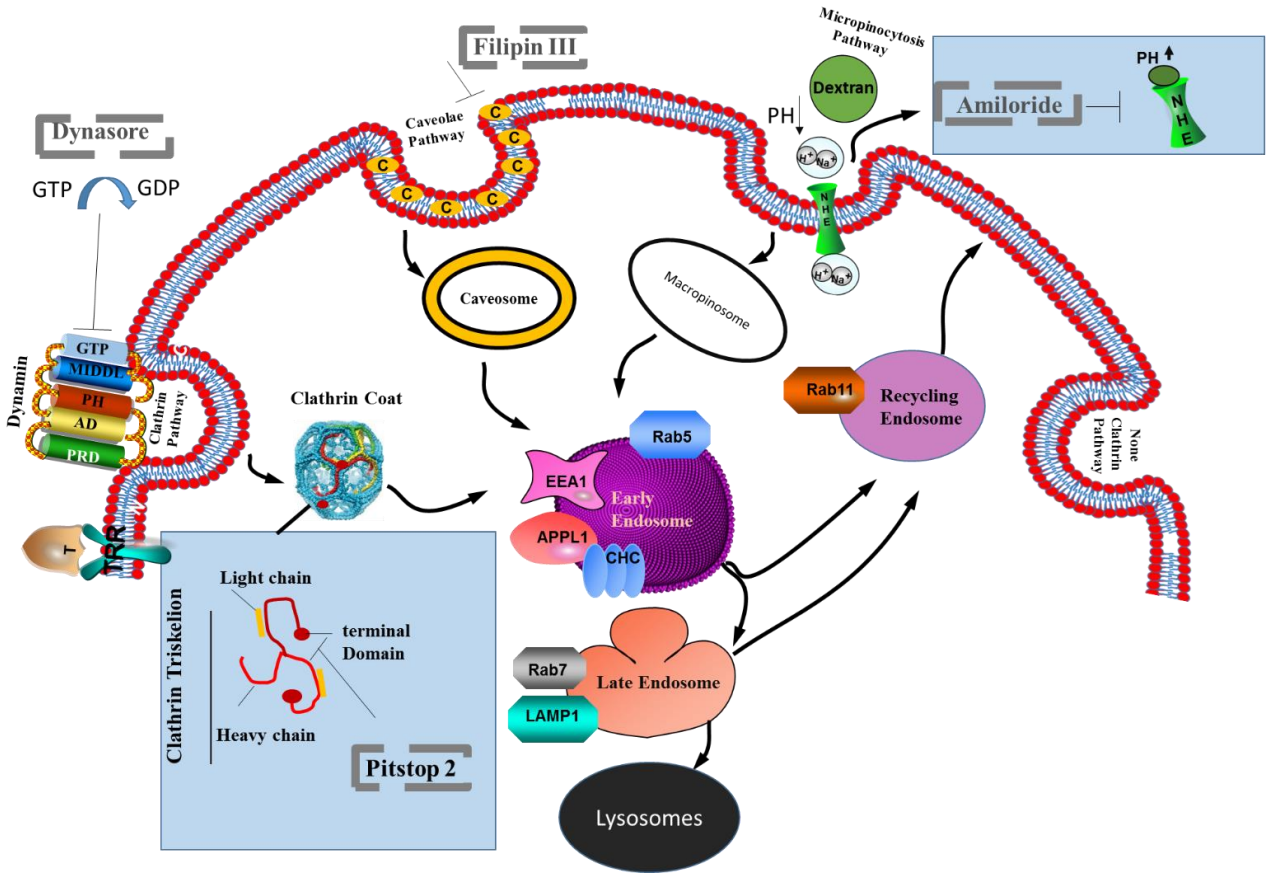

Figure 3.1 Schematic summary representing four endocytosis pathways and chemical inhibitors used in this project.

The internalized cargo are transported from different endocytosis pathways (clathrin, caveolae, micropinocytosis and others) into early endosomes to late endosomes or recycling endosomes. In clathrin pathway, the clathrin coated vesicle are defined before the cargo transported to EE. Similarly, caveosome and macropinsome are defined for caveolae pathways and micropinocytosis, respectively. Dynasore inhibitors block the GTPase activity of Dynamin. Pitstop 2 inhibits the clathrin coat vesicle formation by inhibiting the terminal domains. Amiloride 5-(N-ethyl-N-isopropyl) block the Na + /H+ exchange. Filipin III inhibitor inhibits caveolae by extracting cholesterol from cells. Finally, each endocytotic compartments are defined by markers. Rab5, EEA1, APPL1 and clathrin Heavy chain are constitute early endosomes markers, whereas LAMP1 and Rab7 are late endosomal compartments markers. Finally, Rab4 and Rab11 are recycling endosomes markers.

The third part of this Chapter examines the effect of endocytosis on cell migration. Four different models for investigating cell migration have been wound healing assay, cell tracking assays, cell tracking assays on different cell surfaces and subcellular analysis of endosome localization. Wound healing assays were used to study the role of endocytosis in collective cell migration and were carried

out using two different cell lines, MDA-MB-231 breast cancer cell line and SK-MEL-28 melanoma cell line. These two cell lines were chosen because they displayed invasive properties and different styles of migration. The MDA-MB-231 cells migrate individually whereas SK-MEL-28 cell lines remain as a group and migrate collectively. Cell tracking assays were used to study the effect of endocytosis inhibition on individual cell migration and carried out in MDA-MB-231 breast cancer cells and HT1080 fibrosarcoma cancer cells, due to the fact that these two cell line both display invasive properties and have a similar style of migration.

Several studies have demonstrated that processes such as cell polarization, attachment to surfaces and response to signals can be different on diverse ECM and that may influence cell motility (Kim et al., 2011) (Doyle et al., 2013). More importantly, on extracellular surfaces, many cells use an additional step to migrate via degradation of the extracellular matrix using structures such as invadopodia. Thus, further analysing of this aspect of migration may help to identifying possible link between endocytosis and cell migration.

The final model for investigating cell migration has been subcellular endosome localization. The assessment of endosome localization was carried out by monitoring the endosome localization between leading and trailing edges using fixed and live cell imaging of MDA-MB-231 cells.

After studying the effect of these inhibitors on endocytosis and cell migration, it was decided to extend this study to other ways of targeting endocytosis rather than blocking endocytotic pathways. These ways include prolonged starvation of cells by culturing them in low FBS and low glucose media.

3.2 Hypothesis

Endocytosis pathways increase cell migration by regulating the early endosomal compartments (EEA1 and Rab5).

3.3 Results

3.3.1 Effect of inhibitors of endocytotic pathways on Ligand uptake:

To better understand the relationship between endocytosis pathways and cell migration, it is important to validate the effect of each endocytotic pathway inhibitor on various endocytotic marker uptake. Two ligand uptake markers, Transferrin and Dextran, markers of clathrin dependent endocytosis and fluid marker of micropinocytosis respectively, were examined in MDA-MB-231 or HT1080 cells.

Each cell line was seeded in 6 well plate and allowed to attach to the bottom of the plate overnight. Subsequently, when the plate became 70% confluent, full media was replaced with serum-free media and incubated for 3 hours. Later, the media was replaced with four endocytosis inhibitors at varying concentration and incubation times (Pitstop2 25µM for 15 minutes, Amiloride 50 µM for 30 minutes, DMSO for 30 minutes and Dynasore either at 20 µM or 80 µM for 30 minutes. In the case of Filipin III, the cells were incubated with 16 µM for 24 hours and media replaced with serum-free media containing the inhibitor.

Upon completion of the incubation times, the media replaced with serum-free media containing 20mg/ml Transferrin conjugated to Alexa Fluor 546 or 500µg/ml of dextran conjugated to fluorescein for 30 minutes. Later, the cells were fixed with paraformaldehyde and immunostained for the focal adhesion protein Paxillin to be able to determine the cell surfaces and edges. The effect of four different endocytotic pathway inhibitors on transferrin uptake was measured by selecting the region of interest (ROI) around the cell membrane of individual cells to measure the means of fluorescence intensity. The background intensity was subtracted for each image.

3.3.1.1 Effect of endocytic pathways inhibitors on Transferrin Uptake:

In these experiments, both clathrin dependent endocytosis pathway inhibitors (Dynasore and Pitstop2) inhibited transferrin uptake. Dynasore at high concentration (80 µM) or even at lower concentration (20µM) inhibited the uptake of transferrin in both cell lines tasted. This is supported by Figures 3.2 and 3.3 which showed the average intensity of Transferrin uptake in cells treated with Dynasore 20 µM or 80 µM was 183± 8.73 per/cell (* $p<0.05$) and 153.7 ± 17.84 per/cell (** $p<0.01$), respectively, Compared with 249 ± 13.75 per/cell in control (Figure3.2 B).

Similarly, the Pitstop2 inhibitor at 25 µM for a period of 15 minutes was sufficient to obtain a maximal inhibition of Transferrin uptake in MDA-MB-231 cells. As shown in Figure 3.2 and 3.3 the average intensity of Transferrin in cells treated with Pitstop2 was 67.6 ± 9.73 per/cell (*** $p<0.001$) compared with 249 ± 13.75 per/cell in the control. Interestingly, the micropinocytosis inhibitor Amiloride also showed a significant effect on transferrin uptake with average intensity 108± 19.82 per/cell (** $p<0.01$) compared to 249 ± 13.75 per/cell in the control (Figure3.2 A and B).

To further confirm the effect of clathrin dependent endocytosis inhibitors in MDA-MB-231, the number of transferrin containing endosomes was measured by quantifying the number of transferrin obtained from 3D z-stake video images. The quantification analysis revealed that both inhibitors significantly decreased the mean number of endosomes containing transferrin. As shown in Figure 3. 2 C the average number of endosome containing transferrin in cells treated with Dynasore 20 µM were 66.07± 3.12 per/cell (*** $p<0.001$), Dynasore 80 µM were 52.30 ± 5.29 per/cell (*** $p<0.001$) and Pitstop2 25 µM were 25.47± 5.17 per/cell (*** $p<0.001$) compared with 105.5 ± 2.143 per/cell in untreated cells.

On the other hand, Filipin III even with a long incubation period of 24 hours did not show any significant effect on transferrin uptake and its average intensity were 444 ± 50.68 per/cell $p>0.05$ compared with 402.9± 75.38 per/cell in control in MDA-MB-231 (Figure3.2 D).

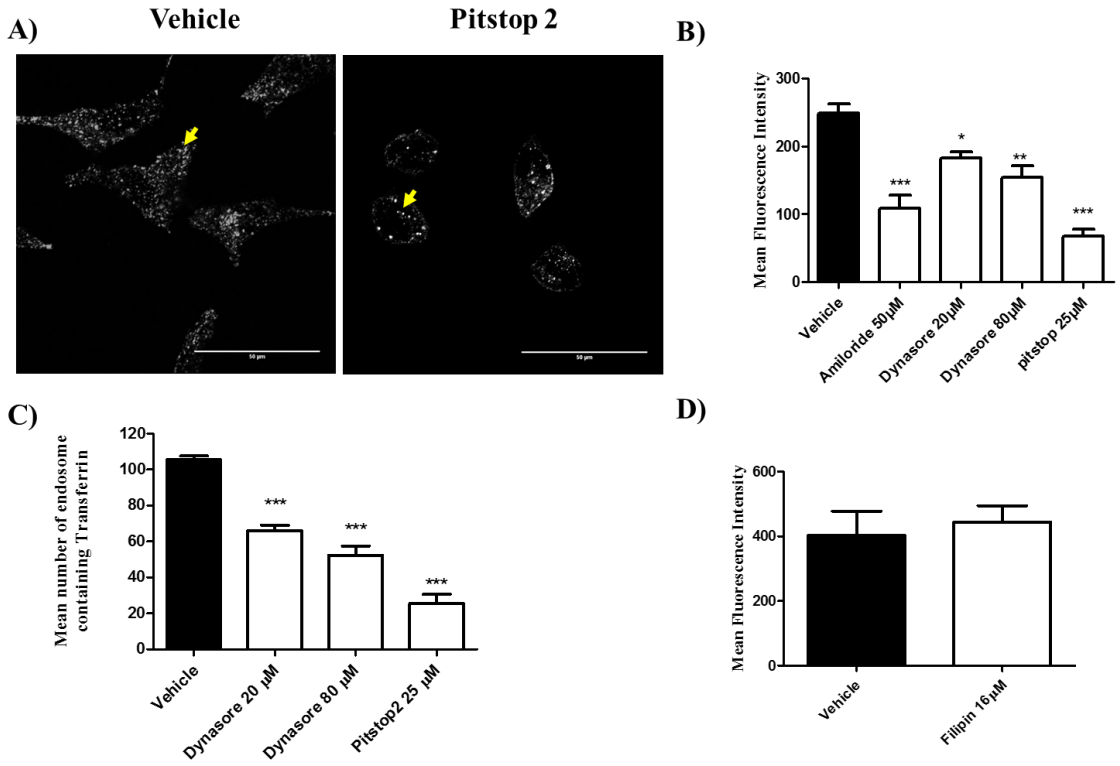

Figure 3. 2 Effect of endocytic pathways inhibitors on endosome containing transferrin and transferrin uptake in MDA-MB-231

MDA-MB-231 cells were serum starved for 3h, treated with vehicle (control) or different endocytic pathways inhibitors at different times (Amiloride 50 µM for 30 minutes, Dynasore 20 µM or 80 µM for 30 minutes, Pistop2 25 µM for 15 minutes and Filipin III 16 µM for 24 hours) prior incubation with 25 µg/ml conjugated transferrin for 30 minutes. Cells were subsequently fixed and subjected to confocal imaging. **A:** Confocal images showing the effect of untreated cells (DMSO) and treated cells (Pitstop2 25µM) on Transferrin uptake in MDA-MB-231. Yellow arrow indicates the amount of transferrin uptake. Scale bar is 50µm. **B:** the transferrin uptake measured by florescence intensity and one way ANOVA with Dunnett's Multiple Comparison were used to compare each treatment with the control. **C:** the endosome containing transferrin was analysed by quantifying the number of transferrin obtained from 3D z-stake video images and one way ANOVA with Dunnett's Multiple Comparison were used to compare each treatment with the control. **D**: Effect of Filipin III inhibitor on transferrin uptake measured by fluorescence intensity and T test was used. Each graph represents the mean ± standard error of three independent experiments, in each experiment at least 20 cells were analysed for each treatment. Statistical significance differences were accepted at * $p<0.05$ ** $p<0.01$ *** $p<0.001$.

To further study the effect of these inhibitors on transferrin uptake, HT1080 cell lines were examined. Similarly to what was observed in MDA-MB-231 cells, Dynasore, Pitstop2 and Amiloride inhibitors significantly decreased transferrin uptake. As shown in Figure 3.3 A and B, mean fluorescence intensity of transferrin in cells treated with Amiloride 50 µM, Dynasore 20 µM, Dynasore 80 µM, and Pitstop2 25 µM were 86.86 ± 20.99 (* $p<0.05$), 66.33 ± 10.45 (** $p<0.01$), 55.33±12.85 (** $p<0.01$) and 58.28 ± 1052 (** $p<0.01$) per/cell, respectively, was reduced compared with 181.8 ± 27.17 in untreated cells.

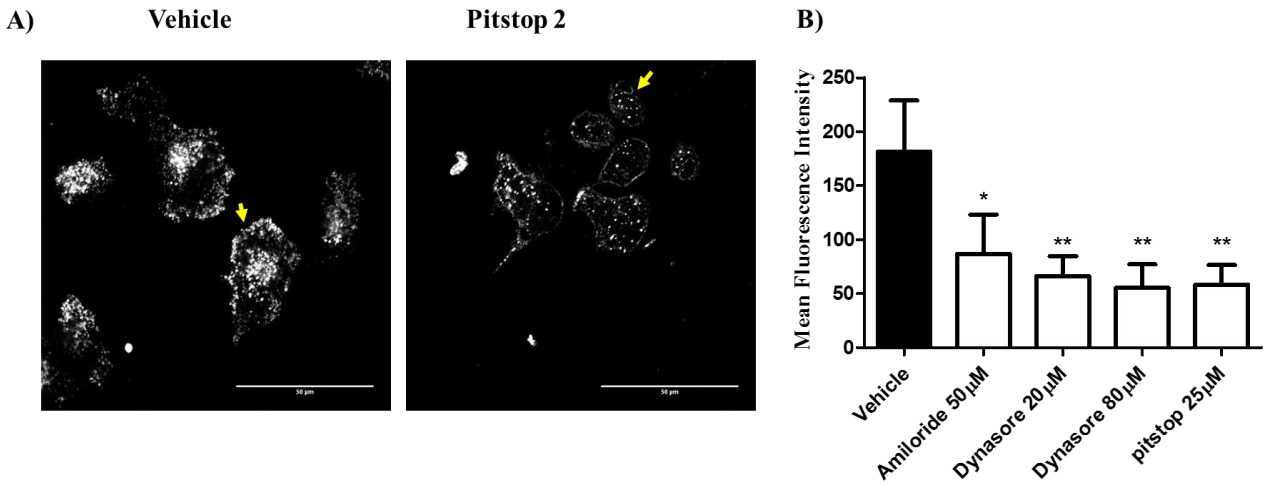

Figure 3. 3 Effect of endocytotic pathways inhibitors on transferrin uptake of HT1080.

HT1080 cells were serum starved for 3h , treated with vehicle (control) or different endocytic pathways inhibitors at different times (Amiloride 50 µM for 30 minute, Dynasore 20 µM or 80 µM for 30minutes and Pistop2) and incubated with 25 µg/ml conjugated transferrin For 30 minutes. Cells were then fixed and subjected to confocal imaging. **A:** Confocal images showing the effect of untreated cells (Vehicle) and treated cells (Pitstop2 25µM) on Transferrin uptake in HT1080. Yellow arrow indicates the amount of transferrin were uptake. Scale bar is 50µm. **B:** the transferrin uptake measured by florescence intensity and one way ANOVA with Dunnett's Multiple Comparison were used to compare each treatment with the control. Graph represents the mean ± standard error of three independent experiments, in each experiment at least 100 cells were analysed. Statistical significance differences were accepted at * $p<0.05$ and ** $p<0.01$.

3.3.1.2 Effect of endocytotic pathways inhibitors on dextran uptake:

In this experiment, dextran uptake was examined by analysing the number and size of endosomes containing dextran per cell. Three inhibitors were involved and carried out only in HT1080. As shown in Figure 3.4 , Amiloride (an inhibitor of fluid uptake), significantly reduces the average number of endosomes containing dextran which was 13.06 ± 3.30 per/cell (* $p<0.05$), compared to 24.52± 2.81 per/cell in control cells. Interestingly, the Pitstop2 inhibitors strongly reduced the average number of endosomes containing dextran to 6.65 ± 2.82 per/cell (** $p<0.01$) compared to 24.52± 2.81 per/cell to control conditions, suggesting that pistop2 interferes with micropinocytosis. A surprising observation was that Dynasore induced the uptake of dextran by almost two fold to 44.54 ± 3.0 per/cell (* $p<0.05$) compared to control 24.52± 2.81.Notably, the mean average size of endosomes containing dextran were similar or not affected between treatment or none treatment conditions (Figure 3.4C).

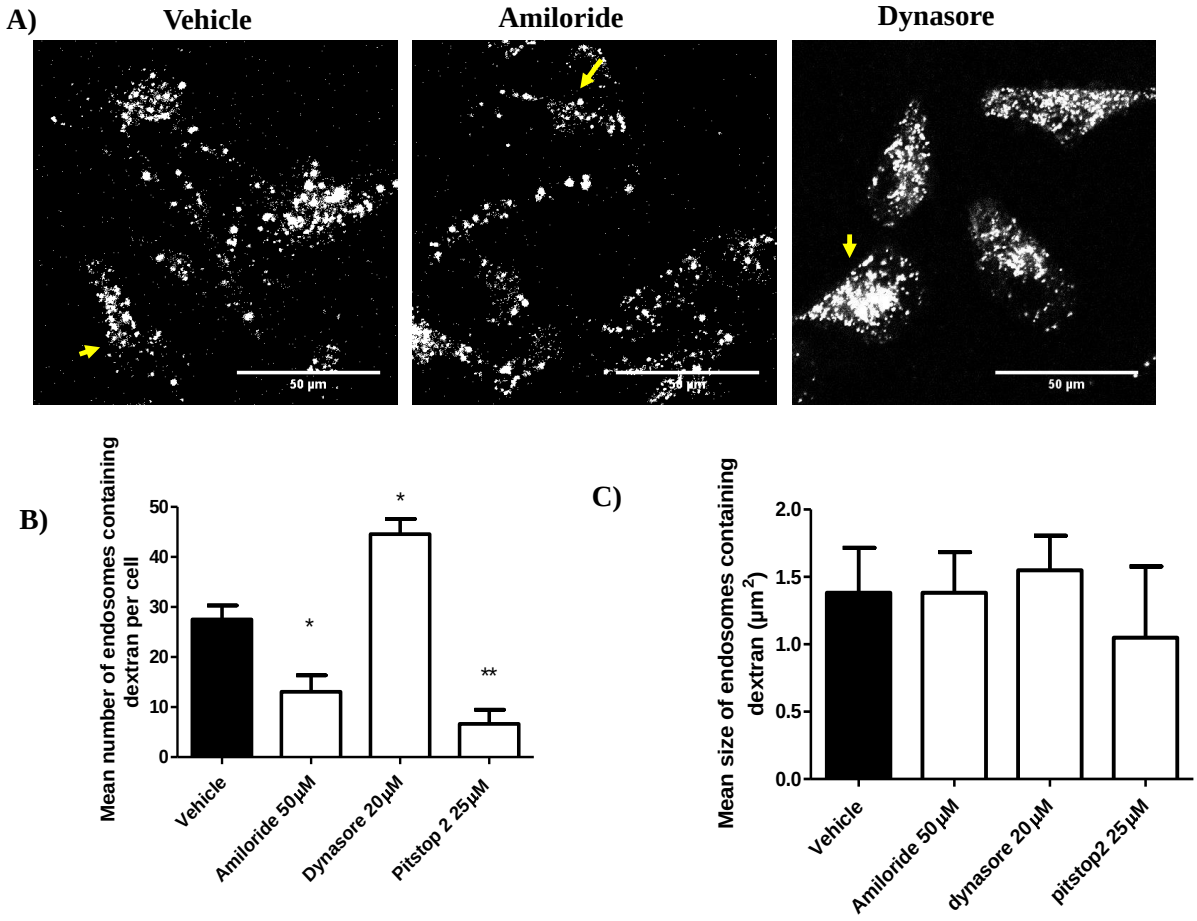

Figure 3. 4 Effect of different endocytotic inhibitors pathways on endosomes containing dextran number and size of HT1080

Cells were serum starved for 3h, treated with Vehicle (control) or different endocytotic pathway inhibitors at incubation times (Amiloride 50 µM for 30 minutes, Dynasore 20 µM or 80 µM for 30 minutes and Pitstop2 25 µM for 15 minutes and incubated with 500 µg/ml Dextran, Fluorescein, 10,000 MW, Anionic, Lysine Fixable for 30 minutes. Cells were subsequently fixed and subjected to confocal imaging. **A:** Confocal images showing the effect of untreated cells and different endocytotic pathways inhibitors on endosomes containing dextran number and size of HT1080. Yellow arrow indicates the amount of dextran uptake. Scale bar is 50µm. **B** and **C**) graphs show the effect of endocytotic inhibitors on endosomes containing dextran number and size. One way ANOVA with Dunnett's Multiple Comparison Test were used to compare each treatment with the control. Graphs represent the mean ± standard error of three independent experiments, in each experiment at least 80 cells were analysed. Statistical significance differences were accepted at * $p<0.05$ ** $p<0.01$.

3.3.2 Effect of inhibitors of endocytotic pathways on Early Endosomal proteins

Early Endosomal proteins play an important role in fission, transport and maturation of vesicles that contain plasma membrane receptors and sort them for transport (Gruenberg et al., 1989). In addition to this, they regulate signalling pathways by recruiting endocytotic adaptors or kinases that have been associated with endosome function (Macia et al., 2006). Although, many internalised pathways exist, the early endosomal proteins are considered to be the centre point for most of these pathways.

The previous results of this chapter showed that treatment with Dynasore or Pitstop2 inhibits the clathrin dependent endocytosis of transferrin. However, they also seemed to have an effect on the micropinocytosis pathway by either stimulating or inhibiting it, respectively. It is possible that this effect could be a result of the inhibitors impairing the function of the early endosomal proteins and thus modulating transferrin trafficking into or from the early endosome. To test this possibility, the expression of three early endosomal markers were examined by western blot analysis. These markers are Early Endosome Antigen 1 (EEA1), Rab5, and APPL1 also with Clathrin Heavy Chain 1 (CHC1). Thus, the MDA-MB-231 cells were grown in T75 flasks and allowed to attach to the bottom of the flask overnight. Subsequently, when the flask became 70% confluent, cells were treated with 20 µM Dynasore inhibitor for 30 minutes or 25 µM Pitstop2 inhibitors for 15 minutes or DMSO as control. Finally, cells were lysed at the end of the incubation time and subjected to western blot analysis. The protein expression was performed by measuring the band intensity of protein normalised to β-actin. The expression were expressed as percentage to the relevant loading control.

3.3.2.1 Effect of inhibitors of endocytotic pathways on Early Endosome Antigen 1(EEA1).

Western blot experiments were employed on MDA-MB-231 cells to investigate the effect of Dynasore or Pitstop2 on Early endosome antigen 1 protein expression.

The band density in Figure 3.5 A shows the expression of EEA1 protein in treated MDA-MB-231 cells, with β Actin used as loading control. The analysed data showed that the MDA-MB-231 cells that were treated with Dynasore inhibitors significantly decreased the expression of EEA1 from 92.68 ± 2.664 to 61.14 ± 7.662 (* $p<0.05$) (EEA1/ β-actin) in comparison with untreated cells. Similarly, pistop2 inhibitor significantly decreased the expression of EEA1 from 92.68 ± 2.664 to 34.12 ± 6.890 (*** $p<0.001$) compared with untreated control Figure 3.5 C. This observation is supported by Figure 3.5 A which shows the band intensity for each sample.

To further confirm and characterize the effect of these inhibitors on early endosome antigen, immunocytochemistry for endosomes containing EEA1 number and size was performed. The results show that both inhibitors significantly decreased the number of endosomes containing EEA1: Dynasore 24.77 ± 4.05 (* $p<0.05$) and Pitstop2 14.17 ± 1.58 (*** $p<0.001$), compared with 43.63 ± 2.765 in control cells. Interestingly, in the presence of Dynasore or Pitstop2, the mean size of endosomes containing EEA1 was significantly increased to 1.09 ± 0.10 (* $p<0.05$) and 1.72 ± 0.2 (** $p<0.01$), respectively, and produces large vesicles (illustrated by white arrow), compared with 0.46 ± 0.08 in control cells (Figures 3.5 B and D). In summary, the results demonstrate that the number of endosomes containing EEA1 and the expression of EEA1 were down regulated after treatment with dynasore or Pitstop2 and the down regulation correlates with morphological change in size. However, both inhibitors significantly increase the size of endosomes containing EEA1. This suggest that the depletion of EEA1 is clathrin and dynamin dependent. Also, it may suggest that these inhibitors impair the maturation of endosomes and thereby affecting internalization pathways.

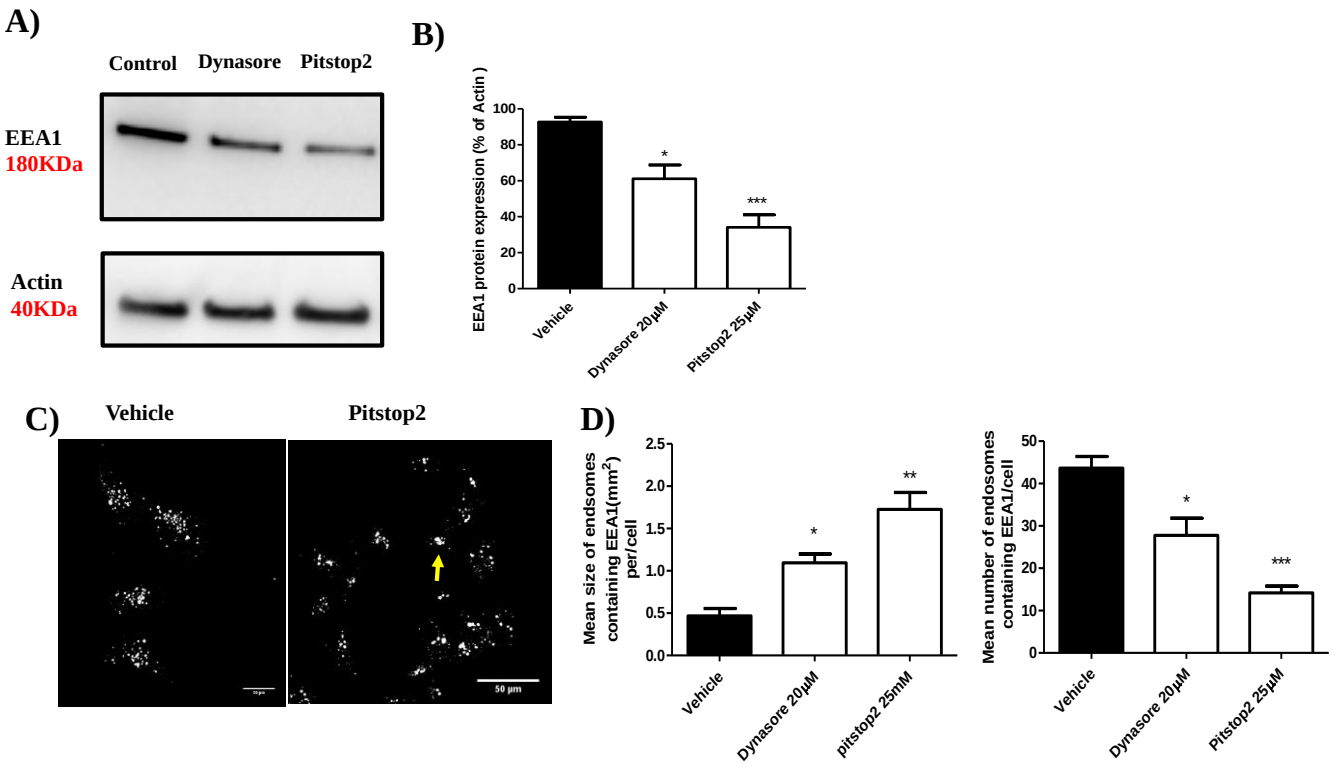

Figure 3. 5 Effect of endocytotic pathways inhibitors on EEA1 expression, number and size in MDA-MB-231.

MDA-MB-231 cells were treated with Vehicle (control) or different endocytotic pathways inhibitors at different times (20 µM Dynasore for 30 minutes and 25 µM Pistop2 for 15 minutes). Cells were then lysed and subjected to Western blot analysis (A and B) or fixed and subjected to immunocytochemistry stain (C and D). A: Western blot images showing the effect of untreated cells and different endocytotic pathway inhibitors on EEA1 expression. B: Graph shows the expression of EEA1 as band intensity normalized to β-actin and expressed as percentage of the control. C: Confocal images showing the effect of untreated cells and treated cells with pitstop2 on endosomes containing EEA1 number and size. In each experiment at least 60 cells were analysed. Yellow arrow illustrates the large-coated vesicle. Scale bar is 50µm. D: graphs show the effect of Dynasore and pitstop2 inhibitors on endosomes containing EEA1 number and size.

One way ANOVA with Dunnett's Multiple Comparison Test were used to compare each treatment with the control. Graphs represent the mean ± standard error of three independent experiments. Statistical significance differences were accepted at * $p<0.05$, ** $p<0.01$ and ***$p<0.001$.

3.3.2.2 Effect of inhibitors of endocytotic pathways on Rab5A.

Since the observed decrease in EEA1 expression and number of EEA1 containing endosomes inversely correlated with increased size, this suggested an effect on regulation of endosome maturation. Rab5 is another early endosome marker that has been shown to be an essential protein in controlling endosome maturation (Jovic et al., 2010). Therefore, it was thought to investigate the effect of Dynasore or Pitstop2 on Rab5 protein expression. Thus, western blot experiments were performed using the same cell line, MDA-MB-231.

The band density in Figure 3.6 A shows the expression of Rab5 protein in treated MDA-MB-231 cells, with β Actin used as loading control. The analysed data showed that Dynasore did not lead to a decrease in expression of Rab5 42.82 ± 4.3 $p > 0.05$ compared with 51.07 ± 1.349 in untreated control. However, Pitstop2 inhibitor significantly decreased the expression of Rab5 to 27.33 ±3.94 (** $p<0.01$) compared with 51.07 ± 1.34 in untreated control Figure 3.6 B. This observation is supported by Figure 3.6A which shows the band intensity for each sample.

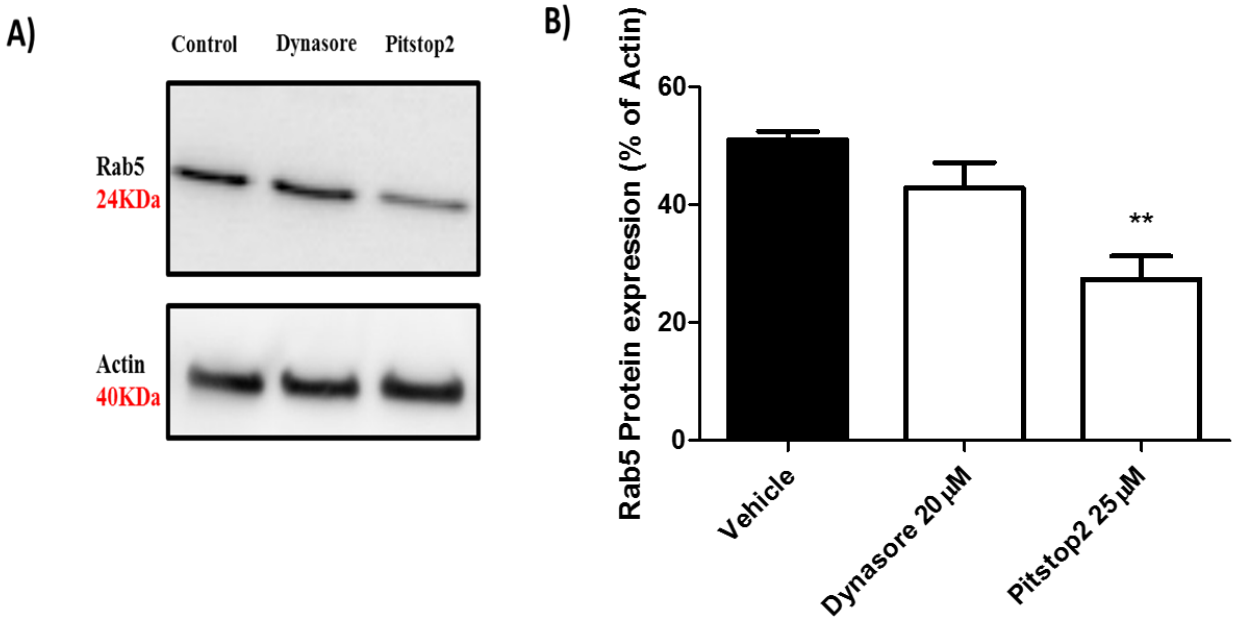

Figure 3. 6 Effect of endocytotic pathways inhibitors on Rab5 expression in MDA-MB-231.

MDA-MB-231 cells were treated with Vehicle (control) or different endocytotic pathways inhibitors at different times (20 µM Dynasore for 30 minutes and 25 µM Pistop2 for 15 minutes). Cells were then lysed and subjected to Western blot analysis. **A:** Western blot images showing the effect of untreated cells and different endocytotic pathways inhibitors on Rab5 expression. **B:** Graph shows the expression of Rab5 as band intensity normalized to β-actin and expressed as percentage of the control. One way ANOVA with Dunnett's Multiple Comparison Test were used to compare each treatment with the control. Graph represents the mean ± standard error of three independent experiments. Statistical significance differences were accepted at ** $p<0.01$.

3.3.2.3 Effect of endocytotic pathways inhibitors on Adaptor protein phosphotyrosine interacting with PH domain and Leucine Zipper 1 (APPL1):

Having established that both endocytotic inhibitors altered early endosomal markers (EEA1 and Rab5), the question was raised whether these inhibitors alter other early endosome markers such as APPL1. Therefore, Western blot experiments were carried out using MDA-MB-231 to investigate the effect of Dynasore or Pitstop2 on APPL1 protein expression.

The band density in Figure 3.7 A shows the expression of APPL1 protein in treated MDA-MB-231 cells, with β Actin used as loading control. The analysed data showed that both inhibitors did not affect the expression of APPL1. Dynasore: 43.58 ± 8.86 $p > 0.05$, Pitstop2: 52.88 ± 4.58 $p > 0.05$and control: 57.66 ± 10.96. This observation is supported by Figure 3.7 B which shows the band intensity for each sample.

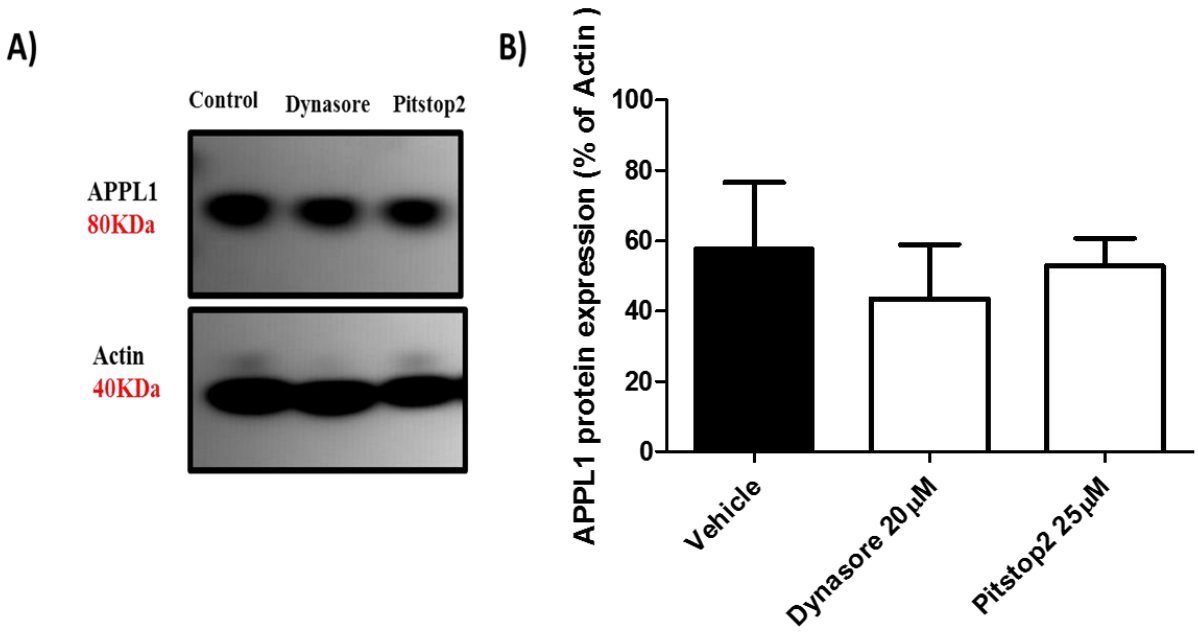

Figure 3. 7 Effect of different endocytotic inhibitors on APPL1 expression of MDA-MB-231

MDA-MB-231 cells were treated with Vehicle (control) or different endocytotic pathways inhibitors at different times (20 µM Dynasore for 30 minutes and 25 µM Pistop2 for 15 minutes). Cells were then lysed and subjected to Western blot analysis. A: Western blot images showing the effect of untreated cells and different endocytotic pathways inhibitors on APPL1 expression. B: Graph shows the expression of APPL1 as band intensity normalized to β-actin and expressed as percentage of the control. One way ANOVA with Dunnett's Multiple Comparison Test were used to compare each treatment with the control. Graph represents the mean ± standard error of three independent experiments.

3.3.3 Effect of inhibitors of endocytotic pathways on Clathrin Heavy Chain 1 (CHC1)

Having confirmed that inhibiting of endocytosis by Dynasore and Pitstop2 impaired the function of early endosomal markers EEA1 and Rab5, the question was raised whether these inhibitors alter clathrin protein levels, thus CHC1 protein expression was studied.

The band density in Figure 3.8 A shows the expression of CHC1 protein in treated MDA-MB-231 cells, with β Actin used as loading control. The analysed data showed that the expression of CHC1 was not affected by both inhibitors. Dynasore: 60.48 ± 5.09 $p > 0.05$, Pitstop2: 65.44 ± 4.73 $p > 0.05$ and control: 62.96 ± 7.72. This observation is supported by Figure 3.8 B which shows the band quantification for each sample.

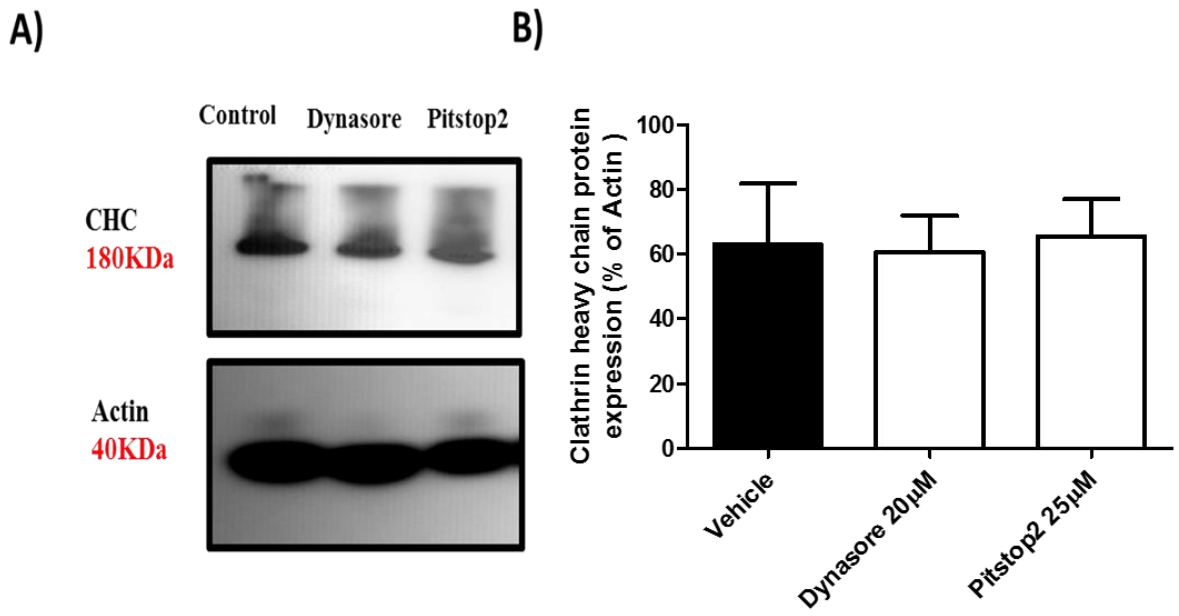

Figure 3. 8 Effect of different endocytotic inhibitors on CHC expression of MDA-MB-231

MDA-MB-231 cells were treated with Vehicle (control) or different endocytotic pathways inhibitors at different times (20 µM Dynasore for 30 minutes and 25 µM Pistop2 for 15 minutes). Cells were then lysed and subjected to Western blot analysis. A: Western blot images showing the effect of untreated cells and different endocytotic pathways inhibitors on CHC expression. B: Graph shows the expression of CHC as band intensity normalized to β-actin and expressed as percentage of the control. One way ANOVA with Dunnett's Multiple Comparison Test were used to compare each treatment with the control. Graph represents the mean ± standard error of three independent experiments.

3.3.4 Effect of inhibitors of endocytotic pathways on Lysosomal associated membrane protein 1 (LAMP1)

The previous data demonstrated that both Dynasore and Pitstop2 inhibitors impaired the function of early endosome proteins and resulted in an enlargement of endosomes. The abnormality in endosome size may indicate the possibility that these inhibitors impair the late endosome function that is associated with lysosomal degradation. To test this possibility, the effect of Dynasore or Pitstop2 on LAMP1 protein expression were examined. The analysed data showed that no significant effect of either Dynasore or Pitstop2 on LAMP1 expression Figure 3.9. Dynasore: 110 ± 12.76 $p > 0.05$, Pitstop2: 106.7 ± 5.88 $p > 0.05$ and control: 94.02 ± 13.92. This observation is supported by Figure 3.9 A and B which shows the band intensity for each sample.

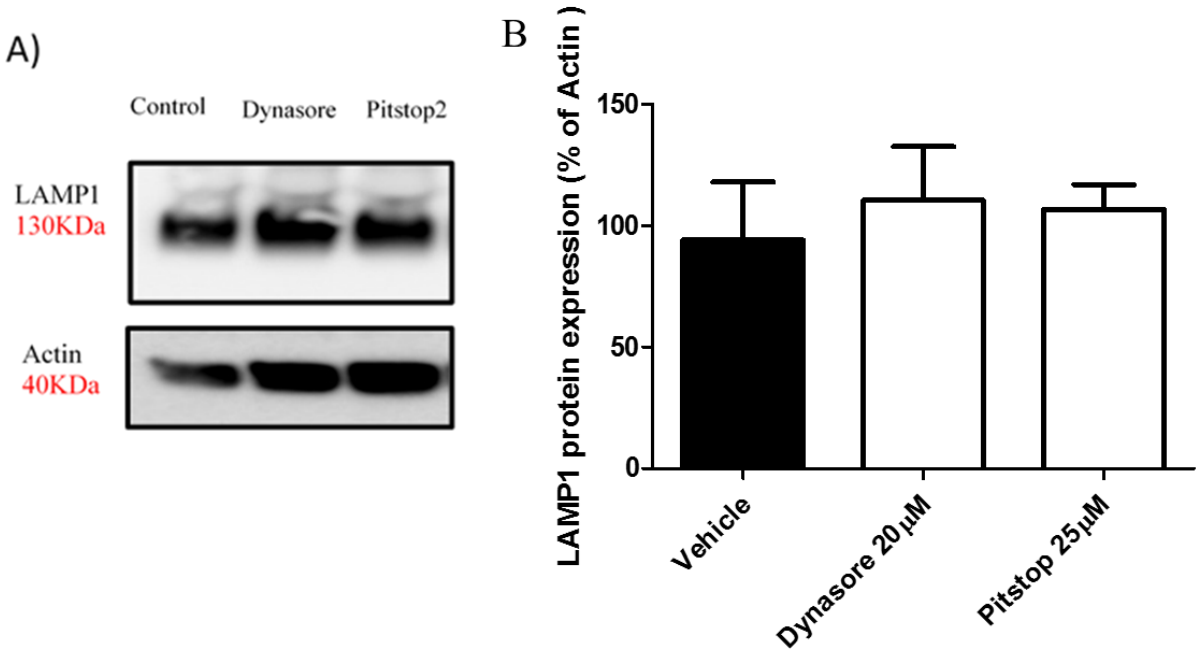

Figure 3. 9 Effect of different endocytotic inhibitors on LAMP1 expression in MDA-MB-231

MDA-MB-231 cells were treated with Vehicle (control) or different endocytotic pathways inhibitors at different times (20 µM Dynasore for 30 minutes and 25 µM Pistop2 for 15 minutes). Cells were then lysed and subjected to Western blot analysis. A: Western blot images showing the effect of untreated cells and different endocytotic pathways inhibitors on LAMP1 expression. B: Graph shows the expression of LAMP1 as band intensity normalized to β-actin and expressed as percentage of the control. One way ANOVA with Dunnett's Multiple Comparison Test were used to compare each treatment with the control. Graph represents the mean ± standard error of three independent experiments.

3.3.5 Role of endocytosis on Cell Migration

It was demonstrated that some endocytotic inhibitors were able to effectively block the endocytosis uptake in both MDA-MB-231 and HT1080 cells lines. In addition, Dynasore or Pitstop2 are able to reduce either the expression of rab5 or number and size of endosomes containing EEA1 and thus seem to affect the endosome trafficking. Therefore, the possible involvement of endocytosis in cell migration was investigated. To test this possibility, various aspects of migration were examined. The first aspect was to test the effect of endocytotic pathways inhibitors on cell motility using two techniques. These techniques include collective migration using a wound healing assay and tracking individual cell migration in plastic or different surfaces using time lapse microscopy. In each technique, two different cancer cell types that originate from different histological organs were examined to establish if this a conserved mechanism across different tissues. The second aspect was to study the role of endocytosis in cell direction by visualization of endosomes on leading and trailing edges using fixed and live cells. The final part was to hypothesize whether the prolonged starvation can increase cell movement in order for the cells to find high nutrient areas and whether this increased movement will increase endocytosis when consuming the nutrients.

3.3.5.1 Effect of endocytotic inhibitors on collective or individual cell migration in MDA-MB-231

To examine whether or not endocytotic pathways inhibitors are required for collective cell migration, a wound-healing assay was performed. MDA-MB-231 cell line was plated on a 6-well-plate and incubated for 48 hours. The confluent cell layers were then treated with DMSO or four endocytotic inhibitors at varying concentrations and incubation times (Pitstop2 25μM for 15 minutes, Amiloride 50 μM for 30 minutes, Filipin III 16 μM for 24 hours, Dynasore 20 μM for 30 minutes with 20μM DMSO for 30 minutes). After wounding the confluent cell layer, the wound closure was captured at 0 and 18 hours in MDA-MB-231. The results of post-scratch analysis show that inhibition of

endocytosis significantly reduces the rate of epithelial cell migration during wound healing in cells treated with either Dynasore or Pitstop2. As shown in Figure 3.10 A and B, the wound on treated cells remained open, while in untreated cells the wound closed completely. In contrast, both inhibitors, Amiloride or Filipin III were unable to significantly reduce the cell migration. Quantification of MDA-MB-231 indicated that 84.72 ± 6.29% of the wound area was covered in untreated cells, compared with 46.56 ± 1.281 (***$p<0.001$) and 52.65 ± 1.17% (***$p<0.001$) in Dynasore and pistop2 treated cells, respectively (Figure 3.10 B). Quantification of MDA-MB-231 indicated that 84.72 ± 6.29% of the wound area was covered in untreated cells, compared with 71.67 ± 2.02 $p >0.05$ and 80.32 ± 3.77% $p >0.05$ in Amiloride and Filipin III treated cells, respectively (Figure 3.10 B).

It was further tested if combinations of these inhibitors had an additive effect compared to individual treatment. The results indicated that a combination of Dynasore and Pitstop2 acted synergistically, significantly reducing collective cell migration (18.99 ± 3.08) compared to Dynasore (46.56 ± 1.28 * $p<0.05$) or pitstop2 (53.68 ± 1.16 ** $p<0.01$) alone. Whereas a combination of Amiloride and Filipin III had no effect on migration (71.09 ± 8.77) compared to Amiloride (71.67 ± 2.02 $p >0.05$) or Filipin III (80.32 ± 3.77 $p >0.05$) alone (Figure 3.10 C).

Additionally, it was established if the inhibition of dynamin or clathrin could decrease the migration when combined with other pathways inhibitors. It seems that Pitstop2 or Dynasore are potent migration inhibitors on their own. However, Pitstop2 in combination with Amiloride (28.16 ± 3.81) or Filipin III (32.60 ± 1.38) is not able to further inhibit wound closure compared to pitstop2 (53.68 ± 1.16 $p >0.05$) (Figure 3.10 C).Whereas Dynasore in combination with Amiloride (87.60 ± 5.58 *** $p<0.001$) or Filipin III (82.77 ± 8.26 ** $p<0.01$) has a much less inhibitory effect – almost close to control compared to Dynasore (46.56 ± 1.28 *** $p<0.001$) (Figure 3.10 C).

Having confirmed that some endocytic pathways inhibitors effectively reduced the cell migration measured by wound healing assay, the question was raised whether or not these inhibitors affect individual cell migration. Thus, migratory speed of individual cells based on the total distance travelling within 24 hours was measured using timelapse microscopy. MDA-MB-231 cells were plated on plastic or different surfaces (0.2% gelatine or 2mg/ml collagen) and incubated overnight. When the plate reached 30% confluence, cells were treated with DMSO or four endocytosis inhibitors at varying concentrations and incubation times (Pistop2 25µM for 15 minutes , Amiloride 50 µM for 30 minutes, Dynasore 20 µM for 30 minutes with 20 µM DMSO for 30 minutes and Filipin III 16 µM at time point 0). Upon completion of the incubation times, the treated media were replaced with fresh media. In case of Caveolae inhibitors, Filipin III 16 µM were kept during the experiment. The cells were then subjected to live imaging using time lapse microscopy. Images were captured every 15 minutes for a period of 24 hours and the speed were represented as the total distance divided by 24 hours (time of the experiment).

As presented in figure 3.10 D, inhibition of endocytosis significantly reduces the average speed during time lapse experiments in cells treated with either Dynasore or Pitstop 2. Whereas, both inhibitors Amiloride or Filipin III were unable to reduce migration speed. The quantification analysis of MDA-MB-231 migration indicated that the average speed was 24.71 ± 1.53 µm/h in DMSO, compared with 17.76 ± 0.65 µm/h ** $p<0.01$ and 20.24 ± 0.34 µm/h * $p<0.05$ in Dynasore and pitstop2 treated cells, respectively.

Interestingly, similar trends were observed when the MDA-MB-231 cells migrated on either gelatine or collagen substrates. Quantification analysis of MDA-MB-231 migration on gelatine indicated that the average speed was 26.56 ± 2.74 in DMSO, compared with 12.93 ± 1.72 µm/h ** $p<0.01$ and 13.35 ± 2.67 µm/h ** $p<0.01$ in Dynasore and pitstop2 treated cells, respectively (figure 3.10 E). Similarly, Quantification analysis of cell migration on collagen showed that the average speed was 26.34 ± 2.02 µm/h in DMSO, compared with 14.60 ± 1.80 µm/h * $p<0.05$ and 15.18 ± 3.04 µm/h *

$p<0.05$ in Dynasore and pitstop2 treated cells, respectively (figure 3.10 F). However, Amiloride or Filipin III were unable to reduce the migration either on gelatine or collagen (figure 3.10 E and F).

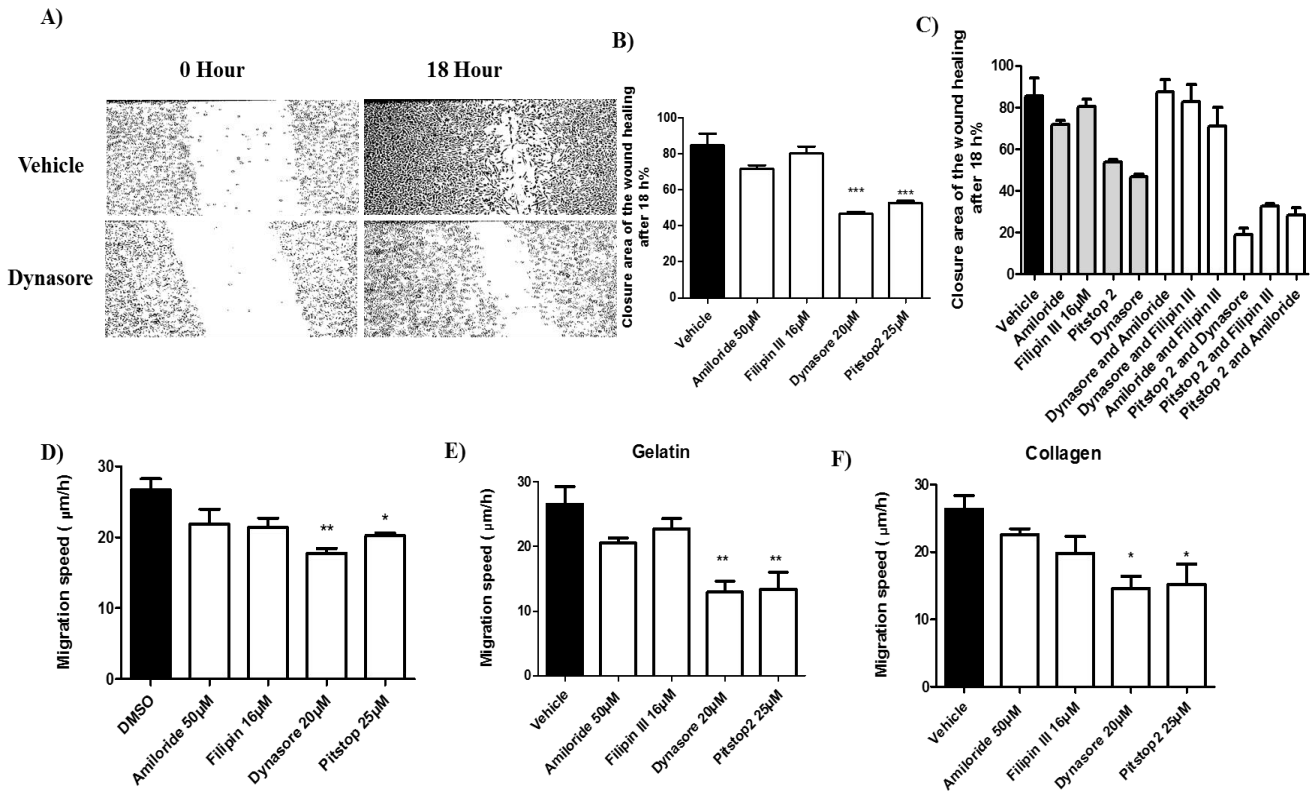

Figure 3. 10 Effect of endocytic inhibitors on cell migration using wound healing and cell tracking in MDA-MB-231

MDA-MB-231 cells were treated with Vehicle or different endocytotic pathways inhibitors for different time periods and subjected to scratch assay using an inverted microscope or tracking individual cell using a time lapse microscope. 50 µM Amiloride and 20 µM Dynasore incubated for 30 minutes. 25 µM Pistop2 and 16 µM Filipin III incubated 15 minutes and 24 hours, respectively. **A)** Inverted microscope images showing the wound closure of MDA-MB-231 cells in the control or dynasore treatment. Closure of the wound was captured at 0 and 18hH. **B)** Effect of different endocytosis inhbitors on the percentage of wound area covered after 18 hours of MDA-MB-231. **C)** Effect of combination of endocytotic inhibitors on the percentage of wound area covered after 18 hours. MDA-MB-231 cells were treated with Vehicle or a combination of indicated inhibitors for different time periods. Filipin III were incubated 24h and then incubated with different endocytosis pathways inhibitors at different times (Amiloride 50 µM for 30 minute, Dynasore 20 µM for 30minutes and Pistop2 25 µM for 15 minutes). Other combination inhibitor were incubated for 30 minutes and subjected to scratch assay. **D)** The mean migration speed of individual cells in plastic surface. **E)** The mean migration speed of individual cells on gelatine. **F)** The mean migration speed of individual cells on collagen.

One way ANOVA with Dunnett's Multiple Comparison Test were used to compare each treatment with the control. Graphs represent the mean ± standard error of three independent experiments. Statistical significance differences were accepted at * $p<0.05$, ** $p<0.01$ and ***$p<0.001$.

Having presented data that some endocytotic pathway inhibitors effectively reduce cell migration of MDA-MB-231 as measured by wound healing assay and cell tracking, the question was raised whether or not these inhibitors affect the migration of other cell lines. Thus, wound-healing assay were performed in the melanoma cell line SK-MEL-28 and the migratory speed of individual cells based on the total distance covered for 24 hours were measured in HT1080 cells.

Measurements of the closing wound showed that inhibition of endocytosis in SK-MEL-28 significantly reduces the rate of epithelial cell migration during wound healing in cells treated with either Dynasore or Pitstop2. About 90.47 ± 3.49 % of the wound area was closed in untreated cells, compared with 44.47 ± 5.42 % * $p<0.05$ and 44.25 ± 15.20 * $p<0.05$ in Dynasore and pitstop2 treated cells, respectively (figure 3.11 A and B).

Consistent with this, the average speed during time lapse in HT1080 cells treated with either Dynasore or Pitstop2 is significantly reduced. As presented in figure 3.11 C, the average speed was 25.52 ± 0.91 µm/h in control conditions, compared with 21.27 ± 0.53 µm/h * $p<0.05$ and 19.68 ± 0.83 µm/h ** $p<0.01$ in Dynasore and pistop2 treated cells, respectively. However, Amiloride was unable to reduce migration.

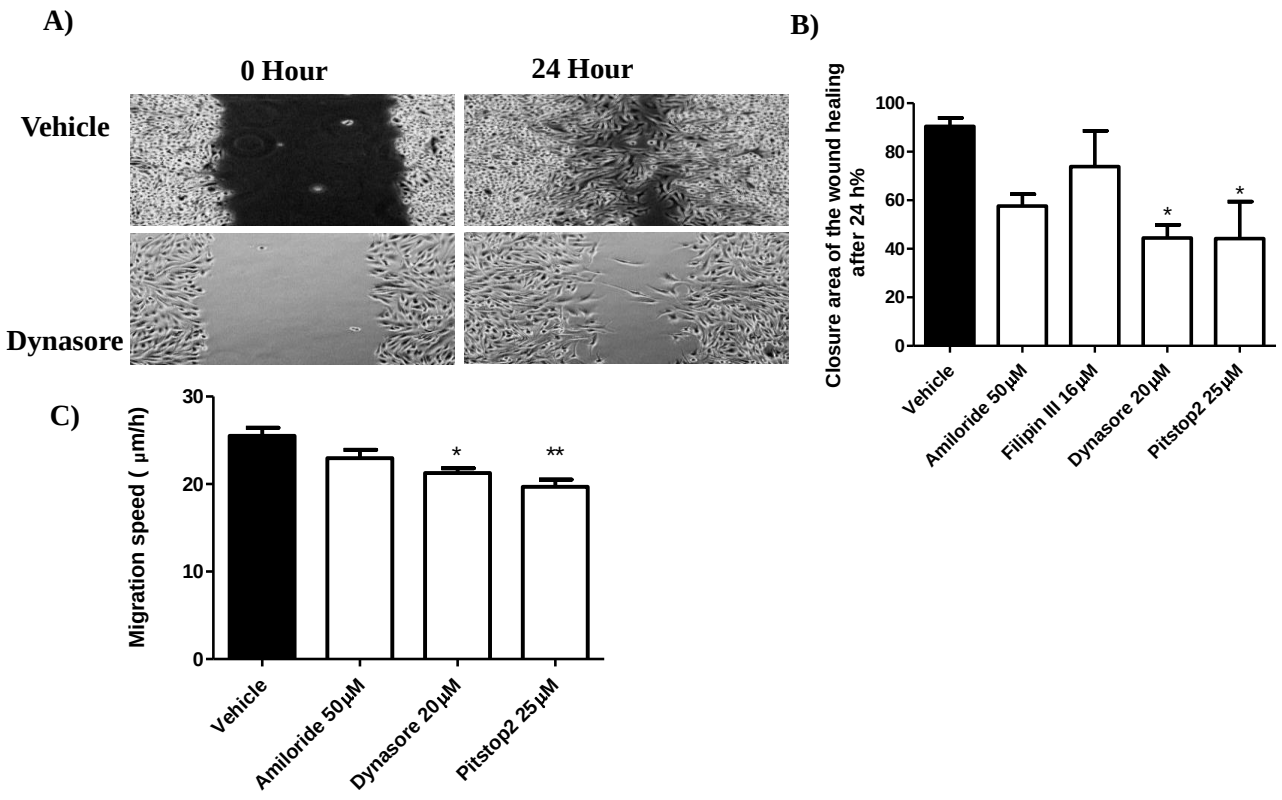

Figure 3. 11 Effect of endocytotic inhibitors on cell migration using wound healing and cell tracking of different cell lines.

SK-MEL-28 and HT1080 cells were treated with Vehicle or different endocytotic pathway inhibitors for different time periods and subjected to scratch assay using an inverted microscope or tracking individual cell using time lapse microscopy. Cell were treated with either 50 µM Amiloride or 20 µM Dynasore and incubated for 30 minutes. 25 µM Pistop2 and 16 µM Filipin III incubated 15 minutes and 24 hours, respectively. **A)** Inverted microscope images showing the wound closure of SK-MEL-28 cells in control and or dynasore treated conditions. Closure of the wound was captured at 0 and 24h. **B)** Effect of different endocytosis inhbitors on the percentage of wound area covered after 24 hours of SK-MEL-28. **C)** The mean migration speed of HT1080 in plastic surface.

One way ANOVA with Dunnett's Multiple Comparison Test were used to compare each treatment with the control. Graphs represent the mean ± standard error of three independent experiments. Statistical significance differences were accepted at * $p<0.05$ and ** $p<0.01$.

3.3.5.2 Visualization of Endosomes on leading and trailing edge in fixed and live cells

The specific localization of proteins in the leading and trailing edge of a cell may play an important role in the direction of migration. Especially since the most important steps of cell migration are occurring on the leading edge and involve attachment of adhesive proteins and stabilizing actin protrusions and formation of lamellipodia.

The Rab5 GTPase has been reported to induce migration by facilitating lamellipodia formation (Spaargaren and Bos, 1999). In addition to this, inhibition of endocytosis by Pitstop2 resulted in reduced expression of both early endosomes markers, EEA1 and Rab5. Thus, it was important to investigate the potential link between early endosomes and cell direction. To test this, MDA-MB-231 were seeded either in a 6 well plate or 1 well glass ibidi slides and allowed to attach to the bottom of the well overnight. Subsequently, when the wells became 70% confluent, they were transfected with GFP-Rab5 and incubated overnight. Later, the cells were fixed with paraformaldehyde, immunostained for focal adhesion protein Paxillin and visualized by confocal laser scanning microscopy. The focal adhesion Paxillin was used to identify the cell edge and speculate the migrational direction of the MDA-MB-231. For live cell imaging, the MDA-MB-231 cells were seeded in 1 well ibidi slides and immediately subjected to a time-lapse movie (1 image every 15 seconds for 10 minutes).

To quantitatively compare the endosomes containing number, size or rate of endosomes, the area of 50 μm^2 from each edge to the nucleus were selected. In fixed cells, the quantification analysis of each leading and trailing area of fixed MDA-MB-231 cells revealed that Rab5 containing endosomes accumulates more at the leading edge (15.16 ± 2.33* $p<0.05$) than at the trailing edge (6.07 ± 0.8). Notably, the size of endosome containing Rab5 did not differ between the two edges (Figures 3.12 A and C).

Live cell imaging used MDA-MB-231 cells that had been transfected with GFP-Rab5 and were directly subjected to time lapse movie imaging to further confirm the localisation of GFP Rab5 in two regions. The quantitative measurement of these movie was performed by taking 1 image every 15 seconds for 10 minutes. This was to illustrate the average number of endosome appearance (rate) at either leading or trailing edges. The results showed that the rate of endosomes containing Rab5 increase at the cell's leading edge 134.3 ± 4.12 ** $p<0.01$ compared to trailing edge 92.67 ± 3.4 (Figure 3.12 B and D), suggesting that Rab5 localisation becomes polarised with directional migration.

The other quantitative measurement performed, was to illustrate the average life time of GFP-Rab5 in whole cells. This was accomplished by taking 1 image every 15 seconds for 20 minutes. The results showed that the average life time of GFP-Rab5 containing endosomes revealed to be 3.66 ± 0.94 minutes.

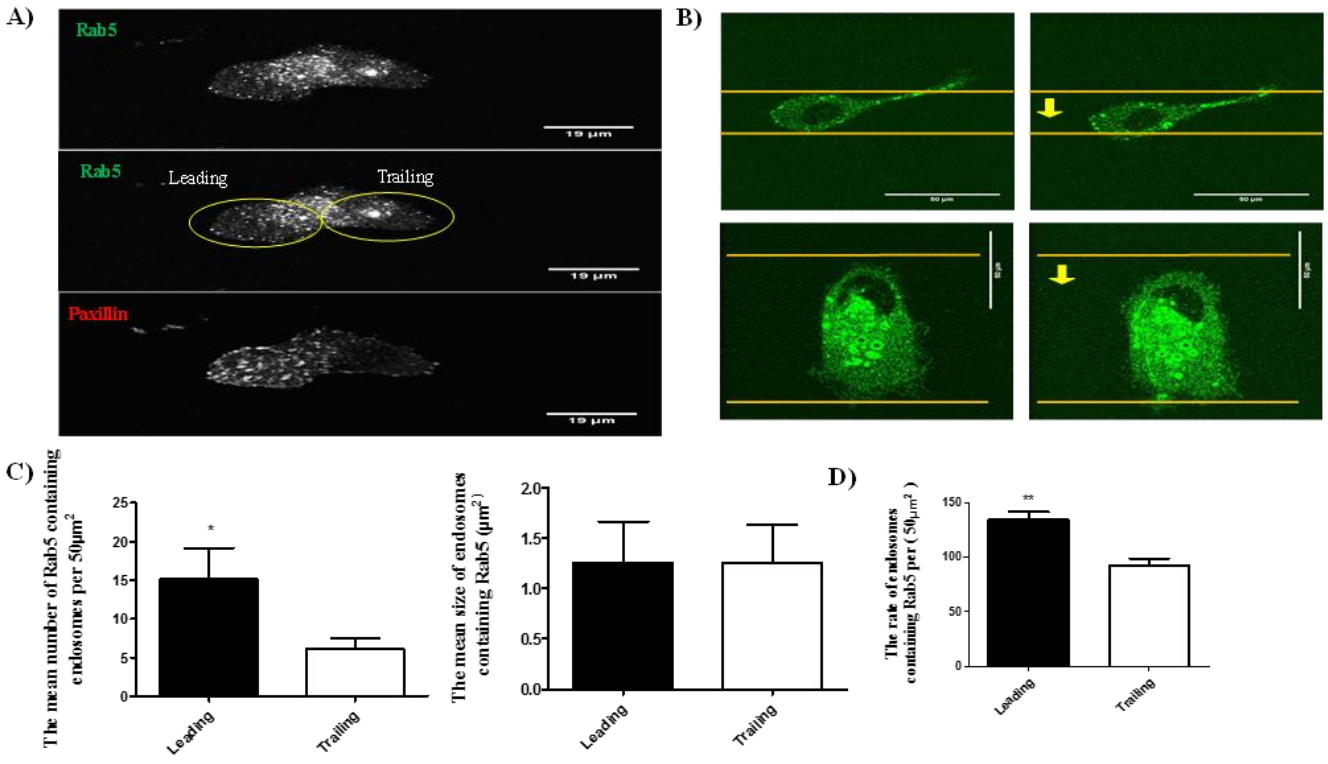

Figure 3. 12 Detection of GFP-Rab5 at the leading and trailing edges of migrating MDA-MB231 cells

Cells were transfected with GFP-Rab5, fixed and visualized by confocal or directly subjected to live confocal imaging where images captured every second for 20 minutes. A: Confocal images showing the localization of GFP Rab5 at the leading edge and trailing edge of MDA-MB-231 cells. The number of GFP-Rab5 endosome was measured through selection ROI (region of interest of an area of 50µm^2) at the leading and trailing edge. Yellow circles indicate the leading and trailing area used to calculate the number of endosomes. The Focal Adhesion molecule paxillin was stained to outline the cell surfaces and the direction of cells. B) Confocal live imaging showing the direction and the distance of GFP Rab5 of MDA-MB-231. The yellow lines indicate the distance that MDA-MB-231 cell move it in 20 minutes and the yellow arrow indicate the direction. C) Two graphs show number and size of GFP Rab5 endosomes per 50µm^2 within two regions (leading and trailing edges) in fixed cells. D) The rate of GFP-Rab5 in leading and trailing edges of live MDA-MB-231 cell. The rate was measured through selection ROI (50µm^2) at the leading and trailing edge. The values are the mean ± standard error of three independent experiments in which 6 cells were measured. T test used to compare means Statistical significance differences were accepted at * $p<0.05$ and ** $p<0.01$.

3.3.6 Effect of nutrient depletion and starvation on Rab5 and cell migration:

Previous results showed that blocking the Clathrin internalization pathway down regulates the early endosomes proteins as a result and this leads to a reduced cell migration. These data led me to suggest whether targeting endocytosis pathways by other mechanisms, rather than blocking the endocytotic pathways using inhibitors, may regulate Rab5. It was suggested that glucose and nutrient depletion can affect endocytosis (Lang et al., 2014). Therefore, it was tested if prolonged starvation affects Rab5 containing endosomes number and size. Two cell lines were employed in this experiment, MDA-MB-231 and HT1080 cells. Each cell line was plated on a 12-well-plate and incubated in low glucose media (MEM) containing 10% FBS overnight. The next day, the media were replaced with low glucose media containing either 10% or 0.5% FBS, transfected with GFP-Rab5 and incubated for additional 24h. Upon completion of the incubation times, cells were fixed with paraformaldehyde and immunostained for the focal adhesion protein Paxillin to be able to outline the cell surfaces and edges.

The quantification analysis of Rab5 revealed that the starvation did not significantly decrease the number of endosomes containing Rab5 in MDA-MB-231 cells but significantly decreased it in HT1080 cells (10% FBS 42.92 ± 0.79 * $p<0.05$ compared with 36.93 ± 1.53 in 0.5% FBS). However, the size of endosome containing Rab5 between two conditions did not differ in both cell lines figure3.13 A and B.

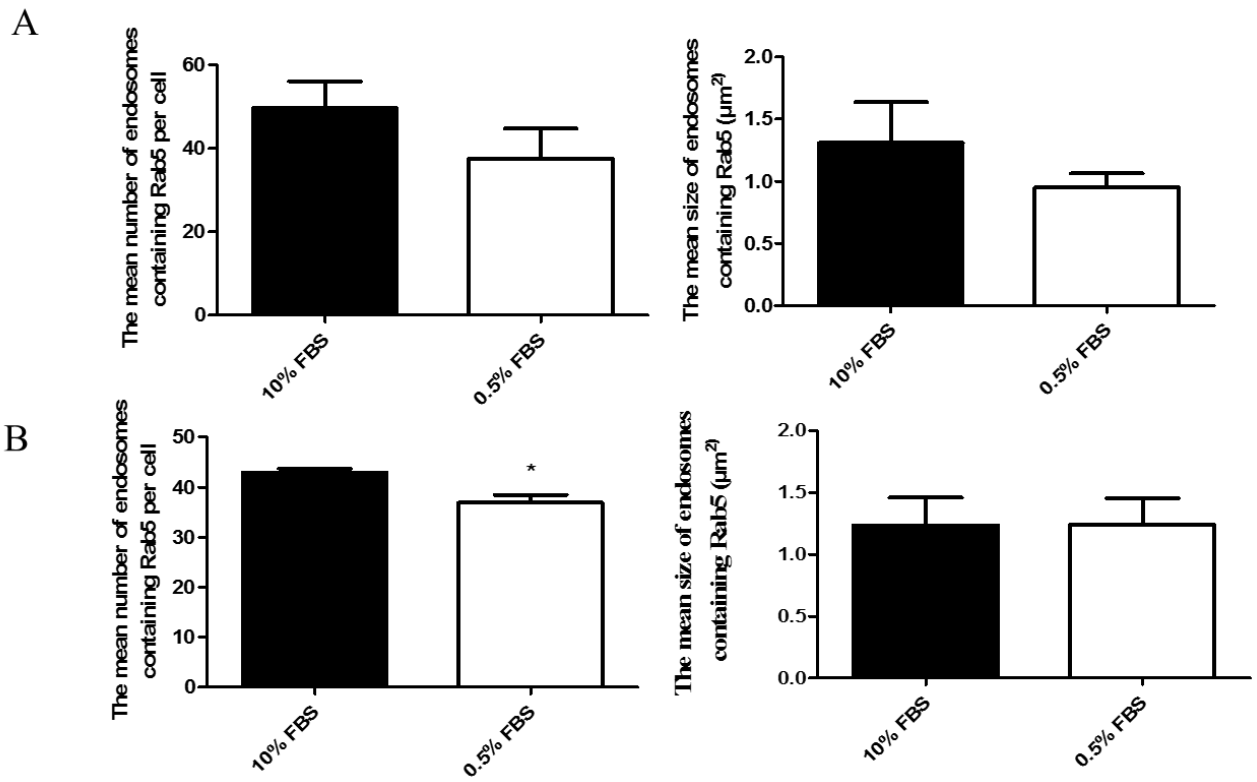

Figure 3. 13 Effect of nutrition depletion on mean endosomes containing Rab5 number and size in MDA-MB-231 and HT1080.

Cells were incubated with 10% FBS or 0.5%FBS continuing cell light GFP Rab5 for 24 hours. Cells were then fixed and subjected to confocal microscope analysis. A) Effect of nutrition depletion on endosome containing Rab5 number and size in MDA-MB-231 cells. B) Effect of nutrition depletion on endosomes containing Rab5 number and size in HT1080 cells.

T Test were used to compare 10% FBS with 0.5% FBS indicate no significant differences. Graphs represent the mean ± standard error of three independent experiments, in each experiment at least 40 cells were analysed for each cell lines.

Next, it was determined whether the prolonged starvation may affect cell migration. Thus, the average distance between two points of migrated cells were examined every 30 minutes during a 24 hour period in order to observe and distinguish a migratory change in both FBS conditions: 10% and 0.5% FBS However, the two way ANOVA analysis failed to confirm that these conditions were statistically different (Figure 3.14).

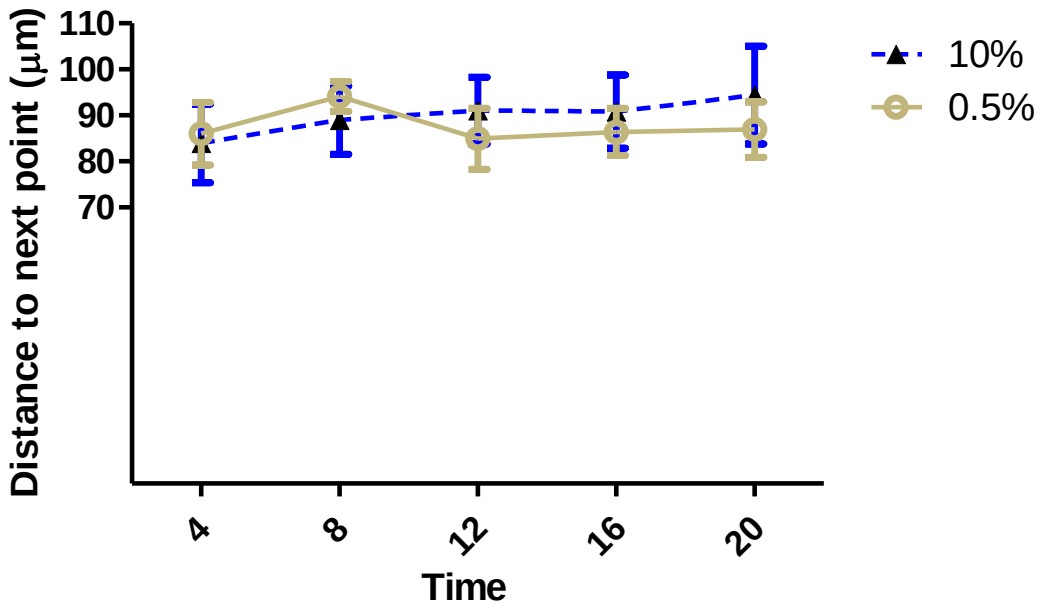

Figure 3. 14 Effect of nutrition depletion on cell tracking assay of MDA-MB-231 cells.

Graph shows the distance between two points of an individual cell over a 24 hour period. Cells were incubated with 10% FBS or 0.5%FBS in low glucose (MEM) media and subjected to cell tracking assay using time lapse microscopy. Two way ANOVA Test was used. Graph represents the mean ± standard error indicates no statistical significant differences. Three independent experiments, in each experiment 40 cells were analysed for 0.5%FBS or 10% FBS.

3.4 Discussion

The first aim of this chapter was to investigate the effectiveness of various endocytosis inhibitors before they were being carried forward to examine their effect on cell migration, therefore initially two different ligand uptakes were examined. Transferrin (clathrin marker) and dextran (micropinocytosis fluid marker).

Transferrin is an iron binding plasma glycoprotein that controls iron uptake in cells (McClelland et al., 1984). The iron uptake occurs when transferrin binds to its receptors and is internalized into cells through Clathrin dependent pathways (Mayle et al., 2012). Dynamin plays an important role in internalising the transferrin complex. Dynamin localizes at the neck of budding vesicles, forming a helix, and acts as a GTPase switch (Shpetner and Vallee, 1989). This switch mediates "pinch" activity, resulting in vesicle scission that contains the transferrin complex from the membrane into the early endosomes (Le Roy and Wrana, 2005). Many inhibitors and tools have been identified to target dynamin. The Dynasore inhibitor is able to inhibit dynamin and thus blocks the formation of clathrin coated vesicles through modulating the GTP hydrolysis without affecting the GTP binding affinity (Macia et al., 2006). In this chapter, fluorescence intensity assays have shown that the Dynasore inhibitor even with short incubation times and low concentration, inhibits transferrin uptake in both MDA-MB-231 and HT1080 cells. Similar results were obtained when the number of endosomes containing transferrin were measured. These finding are consistent with a study which was carried out in Hela cells, showing a similar effect of Dynasore inhibitors on transferrin uptake (Macia et al., 2006). At a higher concentration (80µM) Dynasore also reduced transferrin uptake but was not significant higher than low concentrations of Dynasore. Since the inhibition of endocytosis can be achieved with low concentrations 20 µM and to avoid toxicity or off-target effects, this concentration was used for the upcoming results.

The effect of Dynasore on dextran uptake (a specific maker for micropinocytosis) was also analysed. Many studies have demonstrated that inhibiting the function of dynamin by either using siRNA or chemical inhibitors on different cells can both inhibit or have no effect on dextran uptake depending on the cell type (Cao et al., 2007) (Bonazzi et al., 2005). Here, it was shown that the dextran uptake was not reduced but rather induced by almost two-fold to 44.54 ± 3.0 compared to control conditions 24.52± 2.81. According to Doherty, blocking one pathway of endocytosis may result in up regulation of other endocytotic pathway and that may explain the increased uptake of micropinocytosis marker (dextran) (Doherty and McMahon, 2009). Another possible explanation could be that a subset of dextran was mediated by the clathrin dependent pathways, and blocking the clathrin pathway forced this subset of dextran to use non clathrin pathway for uptake. This is supported by the study of Li and colleagues, who reported that the size of dextran (10K) which was used in this study, can be internalized through the Clathrin pathway (Li et al., 2015b). For example, they showed that inhibition of micropinocytosis with Amiloride alone decrease the uptake of Dextran 10K to 40%, whereas a combination of Amiloride and Dynasore resulted in up to 80% decrease. However, no significant reduction was observed on Dextran 70K uptake by Amiloride alone or Amiloride with Dynasore (Li et al., 2015b). It is likely that these findings and results observed here could indicate that the Dynasore inhibitor could be a good choice for inhibiting the clathrin dependent pathway.

Clathrin dependent pathways were also targeted by inhibiting clathrin proteins. Clathrin proteins play an important role for sorting transferrin entry molecule from the plasma membrane into cells (Mayle et al., 2012). This is initiated via adaptor proteins such as AP2 which recruits the clathrin proteins to the plasma membrane (Edeling et al., 2006). The amino terminal domain of clathrin heavy chain represents a major site for recruiting these adaptors. Pitstop2 has been shown to bind the amino-terminal domain of clathrin and thus prevent various accessory proteins to bind clathrin which inhibits clathrin mediated endocytosis (von Kleist et al., 2011). The result presented here, using two different measurements assays: fluorescence intensity and number of endosomes containing transferrin, shows

that Pitstop2 inhibitor at 25 µM for a period of 15 minutes was sufficient to obtain a maximal inhibition of transferrin uptake in MDA-MB-231. This is consistent with the published results where inhibiting Pitstop2 reduced the uptake of transferrin compared to the control (von Kleist et al., 2011). Their study also monitored the uptake of non clathrin pathway using shiga toxin (a specific maker for clathrin-independent endocytosis) and reported that pitstop2 failed to block shiga toxin internalization, suggesting pitstop2 as a specific inhibitor of the clathrin pathway. A study by Stahlschmidt further supports the specificity of pitstop2 on targeting the amino terminal domain of clathrin heavy chain, and showed that pitstop2 inhibitor did not affect clathrin recruitment to the membrane and clathrin was normally distributed in cells (Stahlschmidt et al., 2014). This is in line with my result, where the inhibition of pitstop2 did not affect the expression of clathrin.

Failure in clathrin recruitment to ligand binding sites via pitstop2 did not only affect ligand uptake but also reduced both dextran uptake and Rab5 expression. Rab5 protein, in addition to regulation of endosomal dynamics and being localized in both clathrin vesicles and the plasma membrane (Chavrier et al., 1990), is associated with macropinosome formation and micropinocytosis process that required the enrichment of phosphoinositide in the plasma membrane (Meier et al., 2005). This is supported by the fact that Rab5 recruits phosphatidylinositol-3 kinase to the plasma membrane which in turn mediates the accumulation of phosphatidylinositol 3,4,5-triphosphate (PI(3,4,5)P3) and results in membrane ruffling and micropinocytosis response (Porat-Shliom et al., 2008). It seems reasonable to speculate that reduction of dextran uptake might be due to an indirect effect of Rab5 expression. This idea is supported by the result obtained here where inhibition of Dynasore did not affect Rab5 expression and as a result the dextran uptake was not blocked.

Additional roles for dynamin and clathrin were also found in regulating expression of early endosomes antigen1 (EEA1). To our knowledge, this was the first study to investigate the effect of endocytosis pathways inhibitors on expression of early endosome proteins. The result here showed

that both inhibitors, Dynasore and pitstop2, decreased the expression of EEA1 and numbers of endosomes containing EEA1, while leading to the enlargement of endosomes.

It has been shown that knock down of proteins located in the membranes of lysosome and late endosomes such as LGP85 (LIMP II) results in morphological changes of both early and late endosomes (Kuronita et al., 2002). Thus, the abnormality in the size of EEA1 containing endosomes observed in this chapter may rule out the possibility that these inhibitors impaired the function of late endosomes that are associated with degradation of proteins. The result obtained here showed that LAMP1 expression was not affected by these inhibitors. In addition, it also did not affect clathrin heavy chain 1. Taken together, these findings suggest that both Dynasore and Pitstop2 appears to regulate early endosomal proteins and likely affect early endocytosis or recycling processes.

In addition, this chapter examined APPL1, a Rab5 effector that directly binds Rab5 via a BAR and a PH domain (Li et al., 2007). APPL1 acts as transporter in very early endosomes that mediates a very early stage of endocytosis process of internalized molecules (close to the plasma membrane) before maturing into EEA1 positive endosomes (Diggins and Webb, 2017) (Zoncu et al., 2009). Here, the results showed that inhibition of clathrin and dynamin did not reduce the expression of APPL1, suggesting that clathrin pathway inhibitors did not affect the early stage of endocytosis. In addition, the internalized transferrin receptor might not necessarily pass through APPL1 to EEA1. This idea is supported by Danson et al who showed that epidermal growth factor receptor (EGFR) can directly fuse to early endosomal compartments without passing through APPL1 (Danson et al., 2013). Taken together, this suggests that clathrin pathway inhibitors appear to specifically regulate EEA1, and the enlargement of endosomes may reduce the rate of recycling.

This project also further investigated other endocytosis pathways (micropinocytosis and caveolae pathways). Micropinocytosis differs from other endocytosis pathways, and pH homeostasis plays an important role in induction of micropinocytosis (West et al., 1989). This is illustrated by the example

of EGF stimulated cells, in which cytosolic pH elevation and subsequent increase of Na^+ influx can result in micropinocytosis activation (West et al., 1989). Amiloride (5-(N-ethyl-N-isopropyl)) was shown to inhibit micropinocytosis as this inhibitor works as a blocker of NHE, a protein that localizes within cell membranes and exchanges intracellular H^+ and extracellular Na^+ (West et al., 1989) (Orlowski and Grinstein, 1997). A study by Koivusalo et al showed that Amiloride inhibits micropinocytosis by lowering the submembranous pH without affecting either cytosolic alkalinisation or Na^+ influx (Koivusalo et al., 2010). As a consequence, Amiloride has been widely used as a micropinocytosis inhibitor. Our study found that Amiloride significantly reduces the uptake of the micropinocytosis marker dextran. This is consistent with a previous result carried out in Human Embryonic Kidney cells (HEK293) where Amiloride concentration of 1mM for 30 minutes decreased the uptake of dextran (Wang et al., 2010). Interestingly, Amiloride also decreased the uptake of transferrin (a specific maker for clathrin-mediated endocytosis) suggesting that Amiloride could interfere with clathrin pathways as well as micropinocytosis.

We also examined the caveolae pathways. This pathway can be distinguished from other endocytosis pathways by the fact that it requires cholesterol components (Hailstones et al., 1998). Removal of cholesterol from the plasma membrane using methyl beta cyclodextrin (MβCD) or exposure to the sterol-binding compound Filipin III can lead to disassembly of caveolae and prevent clustering of receptors that are present in caveolae (Zidovetzki and Levitan, 2007). Here, the clathrin marker were examined and it was found that inhibition of caveola by Filipin III did not affect the uptake of transferrin, indicating that clathrin mediated endocytosis was not affected and suggesting that caveolae is not a route for transferrin uptake.

We confirmed that inhibition of some endocytotic pathways effectively blocked endocytosis uptake and affected early endosome trafficking through either EEA1 or Rab5. This led to the hypothesis that endocytosis may play important roles in cell migration.

One model widely used in the migration field is the wound healing assay, which examines collective directional cell migration. In this study, MDA-MB-231 cells inhibited with low concentrations of dynasore (20μM), significantly reduced the rate of cell migration during wound healing. Our findings are consistent with data published by Eppinga and colleagues, who showed that knockdown of dynamin2 significantly reduced the migration of a highly metastatic pancreatic cancer cell line (Eppinga et al., 2012). In line with this, a short incubation (15 min) with the Pitstop2 inhibitor showed a significant effect on wound closure compared to the control. This is consistent with data obtained on T cell migration, which highlighted a role for clathrin-mediated endocytosis in cell migration using dominant negative mutants of clathrin (Samaniego et al., 2007). Notably, Dynasore and Pitstop2 when combined showed a synergistic effect on wound closure compared to Dynasore or pitstop2 alone. This further indicates a role of both Dynamin and clathrin pathways on cell migration assessed by wound healing.

On the other hand, inhibition of both caveolae and micropinocytosis pathways using Filipin III and Amiloride, respectively, showed no significant effect on wound closure. These inhibitors were further examined when combined with each other or with clathrin inhibitors in order to verify their involvement in directed cell migration. A combination of Amiloride and Filipin III had no additional effect on wound closure, compared to Amiloride or Filipin III alone. Similarly, dynasore in combination with Amiloride or Filipin does not have any additional effect compared to dynasore alone. In addition, when Amiloride was combined with Pitstop2 it had no effect in the migration of MDA-MB-231 cells compared to Pitstop2 alone. Similarly, Filipin III when it combined with Pitstop2 did not decrease the migration of MDA-MB-231 compared to Pitstop2 alone. These observations may suggest that micropinocytosis and caveolae pathways do not play a role in cell migration assessed by a wound healing assay.

This study further examined the involvement of endocytotic pathways inhibitors in the melanoma cell line SK-MEL-28. Similar to what was observed in MDA-MB-231 cells, inhibition of Dynamin and

Clathrin resulted in a significant decrease in cell motility, whereas other pathways failed to demonstrate a significant effect. This may further support the involvement of clathrin and dynamin on cell migration even with cells that display a different style of migration as they remain in groups during movement and there is a clear difference in migration speed between these cell lines. MDA-MB-231 cells only needed 18 hours to close the wound whereas SK-MEL-28 required 24 hours. Fast wound closure could be possibly due to rapid focal adhesion turnover that makes cells move faster (Bijian et al., 2013). Alternatively, it may also be due to different expression levels of molecules such as E-cadherin between these two cell lines, as cells that have collective migration behaviour express high levels of E-cadherin and migrate slower than individual cells (Elisha et al., 2018). Tang and colleagues showed that SK-MEL-28 are strongly positive for E-cadherin more than other forms of melanomas cell lines (Tang et al., 1994), whereas MDA-MB-231 has been shown to be negative or show lower expression for E-cadherin (Kirschmann et al., 1999).

Despite the fact that the wound healing assay is cost effective and is widely used in cell migration studies, it has many disadvantages. The scratches or generated wounds of the cell monolayer can damage neighbouring cells. In addition, they can potentially damage cell borders and especially any ECM present, which in turn can lead to release of growth factors that may influence cell migration activity (Hulkower and Herber, 2011). Size and spacing of the wound as well as varying cell densities are factors which can lead to generation of experimental artefacts. Finally, the examination of migration is only observed in one direction. To avoid these limitations, further analysis of the role of endocytosis pathway inhibitors were carried out using time lapse imaging to track the motility of individual cells in multiple directions. On plastic surfaces, the time lapse data showed a significant decrease in cell migration in MDA-MB-231 cells treated with Dynasore or Pitstop 2. However, Amiloride and Filipin III did not affect migration behaviour. In addition, time lapse data supported the effect of clathrin and dynamin inhibitors dynasore or pitstop2 but not Amiloride in decreasing the cell migration of HT1080 cells. This sarcoma cell line shares a similar style of migration and

metastatic properties as the carcinoma MDA-MB-231 cells, with a similar average speed between MDA-MB-231 (24.71 ± 1.53 μm/h) and HT1080 (25.52 ± 0.91) cells.

It is widely accepted that cell behaviour and responses to signals varies on different surfaces. In extracellular matrix, cells require an extra step for migration, as they need to penetrate the ECM, which is achieved by secretion of matrix metalloproteinase (MMPs) proteins (Doyle et al., 2013). However, the expression of MMPs can vary on different surfaces (Sakai et al., 2011).

In addition, cell attachment to plastic surfaces can be different from ECM surfaces (Davidenko et al., 2016). For example, cell attachment to collagen is mediated via α2ß1 and α1ß1 integrins (Heino, 2000). Whereas, in gelatine the attachment is mediated by integrins such as αVß3 (Grover et al., 2012). These differences can lead to changes in focal adhesions dynamics (assembly and disassembly) as well as cell migration. Our results showed that both Dynasore and Pitstop2 clathrin pathways inhibitors significantly reduced the average migration speed on both gelatine and collagen treated surfaces, whereas non clathrin inhibitors Amiloride and Filipin III were unable to reduce migration speed. Taken together, these findings with regards to different types of attachments that may be present in different surfaces, dynamin and clathrin pathways still play an important role in cell migration.

The project also investigated endocytosis from the angle of nutrient deprivation. Starvation conditions have been shown to regulate protein degradation, and the structure and functions of endocytosis pathways (Krampe and Boles, 2002) (Lang et al., 2014). According to Smith, starved cells caused a decrease in the rate of endocytosis (Smith et al., 2010). Therefore, it can be hypothesized that if serum starvation reduces endocytosis, it should reduce cell migration. In this chapter, early endosomes marker protein Rab5 was not affected in response to serum starvation in MDA-MB-231. Unlike in HT1080, serum deprivation showed a slight decrease in the number of Rab5 containing endosome but no change in endosome size, suggesting the change in early

endosomes in response to starvation is influenced by cell type. This is supported by the study of Levin et al who showed the proteins and phosphoprotein levels between 12 cell lines in response to serum starvation were different (Levin et al., 2010). It seems that the starvation condition can be complex and cell dependent (Pirkmajer and Chibalin, 2011).

Nevertheless, the analysis of migrated distance over time of serum-starved cells provides insight into the migration pattern over the course of the assay. During the first 8 hours of starvation, starved and non-starved cells demonstrated similar motility characteristics. After 8 hours, there was no difference in cell migration of starved cells compared to cells in normal condition. Taken together, these observations suggest that starvation did not affect cell migration, at least in the study conditions and time frames.

Several studies have linked the process of endocytosis, especially clathrin and dynamin dependent endocytosis, with cell migration, as they interfere with actin polymerization (Lee and De Camilli, 2002) (McNiven et al., 2000) (Schlunck et al., 2004) (Ménard et al., 2014). Based on the fact that dynamin proteins can directly bind to actin associated protein cortactin, whereas clathrin protein is involved in recruitment of actin regulator proteins HIP1R (huntingtin-interacting-protein-1 related) which has binding sites for Cortactin, F-actin and clathrin (Wilbur et al., 2008). These findings illustrated that Dynamin or clathrin depletion affects actin remodelling and leads to reduced lamellipodia extension (Wilbur et al., 2008) (Schlunck et al., 2004). A similar conclusion has been reached by Linares and colleagues who used knock down approaches of clathrin in T cells and found that this prevented actin polymerization via inhibiting Arp2/3 protein which is required for actin-polymerizing protein (Calabia-Linares et al., 2011). Although the link between dynamin and clathrin with actin polymerization has been well established, there may be other effects of inhibiting dynamin and clathrin in cells and endocytosis itself might be important in cell migration.

Most of the evidence here suggests a link between decreased cell migration via clathrin pathways and a change in early endosome expression and size. It is well known that early endosome marker expression (Rab5 and EEA1) play a crucial role in primary cancer tissue and more aggressive cancer cells (Johnson et al., 2015). Their expression has been found to be increased in aggressive cancer cells compared to normal tissue and primary cancer tissue and can be used as a prognostic marker for cancer progression (Johnson et al., 2015). This may lead to increased nutrient uptake, cell division and altered signalling and all of these features are hall marks of cancer (Hanahan and Weinberg, 2011). Therefore, it is unsurprising that change of EEA1 and Rab5 dynamics can play a role in cell migration but the critical question still remains how they contribute to cell migration.

There are several possibilities which could explain the effect of early endosomes in cell migration. One possibility is that the association of early endosomes and actin could modulate the cytoskeletal organization. For example, dynamic F- actin has been previously shown to facilitate invagination and removing of vesicles from plasma membranes (Welch and Mullins, 2002) (Merrifield et al., 1999). This idea is supported by the association of dextran with the actin tail that removes the vesicles from the plasma membrane (Gauthier et al., 2007). This study also showed that most actin tail structures are associated with early endosomes but not late endosomes. Later on, Ohashi et al implicated the presence of actin in early endosomes and that impaired intracellular trafficking (Ohashi et al., 2011). In that study, inhibition of actin dynamics induced the formation of large endosomes and suggested that this prevents endosomal transport from early endosomes to recycling endosomes (Ohashi et al., 2011). Thus, it can be suggested that the enlarged endosomes observed in this study upon inhibition of either Dynasore or Pitstop2, might disrupt the function of F-actin and that affects actin network branching leading to a reduced migration.

Another possibility is that the localization of endosomes might enhance lamellipodia protrusion. Immunocytochemistry analysis revealed that more Rab5-positive early endosomes accumulated at the leading edge, where new protrusions are formed, compared to the trailing edge. In addition, the

rate of endocytosis using live cell imaging was higher at the cell's leading edge. The accumulation of Rab5 at areas for cell protrusion might induce the formation of lamellopodia and affect cell morphology (Palamidessi et al., 2008)**.** Simon and colleagues observed accumulation of clathrin mediated endocytosis at the leading edge compared to the trailing edge (Rappoport and Simon, 2003). Despite the differences between proteins used by Simon et al (Dynamin2, clathrin and transferrin) and proteins used in this work (Rab5), their findings are consistent with ours. Thus, it can be hypothesized that there is more happening than just the impact on actin polymerization. For example, cells in order to move, do not only rely on the need to polymerize actin but they also need to form attachments to surfaces. Therefore, we wanted to explore whether endosomes and endocytosis can regulate these attachments (focal adhesions). There is evidence that integrins can be recycled by an endosomes (Roberts et al., 2001a). Thus, we want to see whether other focal adhesion components can be endocytosed.

Chapter 4: Identifying role(s) for endocytosis in focal adhesion regulation

4.1 Introduction

The accumulation of the early endosome marker Rab5 at the leading edge of cells where polarization and focal adhesion recycling takes place, and inhibition of dynamin and clathrin endocytosis pathways down-regulating the early endosomal compartments, resulting in reduced cell migration, prompted the question of how endocytosis contributes to cell migration. One of the key processes underlying cell migration is the formation and turnover of focal adhesions.

Focal adhesions are necessary in many physiological and pathophysiological processes including cell survival, morphology, proliferation and cell migration (Meighan and Schwarzbauer, 2008). They are a complex of many proteins that connect the extracellular matrix to actin cytoskeleton (Wozniak et al., 2004). Connection of these adhesions can allow cells to transmit mechanical cues, generate tension force and promote protrusion by acting as molecular clutches (Giannone et al., 2009). Within the molecular clutches, the stability and turnover of focal adhesion dynamics can control cell movement. For example, the recruitments of many focal adhesion proteins (Vinculin, Paxillin, Talin, Zyxin, etc) and Kinases (FAK, etc) can provide sufficient attachment to ECM (Burridge et al., 1988). The majority of these adhesions can remain stable over minutes or undergo quick turn over which enables cells to migrate forward (Webb et al., 2002).

It is known that focal adhesions are not only structural elements that provide the stability of the cells through its connection to ECM, they also can regulate internal and external signalling to trigger various cellular responses (Humphries et al., 2007). In order to regulate signalling, two major groups of focal adhesion proteins have to be recruited to sites of focal adhesion during the phases of assembly and disassembly. These are scaffolding proteins such as Paxilin, Kindlin, Talin and Vinculin and regulator proteins such as FAK and ERK (Casar and Crespo, 2016). Each protein can be distinguished by its localization between the extracellular matrix and cytoskeleton (van Zanten and Mayor, 2015).

In terms of the possible link between endosomes and focal adhesions, several studies have hypothesised that vesicles might interact with focal adhesions or are implicated in their turnover. One study suggests the link between clathrin and paxillin based on genetic interaction (Brown and Turner, 2004a). For example, scaffolding proteins such as paxillin are comprised of many binding motifs. These are LD motifs (amino terminal), LIM (carboxy terminal) and SH2 domains (Brown and Turner, 2004a).The LD2 domain of Paxillin was demonstrated to bind clathrin heavy chain (Cote et al., 1999). Another study identified the presence of early endosome marker Rab5 and EEA within isolated integrin adhesion complexes based on proteomic analysis (Horton et al., 2015).

Furthermore, other scaffolding proteins such as vinculin was also shown to be associated with intracellular vesicles by either analysing endosome vesicles or their co-localization with transferrin which is taken up by clathrin dependent endocytosis (Márquez et al., 2014) (Macia et al., 2006). In addition, many kinases that are associated with focal adhesion activity or are recruited to the site of focal adhesions during their assembly and disassembly, such as FAK and SRC, have been shown to be localized to the plasma membrane and to perinuclear compartments (Kaplan et al., 1992). FAK and SRC were found to be regulated by endocytosis proteins that are involved in membrane fission and trafficking, called SNARE proteins. Evidence indicates that inhibition of the activity of endocytosis protein SNARE impaired the trafficking of Src and phosphorylation of FAK, and thus reduces the turnover of focal adhesions (Skalski et al., 2011). These results may indicate a possible role for endocytosis in regulating focal adhesion dynamics. However, little attention has been given to investigate the possible link between early endosome compartments and focal adhesions. For example, endocytosis of integrin mediates the disassembly of focal adhesion, whereas recycling integrin can help the formation and reassembly of focal adhesions (Caswell and Norman, 2008). So, whether endocytosis also contributes to the process of focal adhesion disassembly by internalizing and recycling the whole focal adhesions. Therefore, the main aim of this chapter was to examine the possible link between focal adhesions and the early endosomal compartment, including the influence

of clathrin (Pitstop2) and Dynamin (Dynasore) pathway inhibitors on focal adhesion organisation (size, number and turnover).

In order to determine whether the effect on migration by endocytosis pathways happened via effects on focal adhesions, the effect of endocytosis inhibitors Dynasore or Pitstop2 on focal adhesion number, size and turnover were examined in two cell lines (MDA-MB-231 and HT1080).

In order to study the interaction between the early endosomal compartments and focal adhesions, several approaches were performed. First, quantification of the co-localization between focal adhesion proteins and early endosomal compartments or clathrin markers (transferrin) was performed, using either immunostaining of fixed cells or live cell imaging of plasmid co-transfected cell populations. A second approach entailed isolation of endosomes using a cell fractionation assay with a Percoll gradient, followed by identification of proteins found in the endosome fractions. These fractions were then used to determine the presence of a variety of proteins that are specific to endosomal compartments (Rab5, EEA1 and Lamp1), focal adhesions (Vinculin, Zyxin, Paxillin and FAK) and as control nuclear proteins (H2b). A third experimental approach was to develop a new strategy to reduce or exclude contaminating organelles by precipitating endosomes from fractions and identifying the presence of focal adhesion proteins. This was carried out by immunoblotting for EEA1, Rab5 or Lamp1proteins to identify fractions which are enriched for endosome compartments and then incubating the positive one (Fraction 3) with magnetic Dynabeads to precipitate endosomes. Later, vinculin (as a marker for focal adhesions) was determined using SDS PAGE.

4.2 Method

4.2.1 Cell fractionation:

4.2.1.1 Cell fractionation solutions:

- Homogenization buffer (HBA): 0.25 M sucrose/10 mM Hepes pH 7.2/1 mM EDTA.
- PBS containing 0.5× protease inhibitor cocktail (PBS+).
- Stock solution of 90% Percoll (VWr) : 8ml Percoll and 1ml HBA.
- 2.5 M sucrose.

4.2.1.2 Post-nuclear-supernatant (PNS) preparation

After incubation of the cell culture, media were discarded from T75 flasks and the cells were washed twice with 5 mL chilled PBS in order to remove any dead cells. Subsequently, cells were scraped using a rubber policeman with PBS+ and centrifuged at 4°C at 1500 rcf for 15 minutes. The pellets were then re-suspended in 4 ml of chilled homogenization buffer (HBA) and homogenized with a steel dounce homogenizer with plunger (10 times) on ice. Next the homogenization buffer was centrifuged at 750 rcf for 10 minutes to remove unbroken cells, and the postnuclear supernatants were mixed with 90 % percoll to a final concentration of 27% in a volume of 8.5ml. This mixture was layered over 1ml 2.5M sucrose and centrifuged using an ultra-centrifuge at 29,000 rcf for 90 minutes at 4°C. After completed centrifugation, two milky band could be detected (Figure 4.1), all fractions (3 to 9) were collected manually starting from the top of the gradient (1 ml for each fraction). Finally, the fractions were subjected to protein separation, transfer and incubation as discussed above.

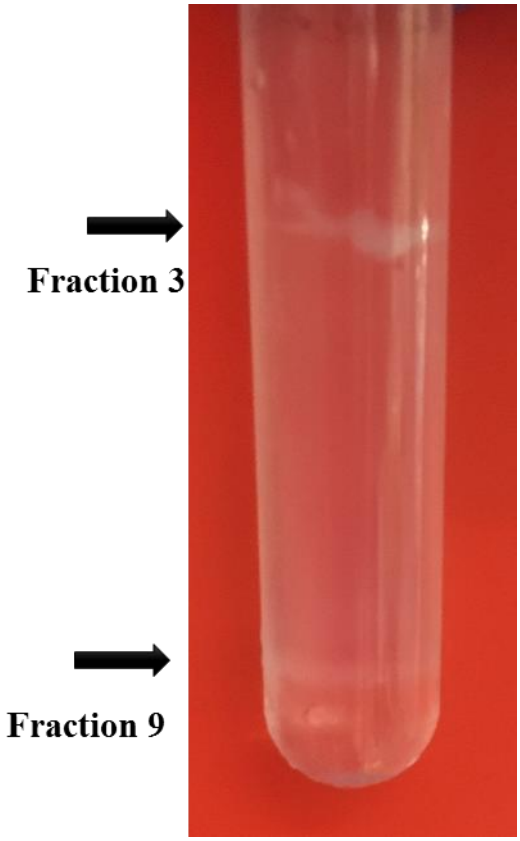

Figure 4. 1 Illustration of fractions

4.2.1.3 Co-Immunoprecipitation:

Once the protein concentrations of fraction 3 was measured using Bradford assay, fraction 3 was transferred into Eppendorf tubes and incubated with primary antibody in the cold room at 4^{o} C overnight. Next day, 100 µL of RIPA buffer containing Protein A/G agarose (20-50 µL) were added to the sample and incubated two hours on the rotating machine at 4^{o} C. The sample was then centrifuged at 2000 rcf for a minute and the pellet was washed with 300 µL with RIPA buffer (this step was repeated 3 times). After the pellet wash, 100 µL of 5X SDS loading buffer was added to the pellet and boiled for 5 minutes at 95^{o} C to denature proteins. Finally, the mixture was subjected to Protein separation (SDS-PAGE), transfer, and antibody incubations and quantifications as illustrated in section 2.4.

4.3 Results:

4.3.1 Effect of endocytotic pathway inhibitors on size, number and turnover of focal adhesions

4.3.1.1 Effect of endocytotic pathways inhibitors on size and number of focal adhesions

The previous results of this project showed that inhibition with Dynasore or Pitstop2 reduced cell migration. It is possible that these inhibitors may affect focal adhesion organization. To test this possibility the effect of these inhibitors on focal adhesions using (Paxillin or Vinculin as markers of focal adhesions), the size and number of focal adhesions were assessed using immunocytochemistry.

MDA-MB-231 cells were treated with two endocytotic inhibitors at varying concentrations and incubation times (20 μM Dynasore for 30 minutes, Pitstop2 25μM for 15 minutes and DMSO for 30 minutes) and subsequently fixed and immunostained for either Paxillin or Vinculin. Images were taken on a Nikon-AIR confocal microscope and analysed in ImageJ for focal adhesion size and number.

Control cells (DMSO treated) showed that the mean size of the focal adhesions containing paxillin was 0.57 ± 0.028 μm^2, while the mean number was 46.52 ± 4.77 per/ cell (Figure 4.2 A and B). In Dynasore treated cells, on the other hand, there was a significant increase in the size of focal-adhesions containing Paxillin to 0.94 ± 0.18 μm^2 (* $p<0.05$). Importantly, the number of focal adhesions containing Paxillin also increased significantly by 2 fold to 89.65 ± 9.05 per cell (** $p<0.01$).

In the control cells (DMSO), the results showed that the mean size of the focal adhesions containing Vinculin was 1.42 ± 0.25 um^2, while the mean number was 34.10 ± 1.05 per cell Figure 4.3 A and B. However, in Pitstop2 treated cells there was no significant increase in size of focal adhesions containing Vinculin with a mean focal area of 1.74 ± 0.35 um^2 ($p>0.05$). While the number of focal adhesions containing Vinculin increased significantly to 43.23 ± 2.22 per cell (* $p<0.05$).

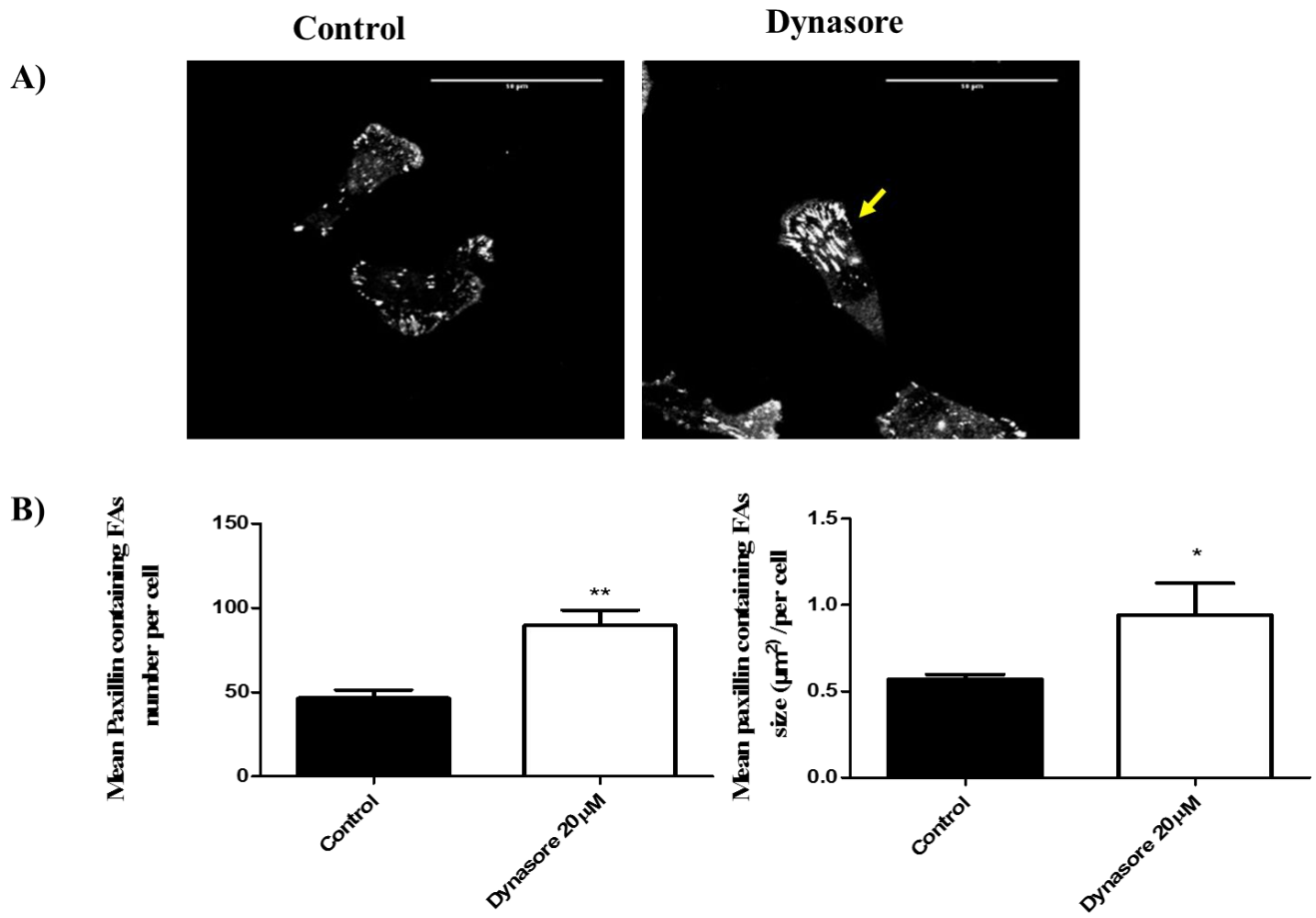

Figure 4. 2 Dynasore increased Paxillin containing focal adhesions number and size in MDA-MB-231.

Cells were treated with control (DMSO) or 20 µM Dynasore for 30 minutes, fixed and subjected to immunocytochemistry staining. A) Confocal images showing Paxillin containing focal adhesion in control compared to Dynasore inhibitor. Yellow arrow illustrates the focal adhesions containing Paxillin. Scale bar 50µm. B) Graphs showing the mean number and size of Paxillin containing focal adhesions. Graphs represent the mean ± standard error of three independent experiments, in each experiment at least 40 cells were analysed. T test used to compare the treatment with control. Statistical significance differences were accepted at * $p<0.05$ ** $p<0.01$.

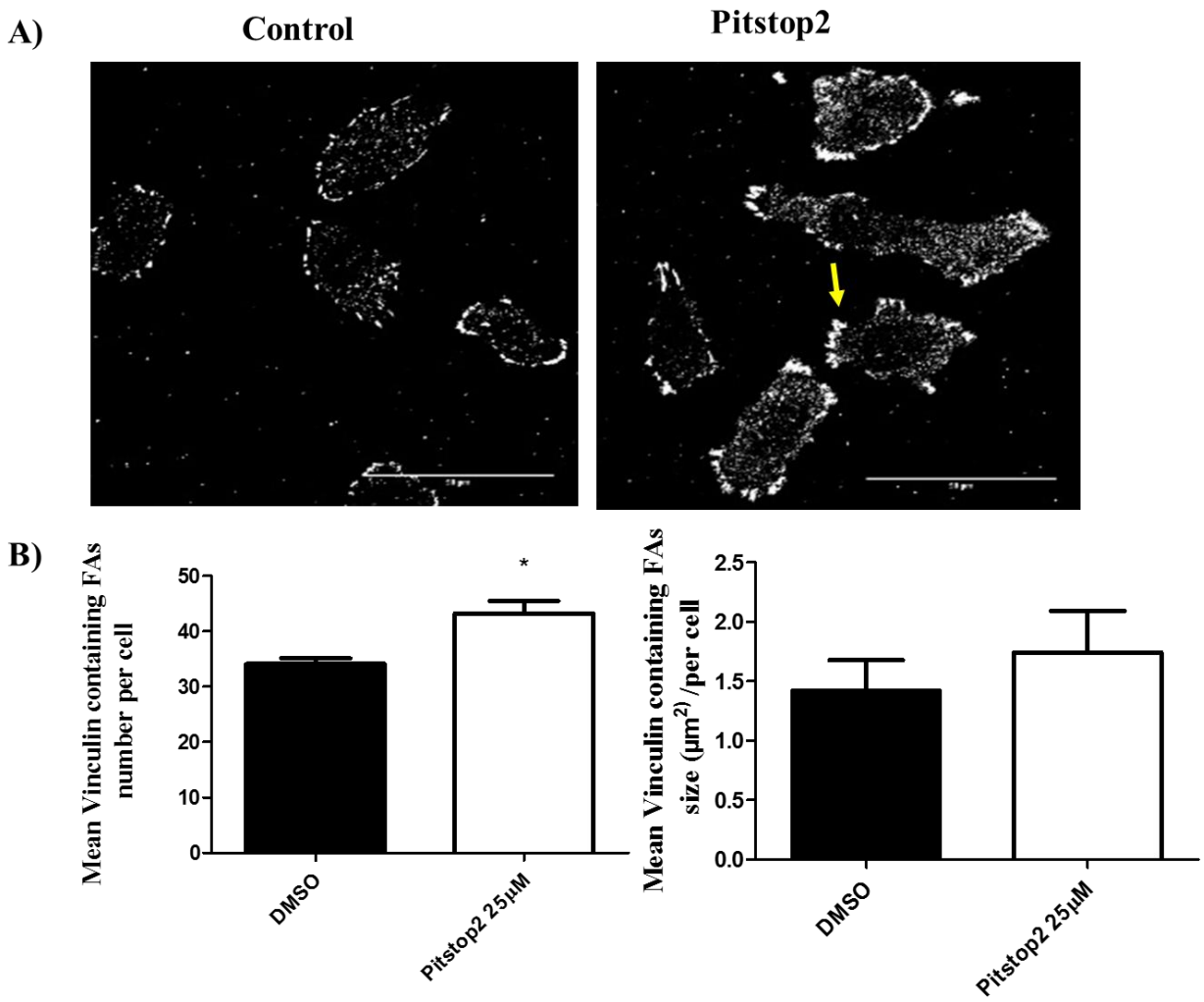

Figure 4. 3 Pitstop2 increased Vinculin containing focal adhesions number but not size in MDA-MB-231.

Cells were treated with control (DMSO) or 25 µM Pitstop2 for 15 minutes, fixed and subjected to immunocytochemistry staining. A) Confocal images showing Vinculin containing focal adhesion in control compared to Pitstop2 inhibitor. Yellow arrow illustrates the focal adhesions containing Vinculin. Scale bar 50µm. B) Graphs showing the mean number and size of Vinculin containing focal adhesions. Graphs represent the mean ± standard error of three independent experiments, in each experiment at least 40 cells were analysed. T test used to compare the treatment with control. Statistical significance differences were accepted at * $p<0.05$ ** $p<0.01$.

To further confirm the effect of these inhibitors with respect to size and number of focal adhesions containing vinculin, the HT1080 cell line was examined. The quantification analysis revealed that both inhibitors significantly increased the mean number of focal adhesions containing Vinculin, as shown in figure 4.4 A and B; the mean number was 36.45 ± 1.28 per cell in untreated cells, compared with 52.64 ± 4.47 per cell (* $p<0.05$) and 63.53 ± 3.42 per cell (** $p<0.01$) in Dynasore and Pitstop2 treated cells, respectively. Consistent to what was observed in MDA-MB-231, only the Dynasore inhibitor significantly increased the size of focal adhesion containing Vinculin and was 1.314 ± 0.095 um^2 (** $p<0.01$) compared to 0.831 ± 0.043 um^2 and 0.789 ± 0.0353 um^2 in DMSO and Pitstop2 treated cells, respectively.

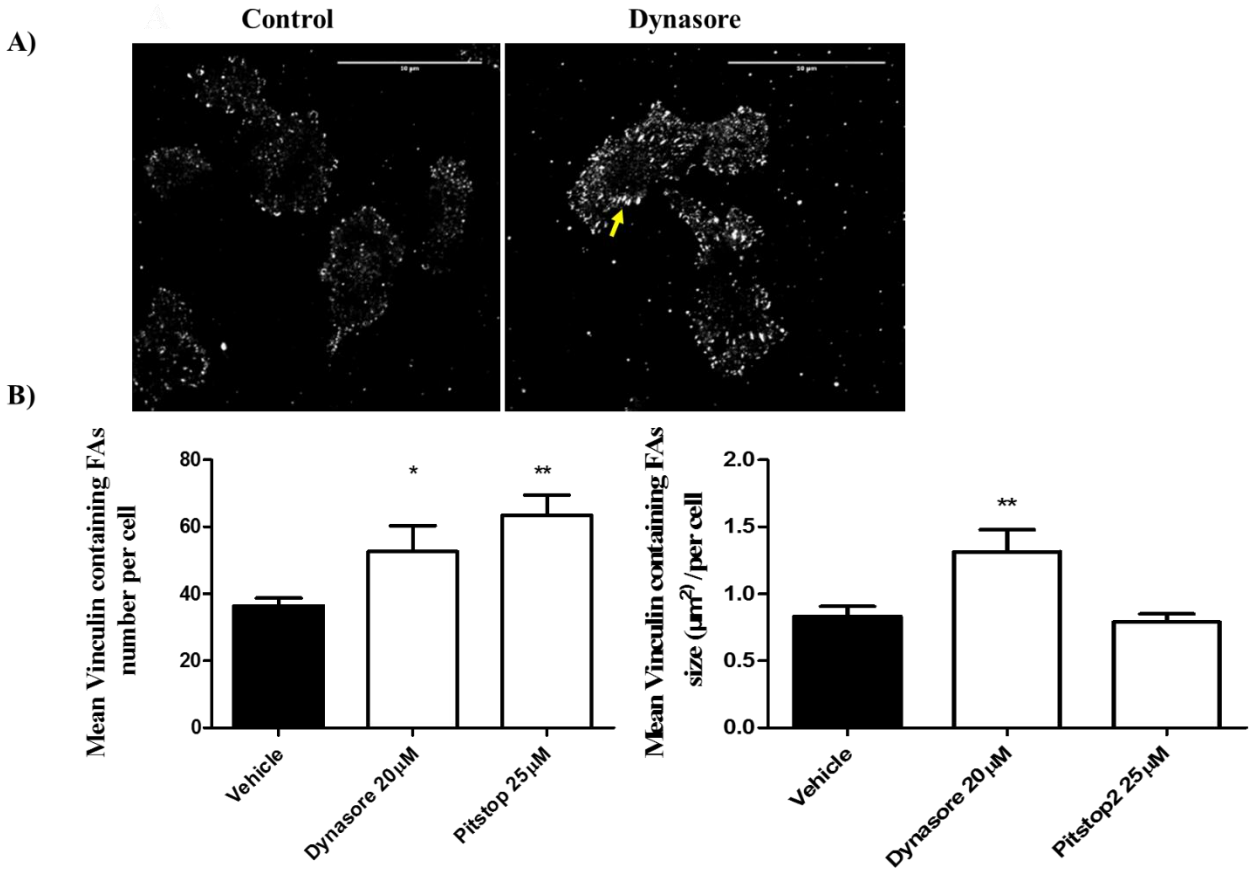

Figure 4. 4 Effect of Pitstop 2 and Dynasore on Vinculin containing focal adhesions number and size in HT1080

Cells were treated with Vehicle (DMSO) or different endocytotic pathways inhibitors at different times, fixed and subjected to immunocytochemistry staining. 20 µM Dynasore and 25 µM Pistop2 were incubated 30 minutes and 15 minutes, respectively. A) Confocal images showing Vinculin containing focal adhesion in control compared to Dynasore inhibitor. Yellow arrow illustrates the focal adhesions containing Vinculin. Scale bar 50µm. B) Graphs showing the mean number and size of Vinculin containing focal adhesions in control compared to Dynasore or Pitstop2. One-way ANOVA with Dunnett's Multiple Comparison Test were used to compare each treatment with the control. Graphs represent the mean ± standard error of three independent experiments, in each experiment at least 60 cells were analysed. Statistical significance differences were accepted at * $p<0.05$ ** $p<0.01$.

4.3.1.2 Effect of endocytosis inhibitors pathways on zyxin containing focal adhesion turnover

To further characterise the effect of Dynasore and Pitstop2 on focal adhesions dynamics, live cell transfection with mCherry-Zyxin for turnover analysis were performed.

MDA-MB-231 cells were seeded on ibidi 50 plastic surface and allowed to attach to the bottom of the plate overnight. When the plate became 60% confluent, cells were transfected with mCherry-Zyxin and then treated with Dynasore 20 µM for 30 minutes, or Pitstop2 25µM for 15 minutes or DMSO for 30 minutes. Subsequently, after the incubation period, the media containing inhibitors was replaced with fresh media containing 10%FBS. Finally, cells were directly subjected to confocal time lapse analysis using excitation 568nm to visualize the mCherry-Zyxin. The live cell imaging of mCherry-Zyxin turnover were monitored by taking images every 5 seconds for 10 minutes. The average life time of Zyxin was determined by measuring the intensity of Zyxin cycle turnover in imageJ. The quantification analysis revealed that both inhibitors significantly increased the turnover time of mCherry-Zyxin (Figure 4.5A). As shown in figure 4.5B, the mean turnover time was 38.11 ± 1.653s in untreated cells, compared with 63.71 ± 4.139 (** $p<0.01$) and 90.85 ± 3.694 (***$p<0.001$) in Dynasore and Pitstop2 treated cells, respectively (Figure 4.4 A and B).

In addition, different cell surfaces (gelatine and collagen) were used to confirm the influence of Dynasore and Pitstop2 on the turnover of focal adhesions containing Zyxin. In this case, the MDA-MB-231 cells were seeded on the top of two different surfaces, 0.2% gelatine or 2mg/ml collagen, and the mCherry-Zyxin turnover and treatment was carried out as described above. Similarly, to what was observed on plastic surfaces the average turnover of mCherry-Zyxin containing focal adhesions on 0.2% gelatine was 41.76 ± 9.41s and 42.29 ± 11.17s on 2mg/ml collagen in control compared to 95.94 ± 5.029s (* $p<0.05$) and 129.9 ± 19.56s (** $p<0.01$) on 0.2% gelatine or 83.80 ± 4.658 (* $p<0.05$) and 99.45 ± 8.798s (** $p<0.01$) on collagen when treated with Dynasore and Pitstop2,

respectively (Figure 4.5 C and D). To further confirm the effect of the influence of Dynasore and Pitstop2 on the focal adhesions containing Zyxin turnover across cell lines, the HT1080 cell line in plastic surface was included. Consistent to the observations in MDA-MB-231, Dynasore and Pitstop2 inhibitors significantly increases the average turnover of mCherry -Zyxin (Figure 4.4 D).

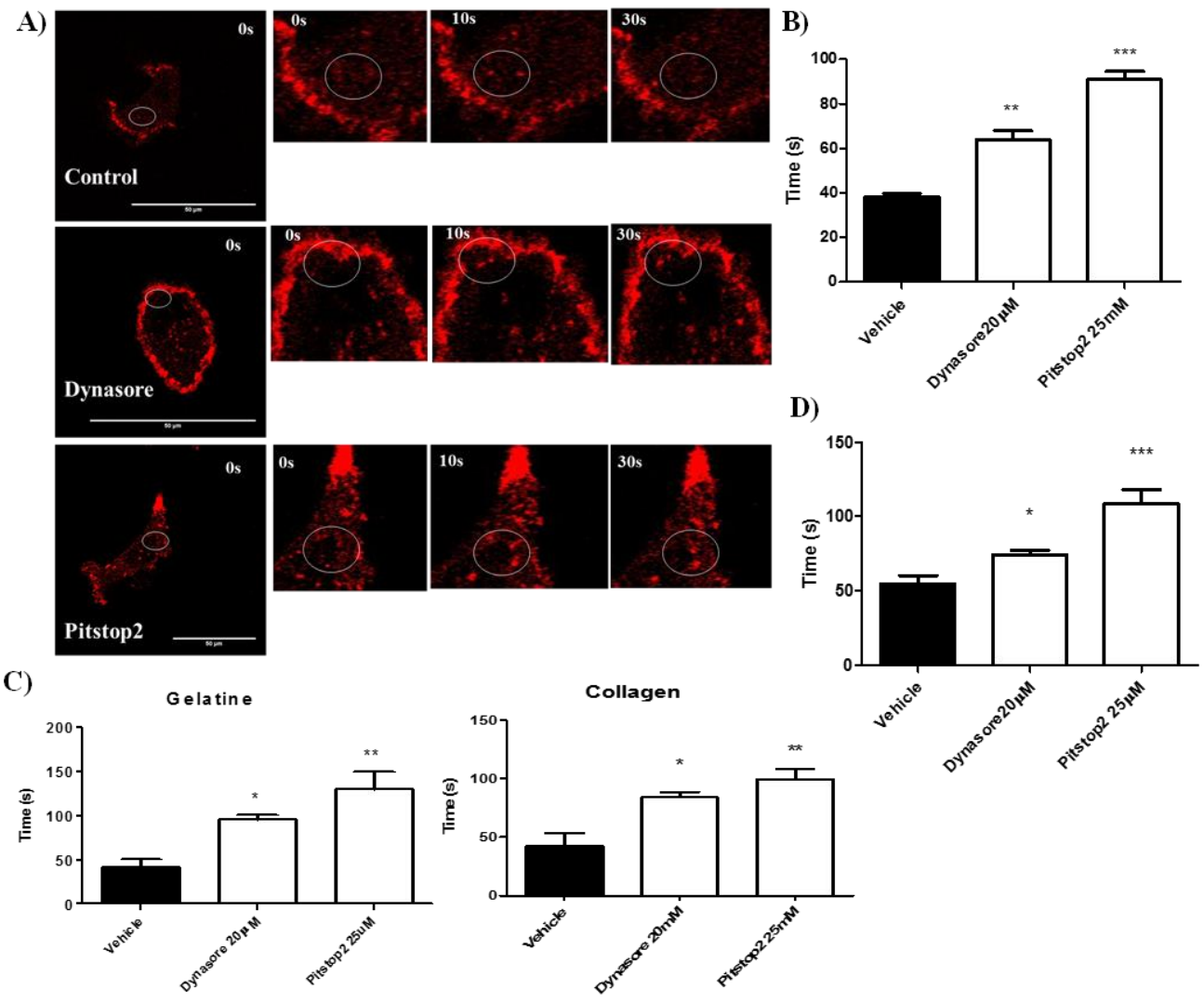

Figure 4. 5 Pitstop2 and Dynasore increased zyxin containing focal adhesions turnover in Live MDA-MB-231 and HT1080 cells.

Cells were plated in different cell surfaces (plastic, gelatine and collagen), transfected with mCherry-Zyxin, treated with Control (DMSO) or different endocytotic pathways inhibitors at different time points (20 µM Dynasore 30 minutes or 25 µM Pistop2 15 minutes) and subjected to live cell imaging. Images were captured every second for five minutes. A) Confocal images showing mCherry- Zyxin containing focal adhesion turnover in control compared to Dynasore or Pitstop2 inhibitors in MDA-MB-231 cells. White circle illustrates zyxin containing focal adhesion turnover. Scale bar 50µm. B) Graph showing the mean turnover time of zyxin containing focal adhesions in control compared to Dynasore or pitstop2 inhibitors in plastic surfaces for MDA-MB-231. C) Graphs showing the mean turnover time of zyxin containing focal adhesions in control compared to Dynasore or Pitstop2 inhibitors in gelatine or collagen surfaces for MDA-MB-231. D) Graph showing the mean turnover time of zyxin containing focal adhesions in control compared to Dynasore or Pitstop2 inhibitors in plastic surfaces for HT1080. One-way ANOVA with Dunnett's Multiple Comparison Test were used to compare each treatment with the control. Graph represents the mean ± standard error of 24 cells (100 focal adhesion) from three independent experiments. Statistical significance differences were accepted at * $p<0.05$, ** $p<0.01$ and ***$p<0.001$.

4.3.2 Association between endosomes and focal adhesions

In order to investigate the potential link between early endosomes and focal adhesions, it is important to assess firstly the localizations of endosomes. To test this, the localisation of early endosome antigen EEA1 with Rab5 or LAMP1 were assessed using immunocytochemistry. The co-localization values were analysed by Spearman's (rho) correlation coefficient analysis, through a selection of the region of interest using ImageJ.

4.3.2.1 Association between Early endosome antigen (EEA1) and Rab5

MDA-MB-231 cells that had been transfected with GFP-Rab5 were fixed and immunostained for EEA1. The results show that 90.3% of EEA1 protein co-localised with GFP-Rab5, demonstrating a high co-localisation value of 0.89 ± 0.017. Similarly, the reverse co-localisation value between GFP-Rab5 and EEA1 scored a high co-localisation value 0.83 ± 0.055 with 87% of EEA1 and GFP-Rab5 being co-located (Figures 4.6 and Table 4.1). The co-localisation suggests that Rab5 association with early endosomes (EEA1) is not affected during cell migration. It also indicates that GFP-Rab5 is a specific target of the early endocytosis pathway.

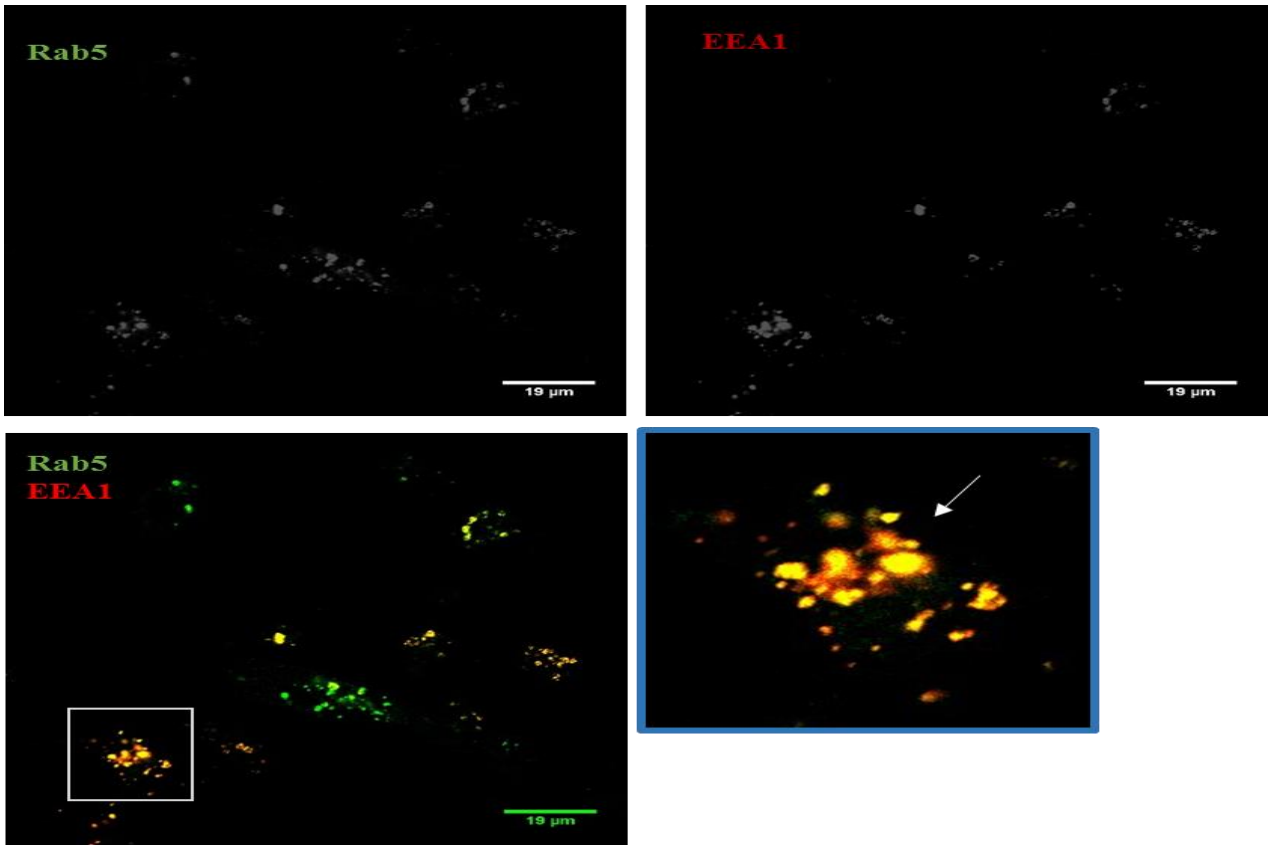

Figure 4. 6 Co-localization between Early endosome (EEA1) and GFP-Rab5

Confocal images of co-localization between GFP-Rab5 and EEA1 in MDA-MB-231 cells. Cells were transfected with GFP-Rab5, fixed and subjected to immunocytochemistry for EEA1 antibody. The co-localisation of GFP Rab5 (green) with the early-endosome marker EEA1 (red) was measured through selection ROI (region of interest) using Spearman's (rho) correlation coefficient analysis. The area highlighted in blue illustrates a magnification of the co-localization and is pointed out with a white arrow. Scale bar 19µm. Three independent experiments were performed.

Table 4. 1 Association between Early endosome antigen and GFP-Rab5

Table summarizing the mean number, percentage and colocalization values ± standard deviation (SD) between endosome markers

protein	Number of positive endosomes	% of co-localization between EEA1 and GFP-Rab5	Spearman Correlation Coefficient Value	(+/- S.D)
EEA1	**15**	**90.3%**	**0.89**	**± 0.01747**
Rab5	**26.2**	**87%**	**0.83**	**± 0.05508**

4.3.2.2 Association between EEA1 and late endosome marker (LAMP1)

The MDA-MB-231 cells were fixed and immunostained for EEA1 and LAMP1. The results show that 40% of EEA1 was co-localised with LAMP1, having a co-localisation value of 0.71 ± 0.106. Similarly, the reverse co-localisation value between LAMP1 and EEA scored a co-localisation value of 0.65 ± 0.102 with 35% of endosomes co-localisations (Figures 4.7 and Table 4.2).

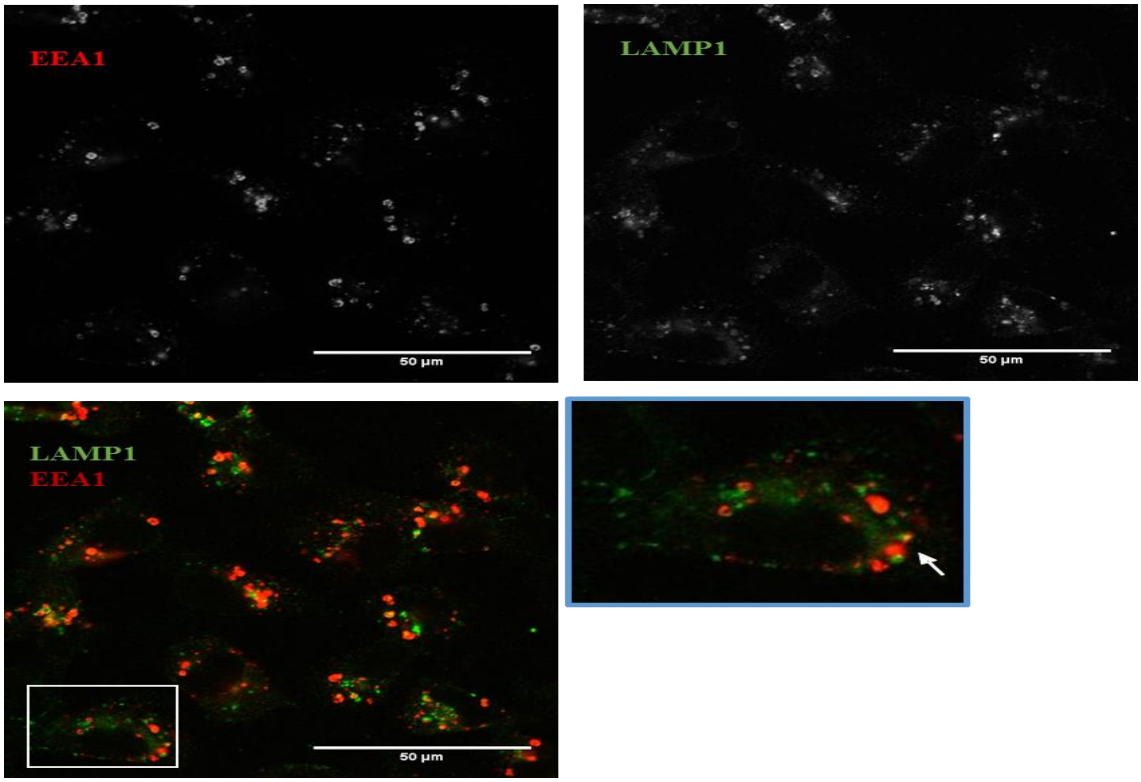

Figure 4. 7 Co-localization between Early endosome (EEA1) and late endosome (LAMP1) Markers

Confocal images of co-localization between EEA1 and LAMP1 in MDA-MB-231 cells. Cells were fixed and subjected to immunocytochemistry for EEA1 and LAMP1 antibodies. The co-localisation of LAMP1 (green) with the early-endosome marker EEA1 (red) was measured through selection ROI (region of interest) using Spearman's (rho) correlation coefficient analysis. The area highlighted in blue illustrates a magnification of the co-localization and pointed out with a white arrow. Scale bar 19µm. Three independent experiments were performed.

Table 4. 2 Association between Early endosome antigen and Late Endosome (LAMP1)

Table summarizing the mean number, percentage and colocalization values ± standard deviation (SD) between endosome markers

protein	Number of positive endosomes	% of co-localization between EEA1 and LAMP1	Spearman Correlation Coefficient Value	(+/- S.D)
EEA1	28	(11) 40%	0.71	± 0.1068
LAMP1	32	(11) 35%	0.65	± 0.102

4.3.2.3 Association between Early-Endocytosis Markers and Paxillin containing focal adhesion in fixed cells

To test the potential of early endosomes for targeting focal adhesion, immunocytochemistry was used to assess whether or not early endosomal markers (EEA1 or Rab5) associates with FA proteins. MDA-MB-231 cells were fixed and immunostained for both paxillin and either Rab5 or EEA1. The co-localization of EEA1 revealed that 9% of the endosomes contained paxillin (Spearman's (rho) correlation coefficient: 0.42 ± 0.078. The reverse approach showed that 6% of paxillin co-localized with EEA1 (estimated Pearson correlation: 0.34 ± 0.126; see Figures 4.8 and Table 4.3).

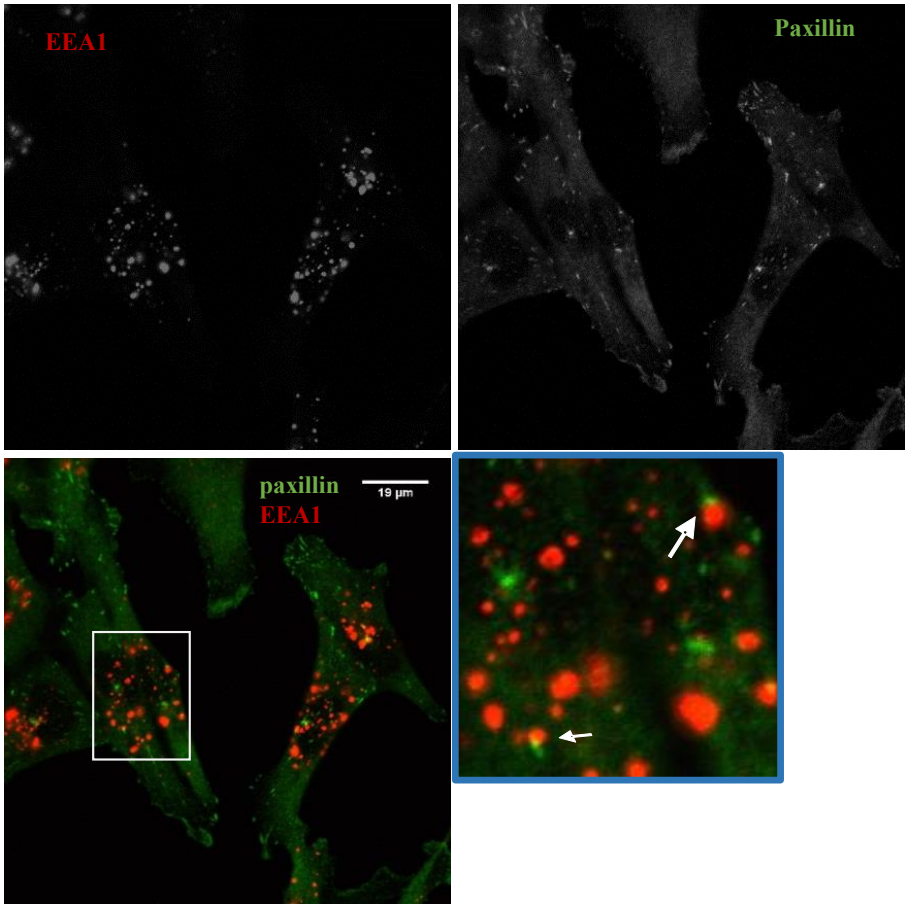

Figure 4. 8 Co-localization of early endosome (EEA1) and Paxillin

Confocal images of co-localization between Paxilin containing focal adhesion and EEA1in MDA-MB-231 cells. Cells were fixed and subjected to immunocytochemistry for EEA1 and Paxilin antibodies. The co-localisation of paxillin (green) with the early-endosome marker EEA1 (red) was measured through selection ROI (region of interest) using Spearman's (rho) correlation coefficient analysis. The area highlighted in blue illustrates a magnification of the co-localization and is pointed out with a white arrow. Scale bar 19µm. Three independent experiments were performed, in each experiment at least 10 cells were analysed.

Table 4. 3 Association between early endosome (EEA1) and Paxillin

Table summarizing the mean number, percentage and co-localization values ± standard deviation (SD) between endosome and Paxillin.

protein	Number of positive endosomes and Paxillin	% of co-localization between EEA1 and Paxillin	Spearman Correlation Coefficient Value	(+/- S.D)
EEA1	33	3 (9%)	0.42	± 0.078
Paxillin	54	3 (6%)	0.34	± 0.1263

The percentage of Rab5 containing endosomes colocalising with Paxillin was higher than that of EEA1 with Paxillin (25% and 15 %, respectively). In addition, Co-localization of Rab5 with Paxillin was higher than that of EEA1 with Paxillin (estimated Spearman's (rho) correlation coefficient: 0.58 ± 0.179 and 0.59 ± 0.173, respectively (Figures 4.9 and Table 4.4). Co-localization of early endosome markers with Paxillin does not reach similar values as observed for the co-localization between Rab5 and EEA1, suggesting only partial co-localization is occurring.

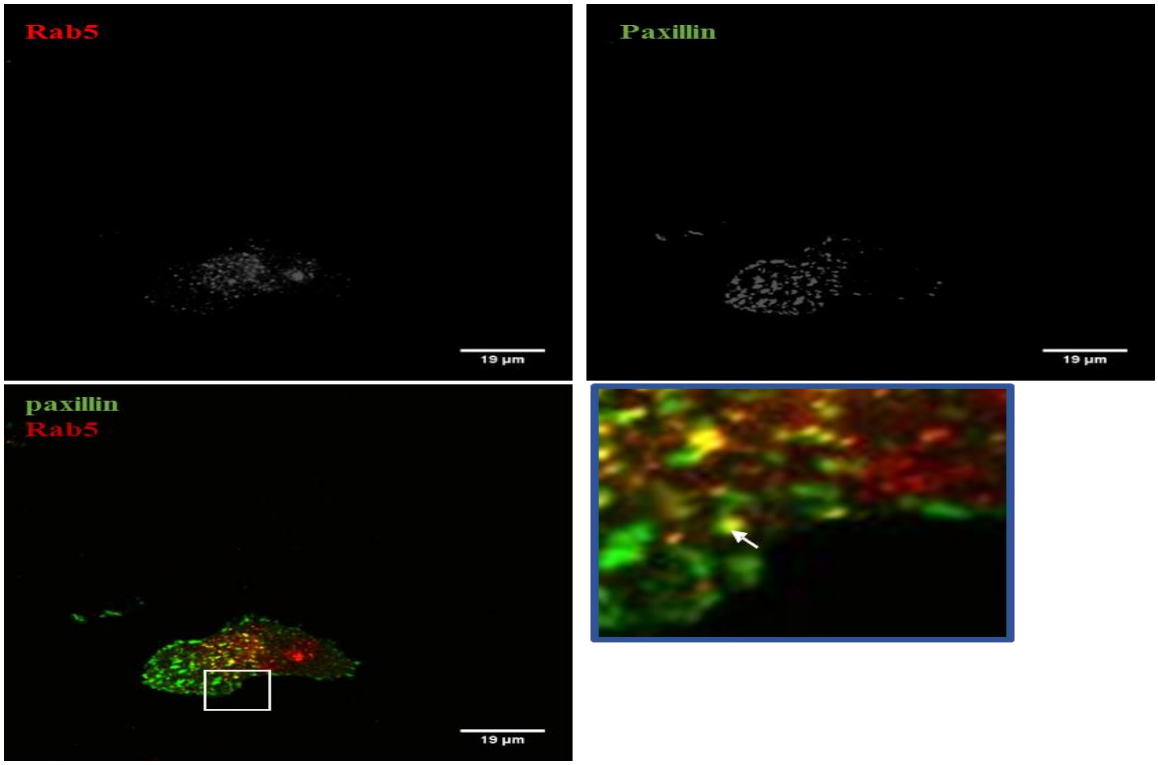

Figure 4. 9 Co-localization between Rab5 and Paxillin

Confocal images of co-localization between Paxillin containing focal adhesion and Rab5 in MDA-MB-231 cells. Cells were fixed and subjected to immunocytochemistry for Paxillin and Rab5 antibodies. The co-localisation of Paxillin (green) with the early-endosome marker Rab5 (red) was measured through selection ROI (region of interest) using Spearman's (rho) correlation coefficient analysis. The area highlighted in blue illustrates a magnification of the co-localization and is pointed out with a white arrow. Scale bar 19µm. Three independent experiments were performed, in each experiment at least 10 cells were analysed.

Table 4. 4 Association between Rab5 and Paxillin

Table summarizing the mean number, percentage and co-localization values ± standard deviation (SD) between Rab5 and Paxillin.

protein	Number of positive endosomes and Paxillin	% of co-localization between Rab5 and Paxillin	Spearman Correlation Coefficient Value	(+/- S.D)
Rab5	32.3	8 (25)%	0.59	± 0.173
Paxillin	45	8 (15)%	0.58	± 0.179

Since the internalization of transferrin receptors is considered to be a well-established method for visualizing endosome transport and recycling, it was sought to test whether transferrin can be enriched around or within the focal adhesion and early endosome markers. Thus, the association between focal adhesion proteins paxillin or vinculin and early endosomal markers (EEA1 or Rab5) within internalized transferrin was examined.

MDA-MB-231 cells that had been incubated with 25mg/ml transferrin conjugated to Alex Fluor 546 were fixed and immunostained for focal adhesions (Paxillin or Vinculin) and either Rab5 or EEA1. The results showed that the co-localization value of Paxillin with transferrin which co-localised with EEA1 were 0.6 ± 0.077 (Figures 4.10). Similarly, the co-localisation value of vinculin with transferrin which co-localised with GFP- Rab5 was 0.57 ± 0.09 (Figures 4.11).

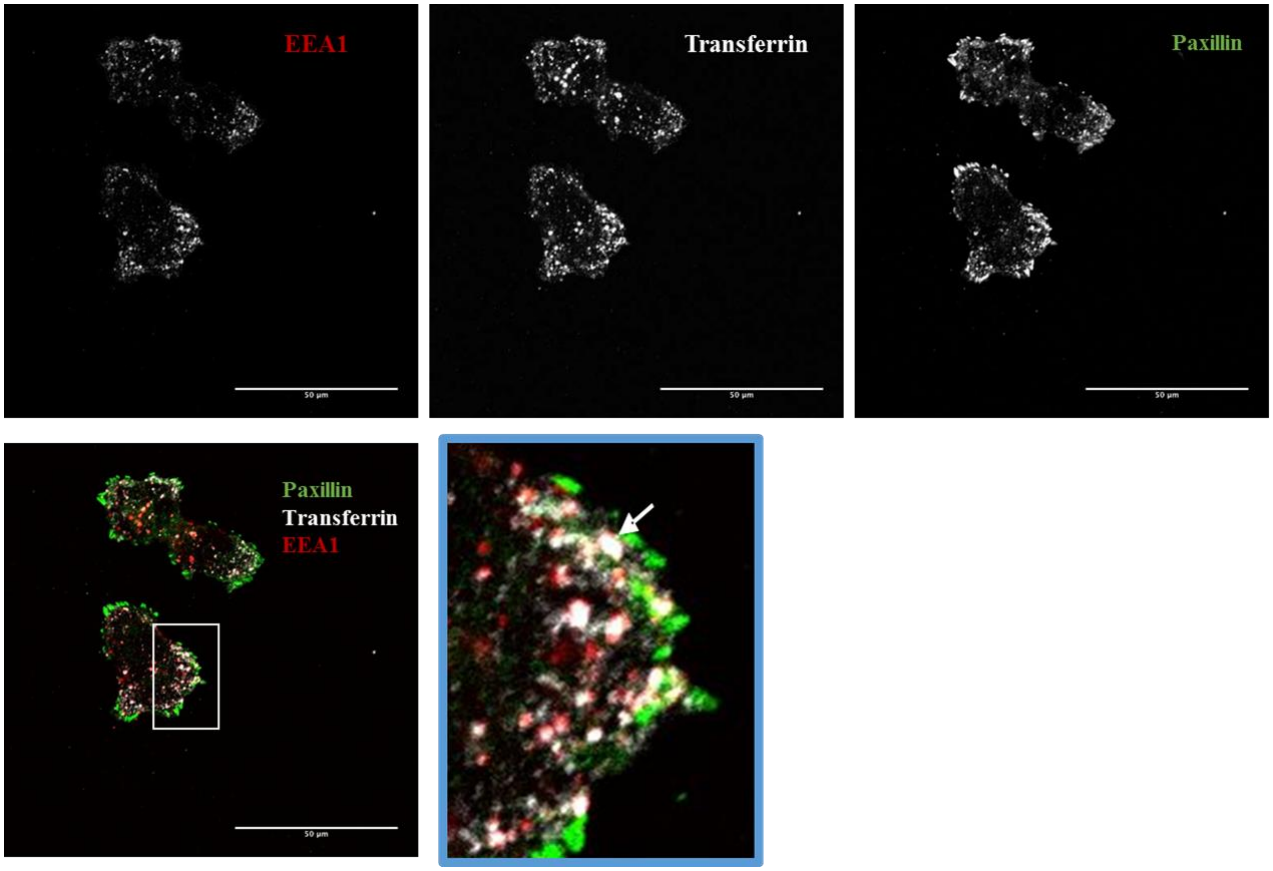

Figure 4. 10 Association of Paxillin containing focal adhesion with transferrin and EEA1

Confocal images of co-localization between Paxillin containing focal adhesion with transferrin and EEA1 in MDA-MB-231 cells. Cells were serum starved for 3h, incubated with 25 mg/ml Alexa Fluor 546 -conjugated transferrin for 30 minutes, fixed and subjected to immunocytochemistry for EEA1 and Paxilin antibodies. The triple co-localisation was measured through selection of a ROI (region of interest) using Spearman's (rho) correlation coefficient analysis. The area highlighted in blue illustrates a magnification of the co-localization and is pointed out with a white arrow. Scale bar 50µm. Three independent experiments were performed, in each experiment at least 10 cells were analysed.

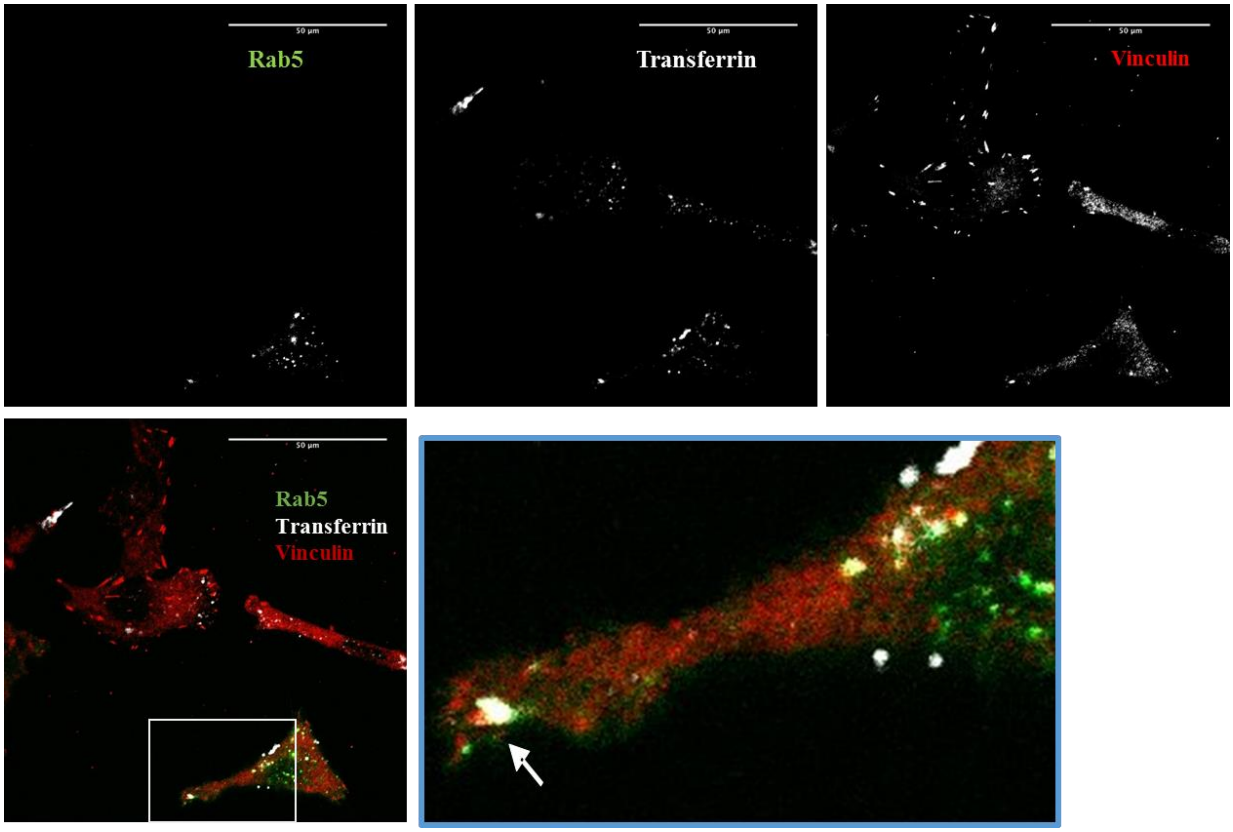

Figure 4. 10 Association of Vinculin containing focal adhesion with transferrin and EEA1

Confocal images of co-localization between Paxillin containing focal adhesion with GFP-Rab5 and transferrin in MDA-MB-231 cells. Cells were transfected with GFP-Rab5, serum starved for 3h, incubated with 25 mg/ml Alexa Fluor 546 -conjugated transferrin for 30 minutes, fixed and subjected to immunocytochemistry for Paxillin antibody. The triple co-localisation was measured through selection of a ROI (region of interest) using Spearman's (rho) correlation coefficient analysis. The area highlighted in blue illustrates a magnification of the co-localization area and is pointed out with a white arrow. Scale bar 50µm. Three independent experiments were performed, in each experiment at least 10 cells were analysed.

4.3.2.4 Association between Rab5 and focal adhesion in live cell co transfection:

To provide further evidence that focal adhesions are partially localized in early endosomes, live cell co-transfection was used to examine their co-localization with the early-endosome marker Rab5. MDA-MB-231 cells were co-transfected with both mCherry-Rab5 and GFP-Paxillin, and the subcellular localization was monitored by live confocal microscopy. Over 5 minutes, it was found that 35% of endosomes contained Paxillin (Spearman's (rho) correlation coefficient: 0.42 ± 0.038) and 23% of Paxillin was co-localized with Rab5 Spearman's (rho) correlation coefficient: 0.47 ± 0.059 (Figures 4.12 and Table 4.5).

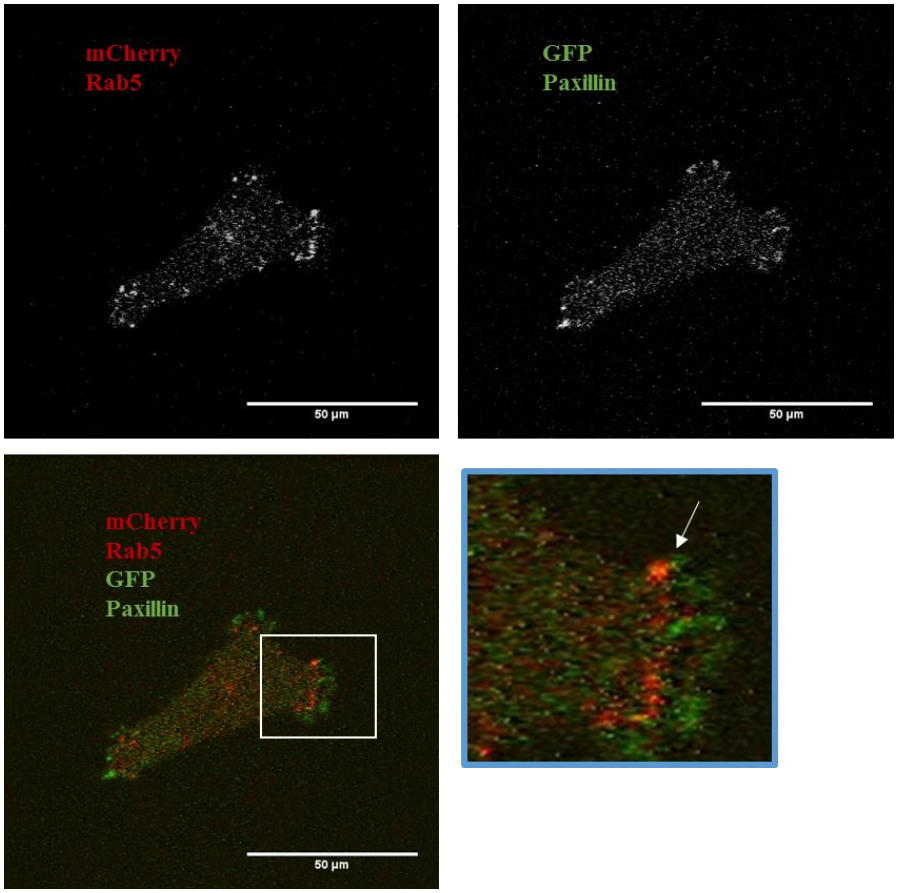

Figure 4. 11 Association between early-endocytosis markers and focal-adhesion molecules in live cells.

Live confocal imaging of mCherry-Rab5 with GFP-Paxillin over 5 minutes in MDA-MB-231 cells. The co-localisation of Paxillin (green) with the early-endosome marker Rab5 (red) was measured through selection of a ROI (region of interest) using Spearman's (rho) correlation coefficient analysis. The area highlighted in blue illustrates a magnification of the co-localization and is pointed out with a white arrow. Scale bar 50µm. Three independent experiments were performed, in each experiment at least 3 cells were analysed.

Table 4. 5 Association between early-endocytosis markers and focal-adhesion Paxillin in live cell

Table summarizing co-localization values ± standard deviation (SD) between mCherry Rab5 with GFP-Paxillin.

protein	Number of positive endosomes and paxillin	% of co-localization between mCherry-Rab5 and GFP-Paxillin	Spearman Correlation Coefficient Value	(+/- S.D)
mCherry Rab5	41	13 (32%)	0.47	± 0.05953
GFP Paxillin	57	13 (23%)	0.42	± 0.038

In addition, analysis of another focal-adhesion molecule mCherry-Zyxin, with GFP-Rab5 was performed to further confirm the observed co-localization pattern. Over 5 minutes, it was found that 40% of endosomes contained Zyxin (Spearman's (rho) correlation coefficient: 0.67 ± 0.0754) and 32% of the Zyxin was co-localized with Rab5 Spearman's (rho) correlation coefficient: 0.65 ± 0.043 (Figures 4.13 and Table 4.6).

This observation was further confirmed through the analysis of Rab5 and Zyxin co-localization over time. This was performed by taking 1 image every 5 seconds for 20 minutes. The results showed that the average live time of the co-localization between GFP-Rab5 and mCherry-Zyxin revealed to be 3.394 ± 0.985 minutes (Figures 4.13), suggest that focal adhesions are targeted by early endosomes.

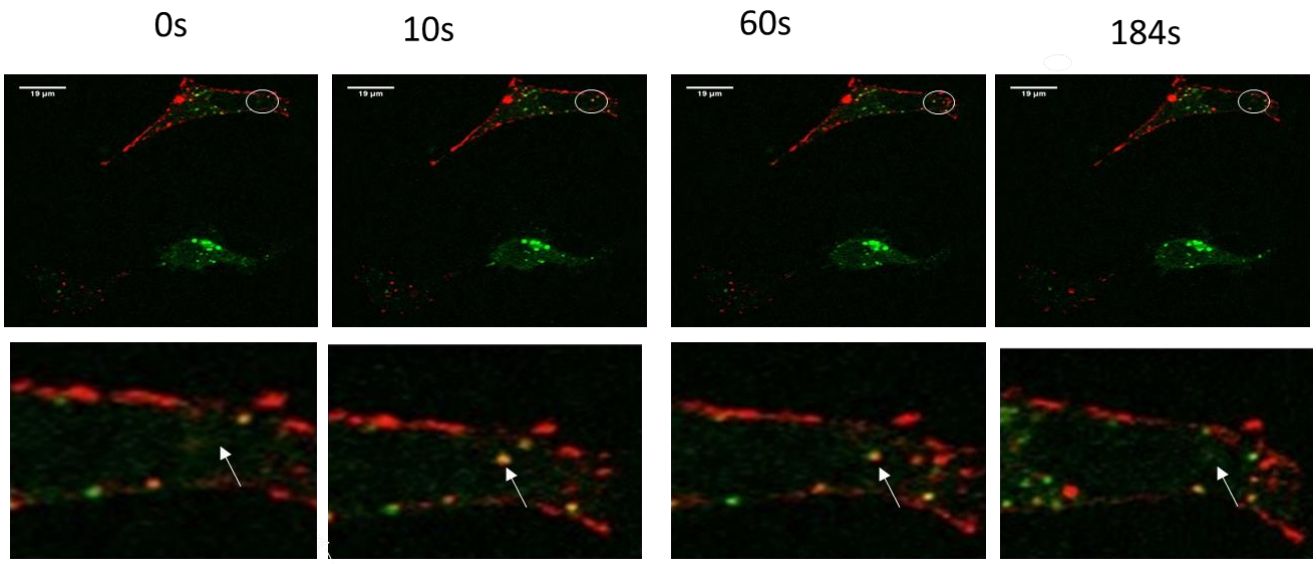

Figure 4. 12 Association between early-endocytosis markers GFP-Rab5 and focal-adhesion protein Zyxin

Live confocal images of mCherry-Zyxin with GFP-Rab5 over 5 minutes in MDA-MB-231 cells. The co-localisation of Zyxin (red) with the early-endosome marker Rab5 (green) was measured through selection of a ROI (region of interest) using Spearman's (rho) correlation coefficient analysis. The highlighted area illustrates the co-localization and the average time that both adhesion and endosomes interaction collapses, and pointed out with a white circle. Three independent experiments were performed, in each experiment at least 3 cells were analysed. Scale bar 19um.

Table 4. 6 Association between early-endocytosis markers and focal-adhesion Zyxin in live cells.

Table summarizing co-localization values ± standard deviation (SD) between GFP-Rab5 and mCherry-Zyxin with GFP-Rab5.

protein	Number of positive endosomes and zyxin	% of co-localization between mCherry-Zyxin and GFP-Rab5	Spearman Correlation Coefficient Value	(+/- S.D)
mCherry Zyxin	37	15 (40%)	0.67	± 0.0745
GFP Rab5	47	15 (32%)	0.65	± 0.043

4.3.2.5 Association between endosomes and focal adhesions using cell fractionation and immuno-precipitation

Having provided evidence that endosome co-localise with focal adhesion proteins in fixed and live cells, the association between endosome and focal adhesions were further investigated using cell fractionation with Percoll gradients and immunoblotting.

4.3.2.5.1 Isolating endosomes by a cell fractionation assay using a Percoll gradient

In order to identify the early and late endosome organelles and determine the proteins that associated with them, two cell lines MDA-MB-231 and HT1080 were centrifuged and homogenized to produce the Post Nuclear Supernatant (PNS). Subsequently, the PNS were subjected to Percoll centrifugation, followed by collecting nine fractions manually (1 ml for each fraction) starting from the top of the gradient stepwise in 1 ml samples from top to bottom. The collected fractions were equally loaded and analysed by SDS-PAGE / western blotting against the organelle markers, which included early endosomal markers (EEA1 and Rab5), Late endosomal compartment markers (LAMP1), Focal adhesion proteins (Vinculin, FAK, Talin, Zyxin and Paxilin), and nuclear proteins H2B (control). This study was also designed to monitor other proteins that have been suggested to be associated with both endosomes and focal adhesions and these proteins were AKT, Actin and GAPDH.

The western blot analysis of MDA-MB-231 revealed that all endosomal organelles were concentrated only in the fractions 3 and 4 with less expression of LAMP1 and Rab5 in fraction 5, compared to the control H2B which showed no band detected in these three fractions (Figure 4.14).

On the other hand, the focal adhesion protein vinculin was found in all fractions but the majority of it was concentrated in fraction 3 and fraction 9. Proteins such as FAK, Zyxin, Talin were found in the same fractions as endosomes as well as fraction 9. The expression of other proteins including Actin, AKT and GAPDH were similar to what was observed with vinculin but with less expression for AKT

in the last three fractions. Finally, the negative control H2B was concentrated in the same fraction (9) that most of the adhesions concentrated.

To further confirm the isolating of endosomal organelles and its association with other proteins, cell fractions were performed on HT1080 cell lines (Figure 4.15). Similar to what has been observed in MDA-MB-231 cells, EEA1 was concentrated in the first two fractions. Furthermore, focal adhesions and other proteins were concentrated on all fractions but with less expression on fraction 9 compared to MDA-MB-231. Finally, the concentration of nuclear proteins H2B was similar to what was observed in MDA-MB-231 cells but with less intensity detected in fraction 9.

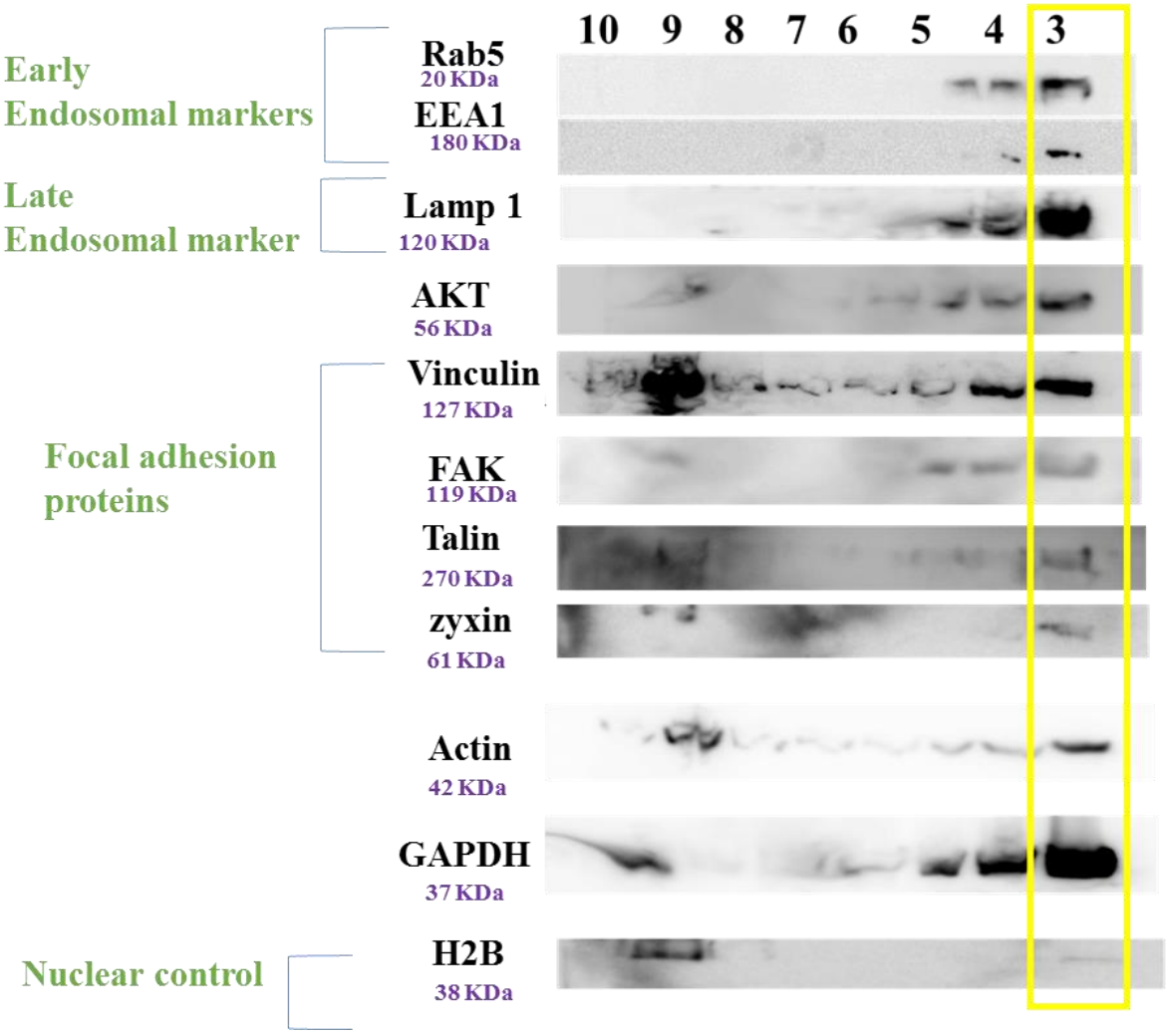

Figure 4. 13 Distribution of proteins in Percoll fractions from MDA-MB-231 cell lysates

Western blot images showing the presence of proteins in cell fractions from a Percoll gradient of MDA-MB-231 cell lysates. Equal volumes from each fraction of Post Nuclear Supernatant (PSN) were subjected to immunoblotting against Early endosomal markers (EEA1) and Rab5, Late endosome marker (LAMP1), focal adhesions proteins (Vinculin, FAK, Talin and Zyxin), nuclear protein (H2B) and other proteins (Actin, AKT and GAPDH). Yellow box highlights fraction three. n= two independent experements.

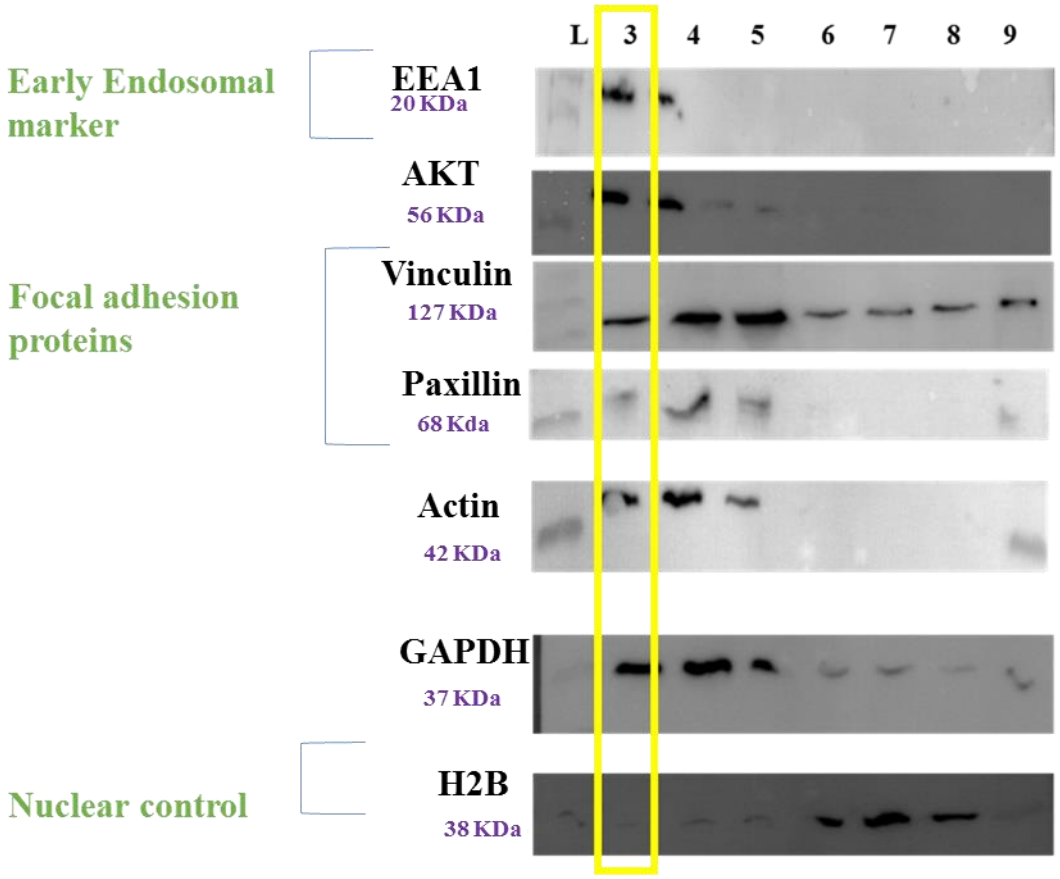

Figure 4. 14 distribution of proteins using continues Percoll in HT1080

Western blot images showing the presence of proteins in cell fractions from a Percoll gradient of HT1080 cell lysates. Equal volumes from each fraction of Post Nuclear Supernatant (PSN) were subjected to immunoblotting against Early endosomal markers (EEA1) and Rab5, Late endosome marker (LAMP1), focal adhesions proteins (Vinculin, FAK, Talin and Zyxin), nuclear protein (H2B) and other proteins (Actin, AKT and GAPDH). Yellow box highlights fraction three. L: Ladder. n= two independent experements.

4.3.2.5.2 Co-immunoprecipitation of endosomes fraction 3 of MDA-MB-231 or HT1080 cells

Having demonstrated that endosomes and focal adhesion proteins are present in the same fractions, this suggests a potential interaction between them. It could be argued that these proteins might have a similar density and thereby would separate in the same fractions. Therefore, co-immunoprecipitation assays were performed from fraction 3, obtained from a Percoll gradient, where endosomes were isolated overnight using anti-rabbit monoclonal antibodies towards EEA1, Rab5, LAMP1 and IgG as control. After antibody – lysate incubation, the precipitated samples or PNS (fraction three control) were loaded onto SDS-PAGE and western blot analysis was performed using an anti-vinculin mouse antibody. In MDA-MB-231 cells, the result indicated that vinculin was found to co-immunoprecipitate with Rab5 (Figure 4.16 A) but not with EEA1 or Lamp1 (Figure 4.16 B and C). Interestingly, in HT1080 cells, vinculin was found to co-immunoprecipitate with all tested endosome markers (figure 4.17).

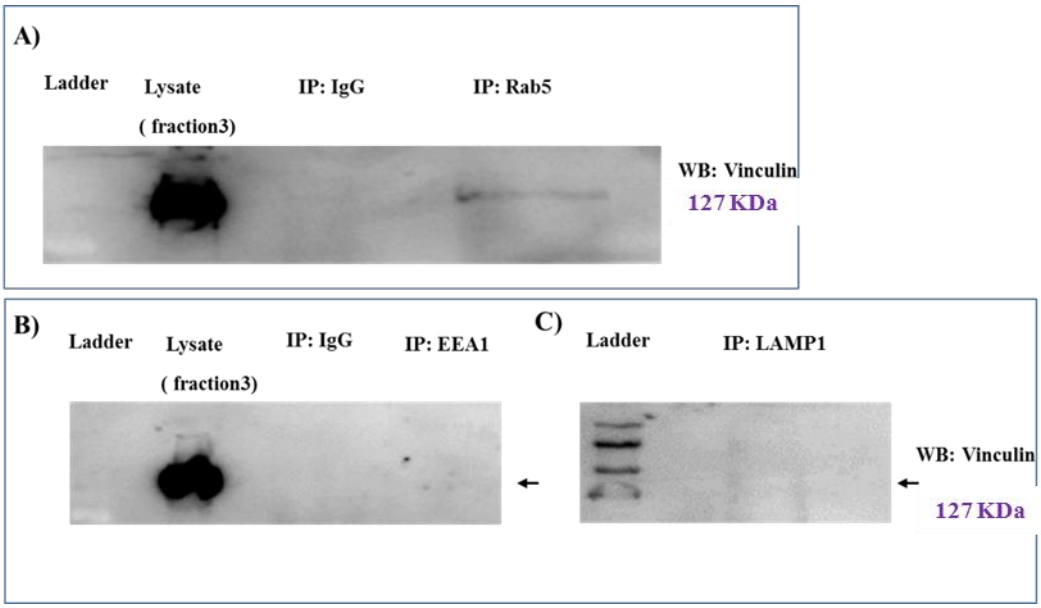

Figure 4. 15 Co-immunoprecipitation of endosomes from MDA-MB-231 Percoll fraction 3

Fraction three, which has been obtained from a Percoll gradient of MDA-MB-231 cell lysate, was incubated with primary antibodies or IgG overnight and precipitated by agarose beads. Precipitated proteins and lysate samples (fraction 3) were then subjected to SDS-PAGE, western blotted onto a PVDF membrane and primary mouse anti-vinculin added. Following this, the secondary antibody was used to detect anti-vinculin. A: Rab5 was precipitated from fraction 3 using anti-rabbit Rab5. B: EEA1 was precipitated from fraction 3 using anti-rabbit EEA1. C: LAMP1 was precipitated from fraction 3 using anti-rabbit LAMP1. IgG was precipitated from fraction 3 using anti-rabbit IgG. Three independent experiments were performed from fraction 3 PNS lysate.

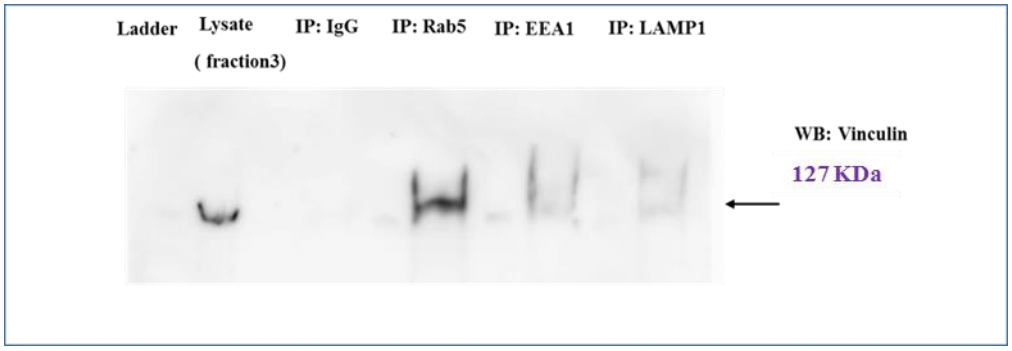

Figure 4. 16 Co-immunoprecipitation of endosomes from HT1080 Percoll fraction 3

Fraction three, which has been obtained from a Percoll gradient of HT1080 cell lysate, was incubated with primary antibodies or IgG overnight and precipitated by agarose beads. Precipitated proteins and lysate samples (fraction 3) were then subjected to SDS-PAGE, western blotted onto a PVDF membrane and primary mouse anti-vinculin added. Following this, the secondary antibody was used to detect anti-vinculin. Three independent experiments were performed from fraction 3 PNS lysate.

4.4 Discussion:

In order to determine whether the effects on cell migration by endocytosis inhibitors seen in chapter 3 was via regulation of focal adhesions, it was important to examine the effect of Dynasore and Pitstop2 on focal adhesion dynamics (number, size and turnover). Thus, immunocytochemistry analysis was carried out to examine the number and size of both Paxillin and Vinculin containing focal adhesions in two different cell lines. In addition, transfection of mCherry-Zyxin and live cell imaging was carried out to examine the turnover of focal adhesion on different surfaces.

The immunocytochemistry-based results obtained showed that both inhibitors (Dynasore and Pitstop2) significantly increase the number of paxillin and vinculin containing focal adhesions in two different cell lines (MDA-MB-231 and HT1080). Previous studies were consistent with our results in terms of effect of endocytosis and focal adhesion dynamics such as number. For example, inhibition of clathrin-mediated endocytosis by the inhibitor monodansylcadaverine markedly increased the number of focal adhesions formed by the human fibrosarcoma cell line HT1080. The authors further observed that other endocytosis inhibitors, such as filipin, which blocks lipid-raft-dependent endocytosis, had no effect on focal adhesion number (Chao and Kunz, 2009).

Other supporting evidence for the increase of focal adhesions number via clathrin dependent endocytosis was published using a microtubule depolymerisation drug as such nocodazole (Ezratty et al., 2009). Basically, once the drug was removed, microtubules grow and contact focal adhesions, which in turn enhance focal adhesion disassembly (Kaverina et al., 1999). Using this method, Ezratty and colleges found that knockdown of dynamin or clathrin heavy chain prevents the disassembly of focal adhesions after drug wash out as the number of focal adhesions increased compared to the control (Ezratty et al., 2009).

However, investigation of the effect of clathrin dependent endocytosis on focal adhesions turnover has not been investigated previously. Here, we examined the effect of both inhibitors on the turnover

of mCherry-Zyxin. To our knowledge, this was the first study that investigated the effect of Dyansore and Pitstop2 on focal adhesions turnover. The results showed that both inhibitors Dynasore and Pitstop2 in both cells lines (MDA-MB-231 and HT1080) significantly increased the turnover time of mCherry-Zyxin, which might slow down the cell speed. Therefore, this provides evidence that inhibition of endocytosis has an impact on focal adhesions dynamics, suggesting endocytosis may be important for the regulation of focal adhesions.

Taken together, Pitstop2 which completely blocks the endocytosis of transferrin, has a greater effect on both number and turnover of focal adhesions. It has been shown that clathrin and its adaptors (Numb and Dab2) bind to focal adhesions at the site where the focal adhesion dissembles (Ezratty et al., 2009). Indeed, both adaptors bind to integrin beta tail NPxY/NxxY motifs via its phosphotyrosine-binding (PTB) domains (Calderwood et al., 2003). It seems that failure in clathrin and its adaptor recruitment via Pitstop2 may lead to failed recruitment of focal adhesion complexes as well as proteins that require to dissemble focal adhesion complexes and thus results in more stable adhesion.

Our results show a significant effect on focal adhesion size upon Dynasore mediated inhibition suggesting Dynasore may delay focal adhesion maturation. This might be due to a dual role of GTPase activity of dynamin on clathrin coated pit maturation and clathrin coat vesicle formation (early and late stage of clathrin formation) (Mettlen et al., 2009). For example, the early stage of dynamin has been suggested to be self-assembled around the coat pit and the late stage is to catalase the membrane fission (Mettlen et al., 2009). The switch of dynamin from one function to another may affect the speed of clathrin maturation and delay focal adhesion complex recruitment. This seems a reasonable suggestion since the direct interaction of dynamin 2 and FAK has been reported in addition to the fact that dynamin directly binds to N-terminal FERM domain of FAK (Wang et al., 2011), potentially inducing focal adhesion maturation.

Based on the fact that focal adhesion dynamics such as FAK phosphorylation, adhesion morphology and composition can vary on different cell surfaces (Harunaga and Yamada, 2011) (Cukierman et al., 2001) (Hakkinen et al., 2011) and that different types of focal adhesions can form on different surfaces (Heino, 2000) (Grover et al., 2012). A further investigation was conducted to observe the potential impact of both inhibitors on focal adhesion turnover on gelatine and collagen surfaces. To our knowledge, this was the first study that has investigated the effect of Dynasore and Pitstop2 on focal adhesions turnover on surfaces coated with gelatine or collagen. Our data demonstrated similar effects to what was observed on plastic surfaces, mainly that both inhibitors increase the average turnover of focal adhesion containing Zyxin proteins on both gelatine and collagen surfaces, indicating that even with formation of different types of focal adhesions, these are still controlled by endocytosis. It also suggests that at least some of the focal adhesions are probably regulated and controlled by endocytosis.

In addition to blocking clathrin and dynamin dependent endocytosis, reduction in early endosomes could be another possible reason for increased focal adhesion number and turnover induced by both inhibitors. This is prompted by the observation in the previous chapter where both inhibitors (Dynasore and Pitstop2) reduced EEA1 expression, and Pitstop2 reduced Rab5 expression. There are several reasons why EEA1 and Rab5 expression may play a role in focal adhesion number and turnover. One possible reason could be the indirect effect of their expression on signalling molecules that are found on these endosomes and are necessary for dynamics of focal adhesions. For example, the non-receptor tyrosine kinase Src plays an important role in regulating a wide range of cellular functions including cell migration and cell adhesion (Frame, 2004). In cell migration, increased activity of Src kinase is believed to increase motility and proliferation in a number of human breast tumour cell lines such as human MCF7 breast tumour (Gonzalez et al., 2006). Similarly, in cell adhesion, Src and FAK are the two most important signalling proteins in regulating the focal adhesion dynamics. For example, in response to integrin engagements, both Src and FAK are recruited to the area where the focal adhesion complex is formed. This leads FAK to be autophosphorylated at tyrosine

residue Y379 which is believed to be an initial step in focal adhesion activation (Schaller et al., 1994a). Subsequently, autophosphorylation of FAK Y379 creates a high affinity to bind Src via its SH2 domain, which in turn phosphorylates FAK on multiple residues, Y576, Y577 and Y861, which recruits the focal adhesion complex (Calalb et al., 1995, Calalb et al., 1996, Schaller et al., 1994a). It is known that localization of Src is controlled by endocytotic trafficking, which is one important mechanism for regulating Src (Sandilands and Frame, 2008). For example, endocytic vesicles containing the small GTPase RhoB translocate the Src in an actin-dependent manner to the cell periphery (Sandilands et al., 2004). The inactive Src localizes to perinuclear endosomes, whereas active Src localizes to focal adhesions (Kaplan et al., 1994). It is possible that decreased early endosomes expression might impair endosome trafficking, and as result affect the translocation of Src to the site of focal adhesion which in turn affect FAK and focal adhesion dynamics. However, another study suggests that the trafficking of Src to focal adhesions requires the function of late endosomes regulated by the ESCRT pathway (Tu et al., 2010). As LAMP1 expression was not affected based on the observation in the previous chapter, this might rule out the involvement of early endosomes on Src localization at the site of focal adhesions. Therefore, future studies will be needed to dissect the specific contribution of early endosomes and late endosomes to Src localization.

The second possible reason for increased number and turnover time of focal adhesion other than the reduction of early endosome expression could be due to impairment of membrane trafficking. Using biochemical techniques, Bretsche showed that integrin endocytosis occurred from the cell surface and recycled back to plasma membrane (Bretscher, 1992). Later on, studies on neutrophils, lymphoid, cervical tumour cells and fibroblasts demonstrated that integrin-containing vesicles were observed in both cell rear and cell front and suggested that integrin is endocytosed from the rear of the cells and recycled to the front (Pierini et al., 2000) (Vacca et al., 2001) (Martel et al., 2000) (Pellinen et al., 2006). Rab5 interacts with these integrins and triggers its internalization as well as delivering it to the perinuclear site of the recycling compartment (Pellinen et al., 2006). From the recycling compartment,

integrin recycles via Rab4 from early endosome and back to plasma membrane near focal adhesion complexes and is suggested to reassemble new focal adhesion (Roberts et al., 2001b). It is therefore tempting to speculate that decreased expression of EEA1 or Rab5 inhibits integrin internalisation, resulting in increased focal adhesion numbers, indicative for a role in focal adhesion disassembly. In addition, the delay of focal adhesion turnover could be attributed to delayed integrin recycling and reassembling of new focal adhesions.

The third possible reason could be the direct effect of endosomes on focal adhesions and that might affect its dynamic. Therefore, we attempted to demonstrate firstly whether early endosome proteins co-localize with its markers (Rab5) or with late endosomes marker LAMP1. The results obtained here showed that 90% of EEA1 and 87% Rab5 co-localized, indicating that the GFP-conjugated Rab5 interacts with its correct tethering factor and can be classified as early endosomes (Merithew et al., 2003). Interestingly, 40% of EEA1 and 35% LAMP1 co-localized suggesting that LAMP1 can be found in both early endosomes and late endosomes. One possible explanation for the localization of LAMP1 with EEA1, is that a subset of LAMP1 might found in a later stage of early endosomes. For example, late endosomal markers (Rab7) regulates the trafficking between early and late endosomes. A study by Humphries et al quantified the co-localization of LAMP1 with Rab7 and found the majority (70 %) of LAMP1 co-localized with Rab7 (Humphries et al., 2011). Thus, it can be proposed that Rab7 may recruit some of the LAMP1 to the later stage of early endosomes.

Yet, the question remains whether endosomes interact with focal adhesion proteins and that may regulate focal adhesion turnover. Considering the accumulation of Rab5- early endosomes at the leading edge of migrating cells, it can be expected that early endosomes may interact with focal adhesions. Therefore, we attempted to demonstrate whether early endosome proteins co-localize with focal adhesion proteins. Our immunocytochemistry data showed low co-localisation correlation co-localization and that 9% of EEA1 co-localized with Paxillin. Similarly, the reverse co-localization

showed 6% of Paxilin co-localized with EEA1. Similar findings were observed in co-localization between EEA1 and α5 Intgerin and found a small percent of co-localization (Lobert et al., 2010).

In contrast, subcellular localization analysis of Rab5 with Paxillin showed a slightly higher co-localisation probability than seen between EEA1 and Paxillin. For example, we observed that 25% Rab5 and 15% Paxilin co-localized. One possible explanation for this difference is that EEA1 can be limited to early endosomes (Wilson et al., 2000), whereas, Rab5 can be found in both early endosomes and in the plasma membrane as it has been shown to be required for budding of vesicles from the plasma membrane (McLauchlan et al., 1998). Therefore, the localization of Rab5 with Paxillin was not as restricted to early endosomes as EEA1, and it can be localized on the cell surfaces (adhesion area). This is supported by the co-localization between focal adhesions (vinculin and FAK) and clathrin adaptors (Dab2, AP-1 and numb), which are believed to be found on both the cell surface and early endosomes (Ezratty et al., 2009). This might be a possible explanation for the increase in localization percentage between Rab5 and Paxillin.

The co-localization data was further supported by live-cell imaging between Rab5 and focal adhesions, and we found that over a period of five minutes 35% of Rab5 contained Paxillin, with a co-localization correlation value of 0.42. Similarly, live co-localization between Rab5 and other focal adhesions like Zyxin were found (0.67). Taken together, these observations indicate that focal adhesion proteins co-localized with early endosomes markers (Rab5 and EEA1), suggesting that Paxillin, vinculin and zyxin in focal adhesions are targeted by early endosomes

Although, not all endosomes have been found to be co-localized with FA but still they were found to be closely located to them. This observation of indirect contact but close proximity could be considered by three possibilities. One possibility is that focal adhesions interact with molecules that bind early endosomes. One of these molecules is the phospholipid phosphatidylinositol-4,5-bisphosphate (PtdIns[4,5]P2). PtdIns[4,5]P2 has been shown to be involved in focal adhesion formation, turnover and directly binds FAK at the FERM domain (Goñi et al., 2014). In addition, it

has been proposed to bind vinculin and controls its dynamics (Thompson et al., 2017). EEA1, in addition to being an effector for Rab5 (Christoforidis et al., 1999), has a region for interacting with phosphatidylinositol-4,5-bisphosphate (PtdIns[4,5]P2) (Simonsen et al., 1998). Interaction of PIP2 with EEA1 has been shown to be required for both clathrin endocytosis and endosome maturation (Simonsen et al., 1998) (Stenmark et al., 1996). Nevertheless, binding of EEA1 and Rab5 controls the production of PtdIns(4,5)P2 by stimulating the activity of PI3K, which in turn affect focal adhesion disassembly (Simonsen et al., 1998) (Goni et al., 2014). Therefore, it can be proposed that the close association between endosomes and focal adhesions might be dependent on PtdIns(4,5)P2 interaction due to the fact that PtdIns(4,5)P2 level is elevated at cell adhesion sites (Chandrasekar et al., 2005).

The second possibility might be that focal adhesions interact with proteins that bind early endosomes such as Zinc Finger FYVE-Type Containing 21 (ZFYVE21). ZFYVE21 is found within cytoplasmic vesicles and shares the FYVE domain that binds EEA1 (Stenmark et al., 1996). In addition to its binding ability to endosomes, this protein is found to directly bind focal adhesions and bind factors involved in focal adhesion dynamins (m-calpain and SHP-2) as well as carrying them via microtubules to the site where focal adhesion disassembly occurs (Nagano et al., 2011). Because ZFYVE21 associates with endosomes, it can be proposed that the close association between endosomes and focal adhesions might be ZFYVE21 dependent.

The third possibility could be that focal adhesions can be found inside the vesicles. Thus, the link between endosomes and focal adhesion were further examined using transferrin uptake studies which can be considered to be a good method for visualizing endosome transport and recycling through the clathrin pathway. Our immunocytochemistry data showed moderate co-localization correlation of paxillin or vinculin with transferrin, which is co-localised with EEA1 or GFP- Rab5. This observation may suggest that focal adhesions may be found with endosomes that required clathrin endocytosis.

This was further supported by recording the time interaction between Rab5 and Zyxin during co-localization. Notably, Zyxin turnover is on average between 30 to 60 (seconds). We found that the average co-localization time between Zyxin and endosomes was 3.3 minutes. Considering the fact that the total life time for clathrin coated pits is between 40 to 330 seconds (Yoshida et al., 2018). Also, the average lifetime (track duration) of GFP-Rab5 was 3.66 minutes and this was in agreement with previous studies (Rink et al., 2005). It can be suggested that focal adhesions need 3 to 5 minutes to be delivered from the plasma membrane to early endosomes compartments or to recycling compartments. However, further analysis is needed such as Z-stacking-timelapse to record the entire co-localization between these proteins in a more three dimensional manner.

The third possibility was further supported by separating endosome using a Percoll gradient of post-nuclear supernatant. The western blot results revealed that two early endosome markers concentrated at the third and fourth fraction and suggested there is in fact separation of early endosomes proteins using this technique. Also, this is supported by the absence of nuclear marker proteins suggesting a contamination free fraction of these endosomes with nuclear proteins/organelles and evidence that this Percoll fraction contains early endosomes. Similarly, late endosomal markers were found in the same fractions in which both early endosomes were present. This was expected, since late endosomes were shown earlier to be found localized with early endosomes. Also, many studies report an overlapping of early endosomes and late endosomes in endosome fractions (Balbis et al., 2007) (Tjelle et al., 1996).

This study also aimed to monitor involvement of other proteins such as AKT. The AKT pathway plays an important role in many cellular functions including cell proliferation, survival and migration (Altomare and Testa, 2005). In addition, it has been found to be upregulated in many human cancers including breast, prostate, ovarian and brain (Sun et al., 2001). In regard to cell migration, there is cross talk between AKT and FAK activation. For example, AKT directly interacts with FAK and

phosphorylates it at different residue sites including S517, S601 and S69 (Wang and Basson, 2011). Following phosphorylation of these site leads subsequently to FAK autophosphorylation at Y397, which is important for FAK activation (Wang and Basson, 2011). This binding promotes cell motility, and is found to regulate focal adhesion disassembly (Wang and Basson, 2011). In our study, the western blot results revealed that both AKT and FAK were found in early endosomes. This finding raises the possibilities that AKT activation and binding to FAK might occur in the endosomes and blocking endocytosis or inhibition of intracellular trafficking may prevent AKT activation. These possibilities were supported by Morisco who showed that Dynamin knock down prevented AKT activation (Morisco et al., 2008). In addition, depletion of early endosome marker APPL inhibits AKT activation/ phosphorylation (Tan et al., 2010). It seems that at a very early stage of endocytosis, AKT binds to the PTB domain of APPL1 (Mitsuuchi et al., 1999). This binding enhances AKT to move to early endosomes where EEA1 is found. EEA1 then facilitates the phosphorylation of AKT at both T308 and S473 (Nazarewicz et al., 2011). This in turn has been suggested to stimulate FAK and induce focal adhesion dynamics. It is worth mentioning that AKT activation can also require FAK activation. For example, inhibition of FAK activity negatively impacts both phosphorylation sites in AKT at S473 and FAK at Y397. Thus, the overall contribution of AKT and FAK on endosomes and that regulate focal adhesion should be investigated further in future studies.

The presence of FAK in endosome fractions was further supported by published data which show that FAK can directly bind endosomes and does not require integrin signalling (Alanko et al., 2015). This seems a reasonable result, as FAK does not directly bind to integrin tails but binds to Talin (Bachir et al., 2014). This binding facilitates the recruitment of focal adhesion complex including kindlin-2 , paxillin and vinculin, which is suggested to control cell motility (Theodosiou et al., 2016) (Lawson et al., 2012). In line with this, our result here showed that focal adhesions containing Vinculin, Paxillin, Zyxin and Talin were found in same fractions that endosomes were found in as well as FAK, indicating that signalling and scaffolding proteins i.e. (focal adhesions complex) are found in

endosomes. So, it can be suggested that endosomes transport non active forms of FAK near to the site where the focal adhesions are attached to cells (Choi et al., 2011). This leads to the activation of FAK on endosomes either via molecules that are found on early endosomes such as Src or via direct interactions between the FERM domain of FAK and vesicle membrane (type I phosphatidylinositol phosphate kinase) (Wang et al., 2011) (Chao et al., 2010). Subsequently, FAK recruits dynamin which is required for vesicle scission (Ezratty et al., 2005). Also, it binds to talin which facilities the recruitment of focal adhesion proteins including paxillin, vinculin and zyxine (Hu et al., 2014). This recruitment would suggest binding to endosomes. To verify this, co-immunoprecipitation data from endosome fractions indicated that vinculin was found to co-immunoprecipitate with Rab5 in both cell lines. Whereas, little co-immunoprecipitation of EEA1 or Lamp1 with vinculin in MDA-MB-231 and HT1080, respectively was observed. There is one possible explanation for the difference between cell lines. There could be varying amounts of EEA1 endosomes present during the subcellular fractions of both cell lines, as large amounts of EEA1 were observed in fraction three of HT1080 compared to MDA-MB-231. This idea is also supported by an increased co-immunoprecipitation band detected between Rab5 and vinculin in HT1080 compared to MDA-MB-231. Therefore, it is possible that amounts of EEA1 proteins in early endosomes of MDA-MB-231 were too low to be detected by co-immunoprecipitation, but sufficient to be detected in HT1080. In addition, this amount might also contain a subset of LAMP1 marker protein that is involved on a late stage of early endosomes as discussed earlier in this chapter and this may explain the observed co- immunoprecipitation of LAMP1 and vinculin. Since we noticed a large quantity of LAMP1 in the early endosomes fraction of MDA-MB-231 but this failed to co-immunoprecipitate with vinculin.

Internalization of integrins may modulate the focal adhesion complexes and lead to disassembly of focal adhesions (Paul et al., 2015). As long as the focal adhesions dissemble, the FAK and Talin scenario could occur at the recycling endosomes as FAK has been found to accumulate at the

perinuclear of recycling endosomes and is co-localized with Rab11 (a marker of recycling endosome) (Nader et al., 2016). From these results, it can be suggested that decreased expression of early endosome markers may impair trafficking of FAK. This in turn may lead to inhibition of FAK activation, and as a result prevents the recruitment of dynamin as well as focal adhesions paxillin, vinculin, zyxin and Talin. These findings could possibly indicate that early endosomes regulate focal adhesions turnover- possibly by delivering FAK to focal adhesions sites as well as recycling endosomes.

Another possible suggestion, independent of FAK trafficking, could be endocytosis of focal adhesions complexes. From our results, it can be hypothesized that the focal adhesions complex can be endocytosed. The invagination of the plasma membrane could surround the focal adhesions complex. This is based on the interactions between focal adhesions, dynamin and clathrin, which suggested that dynamin clustered around focal adhesions (Ezratty et al., 2009). In addition, clathrin coated pits have been reported to occur near focal adhesion areas (Cleghorn et al., 2014). These complexes may then be delivered to early endosomal compartments. This is consistent with our results that focal adhesions co-localise with early endosomes markers as well as with transported transferrin. Further, focal adhesion containing vesicles were detected with focal adhesion proteins appearing in both early endosomes and late endosomes fractions. Bioinformatics analysis supported this finding and indicates the presence of early endosomes markers EEA1 and Rab5 in isolated focal adhesion complexes (Horton et al., 2015). Taken together, these findings add to the growing body of evidence that focal adhesions complexes could be endocytosed and delivered to early endosomes. This scenario is possible, as paxillin has been reported to be targeted by late endosomes (Schiefermeier et al., 2014) and degraded via autophagy (Sharifi et al., 2016). Loss of function of autophagy causes enlargement of focal adhesions and leads to a reduction in cell migration, suggesting that there is a role for autophagy in focal-adhesion disassembly through the targeted degradation of paxillin (Sharifi et al., 2016). The same study also illustrates that the LC3-interacting region (LIR) of the autophagy marker

LC3 interacts with the LIR motif of paxillin, and both paxillin and LC3 co-localised on the cytosolic and at focal adhesions.

Early endosomes contribute to autophagosomes (Tooze et al.), and this may provide evidence that the early endosome might be involved in focal adhesion transport. However, some questions remain to be addressed, such as the mechanisms that regulate both early endosomes and focal adhesion turnover.

Chapter 5: Identifying signalling pathways affecting endocytic regulation of cell migration and focal adhesion turnover

5.1 Introduction:

Having confirmed that endocytosis, specifically the dynamin and clathrin pathways, regulate cell migration through regulating focal adhesion dynamics, the molecular signalling mechanisms that transduce this effect are still unknown. One mechanism that recently has been associated with endocytosis is nitric oxide.

Nitric oxide plays an important role in mediating a number of biological and physiological processes and these include controlling blood flow or blood pressure through control of vasodilation, regulation of cell growth, angiogenesis and platelet aggregation (Hermann et al., 2006). In addition to its physiological roles, nitric oxide has also been implicated in several nervous system diseases (Parkinson's disease and Alzheimer's disease) (Knott and Bossy-Wetzel, 2009) and cancer (Xu et al., 2002). Its production was shown to play an important role in cell migration, either by mediating angiogenesis *in vivo* or modulating endothelial cells growth and migration *in vitro* (Morbidelli et al., 1996) (Bove et al., 2007).

Nitric oxide is colourless, highly lipophilic and a diffusible gas, composed of an oxygen atom bound to a nitrogen atom. It is produced in most mammalian tissues and is synthesized by an enzyme known as nitric oxide synthase (NOS). There are three isoforms of NOS enzymes present: neural NOS (nNOS), inducible NOS (iNOS) and endothelial NOS (eNOS), which control the production and release of nitric oxide (Figure5.1).

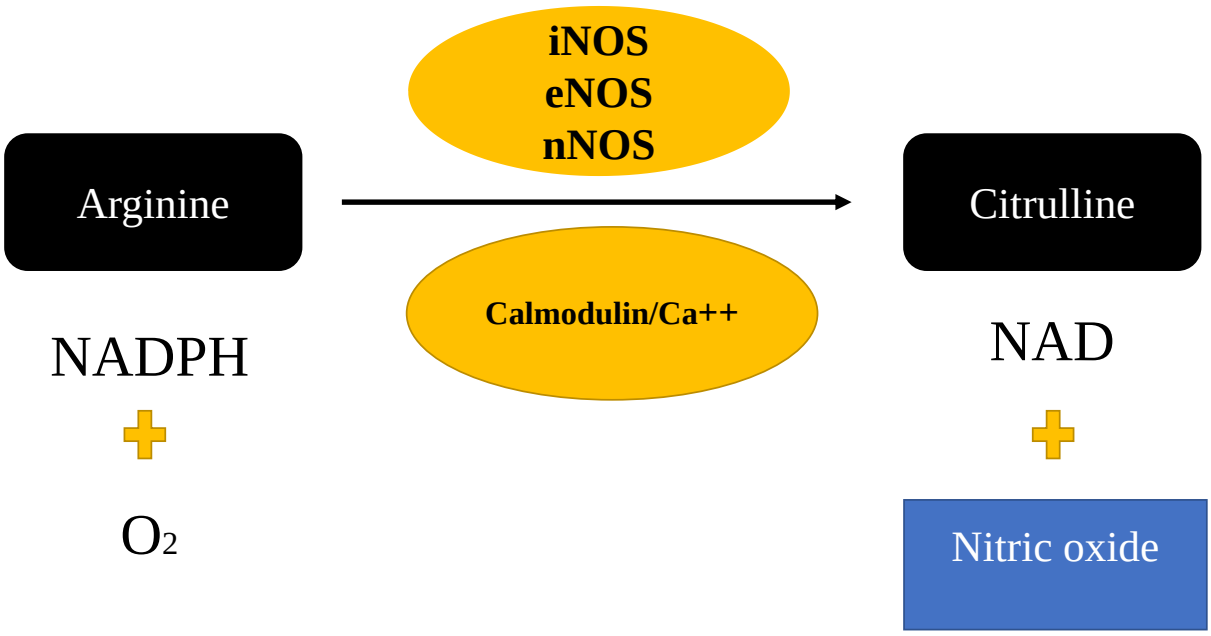

Figure 5. 1 Biosynthesis of nitric oxide.

Illustration of nitric oxide production. The nitric oxide enzyme (iNOS, eNOS and nNOS) and co-factor NADPH and oxygen convert Arginine to Citrulline with release of gaseous Nitric oxide.

Although Nitric oxide can be regulated in a number of ways, its subcellular localization is considered to have a major influence on NO synthesis biology. Subcellular localization of eNOS that is found in the plasma membrane, regulates its activity by determining the proteins that the nitric oxide isoform interacts with (Hecker et al., 1994). Endocytosis pathways such as caveolae were found to play an important role in nitric oxide activity (Figure 5.2 A) (Rath et al., 2009). eNOS directly binds to caveolae and interacts with many signalling molecules that concentrate on the caveolae coat (Feron and Balligand, 2006). Using a subcellular fractionation assay approach employing endothelial cells, eNOS was found particularly in the caveolae fraction (Shaul, 2003). Furthermore, immunofluorescence microscope results demonstrated that eNOS co-localizes with caveolae (Shaul, 2003).

Similarly, the dynamin protein that plays an important role in pinching off vesicles was also shown to bind to eNOS (Cao et al., 2001b). Studies using immunoblotting of eNOS or double labelled confocal immunofluorescence of dynamin 2 and eNOS provided more evidence of the direct interaction of both proteins (Cao et al., 2001b). Interestingly, it was shown that loss of dynamin function by inhibition of GTP hydrolysis through overexpression of a dominant negative construct, K44A, impaired the trafficking of eNOS and its production (Chatterjee et al., 2003).

Nitric oxide mediates many cellular functions through two common processes namely cyclic guanosine monophosphate (cGMP) production and S-nitrosylation of particular proteins. In a process of regulating cyclic guanosine monophosphate (cGMP), nitric oxide interacts with a haem group that is attached to the soluble guanylate cyclase enzyme at His-150 beta subunit. This interaction stimulates the production of cyclic guanosine monophosphate which in turn activates many signalling pathways including phosphodiesterase and protein kinases resulting in functional changes in cells such as muscle relaxation and platelet inhibition (Seth et al., 2018).

The second regulation process is S-nitrosylation of particular proteins. S-nitrosylations occurs when a nitric oxide group is attached to the thiol side of a cysteine in proteins (S-NO) (Smith and Marletta, 2012). On the other hand, denitrosylation is a process of decomposition of S-NO groups, which is mediated by multiple enzymatic systems including: thioredoxin and S-nitrosoglutathione reductase (GSNOR), or ADH5 (Barnett and Buxton, 2017).

Protein S-nitrosylation is an important mechanism that can alter the structure and function of proteins and protein –protein interactions. (Foster et al., 2009). A growing body of evidence suggests that S-nitrosylation is implicated in many cellular functions including: apoptosis (Lee et al., 2005), cell growth (Oliveira et al., 2008), endocytosis (Wang et al., 2006) and membrane trafficking (Matsushita et al., 2003). Apoptosis, which is also known as programmed cell death, plays an important role in removing unwanted cells including damaged or infected cells. Dysregulation of this process is

implicated in diseases such as cancer, where cells are able to evade cell death (Letai, 2017). S-nitrosylation was identified to regulate a number of proteins which carry out functions during signalling in apoptosis (Figure 5.2 B). Caspase 8, a cysteine proteases, which are located in the cytoplasm plays an important role in executing the apoptotic programme or cytokine processing (Shi, 2002). In resting cells, caspase 8 is expressed as a zymogen and is activated by two major pathways - the intrinsic (mitochondria) or extrinsic (death receptors) one (Shi, 2004). In the intrinsic pathway, mitochondria play the central part of apoptosis activation by releasing pro-apoptotic molecules (cytochrome C), which in turn cleaves zymogens to form active tetrameric proteins and trigger other caspase effectors (caspase 3) resulting in cell death (Kim et al., 2000). Considering that caspases is key mediators of apoptosis, S-nitrosylation of caspase 8 was shown to decrease its enzymatic activity (Kim et al., 1997). Similarly, in extrinsic pathways, S-nitrosylation is associated with a key anti-apoptotic death receptors protein Fas - a transmembrane protein that belongs to tumour necrosis factor receptors (TNF) (Leon-Bollotte et al., 2011).

Nitric oxide is known to accelerate receptor mediated endocytosis by S- nitrosylation of dynamin proteins, as nitrosylation of dynamin leads to increase of GTP hydrolysis and thus enhances the cleavage of vesicles (Wang et al., 2006). A good example is the internalization of β2 adrenergic receptors which is mediated via clathrin coated pits (Liang et al., 2004). A mutation in either the site where dynamin is nitrosylated or GTP hydrolysed, decreased the internalization of β2 adrenergic receptor compared to wild type (Wang et al., 2006). In addition to their function on internalization, S-nitrosylation of dynamin was shown to promote cell survival (Figure 5.2 C) (Kang-Decker et al., 2007).

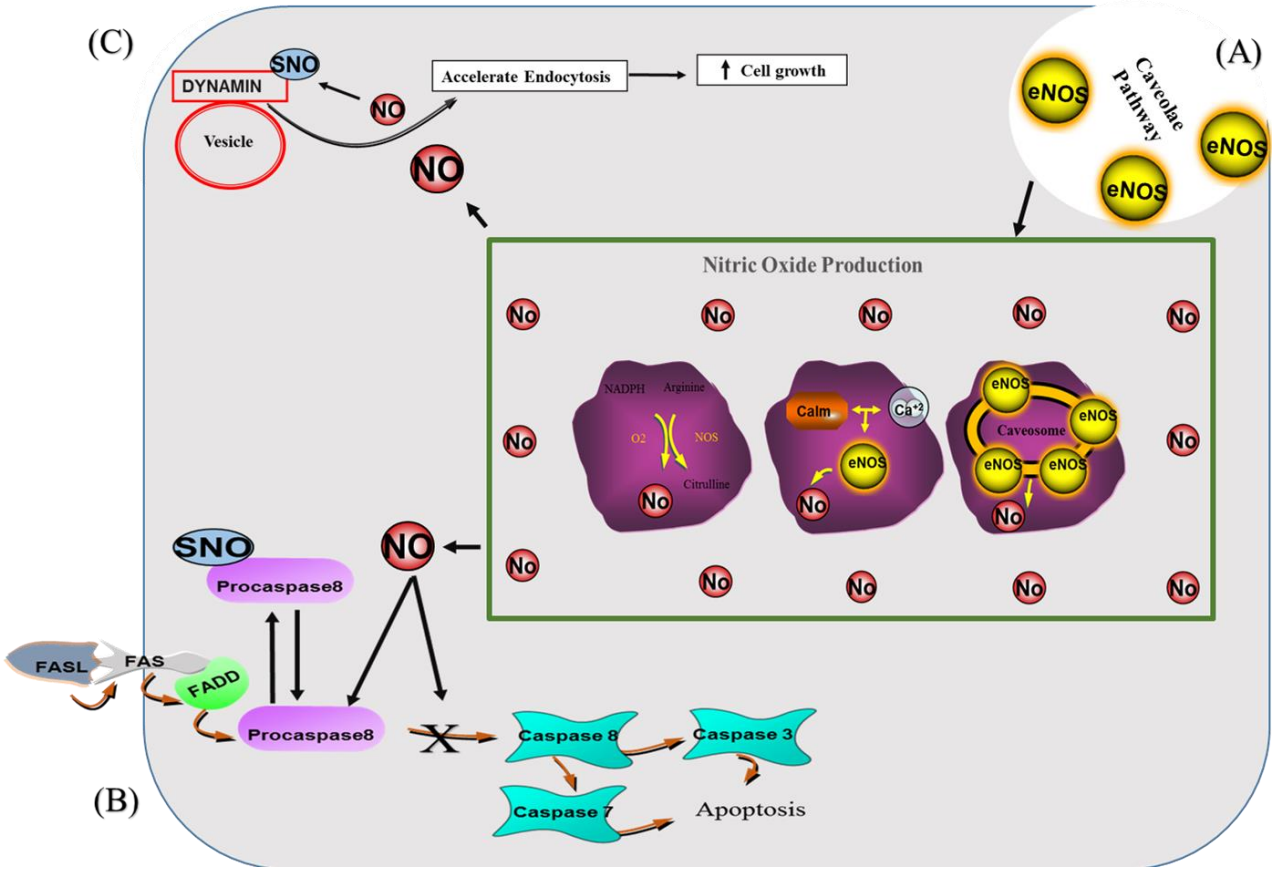

Figure 5. 2 Model summarizing the role of nitric oxide in mediating cellular functions.

A) Subcellular localization of eNOS regulated by Caveolae pathways. B) Mechanism of nitric oxide in apoptosis. Once the apoptosis pathway is induced via death receptors protein Fas, it recruits the Fas-associated death domain (FADD) to its cytosolic death domain which then recruit procaspase-8 causing activation of caspase-8. Activated caspase-8 stimulates apoptosis through the activation of effector caspase-3 or caspase-7. S-nitrosylation of procaspase8 can inhibit the apoptosis through suppression of caspase activity. C) Nitric oxide accelerates receptor mediated endocytosis by S-nitrosylation of dynamin proteins and promotes cell growth.

In addition, S-nitrosylation has been linked to membrane trafficking events between Golgi apparatus and plasma membrane protein transportation through regulation of plasma membrane fusion proteins. SNARE proteins belong to this class and perform fusion of two lipid bilayers. S-nitrosylation of SNARE proteins have been demonstrated to impair membrane trafficking, resulting in inhibition of exocytosis of Weibel-Palade Bodies that mediate vascular inflammation (Matsushita et al., 2003).

Aside from its function in mediating endocytosis, S-nitrosylation has been implicated in focal adhesion disassembly in a process that requires the calcium-dependent protease calpain. Calpain plays an important role in regulating focal adhesion disassembly by proteolytic cleavage of Talin, a focal adhesion protein required for the stability of actin and integrin assembly (Franco et al., 2004). Calpain2 was also found to mediate the proteolysis of other focal adhesions including Paxillin and FAK, which in turn affects the disassembly of focal adhesions and cell motility (Cortesio et al., 2011). Although calpain can be activated in a number of ways including calcium, nitric oxide was shown to be a key regulator of calpain activity (Youn et al., 2009).

Taken together, accumulation of nitric oxide synthase in the endosome compartments and co-localization with dynamin, which was recently shown to promote the cell migration by enhancing focal adhesion turnover, led me to hypothesise that nitric oxide activity stimulates endosome trafficking leading to enhanced focal adhesion turnover. In order to investigate this idea, this chapter will firstly investigate the role of nitric oxide in cell migration using cell tracking assays. This chapter was further extended to investigate the effect of nitric oxide inhibitors on focal adhesion turnover. To do so, two nitric oxide inhibitors Nω -Nitro-L-arginine methyl ester hydrochloride (L-NAME) (a general NOS inhibitors) and 1400W (an iNOS specific inhibitor) were used in order to distinguish between nitric oxide isoforms. Also, the nitric oxide donor: PAPA NONOate (3-(2-Hydroxy-2-nitroso-1-propylhydrazino)-1-propanamine) was used in order to assess whether stimulation of nitric oxide activity had an opposing role on cell migration

After studying the association between nitric oxide and cell migration, this chapter will examine whether inhibition of nitric oxide production will affect the internalization pathways (transferrin and dextran) or early endosomes proteins (EEA1 or Rab5).

This chapter was further extended with two approaches to observe whether there is an interaction between nitric oxide synthases and the early endosome markers. Firstly, quantifying the co-localization between nitric oxide synthases (iNOS or eNOS) and early endosomal compartments using immunostaining of fixed MDA-MB-231 cells. The second approach was to assess whether early endosomes compartment proteins were S-nitrosylated, thus S-nitrosylated cysteine residues of endosome markers were detected by means of a biotin switch assay. The biotin switch assay was developed by Jaffery et al and allows selective conversion of S-nitrosylated moieties to biotinalyted thiols (Jaffrey and Snyder, 2001). It involves three main steps: blocking, reduction and labelling (figure 5.3).

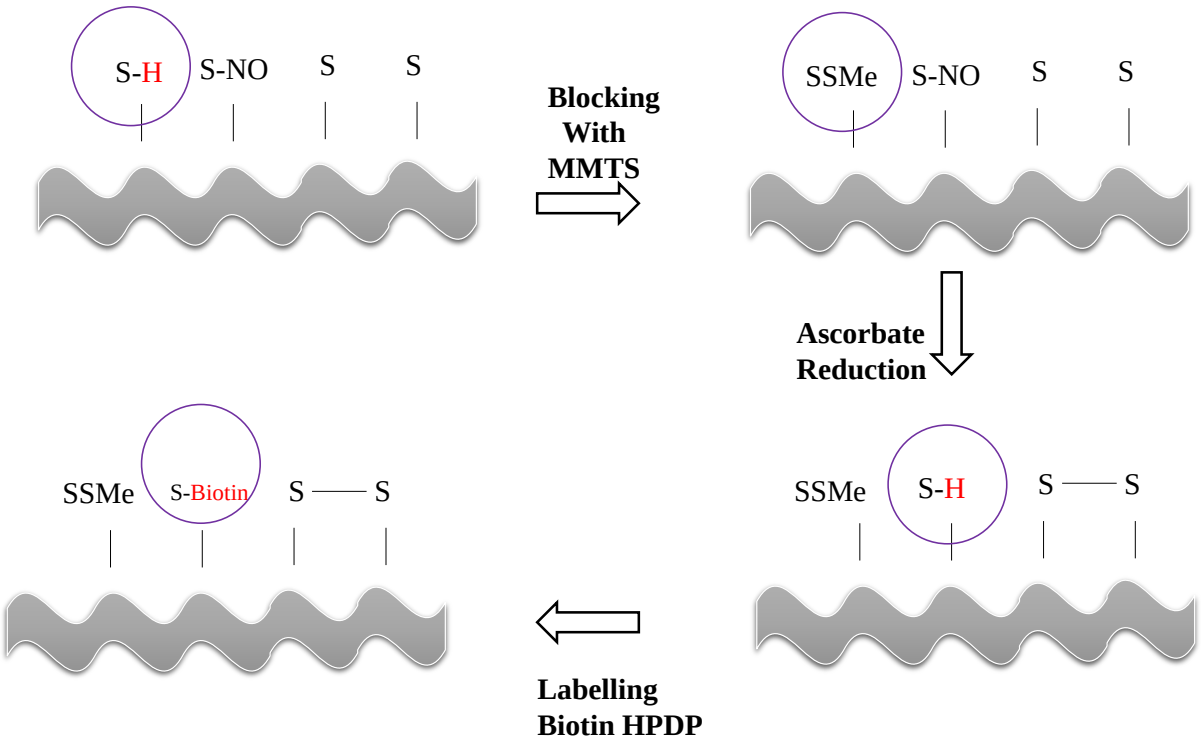

Figure 5. 3 Steps involved in the Biotin Switch Assay

In the first step, free thiols in the protein are blocked with MMTS (S-methyl methanethiosulphonate). After blocking, an ascorbate reduction dissolves the nitrsothiol bond to reduce nitrosothiols to free thiols. Next, the biotinylating reagent (Biotin HPDP ((N-[6-(Biotinamido) hexyl]-3'-(2'-pyridyldithio) propionamide) is labelled to the free thiol. Finally, biotinylated proteins can now be isolated, enriched and detected by western blot.

5.2 Methods:

5.2.1 S-nitrosylation Protein Detection (Biotin Switch):

S-nitrosylation Protein Detection kit (Cayman Chemical) were used to detect S-nitrosylatedcystein residues, according to manufacturer's instructions.

After incubation of the cell culture, media was discarded from T75 flasks and the cells were washed twice with 5 mL cold wash buffer. Subsequently, cells were scraped using a rubber policeman with wash buffer and centrifuged at 500 g for 5 minutes at 4^{o} C. The pellets were then re-suspend with 0.5 ml Buffer A containing blocking reagent and incubated for 30 minutes at 4°C on a shaker. Next, supernatants were mixed with 2 ml of ice-cold acetone and incubated at -20^{o} C for one hour. Later, samples were centrifuged at 3000 rcf for 10 minutes at 4^{o} C and the pellet was mixed with Buffer B containing Reducing and Labelling reagents and incubated for one hour at room temperature. After, 2 ml of ice-cold acetone were added to the sample and incubated at -20^{o} C for one hour, and a pellet was generated by centrifugation at 3000 rcf for 10 minutes at 4^{o} C. The pellet was then mixed with a 100 µL of cold wash buffer and incubated with 100 µL of RIPA buffer containing Streptavidin-agarose bead (20µL) overnight at 4^{o} C on the rotating machine. The sample was then centrifuged at 14000 rcf for 30 seconds and the pellet was washed with 300 µL with RIPA buffer (this step was repeated 3 times). Post-streptavidin pull down, samples were subjected to Protein separation (SDS-PAGE), transfer, and antibody incubations and quantifications as illustrated in section 2.4.

5.3 Results:

5.3.1 Effect of nitric oxide on cell migration as measured by tracking individual cells:

MDA-MB-231 breast-cancer cells were plated on a 6-well-plate and incubated overnight. When the plate reached 30% confluence, cells were treated with either vehicle (PBS), nitric oxide inhibitors (L-NAME or 1400W) or nitric oxide donors (PAPA NONOate) at varying concentrations (L-NAME 5 mM, 1400W 2 mM and PAPA NONOate 50 µM) for a 24 hour incubation. Upon completion of the incubation times, cells were directly subjected to live imaging using time lapse microscopy. Images were captured every 15 minutes for a period of 24 hours and the speed was calculated as the total distance moved divided by 24 hours.

As illustrated in figure 5.4, inhibition of nitric oxide production via iNOS (1400W) and inhibition of the three isoforms of NOS (L-NAME) significantly reduces the average speed of cell migration with a higher effect for L-NAME compared to control. Whereas nitric oxide donors (PAPA NONOate) had no effect on the migration speed.

Quantification analysis of MDA-MB-231 migration indicated that the average speed was 23.49 ± 0.832 µm/h in vehicle and 22.95 ± 0.858 $p<0.05$ in PAPA NONOate, compared to 14.78 ± 1.05 µm/h ** $p<0.01$ and 18.37 ± 1.288 µm/h * $p<0.05$ in L-NAME and 1400W treated cells, respectively (Figure 5.3).

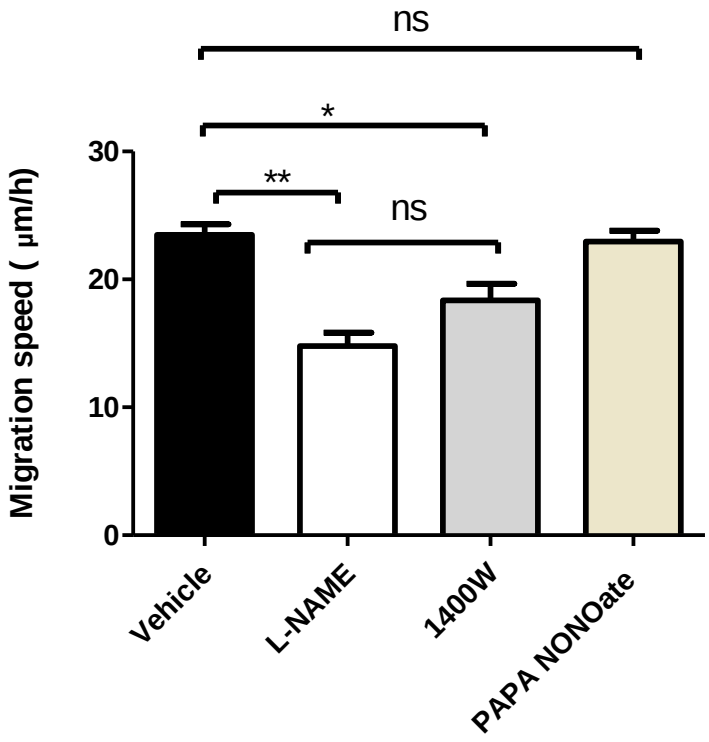

Figure 5. 4 Effect of nitric oxide inhibitors or donors on cell migration using cell tracking of MDA-MB-231 cells.

Mean migration speed of individual cells in 24 hours. MDA-MB-231 cells were treated with Vehicle, different nitric oxide inhibitors (L-NAME 5 mM or 1400W 2 mM) or NO Donors (PAPA NONOate 50 µM) for 24 hours and subjected to a cell tracking assay using time lapse microscopy. One way ANOVA with Tukey Multiple Comparison Test were used to compare each treatment with the control. Graph represents the mean ± standard error of three independent experiments, in each experiment 40 cells were analysed for vehicle or each inhibitor. Statistical significance differences were accepted at * $p<0.05$ ** $p<0.01$.

5.3.2 Effect of nitric oxide on focal adhesion turnover:

As shown in previous results, inhibition of nitric oxide reduces cell migration. The question was raised whether the inhibition of nitric oxide (L-NAME or 1400W) could also affect focal adhesion turnover. Therefore, live cell transfection with mCherry- Zyxin were performed.

The MDA-MB-231 cells were seeded on ibidi 50 plastic surface and allowed to attach to the bottom of the plate overnight. When the plate became 60% confluent, cells were transfected with mCherry -Zyxin and then treated with 5mM L-NAME or 2mM 1400W or Vehicle for 24 hours. Subsequently, after completion of the incubation time, cells were directly subjected to confocal time lapse microscopy at a wave length of 568nm to visualize mCherry -Zyxin turnover. The mCherry -Zyxin turnover was monitored by taking 1 image every 5 seconds for the duration of 10 minutes and the average life time of Zyxin concluded by measuring the intensity of Zyxin in focal adhesions overtime.

The quantification measurements revealed that both nitric oxide inhibitors significantly increased the turnover time of mCherry -Zyxin compared to control. As shown in figure 5.5, the mean turnover time was 36.03 ± 3.8s in vehicle, compared with 74.57 ± 2.667s (** $p<0.01$) and 58.79 ± 7.69s (* $p<0.05$) in L-NAME and 1400W treated cells, respectively.

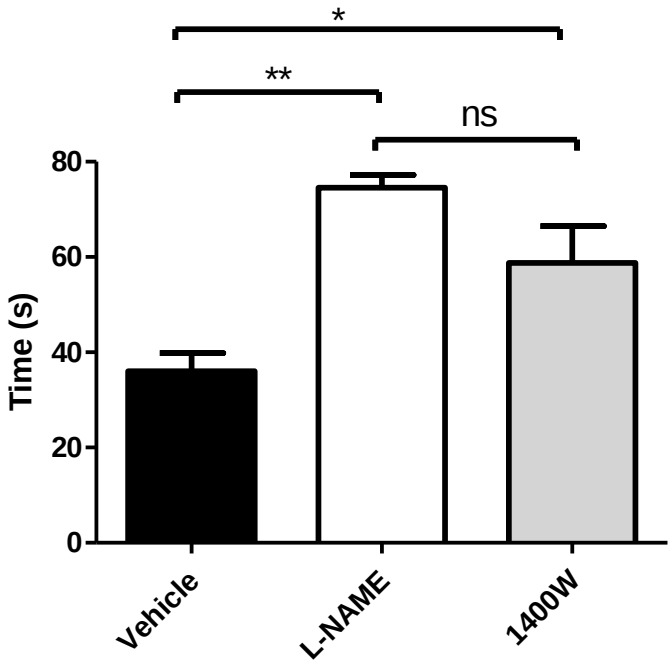

Figure 5. 5 L-NAME and 1400W increased zyxin containing focal adhesions turnover in live MDA-MB-231 cells.

Mean turnover time of zyxin containing focal adhesions in control compared to L-NAME or 1400W inhibitors of MDA-MB-231 cells. MDA-MB-231 cells were transfected with mCherry-Zyxin, treated with vehicle, different nitric oxide inhibitors (L-NAME or 1400W) or Donors for 24 hours and subjected to live cell imaging. Images were captured every seconds for five minutes. One way ANOVA with Tukey Multiple Comparison Test were used to compare each treatment with the control. Graph represents the mean ± standard error of 24 cells (100 focal adhesion) from three independent experiments. Statistical significance differences were accepted at * $p<0.05$ and ** $p<0.01$.

5.3.3 Effect of nitric oxide on endocytosis:

5.3.3.1 Effect of nitric oxide inhibitors on transferrin and dextran internalization:

This approach was used to demonstrate whether inhibition of nitric oxide interferes with endocytosis in terms of clathrin or non clathrin internalization pathways. Therefore, the effect on ligand uptake in the presence of nitric oxide inhibitors on two ligands, transferrin and dextran, was examined.

In each experiment of dextran or transferrin internalization, MDA-MB-231cells were allowed to attach to the bottom of the plate overnight. Next day, cells were treated with 5mM L-NAME or 2mM 1400W or vehicle for 48 hours. Subsequently, the media was replaced with 0% FBS containing 500µg/ml of dextran conjugated to Fluorescein or 20mg/ml transferrin conjugated to Alex Fluor 546 for 30 minutes. Finally, cells were fixed with paraformaldehyde, subjected to confocal microscopy and fluorescence intensity measured for transferrin uptake or the number and size of endosomes containing dextran.

The quantification analysis of transferrin uptake indicated that both nitric oxide inhibitors failed to inhibit transferrin uptake (figure 5.6). Similarly, these inhibitors also did not show any significant effect on number or size of dextran containing vesicles (figure 5.7).

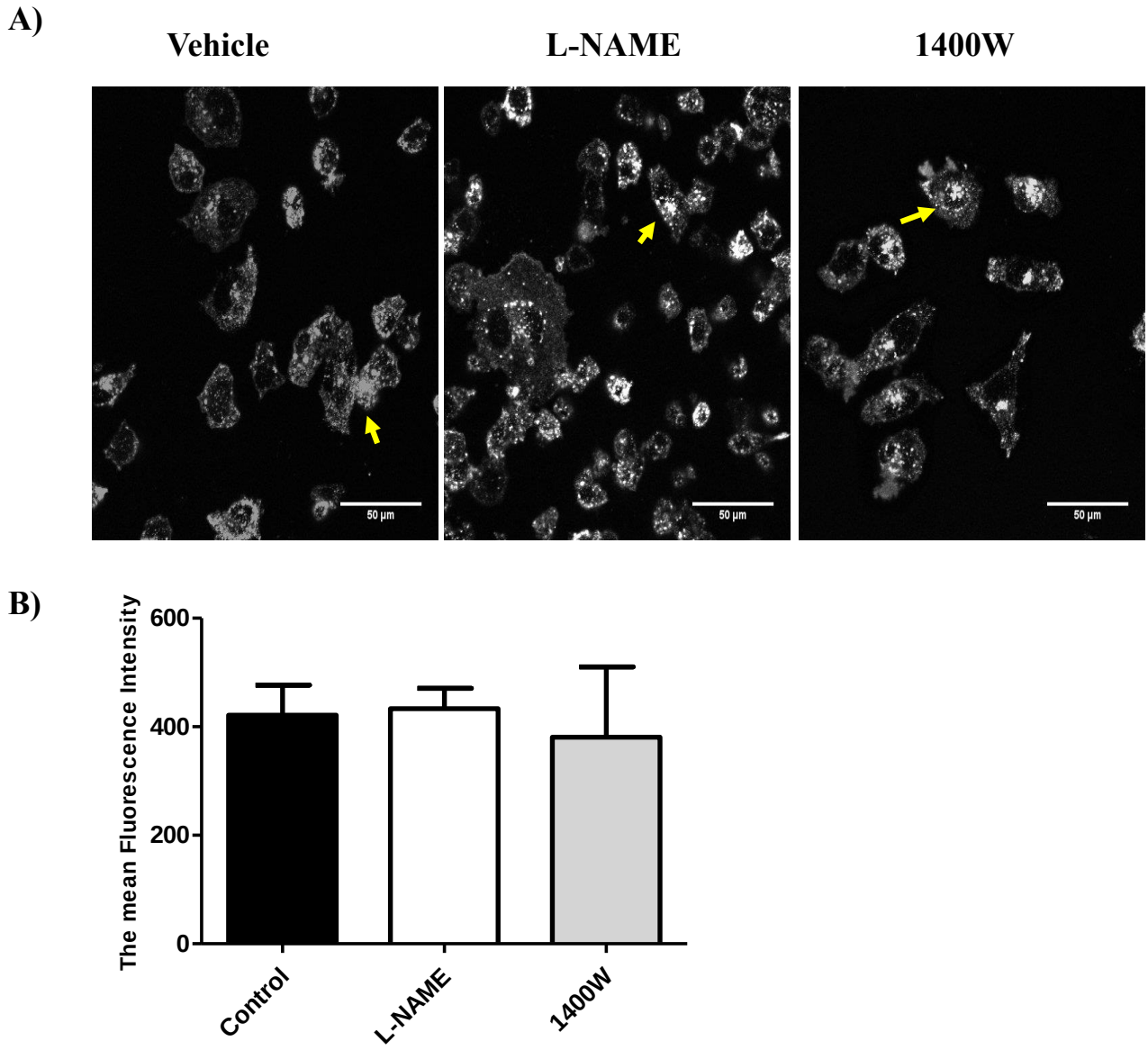

Figure 5. 6 L-NAME and 1400W did not affect transferrin uptake in MDA-MB-231 cells

MDA-MB-231 cells were treated with vehicle, different nitric oxide inhibitors (L-NAME or 1400w) for 48 hours, serum starved for 3h and incubated with 25 µg/ml Alexa Fluor 546 -conjugated transferrin for 30 minutes. Cells were then fixed and subjected to confocal imaging. **A:** Confocal images representing the effect of untreated cells (vehicle) and treated cells (L-NAME 5 mM or 1400W 2mM) on Transferrin uptake in MDA-MB-231. Yellow arrows indicate the amount of transferrin uptake. Scale bar is 50µm. **B:** the transferrin uptake measured by fluorescence intensity and one way ANOVA with Dunnett's Multiple Comparison were used to compare each treatment with the control.

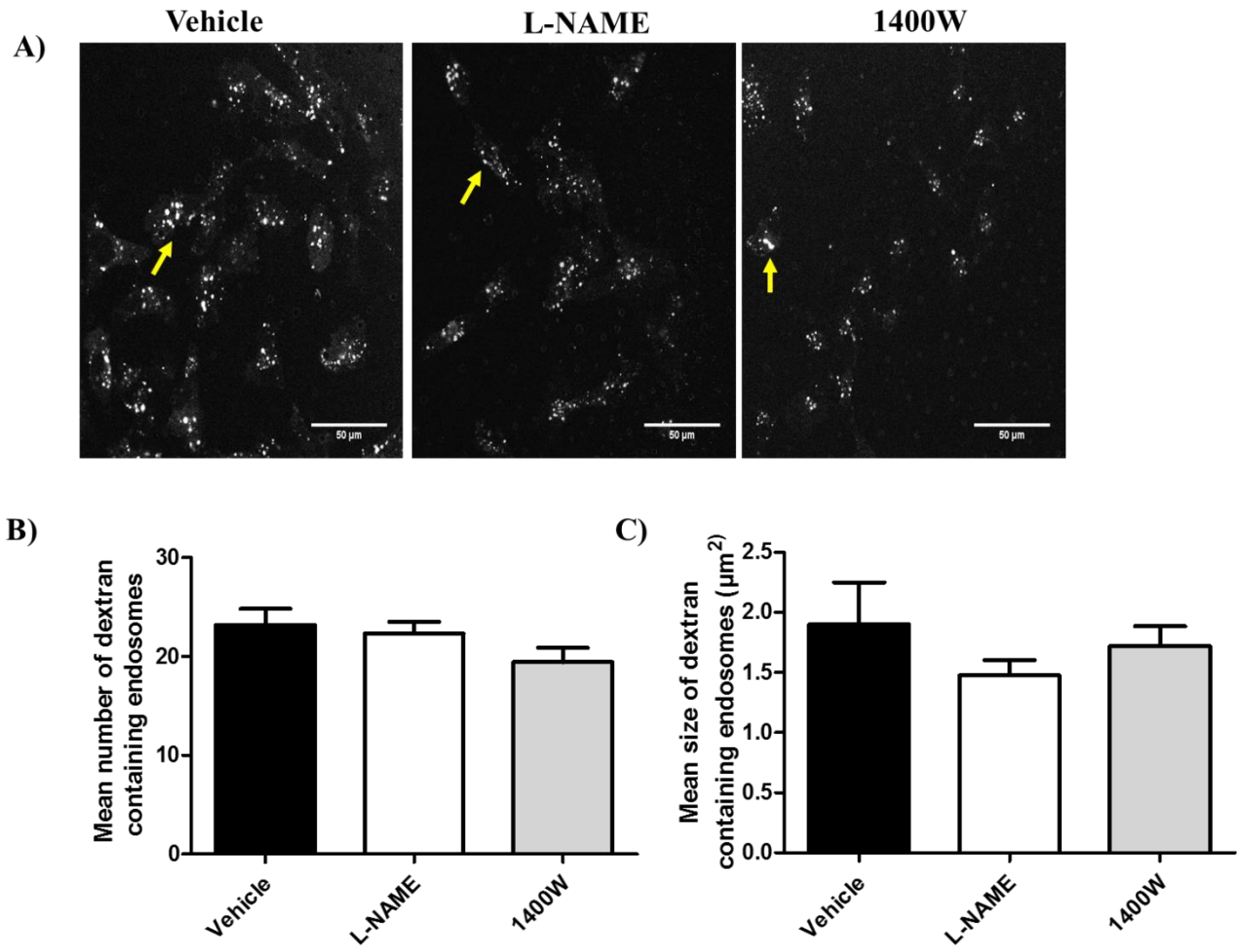

Figure 5. 7 L-NAME and 1400W did not affect dextran uptake or size in MDA-MB-231 cells

MDA-MB-231 cells were treated with vehicle or different nitric oxide inhibitors (L-NAME or 1400w) for 48 hours, serum starved for 3h and incubated with 500 µg/ml Dextran, Fluorescein, 10,000 MW, Anionic, Lysine Fixable for 30 minutes. Cells were then fixed and subjected to confocal imaging. **A:** Confocal images showing the effect of untreated cells (vehicle) and treated cells (L-NAME or 1400W) on dextran number and size in MDA-MB-231 cells. Yellow arrows indicate the amount of dextran uptake. Scale bar is 50µm. **B** and **C**) graphs show the effect of nitric oxide inhibitors on dextran number and size**.** One way ANOVA with Dunnett's Multiple Comparison were used to compare each treatment with the control.

5.3.3.2 Effect of nitric oxide inhibitors on early endosome markers:

To examine whether nitric oxide is involved in endocytosis regulation through early endosomal compartments, the effect of nitric oxide inhibition or donors on Rab5 or EEA1 markers was examined. Thus, MDA-MB-231 cells were treated with nitric oxide inhibitors (L-NAME or 1400W) or donor (PAPA NONOate) and then immunostained for either Rab5 or EEA1.

The results show that both inhibitors and donors had no significant effect on number or size of Rab5 containing endosomes compared to control (Figure 5.8). However, L-NAME and 1400W but not PAPA NONOate significantly reduced the number of EEA1 containing endosomes and increased their size compared to control cells. As shown in figure 5.9, the mean average number of EEA1 in cells treated with L-NAME or 1400W were 23.7 ± 2.00 (* $p<0.05$) and 20.1 ± 6.87 (* $p<0.05$), respectively, compared with 43.5 ± 3.20 in control and 40.9 ± 1.37 in PAPA NONOate. Similarly, the mean average size of EEA1 containing endosomes in cells treated with L-NAME or 1400W were 0.99 ± 0.068 μm^2 (** $p<0.01$) and 1.11 ± 0.09 μm^2 (** $p<0.01$) respectively, compared with 0.47 ± 0.066 μm^2 in control and 0.80 ± 0.092 μm^2 in PAPA NONOate.

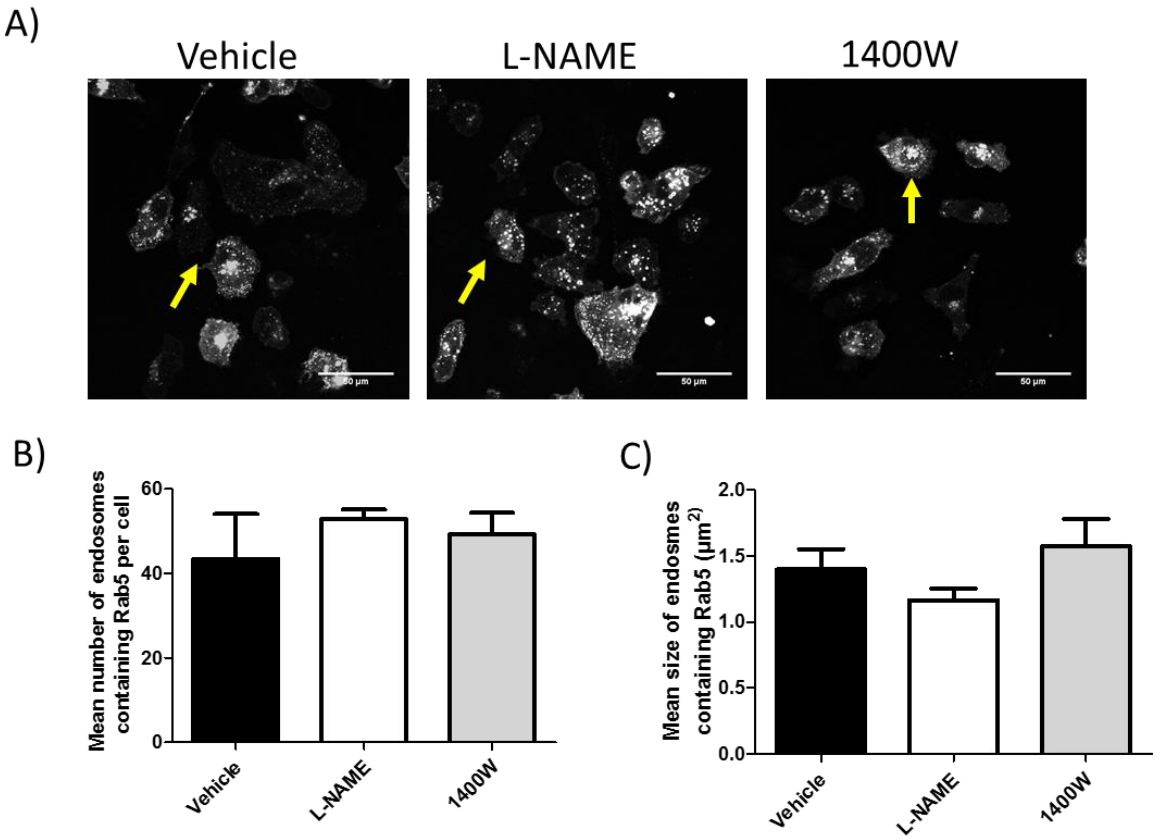

Figure 5. 8 Nitric oxide inhibitors do not effect number and size of Rab5 containing endosomes in MDA-MB-231 cells.

MDA-MB-231 cells were treated with vehicle or different nitric oxide inhibitors (L-NAME or 1400w) for 48 hours, fixed and subjected to immunocytochemistry staining of anti-Rab5. **A)** Confocal images showing the effect of untreated cells and treated cells with L-NAME or 1400W on Rab5 number and size. Yellow arrows illustrate Rab5. Scale bar is 50µm. **B** and **C**) graphs show the effect of L-NAME and 1400W inhibitors on Rab5 number and size. One way ANOVA with Dunnett's Multiple Comparison Test were used to compare each treatment with the control. Graphs represent the mean ± standard error of three independent experiments, in each experiment at least 60 cells were analysed.

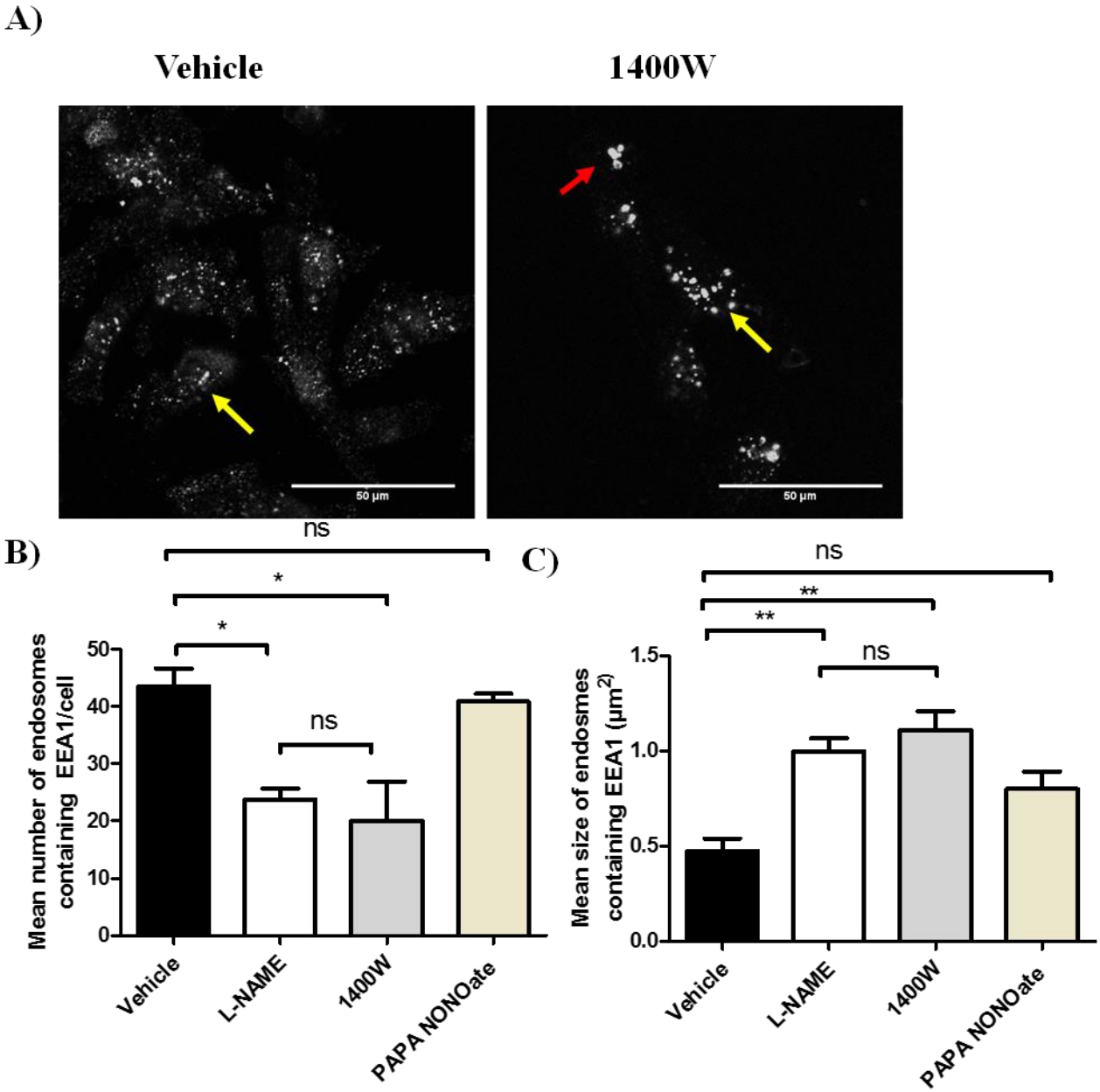

Figure 5. 9 Effect nitric oxide inhibitors or donors on number and size of EEA1 containing endosomes in MDA-MB-231 cells.

MDA-MB-231 cells were treated with vehicle or different nitric oxide inhibitors (L-NAME or 1400w) for 48 hours, fixed and subjected to immunocytochemistry staining of anti-EEA1. **A)** Confocal images representing the effect of untreated cells and treated cells with 1400W on EEA1 number and size. Yellow arrows illustrate EEA1. Red arrow illustrates the large-coated vesicle. Scale bar is 50µm. **B** and **C)** graphs show the effect of L-NAME and 1400W inhibitors or donors on EEA1 number and size. One way ANOVA with Dunnett's Multiple Comparison Test were used to compare each treatment with the control. Graphs represent the mean ± standard error of three independent experiments, in each experiment at least 80 cells were analysed. Statistical significance differences were accepted at * $p<0.05$ and ** $p<0.01$.

5.3.4 Association between nitric oxide and endosomes:

Since the previous results demonstrated that inhibition of nitric oxide regulates number and size of EEA1 containing endosomes, it was thought to investigate the potential link between early endosomes and nitric oxide. Therefore, two methods were applied. The first method was immunocytochemistry to assess the co-localization between early endosomes and nitric oxide synthase. The second method was the biotin switch assay to detect whether early endosomes antigens are S-nitrosylated.

5.3.4.1 Association between Early endosome antigen and eNOS or iNOS using immunocytochemistry:

MDA-MB-231 cells were fixed and immunostained for EEA1 and eNOS or iNOS. The results show that the co-localisation value between EEA1 and eNOS was 0.64 ± 0.17 (Figures 5.10). Similarly, the co-localisation value between EEA1 and iNOS were 0.63 ± 0.11 (Figure 5.11).

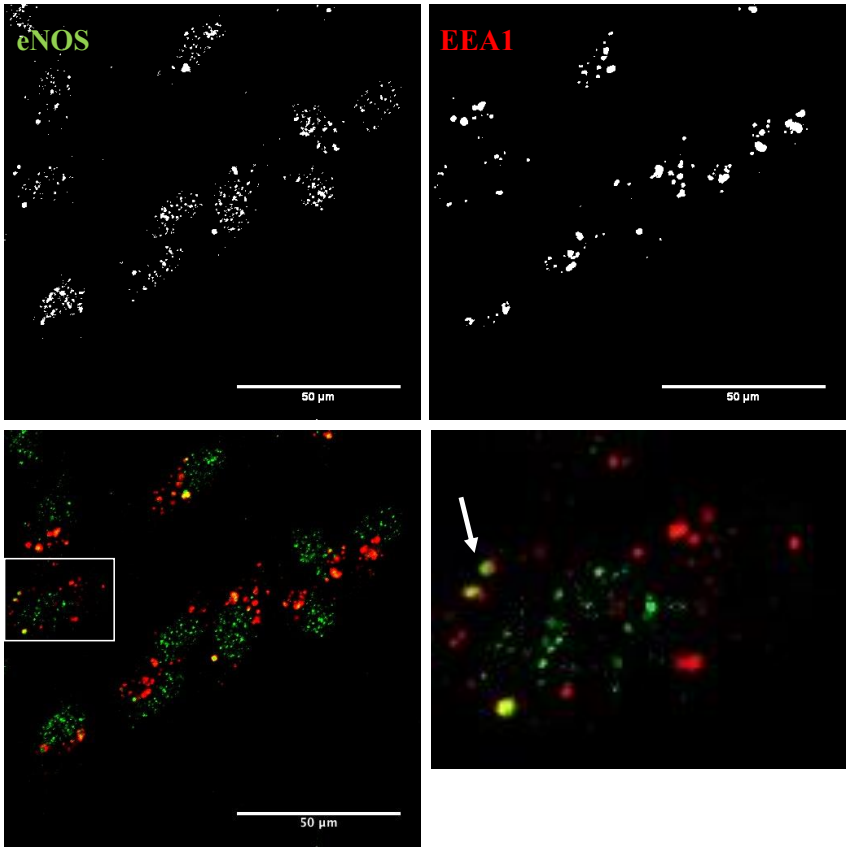

Figure 5. 10 Co-localization between eNOS and Early Endosome Antigen (EEA1).

Confocal images of co-localization between eNOS and EEA1 antibodies in MDA-MB-231 cells. Cells were fixed and subjected to immunocytochemistry for eNOS and EEA1 antibodies. The co-localisation of eNOS (green) with the early-endosome marker EEA1 (red) was measured through selection of a ROI (region of interest) using Spearman's (rho) correlation coefficient analysis. Scale bar is 50µm. The highlighted area illustrates a magnification of the co-localization and is pointed out with a white arrow. Three independent experiments were performed.

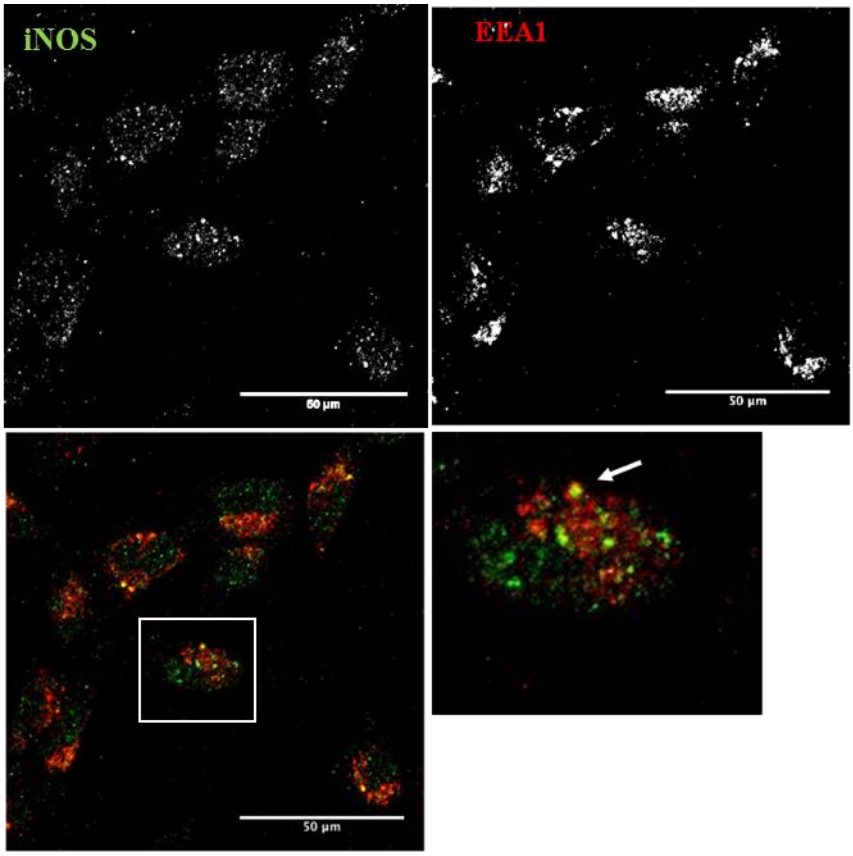

Figure 5. 11 Co-localization between iNOS and Early Endosome Antigen (EEA1).

Confocal images of co-localization between iNOS and EEA1 antibodies in MDA-MB-231 cells. Cells were fixed and subjected to immunocytochemistry for eNOS and EEA1 antibodies. The co-localisation of iNOS (green) with the early-endosome marker EEA1 (red) was measured through selection of a ROI (region of interest) using Spearman's (rho) correlation coefficient analysis. Scale bar is 50µm. The highlighted area illustrates a magnification of the co-localization and is pointed out with a white arrow. Three independent experiments were performed.

5.3.4.2 Association between endocytosis and nitric oxide through detection of S-nitrosylation:

Once it was ascertained that an early endosomes antigen is affected by nitric oxide inhibitors and co-localized with both iNOS and eNOS, it was decided to investigate whether early endosome proteins or proteins associated with early endosomes are S-nitrosylated. Thus, a biotin switch assay was conducted as described in materials and methods.

Western blot analysis revealed that several early endosomal markers (APPL1, EEA1 and Rab5), associated proteins (CHC1) and late endosomal markers (LAMP1) were all found to be S-nitrosylated. There was a lower signal for S-nitrosylated Rab5 than the other endosomal markers and no signal was detected with H2B proteins or Ubiquitin which were used a control as they do not contain S-nitrosylation. To ensure the accurate detection of S-nitrosothiols, samples were treated with mercury chloride (HgCl2) to cleave S-NO bonds as a negative assay control prior the biotin switch assay, which showed no detected bands in all proteins tested (figure 5.12A).

Once it was ascertained that these endosome markers were S-nitrosylated, the GPS-SNO S-nitrosylation site prediction algorithm was used (Xue et al., 2010) to predict the specific cysteine residue that is likely to be S-nitrosylated. The prediction algorithm was applied to APPL1, Clathrin Heavy Chain 1, EEA1, LAMP1, Rab5 and others proteins including H2B and ubiquitin (figure 5.12B).

A

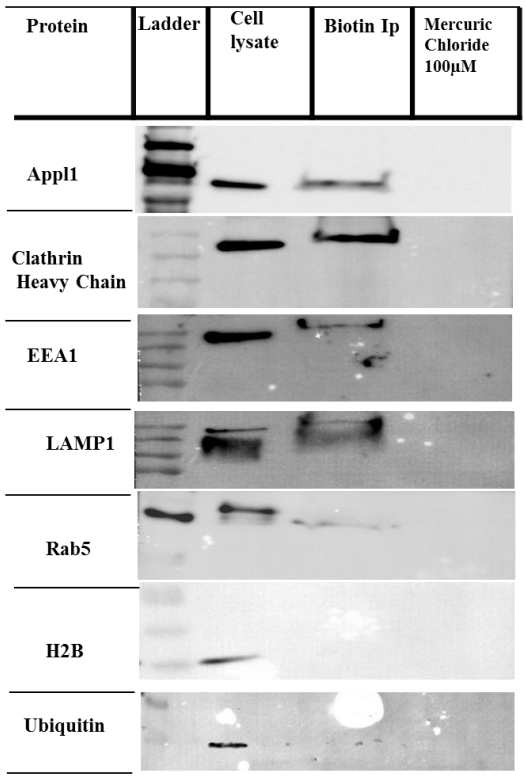

B

Site prediction	Positions of cysteine residue and score
- VIDELSSCHAVLSTQ - ESNLSSVCYIFESN	Position 99 (2.4) Position 603 (20.7)
- RHSSLAGCQIINYRT - LKEDKLECSEELGD - VPNKVIQCFAETGQV - SVEDSLECLRAMLSA - GGLLDVDCSEDVIKN - EARIHEGCEEPATHN - DLELINVCNENSLFK - EFRLAQMCGLHIVVH	Position 151 (21) , Position 459 (5) Position 491 (3.1), Position 666 (3.2) Position 824 (3.3), Position 870 (2.3) Position 934 (2.4), Position 1272 (21)
- EGFICPQCMKSLGSA - SEKLKDECKKLQSQY - ILDLEKTCKELKHQL - EQQLQERCKALQDIQ	Position 46 (2.4) Position 255 (2.0) Position 894 (1.6) Position 1102 (2.2)
- LLLGLMHCASAAMFM	Position 25 (2.7)
- TQPTRNQCCSN	Position 212 (3.3)
No site predicted	None
No site predicted	None

Figure 5. 12 Detection of S-nitrosylation proteins on western blot

Western blots images showing the S-nitrosylation proteins detected using the biotin switch assay. MDA-MB-231 cell lysate was either left untreated or treated with 100µM Mercuric chloride before performing the biotin switch assay. Biotinylated proteins were then precipitated by streptavidin-agarose, subjected to western blot against early endosomal markers (EEA1, Rab5 and APPL1), late endosome marker (LAMP1), Clathrin Heavy Chain (CHC1), nuclear proteins (H2B) and Ubiquitin. Three independent experiments were performed and a representative image shown. B) List of predicted S-nitrosylation for endosomes. Predicted S-nitrosylated cysteine residue in the amino acid sequences are highlighted in red

5.3.4.3 Bioinformatics analysis of endosome proteins S-nitrosylation:

The predicted three-dimensional structures of early endosome proteins were generated using IntFOLD software (McGuffin et al., 2015) (McGuffin et al., 2018). This tool was used to identify the buried and exposed cysteines to determine which are most likely to be S-nitrosylated. The structure of EEA1 indicates that two cysteines, at position 255 and 1102, are buried and not likely to be a site of S-nitrosylation (Figure 5.13 B and D). However, other two cysteines, at positions 46 and at position 894, are both exposed and are possible sites of S-nitrosylation (Figure 5.13 C).

A three dimensional model of clathrin heavy chain 1 was also generated. From the structure in Figure 5.13 B, C and D, it can be seen from the surface render image that Cys-151, Cys-491, Cys-666, Cys-934 and Cys-1272 are buried, and thus would be unlikely to be potentially S-nitrosylated. However, Cy459, Cys824, Cys 934 and Cys 870 are exposed and are all possible targets for S-nitrosylation (Figure 5.14 B, C and D).

The three dimensional model was also generated for the other endosome proteins. From the structures in Figure 5.15 and 5.16, it can be seen that only one cysteine was detected for both Rab5 and LAMP1 and is likely to be S-nitrosylated as both were exposed. However, a three dimensional model for APLL1 indicated that the location of both cysteines was buried and thus would be unlikely to be a target for S-nitrosylation (Figure 5.17).

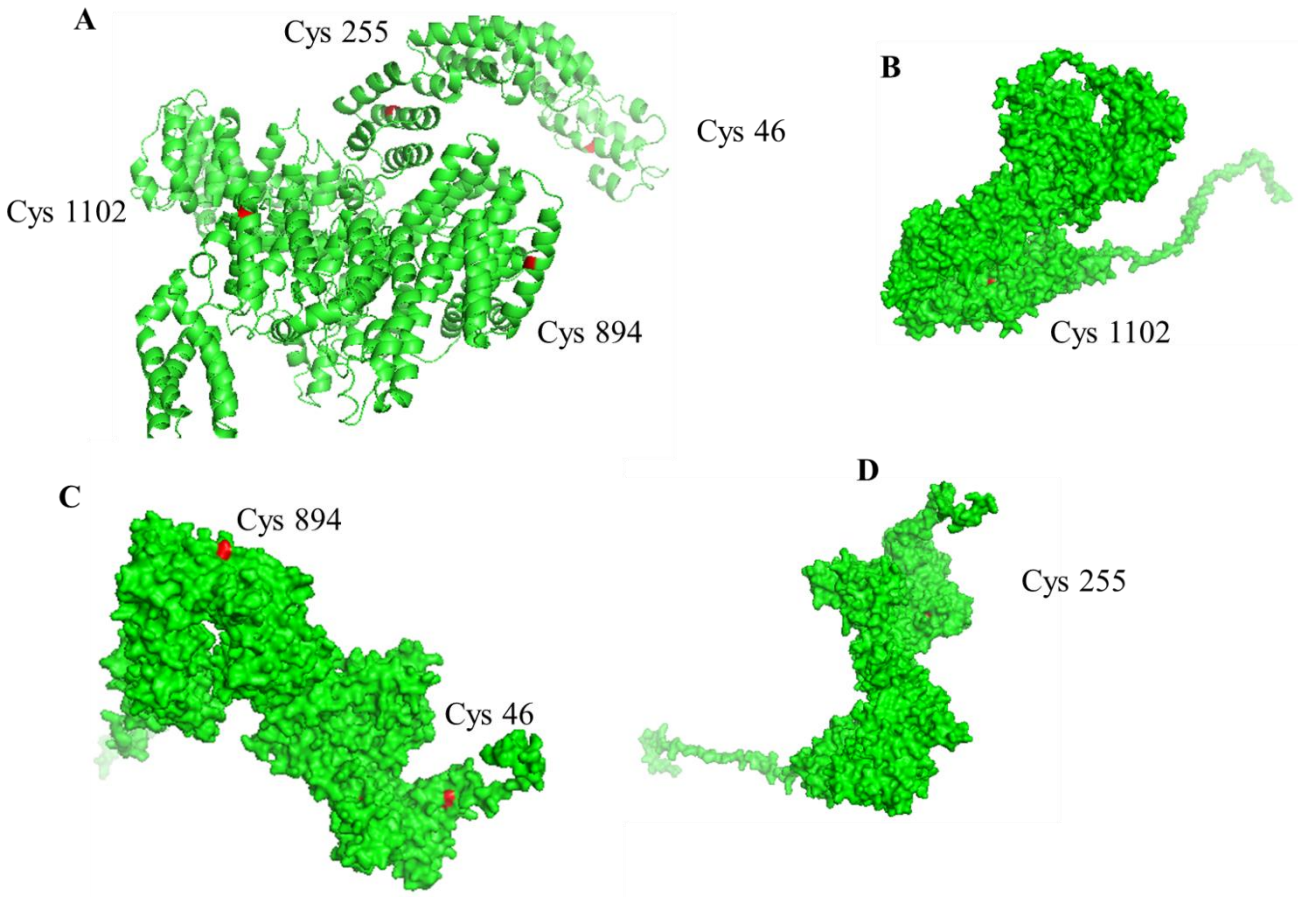

Figure 5. 13 The human EEA1 structure

A cartoon representation of EEA1 with cysteine residues highlighted in red. A) All potential cysteine residues identified from GPS-SNO analysis. B) Cys 1102. C) Cys 894 and Cys 46. D) Cys255.

.

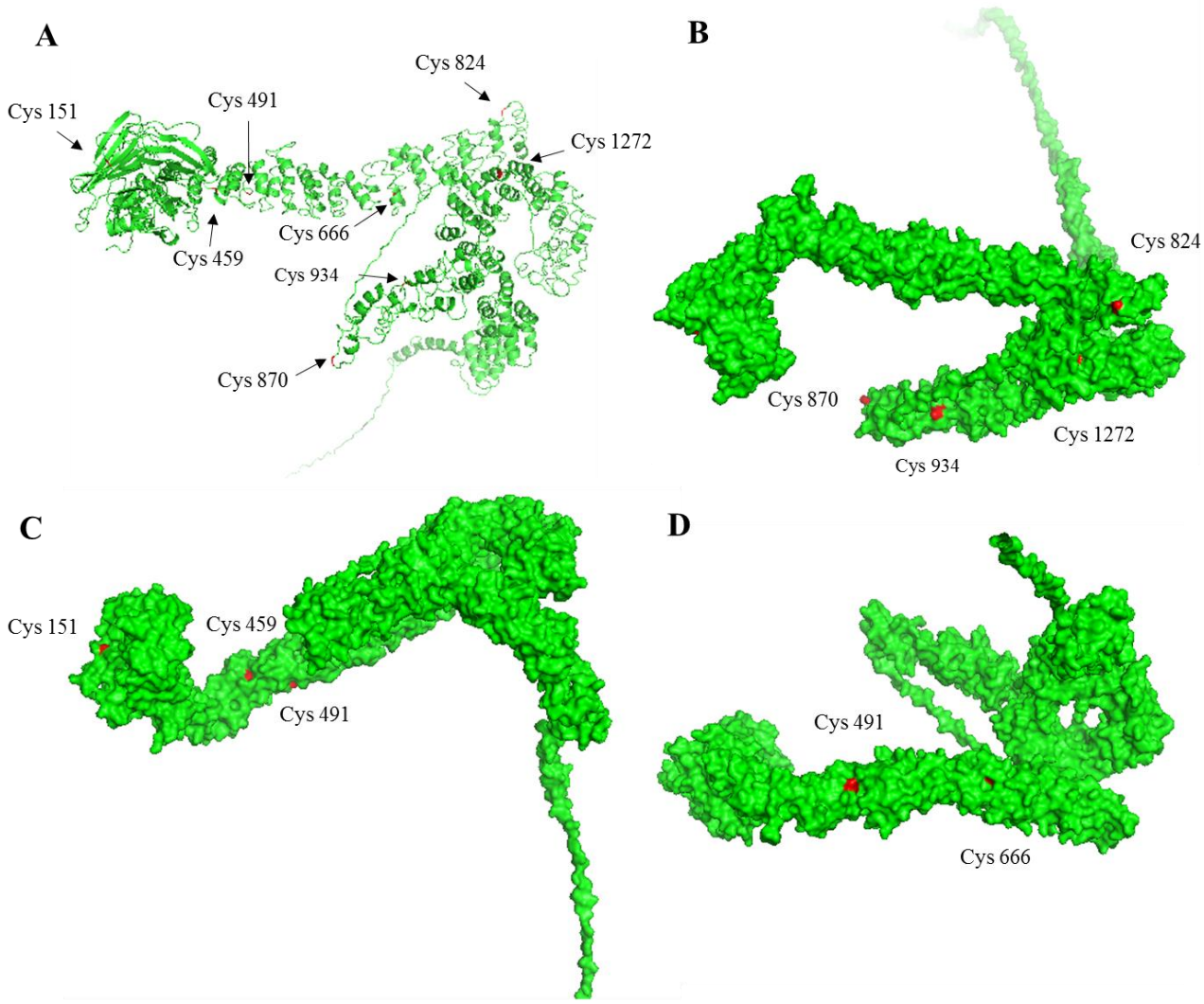

Figure 5. 14 The human Clathrin Heavy Chain structure

A cartoon representation of CHC with cysteine residues highlighted in red. A) All potential cysteine residues identified from GPS-SNO analysis. B) Cys 824, Cys 870, Cys 934 and Cys 1272. C) Cys 151, Cys 459 and Cys 491. D) Cys 491 and Cys 666.

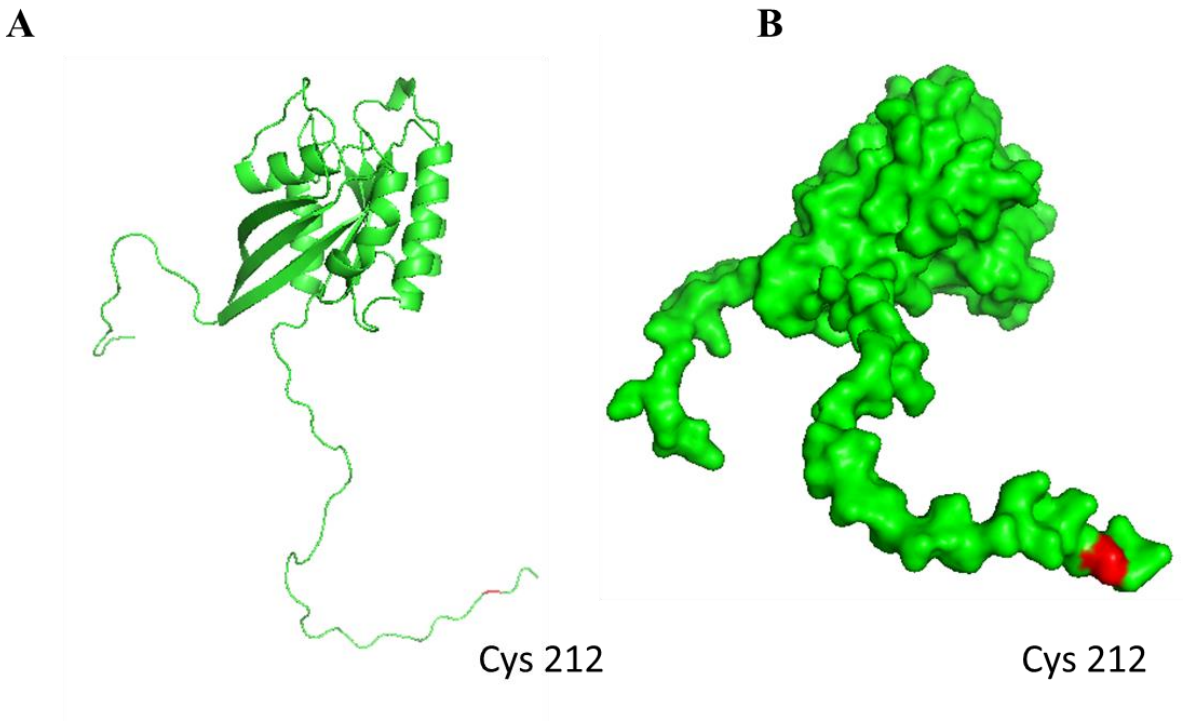

Figure 5. 15 The human Rab5a structure

A cartoon representation of EEA1 with cysteine residues highlighted in red. A) Potential cysteine residue identified from GPS-SNO analysis. B) Cys 212.

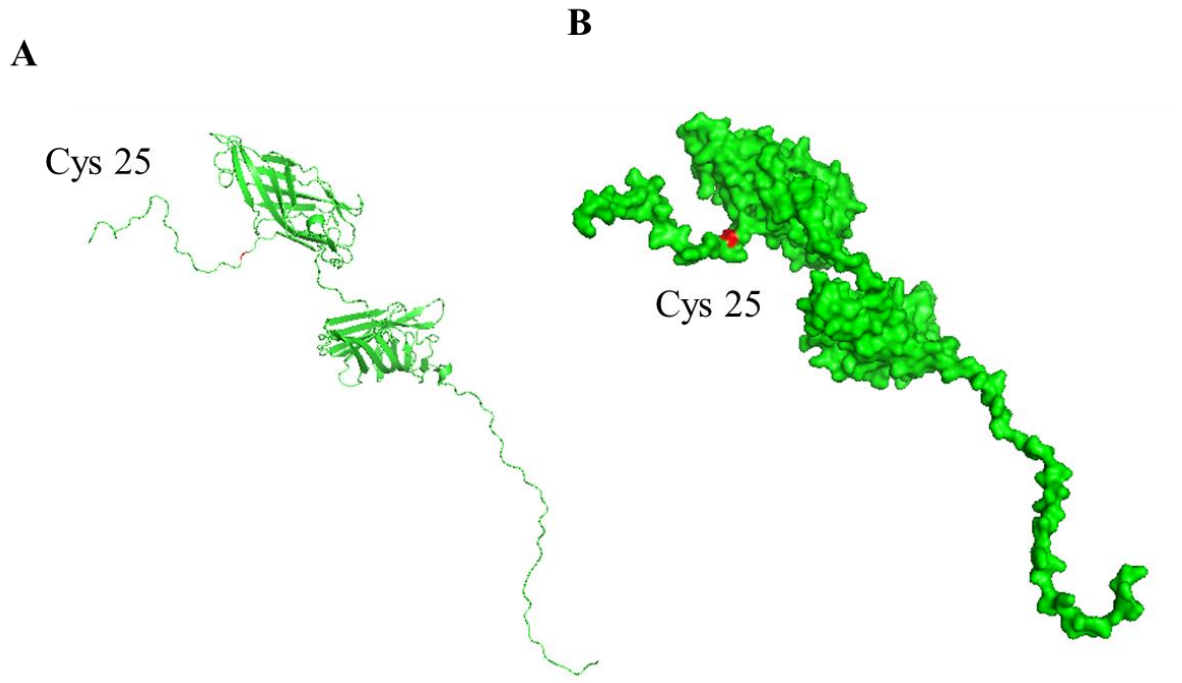

Figure 5. 16 The human LAMP1 structure

A cartoon representation of LAMP1 with cysteine residues highlighted in red. A) Potential cysteine residue identified from GPS-SNO analysis. B) Cys 25.

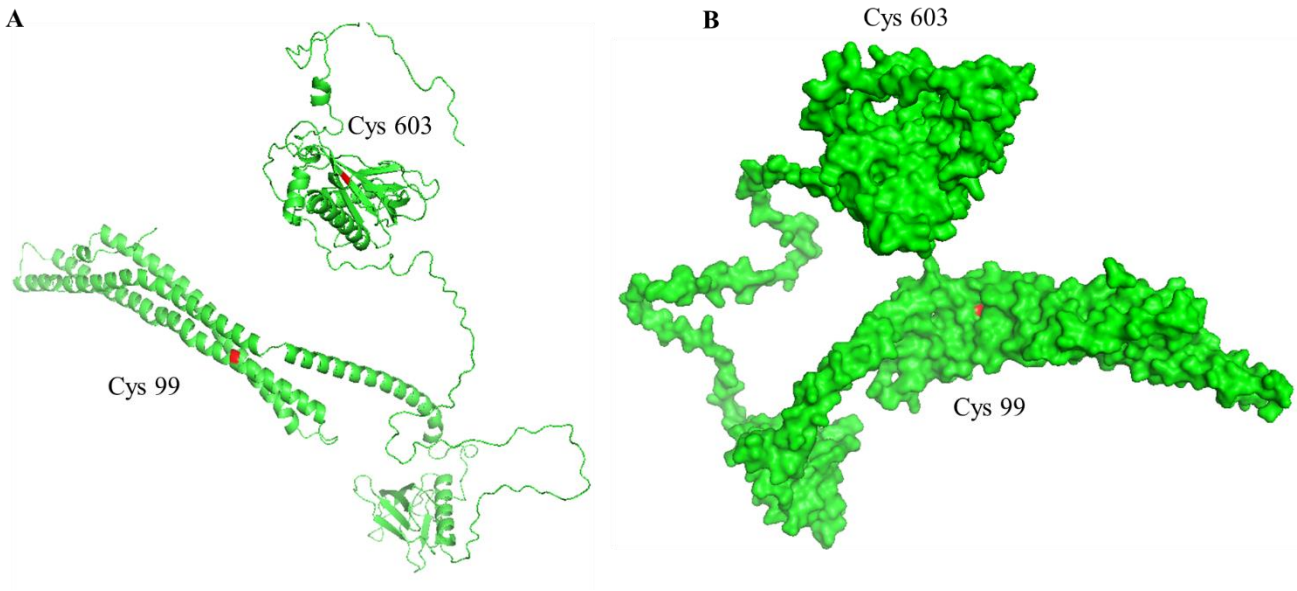

Figure 5. 17 The human APPL1 structure

A cartoon representation of APPL1 with cysteine residues highlighted in red. A) Potential cysteine residue identified from GPS-SNO analysis. B) Cys 99 and Cys 603.

5.4 Discussion:

The gas nitric oxide (NO) plays an important role in many physiological and pathological processes including smooth-muscle relaxation, the cardiovascular system (Bian et al., 2008) and cancer (Choudhari et al., 2013). Three different isoforms of nitric oxide synthase (NOS): endothelial (eNOS), neuronal (nNOS) and inducible (iNOS) which produce nitric oxide, have been detected in a wide range of human cell lines. The expression of these isoforms has been reported to be increased in breast cancer (Thomsen et al., 1995) and other cancers such as colon cancer cells (Cianchi et al., 2003), lung cancer (Okayama et al., 2013), lymphoma (Barreiro Arcos et al., 2003), and melanoma (Massi et al., 2001).

A number of studies have demonstrated a relationship between nitric oxide expression and cell migration. For example, in wound healing assays high levels of nitric oxide promote wound healing and proliferation of human keratinocyte cells (Zhan et al., 2015). Whereas, low levels of nitric oxide leads to delayed wound healing (Schaffer et al., 1996). Expression of nitric oxide in wound healing is therefore an important component and might play a role in breast cancer metastasis.

In this chapter, L-NAME and 14000W have been used to inhibit total NO synthesis and inducible NO synthase (iNOS), respectively in MDA-MB-231 cells. Cell tracking was employed to identify its effect on migration. Cell tracking assays revealed a significant decrease in migration speed in MDA-MB-231 cells when treated with L-NAME (5 mM) or 1400W (2 mM) compared to control conditions. The migration speed for both inhibitors combined was not significantly altered, suggesting a role for iNOS. This is supported by the data obtained from invasive tumours, benign and normal tissue highlighting the role of iNOS protein levels (Thomsen et al., 1995).

It has been demonstrated that NO donors play a role in endothelial cell migration by increasing its ability to migrate and proliferate during wound healing of endothelial cells and human keratinocyte cells, suggesting the release of nitric oxide at the leading edge of the wound (Noiri et al., 1997) (Zhan

et al., 2015). However, cells treated with NO donor (PAPA NONOate) at 50 µM showed no significant effect on migration speed compared to the control. It is possible that the lack of an effect with the NO donor may indicate that the cells already produce enough NO to have a maximal effect on cell migration or that the NO needs to be produced locally (e.g. in endosomes or near the plasma membrane) in order to stimulate cell migration. Another possibility is that the NO is released too quickly and needs more sustained production of NO. This would suggest that future work could look at other NO donors.

Focal adhesion dynamics and turnover is considered to be an essential component of cell motility (Broussard et al., 2008). Previous studies indicate that nitric oxide is involved in the maintenance and attachment of adhesions to extracellular matrix in various cell types including endothelial cells, vascular smooth muscle cells and renal meningeal cells (Fang et al., 1997, Yao et al., 1998). In addition, the production of nitric oxide was shown to stimulate cell migration of intestinal epithelial cell line through FAK activation (Rhoads et al., 2004). However, the role of nitric oxide on focal adhesion turnover of cancer cell has not been well studied. Here, live cell imaging of mCherry -Zyxin revealed a significant increase in focal adhesion turnover time in cells treated with 5 mM L-NAME or 2 mM 1400W compared to control. The turnover rate for these cells was approximately 36.03 ± 3.8s in vehicle, compared with 74.57 ± 2.66s and 58.79 ± 7.69s in L-NAME and 1400W treated cells, respectively. This reduction supports the data obtained in cell tracking assays, suggesting that nitric oxide may regulate the migration of cells through regulating focal adhesion turnover. Another possibility is the inhibiting NO production stops migration through some other mechanism and once the cells stop migrating they also stop the turnover of FAs.

As L-NAME and 1400W regulate both cell migration and focal adhesion turnover, it was decided to investigate the mechanisms by which nitric oxide regulate focal adhesions turnover. One possible mechanism, as hypothesized in this chapter, could be via a direct effect of nitric oxide on proteins through the mechanism of S-nitrosylation. Nitric oxide has been reported to S-nitrosylate dynamin

and this in turn promotes cell survival and endocytosis (Kang-Decker et al., 2007). Nitric oxide nitrosylates dynamin within its pleckstrin homology (PH) domain on C607 (Wang et al., 2006). S-nitrosylation of dynamin Cys-607 induces GTPase activity and dynamin oligomerization, which in turn leads to increased receptor mediated endocytosis (Wang et al., 2006). For example, endothelial HEK cells expressing eNOS, increases β2adrenergic receptor internalization. Here however, we demonstrate that MDA-MB-231 cells inhibited with L-NAME and 1400W showed no significant effect on both dynamin dependent endocytosis marker (transferrin) and micropinocytosis (dextran), compared to control. One possible reason for these contradictory findings could be variation in experimental designs. For example, Wang et al used endothelial HEK cells expressing eNOS (cotransfected with expression plasmids encoding eNOS) and compered to non-transfected HEK cells (Wang et al., 2006). Also, Kang-Decker et al measured the uptake of transferrin, with the NO donor GSNO (Kang-Decker et al., 2007). While the transferrin uptake of this work was carried out in non-modified cells and via inhibition rather than inducing the nitric oxide. HEK cells also express little nitric oxide synthase isoforms (Gui et al., 2018). So, adding nitric oxide to these cells can increase the level of nitric oxide which in turn have a strong impact on cellular signalling events. Whereas, MDA-MB-231 cells already have high endogenous levels of nitric oxide synthase and further addition of nitric oxide might not be able to further increase any response. Therefore, such differences in cell types and experiments might explain these contradictory findings.

Another possible reason could be that S- nitrosylation of Dynamin may not occur at the plasma membrane where endocytosis uptake takes place. This is supported by an existing study highlighting a role of eNOS and Dynamin interactions in endothelial cells which found that endogenous eNOS and dynamin localize and interact within Golgi membranes (Cao et al., 2001a). They suggest that eNOS protein interactions occur in other membrane compartments within which eNOS resides (Cao et al., 2001a). Taken together, these observations with our findings may suggest that the inhibition of nitric oxide synthase did not affect internalization but might be involved in trafficking.

No change in transferrin uptake following NOS inhibition led us to hypothesise that nitric oxide might disrupt trafficking and fusion with lysosomes or recycling vesicles rather than internalization. This hypothesis was supported by a study which examined the role of nitric oxide in regulating membrane fusion by acting on a SNARE complex, resulting in induction of the exocytosis of Weibel-Palade Bodies (Matsushita et al., 2003). These findings imply the mode of action for nitric oxide is in the regulation of vesicle trafficking. Here, treatments with general NOS inhibitors such as L-NAME and the selective iNOS inhibitor 1400W resulted in a significant increase in the size of endosomes containing EEA1 and simultaneously decreased the number of these endosomes. This observation was further confirmed by immunocytochemistry results where EEA1 was found to moderately co-localize with eNOS and iNOS. Therefore, a significant reduction in the number and an increase in the size of endosomes containing EEA1 in addition to the co-localization of EEA1 with nitric oxide isoforms, suggests that nitric oxide may act on EEA1. These results encouraged us to employ the biotin switch assay to determine if these effects were due to S-nitrosylation of EEA1. Western blot analysis revealed that EEA1 was indeed S-nitrosylated compared to non-modified control proteins like H2B or ubiquitin. This result was further confirmed by bioinformatics analysis using GPS-SNO algorithm where EEA1 was predicted to be S-nitrosylated at four cysteine residues - Cys-46, Cys-255, Cys-894 and Cys-1102, with a high confidence score. Although, the score for these four site is high, the three-dimensional structure indicated that only two sites are exposed: Cys-46 and Cys-894, while the remaining two were buried: Cys-255 and Cys-1102. The two exposed cysteines are therefore more likely to be S-nitrosylated. Cys 894 is proposed to be located within the N-terminal C2H2 zinc finger (ZF) (Callaghan et al., 1999). EEA1 C2H2 ZF were shown to be highly selective to bind Rab5 switch regions as well as influence the active switch conformation (Mishra et al., 2010). The localization of Cys-894 in EEA1 suggests a mechanism of action for nitric oxide on EEA1 activity, specifically affecting the dimerization of EEA1, which is thought to be essential for the tethering function (Dumas et al., 2001) as cysteine residues form disulphide bonds and serve a

principal structural function during protein folding (Berndt et al., 2008). It may be that nitric oxide activity leads EEA1 to dimerize into a large protein complex that contains multiple Rab5 effectors such as Rab5a, Rabex-5 and Rabaptin as well as other endosome markers such as Syntaxin-13 and SNARE, and this results in the fusion and trafficking of endosomes (McBride et al., 1999). Therefore, S-nitrosylation of EEA1 at Cys-894 may induce the dimerization and thus promotes docking and fusion of endosomes.

As EEA1 is S-nitrosylated, it would seem reasonable to assume that other proteins that were found to interact with it or with early endosomes may also be S-nitrosylated. Clathrin heavy chain 1 was shown here to be S-nitrosylated in the MDA-MB-231 cell line, and was also analysed by a bioinformatics approach using the aforementioned GPS-SNO algorithm. Although seven cysteine residues are present in clathrin heavy chain 1 with a high confidence score, four cysteines: Cys-459, Cys-827, Cys-870 and Cys-934 are exposed and the remaining three are buried. Note that clathrin heavy chain consists of several domains including terminal domains, Linker domains, Ankle domains, distal segment domains and Knee domains (Xing et al., 2010). Cys 459 is located near the terminal domain that is critical for several accessory proteins bindings. These accessory proteins include Epsin (Rosenthal et al., 1999), β-subunits of adaptor complexes (Musacchio et al., 1999), AP-180 (Murphy et al., 1991) and Amphiphysin were reported to bind the NH2-terminal domain of clathrin (Slepnev et al., 2000). The location of Cys 459 at this region may allow nitric oxide to promote, via S-nitrosylation, modulation of the interaction between clathrin and these accessory proteins and thereby mediate vesicle trafficking. This concept is supported by Ozawa et al who found that S-nitrosylation of β-arrestin2 influences its interaction with clathrin and thereby regulates the receptor trafficking (Ozawa et al., 2008). Whereas, the localization of cys-827, cys-870 and cys-934 are located at distal segments (Xing et al., 2010). This region was shown to be important for clathrin heavy chain and vinculin interactions as well as interaction with α-actinin that mediates vesicle formation in muscle cells (Vassilopoulos et al., 2014) (Fausser et al., 1993). It may be possible that S-nitrosylations of

these cysteine residues in clathrin heavy chain may affect these interactions and thus result in enlargement of vesicles as previously seen in EEA1 containing vesicles following inhibition of NO synthesis.

On the other hand, two cysteines residues were found in APPL1. Although, the prediction score was quite high, especially for Cys-603 (score 20), both predicted were buried in the three-dimensional structure making them unlikely targets for S-nitrosylation. Similarly, there was only one cysteine residue predicted as a nitrosylation target in Rab5. Although, the score was high the cysteine was located outside of all obvious functional domains. This is plausible since, in this study, I found that treatments with general NOS inhibitors L-NAME and iNOS inhibitor 1400W did not affect the number or size of Rab5 containing endosomes.

In the case of LAMP1, this protein has a large N-terminal glycosylated luminal domain in the lysosomal lumen followed by a short C-terminal cytosolic tail (10–11 amino acids) and a lysosomal targeting signal (Eskelinen et al., 2003). It was shown that the main role of the luminal domain of LAMP1 was to maintain the structural integrity of the lysosome membrane and to protect it from degradation (Fukuda, 1991) due to heavy glycosylation of these proteins (Fukuda, 1991). Whereas, the cytosolic tail is necessary for the lysosomal targeting signal i.e. sorting this protein to late endosomes and lysosome (Cherqui et al., 2001). In regards to S-nitrosylation, the biotin switch assay showed that LAMP1 is S-nitrosylated in MDA-MB-231 cells and the GPS-SNO software predicted nitrosylation only on Cys-25 site. This cysteine is exposed and is located on the luminal domain near the cytosolic tail. At this site, the adaptor protein AP-2, which mediates the trafficking from the plasma membrane into the lysosome, was shown to directly bind (Bonifacino and Dell'Angelica, 1999). Thus, it is tempting to speculate that S-nitrosylation on Cys-25 may regulate AP2 binding and thereby promote the movement of endosome's fusion with lysosomes.

Taken together, nitric oxide is a crucial signalling molecule that regulates several processes and modulates a wide range of cell functions (Iwakiri, 2011) including endosome trafficking. In this chapter we identified that nitric oxide may be as positive regulator of cell migration and focal adhesion turnover and that relies on early endosomes trafficking. Therefore, mutagenesis approaches and the introduction of mutations of cysteine residues within EEA1 in dimerization sites or Rab5 binding regions should be introduced to enable S-nitrosylation inhibition and further clarify the role of nitric oxide in the regulation of endosome trafficking. Similar approaches should be used with other endosome proteins such as CHC1 and LAMP1. This will increase our knowledge how nitric oxide regulates their activity in cell migration and focal adhesion dynamics. It may also represent a new mechanism for cell migration and focal adhesion turnover, which could be targeted in the future.

Chapter 6 General discussion:

6.1 Future work and perspective:

The results in this thesis support the hypothesis that endocytosis modulates cell migration via regulating trafficking of focal adhesion, and nitric oxide accelerates this trafficking. One vital question is whether targeting endocytosis can be useful for development of molecular therapies to inhibit metastasis.

There is growing interest in clinical trials that target endocytosis in the delivery of anti-cancer drugs (Kim et al., 2013). Endocytosis has also gained high interest as a target for delivering and escaping the degradation of siRNA-based therapeutics. These siRNA-based therapeutics are being evaluated in preclinical trials to be used to target specific types of genes including anti-protein kinase N3 (PKN3) for pancreatic cancer (Aleku et al., 2008), vascular endothelial growth factor (VEGF) to modulate tumour angiogenesis (Forooghian and Das, 2007) and kinesin spindle protein (KSP1) for mitotic spindle formation (Zhang and Xu, 2008). Endocytosis of these siRNA is one of the main concerns that has prompted research to explore solutions that would enhance drug uptake into cancer cells in order to achieve a gene silencing effect by siRNA therapeutics. The specific drug needs to be able to cross the cellular membrane and gain access into the cytoplasm. However, siRNA molecules are not able to cross the plasma membrane on its own but need guides such as ligands which are highly expressed on cancer cells with lower expression on non-cancer cells (Teesalu et al., 2013) (Leng et al., 2017)

Clathrin mediated endocytosis receptors on the surface of cancer cells have been widely explored for targeted therapy and other literature reported examples are Epidermal Growth Factor Receptor (EGFR), Transforming Growth Factor Beta Receptor (TGFβR), Folate receptor (FR) and transferrin receptor (Daniels et al., 2012). Levels of transferrin are higher in high-grade ductal carcinoma in comparison with normal and benign tumours. Moreover, transforming growth factor beta (TGFβ)

expression has been found to increase in the late stages of tumour progression (Singh et al., 2011) (Jakowlew, 2006).Therefore, enhancing endocytosis pathways especially clathrin mediated endocytosis could lead to a higher take up of anti-cancer drugs (Alshehri et al., 2018). However, it may have possible side effects. For example excessive transferrin can be linked to iron requirements, which seem to impair the function of RNA and DNA resulting in rapidly dividing cells (Daniels et al., 2006). It also has been observed that this generates free radicals in cells resulting in damage of proteins, lipids and nucleic acids (Tarangelo and Dixon, 2016). In addition, it induces tumorigenesis and cancer growth (Schoenfeld et al., 2017). Our investigation shows that enhancing the endocytosis rate through clathrin pathways can enhance the turnover of focal adhesion and increase cancer cell migration. This finding may explains the reason for the progression of cancer among endocytosis which is characterized by excessive receptors such as transferrin (Jung et al., 2017). However, enhancing endocytosis through other pathways such as caveola and micropinocytosis can be targeted for delivering the drug as both micropinocytosis and caveola pathways had no effect with regards to cancer migration.

Endosomal escape is another challenge during cancer treatment. SiRNA molecules need to be released from endosomal vesicles into the cytoplasm avoiding the degradation system (late endosomes/lysosomes) to achieve arrival at its target destination. Several chemical compounds in combination with anti-cancer therapy have been used to facilitate endosomal escape such as chloroquine (CQ) (Cook et al., 2014) (Chude and Amaravadi, 2017) (Pellegrini et al., 2014). This compound has the ability to increase the time of siRNAs in early endosomes to escape the degradation through prevention of acidification of the endosomes and enhancement of the formation of large vesicles (Mauthe et al., 2018). Although chloroquine is very promising for cancer therapy, side effects have been reported during short term administration as well as severe side effects such as retinal toxicity and bone suppression during long term exposure (Costedoat-Chalumeau et al., 2015) (Verbaanderd et al., 2017).

Wittrup et al. 2015 showed that the release of siRNA, which presumably resulted from a damaged endosomal membrane, occurs from early endosomes (Wittrup et al., 2015). In addition, knocking down of endosomal sorting complexes required for transport (ESCRT) members has also been shown to improve *in vitro* and *in vivo* efficacy of anti-miRNA compounds (miRNA inhibitors). Our results showed that impairment of the site of EEA1 protein where endosomes need to polymerise showed no effect on the uptake of transferrin and prevented the fusion of endosomes by increasing the size of vesicle containing EEA1. This may indicates that knock down of endosomal EEA1 may enhance the uptake of siRNA and its release and could be a good choice for siRNA delivery. However, future work is needed to investigate whether knock down of endosome proteins involved in cell internalization is sufficient to overcome issues of delivering siRNA.

Besides its delivery, targeting endosomes can be a good choice for treatment of cancer and metastases. In real tumours, Rab5 and EEA1 expression has been found to be increased in aggressive cancer cells compared to normal and primary cancer tissue. Indicating that these proteins are over expressed in cancer cells compared to normal tissue. This can be employed as a prognostic marker for cancer progression especially on triple negative breast cancers as these cells lack receptors that can be targeted for cancer treatments such as Estrogenic Receptors, progesterone-receptors and HER2 (Sorlie et al., 2003) (Brenton et al., 2005).

In metastatic studies, through the examination of migration and invasiveness activity, endosomes have been shown to be involved in regulation of many aspects of cell migration. The action of these proteins has been shown to traffic c-Met to activate Rac1 which is implicated in polarized protrusion of lamellipodia and directed migration (Ménard et al., 2014) They also have been reported in recycling metalloproteases and integrins to the plasma membrane, thus promoting invasive properties of cancer cells (Schiefermeier et al., 2011).

Since delivery of these factors like integrin and metalloproteases to the plasma membrane is very common in metastatic phenotypes, our results support this concept by addressing a new role for endosomes in metastatic cells, as focal adhesions (Paxillin, Vinculin, and Zyxin) can be internalized and delivered to early endosomes. Internalization of these adhesions mediate focal adhesion disassembly, turnover and spread of cell migration. In this regard, endosomes - because of their ability to regulate polarity, motility, and endocytosis of integrin and focal adhesions, appear to be a good choice for metastatic intervention.

However, endosome treatment in combination with nitric oxide can pose a major challenge. Nitric oxide synthase expression has been shown to be associated with cancer development (Xu et al., 2002). For example the endothelial nitric oxide synthase was shown to be over expressed in cholangiocarcinoma cell lines and tissues (Suksawat et al., 2018). In addition, the expression of eNOS were found to be involved in proliferation of oral squamous cancer cell lines (Shang et al., 2006), enhanced the invasion of mammary cancer cells (Tu et al., 2006), tumor angiogenesis in gastric cancer (Wang et al., 2005), human breast cancer (Thomsen et al., 1995) and protected prostate cancer cells from induced apoptosis (Tong and Li, 2004).

Besides eNOS expression, NOS expression was shown to support tumour progression of melanoma by inducing chronic inflammation (Tanese et al., 2012). It elevates the caveolin-1 expression to increase the migration of breast cancer (Sanuphan et al., 2013). High NOS expression was found in colon cancer patients, and induced tumour growth in mice and increased incidences of lymph node metastasis (Erdman et al., 2009) (de Oliveira et al., 2017) (Salimian Rizi et al., 2017).

In contrast, several studies demonstrated that the expression of nitric oxide exhibited tumour-suppressive functions, suggesting that conflicting observations might depend on the type of tumour and stage of cancer progression. In this regard, the employed metastatic cell line MDA-MB-231

showed that inhibition of nitric oxide decreased the migration speed and the focal adhesion turnover, suggesting the expression of nitric oxide is associated with breast metastases migration.

Although nitric oxide is intrinsic to cancer metastases, there are still several challenges regarding therapeutically inhibiting it. One of the most common adverse effects of inhibiting NOS is hypertension. Hypertension can increase the risk of development of the cancer and increase the risk of metastasis (Han et al., 2017). Inhibition of nitric oxide increases blood pressure and this may also elevate the risk of developing cancer. In addition, inhibitor concentrations and the duration of nitric oxide exposure poses another challenge (Burke et al., 2013). Emerging evidence suggested that the posttranslational protein modification S-nitrosylation might represent a potentially viable therapeutic target (Nakamura and Lipton, 2016). In this regard, early endosomal marker EEA1 which co-localized with eNOS was found to be s-nitrosylated and inhibition of nitric oxide resulted in a significant increase in size of endosomes containing EEA1 and simultaneously decreased their number. This suggested that the dimerization of EEA1 and thus impaired docking and fusion of endosomes resulted in inhibition of cell migration and focal adhesion turnover. Therefore, mutagenesis approaches and introduction of mutations of cysteine residues within EEA1 in dimerization sites could be considered as a therapeutic target especially when combined with other cancer therapy as these inhibitors had no effect on the uptake of transferrin.

Endocytosis and recycling of integrin from the plasma membrane at the site of cell protrusions is an important step in cell migration and participates in tumour growth, invasion, and metastasis (Mosesson et al., 2008). It is estimated that integrins are recycled by the endosomal system every 30 minutes (Roberts et al., 2001a). In addition, it has been shown that endocytosis of integrins mediates the disassembly of focal adhesion, whereas recycling integrins can help the formation and reassembly of focal adhesions (Caswell and Norman, 2008). In this regard, the results of this project provided new evidence that focal adhesions also can be endocytosed and offered a link between focal adhesions (Paxillin, Vinculin and Zyxine) and the early endosome markers Rab5 and EEA1. These adhesions

were demonstrated to be internalised and that the early endosome compartment is involved in their transport. In addition, clatherin mediated pathways and early endosomes may contribute to the process of focal adhesion disassembly by internalizing these focal adhesions (Paxillin, Vinculin and Zyxin). Therefore, this prompted the question whether the whole FA complex is internalized. In this work it was shown that Zyxine, which is located up to 80nm from integrin and the plasma membrane (Kanchanawong et al., 2010), could be internalized (Figure 4.13). Therefore, α-actinin - which is located much further away from Zyxin – could be used to elucidate whether the whole complex internalized or just some focal adhesions. In addition, visualizing integrins, Rab5, and focal adhesions (Paxillin, Zyxin, Vinculin, α-actinin etc) with a triple immunostaining approach or isolating early endosomes and analysis with mass spectrometry will elucidate whether the whole complex is located in the same endosome meaning endocytosed as a whole. Super-resolution fluorescence microscopy STORM is a very effective method for studying co-localization, and could be used to examine endosomes that contain focal adhesions. Moreover, this technique could be used to acquire three-dimensional images that provide more precise information about whole cell layers (Huang et al., 2009).

Having demonstrated that focal adhesions are delivered to the early endosome compartment, the critical question became whether the internalized focal adhesion are delivered to late endosomes (Schiefermeier et al., 2014) to be degraded via autophagy (Sharifi et al., 2016) or recycled back to plasma membrane. Thus, the importance of other endosome proteins such a marker of endosome recycling, must also be considered. Immunostaining of these specific compartment markers will help to dissect the trafficking routes of focal adhesion proteins.

6.2 Future work:

There are several future research lines arising from this project that would complement the idea and could be tested in the future. For example, siRNA knock down of Rab5 or EEA1 to understand the complex process involved in cell internalization and to overcome issues of non-specificity of several pharmacological inhibitors. Further investigations that could be carried out here would be asking which endocytosis pathways or endosomes have the most effect on cell migration and focal adhesion turnover.

Further research would include mutagenesis approaches by introduction of mutations of cysteine residues within EEA1 in dimerization sites or Rab5 binding regions. This will increase our knowledge of how nitric oxide regulates their activity in cell migration and focal adhesion dynamics. It may also represent a new mechanism for cell migration and focal adhesion turnover, which could be targeted in the future.

Together with all future works that has been suggested above and in the general discussion will provide a far more complete understanding of the role of endocytosis in cell migration, focal adhesion endocytosis and its implication on focal adhesion disassembly. By understanding in detail the role of endocytosis in these main processes, we will lay the foundation in understanding the role of endocytosis in cancer cell migration.

References

ABERCROMBIE, M., JOAN, E., HEAYSMAN, M. & PEGRUM, S. M. 1970. The locomotion of fibroblasts in culture. *Experimental Cell Research,* 60**,** 437-444.

ALANKO, J., MAI, A., JACQUEMET, G., SCHAUER, K., KAUKONEN, R., SAARI, M., GOUD, B. & IVASKA, J. 2015. Integrin endosomal signalling suppresses anoikis. *Nature cell biology,* 17**,** 1412-1421.

ALEKU, M., SCHULZ, P., KEIL, O., SANTEL, A., SCHAEPER, U., DIECKHOFF, B., JANKE, O., ENDRUSCHAT, J., DURIEUX, B., RODER, N., LOFFLER, K., LANGE, C., FECHTNER, M., MOPERT, K., FISCH, G., DAMES, S., ARNOLD, W., JOCHIMS, K., GIESE, K., WIEDENMANN, B., SCHOLZ, A. & KAUFMANN, J. 2008. Atu027, a liposomal small interfering RNA formulation targeting protein kinase N3, inhibits cancer progression. *Cancer Res,* 68**,** 9788-98.

ALSHEHRI, A., GRABOWSKA, A. & STOLNIK, S. 2018. Pathways of cellular internalisation of liposomes delivered siRNA and effects on siRNA engagement with target mRNA and silencing in cancer cells. *Scientific Reports,* 8**,** 3748.

ALTOMARE, D. A. & TESTA, J. R. 2005. Perturbations of the AKT signaling pathway in human cancer. *Oncogene,* 24**,** 7455-64.

ANANTHAKRISHNAN, R. & EHRLICHER, A. 2007. The forces behind cell movement. *International journal of biological sciences,* 3**,** 303-317.

ANTONNY, B., BURD, C., DE CAMILLI, P., CHEN, E., DAUMKE, O., FAELBER, K., FORD, M., FROLOV, V. A., FROST, A., HINSHAW, J. E., KIRCHHAUSEN, T., KOZLOV, M. M., LENZ, M., LOW, H. H., MCMAHON, H., MERRIFIELD, C., POLLARD, T. D., ROBINSON, P. J., ROUX, A. & SCHMID, S. 2016. Membrane fission by dynamin: what we know and what we need to know. *Embo j,* 35**,** 2270-2284.

ARTYM, V. V., ZHANG, Y., SEILLIER-MOISEIWITSCH, F., YAMADA, K. M. & MUELLER, S. C. 2006. Dynamic interactions of cortactin and membrane type 1 matrix metalloproteinase at invadopodia: defining the stages of invadopodia formation and function. *Cancer Res,* 66**,** 3034-43.

BACHIR, A. I., ZARENO, J., MOISSOGLU, K., PLOW, E. F., GRATTON, E. & HORWITZ, A. R. 2014. Integrin-associated complexes form hierarchically with variable stoichiometry in nascent adhesions. *Curr Biol,* 24**,** 1845-53.

BAKER, N. & TUAN, R. S. 2013. The less-often-traveled surface of stem cells: caveolin-1 and caveolae in stem cells, tissue repair and regeneration. *Stem Cell Research & Therapy,* 4**,** 90.

BALBIS, A., PARMAR, A., WANG, Y., BAQUIRAN, G. & POSNER, B. I. 2007. Compartmentalization of signaling-competent epidermal growth factor receptors in endosomes. *Endocrinology,* 148**,** 2944-54.

BAMBURG, J. R. & BERNSTEIN, B. W. 2010. Roles of ADF/cofilin in actin polymerization and beyond. *F1000 biology reports,* 2**,** 62-62.

BAR-SAGI, D., FERNANDEZ, A. & FERAMISCO, J. R. 1987. Regulation of membrane turnover by ras proteins. *Biosci Rep,* 7**,** 427-34.

BARNETT, S. D. & BUXTON, I. L. O. 2017. The role of S-nitrosoglutathione reductase (GSNOR) in human disease and therapy. *Critical Reviews in Biochemistry and Molecular Biology,* 52**,** 340-354.

BAROUCH, W., PRASAD, K., GREENE, L. E. & EISENBERG, E. 1994. ATPase activity associated with the uncoating of clathrin baskets by Hsp70. *J Biol Chem,* 269**,** 28563-8.

BARREIRO ARCOS, M. L., GORELIK, G., KLECHA, A., GOREN, N., CERQUETTI, C. & CREMASCHI, G. A. 2003. Inducible nitric oxide synthase-mediated proliferation of a T lymphoma cell line. *Nitric Oxide,* 8**,** 111-8.

BASQUIN, C., TRICHET, M., VIHINEN, H., MALARDÉ, V., LAGACHE, T., RIPOLL, L., JOKITALO, E., OLIVO-MARIN, J.-C., GAUTREAU, A. & SAUVONNET, N. 2015. Membrane protrusion powers clathrin-independent endocytosis of interleukin-2 receptor. *The EMBO Journal,* 34**,** 2147-2161.

BAUM, B., SETTLEMAN, J. & QUINLAN, M. P. 2008. Transitions between epithelial and mesenchymal states in development and disease. *Seminars in Cell & Developmental Biology,* 19**,** 294-308.

BERNDT, C., LILLIG, C. H. & HOLMGREN, A. 2008. Thioredoxins and glutaredoxins as facilitators of protein folding. *Biochim Biophys Acta,* 1783**,** 641-50.

BIAN, K., DOURSOUT, M. F. & MURAD, F. 2008. Vascular system: role of nitric oxide in cardiovascular diseases. *J Clin Hypertens (Greenwich),* 10**,** 304-10.

BIJIAN, K., LOUGHEED, C., SU, J., XU, B., YU, H., WU, J. H., RICCIO, K. & ALAOUI-JAMALI, M. A. 2013. Targeting focal adhesion turnover in invasive breast cancer cells by the purine derivative reversine. *British journal of cancer,* 109**,** 2810-2818.

BISHOP, N. & WOODMAN, P. 2000. ATPase-defective mammalian VPS4 localizes to aberrant endosomes and impairs cholesterol trafficking. *Mol Biol Cell,* 11**,** 227-39.

BLASCO, M. A. 2005. Telomeres and human disease: ageing, cancer and beyond. *Nature Reviews Genetics,* 6**,** 611.

BONAZZI, M., SPANO, S., TURACCHIO, G., CERICOLA, C., VALENTE, C., COLANZI, A., KWEON, H. S., HSU, V. W., POLISHCHUCK, E. V., POLISHCHUCK, R. S., SALLESE, M., PULVIRENTI, T., CORDA, D. & LUINI, A. 2005. CtBP3/BARS drives membrane fission in dynamin-independent transport pathways. *Nat Cell Biol,* 7**,** 570-80.

BONIFACINO, J. S. & DELL'ANGELICA, E. C. 1999. Molecular Bases for the Recognition of Tyrosine-based Sorting Signals. *The Journal of Cell Biology,* 145**,** 923-926.

BORTHS, E. L. & WELCH, M. D. 2002. Turning on the Arp2/3 Complex at Atomic Resolution. *Structure,* 10**,** 131-135.

BOVE, P. F., WESLEY, U. V., GREUL, A. K., HRISTOVA, M., DOSTMANN, W. R. & VAN DER VLIET, A. 2007. Nitric oxide promotes airway epithelial wound

repair through enhanced activation of MMP-9. *Am J Respir Cell Mol Biol,* 36**,** 138-46.

BRAY, F., FERLAY, J., SOERJOMATARAM, I., SIEGEL, R. L., TORRE, L. A. & JEMAL, A. 2018. Global cancer statistics 2018: GLOBOCAN estimates of incidence and mortality worldwide for 36 cancers in 185 countries. *CA: a cancer journal for clinicians,* 68**,** 394-424.

BRETSCHER, M. S. 1992. Circulating integrins: alpha 5 beta 1, alpha 6 beta 4 and Mac-1, but not alpha 3 beta 1, alpha 4 beta 1 or LFA-1. *Embo j,* 11**,** 405-10.

BRIDGEWATER, R. E., NORMAN, J. C. & CASWELL, P. T. 2012. Integrin trafficking at a glance. *Journal of Cell Science,* 125**,** 3695-3701.

BROOKS, P. C. 1996. Cell adhesion molecules in angiogenesis. *Cancer Metastasis Rev,* 15**,** 187-94.

BROUSSARD, J. A., WEBB, D. J. & KAVERINA, I. 2008. Asymmetric focal adhesion disassembly in motile cells. *Curr Opin Cell Biol,* 20**,** 85-90.

BROWN, M. C. & TURNER, C. E. 2004a. Paxillin: Adapting to Change. *Physiological Reviews,* 84**,** 1315-1339.

BROWN, M. C. & TURNER, C. E. 2004b. Paxillin: adapting to change. *Physiol Rev,* 84**,** 1315-39.

BUCCIONE, R., CALDIERI, G. & AYALA, I. 2009. Invadopodia: specialized tumor cell structures for the focal degradation of the extracellular matrix. *Cancer Metastasis Rev,* 28**,** 137-49.

BUGYI, B. & CARLIER, M. F. 2010. Control of actin filament treadmilling in cell motility. *Annu Rev Biophys,* 39**,** 449-70.

BURKE, A. J., GLYNN, S. A., SULLIVAN, F. J. & GILES, F. J. 2013. The yin and yang of nitric oxide in cancer progression. *Carcinogenesis,* 34**,** 503-512.

BURRIDGE, K., FATH, K., KELLY, T., NUCKOLLS, G. & TURNER, C. 1988. Focal adhesions: transmembrane junctions between the extracellular matrix and the cytoskeleton. *Annu Rev Cell Biol,* 4**,** 487-525.

CALABIA-LINARES, C., ROBLES-VALERO, J., DE LA FUENTE, H., PEREZ-MARTINEZ, M., MARTÍN-COFRECES, N., ALFONSO-PÉREZ, M., GUTIERREZ-VÁZQUEZ, C., MITTELBRUNN, M., IBIZA, S., URBANO-OLMOS, F. R., AGUADO-BALLANO, C., SÁNCHEZ-SORZANO, C. O., SANCHEZ-MADRID, F. & VEIGA, E. 2011. Endosomal clathrin drives actin accumulation at the immunological synapse. *Journal of Cell Science,* 124**,** 820-830.

CALALB, M. B., POLTE, T. R. & HANKS, S. K. 1995. Tyrosine phosphorylation of focal adhesion kinase at sites in the catalytic domain regulates kinase activity: a role for Src family kinases. *Mol Cell Biol,* 15**,** 954-63.

CALALB, M. B., ZHANG, X., POLTE, T. R. & HANKS, S. K. 1996. Focal adhesion kinase tyrosine-861 is a major site of phosphorylation by Src. *Biochem Biophys Res Commun,* 228**,** 662-8.

CALLAGHAN, J., SIMONSEN, A., GAULLIER, J. M., TOH, B. H. & STENMARK, H. 1999. The endosome fusion regulator early-endosomal autoantigen 1 (EEA1) is a dimer. *Biochem J,* 338 (Pt 2)**,** 539-43.

CANTON, I. & BATTAGLIA, G. 2012. Endocytosis at the nanoscale. *Chem Soc Rev,* 41**,** 2718-39.

CAO, H., CHEN, J., AWONIYI, M., HENLEY, J. R. & MCNIVEN, M. A. 2007. Dynamin 2 mediates fluid-phase micropinocytosis in epithelial cells. *Journal of Cell Science,* 120**,** 4167.

CAO, S., YAO, J., MCCABE, T. J., YAO, Q., KATUSIC, Z. S., SESSA, W. C. & SHAH, V. 2001a. Direct interaction between endothelial nitric-oxide synthase and dynamin-2 implications for nitric-oxide synthase function. *Journal of Biological Chemistry,* 276**,** 14249-14256.

CAO, S., YAO, J., MCCABE, T. J., YAO, Q., KATUSIC, Z. S., SESSA, W. C. & SHAH, V. 2001b. Direct interaction between endothelial nitric-oxide synthase and dynamin-2. Implications for nitric-oxide synthase function. *J Biol Chem,* 276**,** 14249-56.

CARLIER, M. F., DUCRUIX, A. & PANTALONI, D. 1999. Signalling to actin: the Cdc42-N-WASP-Arp2/3 connection. *Chem Biol,* 6**,** R235-40.

CASAR, B. & CRESPO, P. 2016. ERK Signals: Scaffolding Scaffolds? *Frontiers in cell and developmental biology,* 4**,** 49-49.

CASTELLANO, F., LE CLAINCHE, C., PATIN, D., CARLIER, M.-F. & CHAVRIER, P. 2001. A WASp–VASP complex regulates actin polymerization at the plasma membrane. *The EMBO Journal,* 20**,** 5603-5614.

CASWELL, P. & NORMAN, J. 2008. Endocytic transport of integrins during cell migration and invasion. *Trends Cell Biol,* 18**,** 257-63.

CHAMBERS, A. F., GROOM, A. C. & MACDONALD, I. C. 2002. Dissemination and growth of cancer cells in metastatic sites. *Nat Rev Cancer,* 2**,** 563-72.

CHANDRASEKAR, I., STRADAL, T. E. B., HOLT, M. R., ENTSCHLADEN, F., JOCKUSCH, B. M. & ZIEGLER, W. H. 2005. Vinculin acts as a sensor in lipid regulation of adhesion-site turnover. *Journal of Cell Science,* 118**,** 1461.

CHAO, W.-T., ASHCROFT, F., DAQUINAG, A. C., VADAKKAN, T., WEI, Z., ZHANG, P., DICKINSON, M. E. & KUNZ, J. 2010. Type I Phosphatidylinositol Phosphate Kinase Beta Regulates Focal Adhesion Disassembly by Promoting β1 Integrin Endocytosis. *Molecular and Cellular Biology,* 30**,** 4463-4479.

CHAO, W.-T. & KUNZ, J. 2009. Focal adhesion disassembly requires clathrin-dependent endocytosis of integrins. *FEBS Letters,* 583**,** 1337-1343.

CHARRAS, G. & PALUCH, E. 2008. Blebs lead the way: how to migrate without lamellipodia. *Nat Rev Mol Cell Biol,* 9**,** 730-736.

CHATTERJEE, S., CAO, S., PETERSON, T. E., SIMARI, R. D. & SHAH, V. 2003. Inhibition of GTP-dependent vesicle trafficking impairs internalization of plasmalemmal eNOS and cellular nitric oxide production. *Journal of Cell Science,* 116**,** 3645-3655.

CHAVRIER, P., PARTON, R. G., HAURI, H. P., SIMONS, K. & ZERIAL, M. 1990. Localization of low molecular weight GTP binding proteins to exocytic and endocytic compartments. *Cell,* 62**,** 317-29.

CHENG, J., GRASSART, A. & DRUBIN, D. G. 2012. Myosin 1E coordinates actin assembly and cargo trafficking during clathrin-mediated endocytosis. *Molecular Biology of the Cell,* 23**,** 2891-2904.

CHENG, N., CHYTIL, A., SHYR, Y., JOLY, A. & MOSES, H. L. 2008. Transforming growth factor-β signaling–deficient fibroblasts enhance hepatocyte growth factor signaling in mammary carcinoma cells to promote scattering and invasion. *Molecular Cancer Research,* 6**,** 1521-1533.

CHERQUI, S., KALATZIS, V., TRUGNAN, G. & ANTIGNAC, C. 2001. The targeting of cystinosin to the lysosomal membrane requires a tyrosine-based signal and a novel sorting motif. *J Biol Chem,* 276**,** 13314-21.

CHOI, C. K., ZARENO, J., DIGMAN, M. A., GRATTON, E. & HORWITZ, A. R. 2011. Cross-correlated fluctuation analysis reveals phosphorylation-regulated paxillin-FAK complexes in nascent adhesions. *Biophys J,* 100**,** 583-592.

CHOUDHARI, S. K., CHAUDHARY, M., BAGDE, S., GADBAIL, A. R. & JOSHI, V. 2013. Nitric oxide and cancer: a review. *World journal of surgical oncology,* 11**,** 118-118.

CHRISTOFORIDIS, S., MCBRIDE, H. M., BURGOYNE, R. D. & ZERIAL, M. 1999. The Rab5 effector EEA1 is a core component of endosome docking. *Nature,* 397**,** 621-5.

CHUDE, C. I. & AMARAVADI, R. K. 2017. Targeting Autophagy in Cancer: Update on Clinical Trials and Novel Inhibitors. *International journal of molecular sciences,* 18**,** 1279.

CIANCHI, F., CORTESINI, C., FANTAPPIE, O., MESSERINI, L., SCHIAVONE, N., VANNACCI, A., NISTRI, S., SARDI, I., BARONI, G., MARZOCCA, C., PERNA, F., MAZZANTI, R., BECHI, P. & MASINI, E. 2003. Inducible nitric oxide synthase expression in human colorectal cancer: correlation with tumor angiogenesis. *Am J Pathol,* 162**,** 793-801.

CLEGHORN, W. M., BRANCH, K. M., KOOK, S., ARNETTE, C., BULUS, N., ZENT, R., KAVERINA, I., GUREVICH, E. V., WEAVER, A. M. & GUREVICH, V. V. 2014. Arrestins regulate cell spreading and motility via focal adhesion dynamics. *Molecular Biology of the Cell,* 26**,** 622-635.

COCUCCI, E., AGUET, F., BOULANT, S. & KIRCHHAUSEN, T. 2012. The first five seconds in the life of a clathrin-coated pit. *Cell,* 150**,** 495-507.

COLLINS, B. M., MCCOY, A. J., KENT, H. M., EVANS, P. R. & OWEN, D. J. 2002. Molecular architecture and functional model of the endocytic AP2 complex. *Cell,* 109**,** 523-35.

COOK, K. L., WARRI, A., SOTO-PANTOJA, D. R., CLARKE, P. A., CRUZ, M. I., ZWART, A. & CLARKE, R. 2014. Hydroxychloroquine inhibits autophagy to potentiate antiestrogen responsiveness in ER+ breast cancer. *Clin Cancer Res,* 20**,** 3222-32.

COPPOLINO, M. G., KRAUSE, M., HAGENDORFF, P., MONNER, D. A., TRIMBLE, W., GRINSTEIN, S., WEHLAND, J. & SECHI, A. S. 2001. Evidence for a molecular complex consisting of Fyb/SLAP, SLP-76, Nck, VASP and WASP that

links the actin cytoskeleton to Fcγ receptor signalling during phagocytosis. *Journal of Cell Science,* 114**,** 4307-4318.

CORTESIO, C. L., BOATENG, L. R., PIAZZA, T. M., BENNIN, D. A. & HUTTENLOCHER, A. 2011. Calpain-mediated proteolysis of paxillin negatively regulates focal adhesion dynamics and cell migration. *J Biol Chem,* 286**,** 9998-10006.

COSTEDOAT-CHALUMEAU, N., DUNOGUE, B., LEROUX, G., MOREL, N., JALLOULI, M., LE GUERN, V., PIETTE, J. C., BREZIN, A. P., MELLES, R. B. & MARMOR, M. F. 2015. A Critical Review of the Effects of Hydroxychloroquine and Chloroquine on the Eye. *Clin Rev Allergy Immunol,* 49**,** 317-26.

COTE, J. F., TURNER, C. E. & TREMBLAY, M. L. 1999. Intact LIM 3 and LIM 4 domains of paxillin are required for the association to a novel polyproline region (Pro 2) of protein-tyrosine phosphatase-PEST. *J Biol Chem,* 274**,** 20550-60.

CUKIERMAN, E., PANKOV, R., STEVENS, D. R. & YAMADA, K. M. 2001. Taking cell-matrix adhesions to the third dimension. *Science,* 294**,** 1708-12.

DAMM, E. M., PELKMANS, L., KARTENBECK, J., MEZZACASA, A., KURZCHALIA, T. & HELENIUS, A. 2005. Clathrin- and caveolin-1-independent endocytosis: entry of simian virus 40 into cells devoid of caveolae. *J Cell Biol,* 168**,** 477-88.

DANIELS, T. R., BERNABEU, E., RODRÍGUEZ, J. A., PATEL, S., KOZMAN, M., CHIAPPETTA, D. A., HOLLER, E., LJUBIMOVA, J. Y., HELGUERA, G. & PENICHET, M. L. 2012. The transferrin receptor and the targeted delivery of therapeutic agents against cancer. *Biochimica et biophysica acta,* 1820**,** 291-317.

DANIELS, T. R., DELGADO, T., RODRIGUEZ, J. A., HELGUERA, G. & PENICHET, M. L. 2006. The transferrin receptor part I: Biology and targeting with cytotoxic antibodies for the treatment of cancer. *Clinical Immunology,* 121**,** 144-158.

DANSON, C., BROWN, E., HEMMINGS, O. J., MCGOUGH, I. J., YARWOOD, S., HEESOM, K. J., CARLTON, J. G., MARTIN-SERRANO, J., MAY, M. T., VERKADE, P. & CULLEN, P. J. 2013. SNX15 links clathrin endocytosis to the PtdIns3P early endosome independently of the APPL1 endosome. *Journal of Cell Science,* 126**,** 4885.

DAS, S. & LAMBRIGHT, DAVID G. 2016. Membrane Trafficking: An Endosome Tether Meets a Rab and Collapses. *Current Biology,* 26**,** R927-R929.

DAVIDENKO, N., SCHUSTER, C. F., BAX, D. V., FARNDALE, R. W., HAMAIA, S., BEST, S. M. & CAMERON, R. E. 2016. Evaluation of cell binding to collagen and gelatin: a study of the effect of 2D and 3D architecture and surface chemistry. *Journal of materials science. Materials in medicine,* 27**,** 148-148.

DE FORGES, H., BOUISSOU, A. & PEREZ, F. 2012. Interplay between microtubule dynamics and intracellular organization. *The international journal of biochemistry & cell biology,* 44**,** 266-274.

DE OLIVEIRA, G. A., CHENG, R. Y. S., RIDNOUR, L. A., BASUDHAR, D., SOMASUNDARAM, V., MCVICAR, D. W., MONTEIRO, H. P. & WINK, D.

A. 2017. Inducible Nitric Oxide Synthase in the Carcinogenesis of Gastrointestinal Cancers. *Antioxid Redox Signal,* 26**,** 1059-1077.

DEBATIN, K. M. 2004. Apoptosis pathways in cancer and cancer therapy. *Cancer Immunol Immunother,* 53**,** 153-9.

DEBERARDINIS, R. J., LUM, J. J., HATZIVASSILIOU, G. & THOMPSON, C. B. 2008. The biology of cancer: metabolic reprogramming fuels cell growth and proliferation. *Cell metabolism,* 7**,** 11-20.

DEVITA, V. T., JR., YOUNG, R. C. & CANELLOS, G. P. 1975. Combination versus single agent chemotherapy: a review of the basis for selection of drug treatment of cancer. *Cancer,* 35**,** 98-110.

DI FIORE, P. P. & VON ZASTROW, M. 2014. Endocytosis, Signaling, and Beyond. *Cold Spring Harbor Perspectives in Biology,* 6**,** a016865.

DIGGINS, N. L. & WEBB, D. J. 2017. APPL1 is a multifunctional endosomal signaling adaptor protein. *Biochemical Society transactions,* 45**,** 771-779.

DOHERTY, G. J. & MCMAHON, H. T. 2009. Mechanisms of endocytosis. *Annu Rev Biochem,* 78**,** 857-902.

DOMINGUEZ, R. & HOLMES, K. C. 2011. Actin structure and function. *Annual review of biophysics,* 40**,** 169-186.

DOYLE, A. D., PETRIE, R. J., KUTYS, M. L. & YAMADA, K. M. 2013. Dimensions in Cell Migration. *Current opinion in cell biology,* 25**,** 642-649.

DOZYNKIEWICZ, M. A., JAMIESON, N. B., MACPHERSON, I., GRINDLAY, J., VAN DEN BERGHE, P. V. E., VON THUN, A., MORTON, J. P., GOURLEY, C., TIMPSON, P., NIXON, C., MCKAY, C. J., CARTER, R., STRACHAN, D., ANDERSON, K., SANSOM, O. J., CASWELL, P. T. & NORMAN, J. C. 2012. Rab25 and CLIC3 collaborate to promote integrin recycling from late endosomes/lysosomes and drive cancer progression. *Developmental cell,* 22**,** 131-145.

DUCHEK, P., SOMOGYI, K., JÉKELY, G., BECCARI, S. & RØRTH, P. 2001. *Guidance of cell migration by the Drosophila PDGF/VEGF receptor*.

DUMAS, J. J., MERITHEW, E., SUDHARSHAN, E., RAJAMANI, D., HAYES, S., LAWE, D., CORVERA, S. & LAMBRIGHT, D. G. 2001. Multivalent endosome targeting by homodimeric EEA1. *Mol Cell,* 8**,** 947-58.

DUTTA, D. & DONALDSON, J. G. 2012. Search for inhibitors of endocytosis: Intended specificity and unintended consequences. *Cell Logist,* 2**,** 203-208.

EDELING, M. A., SMITH, C. & OWEN, D. 2006. Life of a clathrin coat: insights from clathrin and AP structures. *Nat Rev Mol Cell Biol,* 7**,** 32-44.

EFIMOV, A., SCHIEFERMEIER, N., GRIGORIEV, I., BROWN, M. C., TURNER, C. E., SMALL, J. V. & KAVERINA, I. 2008. Paxillin-dependent stimulation of microtubule catastrophes at focal adhesion sites. *Journal of Cell Science,* 121**,** 196-204.

ELISHA, Y., KALCHENKO, V., KUZNETSOV, Y. & GEIGER, B. 2018. Dual role of E-cadherin in the regulation of invasive collective migration of mammary carcinoma cells. *Scientific reports,* 8**,** 4986-4986.

ELKIN, S. R., LAKODUK, A. M. & SCHMID, S. L. 2016. Endocytic pathways and endosomal trafficking: a primer. *Wiener Medizinische Wochenschrift,* 166**,** 196-204.

EPPINGA, R. D., KRUEGER, E. W., WELLER, S. G., ZHANG, L., CAO, H. & MCNIVEN, M. A. 2012. Increased expression of the large GTPase dynamin 2 potentiates metastatic migration and invasion of pancreatic ductal carcinoma. *Oncogene,* 31**,** 1228-41.

ERDMAN, S. E., RAO, V. P., POUTAHIDIS, T., ROGERS, A. B., TAYLOR, C. L., JACKSON, E. A., GE, Z., LEE, C. W., SCHAUER, D. B., WOGAN, G. N., TANNENBAUM, S. R. & FOX, J. G. 2009. Nitric oxide and TNF-alpha trigger colonic inflammation and carcinogenesis in Helicobacter hepaticus-infected, Rag2-deficient mice. *Proc Natl Acad Sci U S A,* 106**,** 1027-32.

ESKELINEN, E.-L., TANAKA, Y. & SAFTIG, P. 2003. At the acidic edge: emerging functions for lysosomal membrane proteins. *Trends in Cell Biology,* 13**,** 137-145.

EVANGELISTA, M., ZIGMOND, S. & BOONE, C. 2003. Formins: signaling effectors for assembly and polarization of actin filaments. *J Cell Sci,* 116**,** 2603-11.

EZRATTY, E. J., BERTAUX, C., MARCANTONIO, E. E. & GUNDERSEN, G. G. 2009. Clathrin mediates integrin endocytosis for focal adhesion disassembly in migrating cells. *The Journal of Cell Biology,* 187**,** 733.

EZRATTY, E. J., PARTRIDGE, M. A. & GUNDERSEN, G. G. 2005. Microtubule-induced focal adhesion disassembly is mediated by dynamin and focal adhesion kinase. *Nature Cell Biology,* 7**,** 581.

FANG, S., SHARMA, R. V. & BHALLA, R. C. 1997. Endothelial nitric oxide synthase gene transfer inhibits platelet-derived growth factor-BB stimulated focal adhesion kinase and paxillin phosphorylation in vascular smooth muscle cells. *Biochem Biophys Res Commun,* 236**,** 706-11.

FAUSSER, J. L., UNGEWICKELL, E., RUCH, J. V. & LESOT, H. 1993. Interaction of vinculin with the clathrin heavy chain. *J Biochem,* 114**,** 498-503.

FERGUSON, S. M. & DE CAMILLI, P. 2012. Dynamin, a membrane-remodelling GTPase. *Nature Reviews Molecular Cell Biology,* 13**,** 75.

FERON, O. & BALLIGAND, J.-L. 2006. Caveolins and the regulation of endothelial nitric oxide synthase in the heart. *Cardiovascular Research,* 69**,** 788-797.

FORD, M. G., PEARSE, B. M., HIGGINS, M. K., VALLIS, Y., OWEN, D. J., GIBSON, A., HOPKINS, C. R., EVANS, P. R. & MCMAHON, H. T. 2001. Simultaneous binding of PtdIns(4,5)P2 and clathrin by AP180 in the nucleation of clathrin lattices on membranes. *Science,* 291**,** 1051-5.

FOROOGHIAN, F. & DAS, B. 2007. Anti-angiogenic effects of ribonucleic acid interference targeting vascular endothelial growth factor and hypoxia-inducible factor-1alpha. *Am J Ophthalmol,* 144**,** 761-8.

FOSTER, M. W., HESS, D. T. & STAMLER, J. S. 2009. Protein S-nitrosylation in health and disease: a current perspective. *Trends Mol Med,* 15**,** 391-404.

FRAME, M. C. 2004. Newest findings on the oldest oncogene; how activated src does it. *J Cell Sci,* 117**,** 989-98.

FRANCO, S. J., RODGERS, M. A., PERRIN, B. J., HAN, J., BENNIN, D. A., CRITCHLEY, D. R. & HUTTENLOCHER, A. 2004. Calpain-mediated proteolysis of talin regulates adhesion dynamics. *Nat Cell Biol,* 6**,** 977-83.

FRIEDL, P. & GILMOUR, D. 2009. Collective cell migration in morphogenesis, regeneration and cancer. *Nat Rev Mol Cell Biol,* 10**,** 445-457.

FUCHS, E. & KARAKESISOGLOU, I. 2001. Bridging cytoskeletal intersections. *Genes Dev,* 15**,** 1-14.

FUKUDA, M. 1991. Lysosomal membrane glycoproteins. Structure, biosynthesis, and intracellular trafficking. *J Biol Chem,* 266**,** 21327-30.

GAGLIARDI, P. A., DI BLASIO, L. & PRIMO, L. 2015. PDK1: A signaling hub for cell migration and tumor invasion. *Biochimica et Biophysica Acta (BBA)-Reviews on Cancer,* 1856**,** 178-188.

GALLOP, J. L., WALRANT, A., CANTLEY, L. C. & KIRSCHNER, M. W. 2013. Phosphoinositides and membrane curvature switch the mode of actin polymerization via selective recruitment of toca-1 and Snx9. *Proc Natl Acad Sci U S A,* 110**,** 7193-8.

GAUTHIER, N. C., MONZO, P., GONZALEZ, T., DOYE, A., OLDANI, A., GOUNON, P., RICCI, V., CORMONT, M. & BOQUET, P. 2007. Early endosomes associated with dynamic F-actin structures are required for late trafficking of H. pylori VacA toxin. *The Journal of cell biology,* 177**,** 343-354.

GEIGER, B., SPATZ, J. P. & BERSHADSKY, A. D. 2009. Environmental sensing through focal adhesions. *Nature reviews Molecular cell biology,* 10**,** 21.

GIANNONE, G., MEGE, R. M. & THOUMINE, O. 2009. Multi-level molecular clutches in motile cell processes. *Trends Cell Biol,* 19**,** 475-86.

GONI, G. M., EPIFANO, C., BOSKOVIC, J., CAMACHO-ARTACHO, M., ZHOU, J., BRONOWSKA, A., MARTIN, M. T., ECK, M. J., KREMER, L., GRATER, F., GERVASIO, F. L., PEREZ-MORENO, M. & LIETHA, D. 2014. Phosphatidylinositol 4,5-bisphosphate triggers activation of focal adhesion kinase by inducing clustering and conformational changes. *Proc Natl Acad Sci U S A,* 111**,** E3177-86.

GOÑI, G. M., EPIFANO, C., BOSKOVIC, J., CAMACHO-ARTACHO, M., ZHOU, J., BRONOWSKA, A., MARTÍN, M. T., ECK, M. J., KREMER, L., GRÄTER, F., GERVASIO, F. L., PEREZ-MORENO, M. & LIETHA, D. 2014. Phosphatidylinositol 4,5-bisphosphate triggers activation of focal adhesion kinase by inducing clustering and conformational changes. *Proceedings of the National Academy of Sciences,* 111**,** E3177-E3186.

GONZALEZ, D. M. & MEDICI, D. 2014. Signaling mechanisms of the epithelial-mesenchymal transition. *Science Signaling,* 7**,** re8-re8.

GONZALEZ, L., AGULLO-ORTUNO, M. T., GARCIA-MARTINEZ, J. M., CALCABRINI, A., GAMALLO, C., PALACIOS, J., ARANDA, A. & MARTIN-PEREZ, J. 2006. Role of c-Src in human MCF7 breast cancer cell tumorigenesis. *J Biol Chem,* 281**,** 20851-64.

GROVER, C. N., CAMERON, R. E. & BEST, S. M. 2012. Investigating the morphological, mechanical and degradation properties of scaffolds comprising

collagen, gelatin and elastin for use in soft tissue engineering. *Journal of the Mechanical Behavior of Biomedical Materials,* 10**,** 62-74.

GRUENBERG, J., GRIFFITHS, G. & HOWELL, K. E. 1989. Characterization of the early endosome and putative endocytic carrier vesicles in vivo and with an assay of vesicle fusion in vitro. *The Journal of Cell Biology,* 108**,** 1301-1316.

GUI, L., ZHU, J., LU, X., SIMS, S. M., LU, W.-Y., STATHOPULOS, P. B. & FENG, Q. 2018. S-Nitrosylation of STIM1 by Neuronal Nitric Oxide Synthase Inhibits Store-Operated Ca2+ Entry. *Journal of Molecular Biology,* 430**,** 1773-1785.

GUPTON, S. L. & GERTLER, F. B. 2007. Filopodia: The Fingers That Do the Walking. *Science Signaling,* 2007**,** re5-re5.

HAILSTONES, D., SLEER, L. S., PARTON, R. G. & STANLEY, K. K. 1998. Regulation of caveolin and caveolae by cholesterol in MDCK cells. *J Lipid Res,* 39**,** 369-79.

HAKKINEN, K. M., HARUNAGA, J. S., DOYLE, A. D. & YAMADA, K. M. 2011. Direct comparisons of the morphology, migration, cell adhesions, and actin cytoskeleton of fibroblasts in four different three-dimensional extracellular matrices. *Tissue Eng Part A,* 17**,** 713-24.

HAN, H., GUO, W., SHI, W., YU, Y., ZHANG, Y., YE, X. & HE, J. 2017. Hypertension and breast cancer risk: a systematic review and meta-analysis. *Scientific reports,* 7**,** 44877-44877.

HANAHAN, D. & WEINBERG, R. A. 2000. The hallmarks of cancer. *Cell,* 100**,** 57-70.

HANAHAN, D. & WEINBERG, R. A. 2011. Hallmarks of cancer: the next generation. *Cell,* 144**,** 646-74.

HANAKI, H., YAMAMOTO, H., SAKANE, H., MATSUMOTO, S., OHDAN, H., SATO, A. & KIKUCHI, A. 2012. An anti-Wnt5a antibody suppresses metastasis of gastric cancer cells in vivo by inhibiting receptor-mediated endocytosis. *Mol Cancer Ther,* 11**,** 298-307.

HARUNAGA, J. S. & YAMADA, K. M. 2011. Cell-matrix adhesions in 3D. *Matrix Biol,* 30**,** 363-8.

HECKER, M., MULSCH, A., BASSENGE, E., FORSTERMANN, U. & BUSSE, R. 1994. Subcellular localization and characterization of nitric oxide synthase(s) in endothelial cells: physiological implications. *Biochem J,* 299 (Pt 1)**,** 247-52.

HEINO, J. 2000. The collagen receptor integrins have distinct ligand recognition and signaling functions. *Matrix Biol,* 19**,** 319-23.

HELENIUS, A., MELLMAN, I., WALL, D. & HUBBARD, A. 1983. Endosomes. *Trends in Biochemical Sciences,* 8**,** 245-250.

HENNE, W. M., BOUCROT, E., MEINECKE, M., EVERGREN, E., VALLIS, Y., MITTAL, R. & MCMAHON, H. T. 2010. FCHo proteins are nucleators of clathrin-mediated endocytosis. *Science,* 328**,** 1281-4.

HERMANN, M., FLAMMER, A. & LUSCHER, T. F. 2006. Nitric oxide in hypertension. *J Clin Hypertens (Greenwich),* 8**,** 17-29.

HOOD, J. D. & CHERESH, D. A. 2002. Role of integrins in cell invasion and migration. *Nature Reviews Cancer,* 2**,** 91.

HORTON, E. R., BYRON, A., ASKARI, J. A., NG, D. H. J., MILLON-FREMILLON, A., ROBERTSON, J., KOPER, E. J., PAUL, N. R., WARWOOD, S., KNIGHT, D., HUMPHRIES, J. D. & HUMPHRIES, M. J. 2015. Definition of a consensus integrin adhesome and its dynamics during adhesion complex assembly and disassembly. *Nat Cell Biol,* 17**,** 1577-1587.

HU, Y. L., LU, S., SZETO, K. W., SUN, J., WANG, Y., LASHERAS, J. C. & CHIEN, S. 2014. FAK and paxillin dynamics at focal adhesions in the protrusions of migrating cells. *Sci Rep,* 4**,** 6024.

HUANG, B., BATES, M. & ZHUANG, X. 2009. Super resolution fluorescence microscopy. *Annual review of biochemistry,* 78**,** 993-1016.

HULKOWER, K. I. & HERBER, R. L. 2011. Cell migration and invasion assays as tools for drug discovery. *Pharmaceutics,* 3**,** 107-124.

HUMPHRIES, J. D., BYRON, A. & HUMPHRIES, M. J. 2006. Integrin ligands at a glance. *Journal of Cell Science,* 119**,** 3901-3903.

HUMPHRIES, J. D., WANG, P., STREULI, C., GEIGER, B., HUMPHRIES, M. J. & BALLESTREM, C. 2007. Vinculin controls focal adhesion formation by direct interactions with talin and actin. *The Journal of cell biology,* 179**,** 1043-1057.

HUMPHRIES, W. H. T., SZYMANSKI, C. J. & PAYNE, C. K. 2011. Endo-lysosomal vesicles positive for Rab7 and LAMP1 are terminal vesicles for the transport of dextran. *PLoS One,* 6**,** e26626.

HUOTARI, J. & HELENIUS, A. Endosome maturation. *The EMBO journal,* 30**,** 3481-3500.

IWAKIRI, Y. 2011. S-nitrosylation of proteins: a new insight into endothelial cell function regulated by eNOS-derived NO. *Nitric oxide : biology and chemistry,* 25**,** 95-101.

JAFFREY, S. R. & SNYDER, S. H. 2001. The biotin switch method for the detection of S-nitrosylated proteins. *Sci STKE,* 2001**,** pl1.

JAKOWLEW, S. B. 2006. Transforming growth factor-β in cancer and metastasis. *Cancer and Metastasis Reviews,* 25**,** 435-457.

JOHNSON, I. R. D., PARKINSON-LAWRENCE, E. J., KEEGAN, H., SPILLANE, C. D., BARRY-O'CROWLEY, J., WATSON, W. R., SELEMIDIS, S., BUTLER, L. M., O'LEARY, J. J. & BROOKS, D. A. 2015. Endosomal gene expression: a new indicator for prostate cancer patient prognosis? *Oncotarget,* 6**,** 37919-37929.

JOVIC, M., SHARMA, M., RAHAJENG, J. & CAPLAN, S. 2010. The early endosome: a busy sorting station for proteins at the crossroads. *Histology and histopathology,* 25**,** 99-112.

JOYCE, J. A. & POLLARD, J. W. 2009. Microenvironmental regulation of metastasis. *Nat Rev Cancer,* 9**,** 239-52.

JUNG, M., WEIGERT, A., MERTENS, C., REHWALD, C. & BRUNE, B. 2017. Iron Handling in Tumor-Associated Macrophages-Is There a New Role for Lipocalin-2? *Front Immunol,* 8**,** 1171.

JUNTTILA, M. R. & EVAN, G. I. 2009. p53—a Jack of all trades but master of none. *Nature reviews cancer,* 9**,** 821.

KAKSONEN, M. & ROUX, A. 2018. Mechanisms of clathrin-mediated endocytosis. *Nat Rev Mol Cell Biol,* 19**,** 313-326.

KANCHANAWONG, P., SHTENGEL, G., PASAPERA, A. M., RAMKO, E. B., DAVIDSON, M. W., HESS, H. F. & WATERMAN, C. M. 2010. Nanoscale architecture of integrin-based cell adhesions. *Nature,* 468**,** 580-584.

KANG-DECKER, N., CAO, S., CHATTERJEE, S., YAO, J., EGAN, L. J., SEMELA, D., MUKHOPADHYAY, D. & SHAH, V. 2007. Nitric oxide promotes endothelial cell survival signaling through S-nitrosylation and activation of dynamin-2. *J Cell Sci,* 120**,** 492-501.

KAPLAN, K. B., BIBBINS, K. B., SWEDLOW, J. R., ARNAUD, M., MORGAN, D. O. & VARMUS, H. E. 1994. Association of the amino-terminal half of c-Src with focal adhesions alters their properties and is regulated by phosphorylation of tyrosine 527. *Embo j,* 13**,** 4745-56.

KAPLAN, K. B., SWEDLOW, J. R., VARMUS, H. E. & MORGAN, D. O. 1992. Association of p60c-src with endosomal membranes in mammalian fibroblasts. *The Journal of Cell Biology,* 118**,** 321-333.

KARDOS, R., POZSONYI, K., NEVALAINEN, E., LAPPALAINEN, P., NYITRAI, M. & HILD, G. 2009. The effects of ADF/cofilin and profilin on the conformation of the ATP-binding cleft of monomeric actin. *Biophysical journal,* 96**,** 2335-2343.

KAVERINA, I., KRYLYSHKINA, O. & SMALL, J. V. 1999. Microtubule Targeting of Substrate Contacts Promotes Their Relaxation and Dissociation. *The Journal of Cell Biology,* 146**,** 1033.

KAVERINA, I., ROTTNER, K. & SMALL, J. V. 1998. Targeting, capture, and stabilization of microtubules at early focal adhesions. *The Journal of cell biology,* 142**,** 181-190.

KIM, S. H., TURNBULL, J. & GUIMOND, S. 2011. Extracellular matrix and cell signalling: the dynamic cooperation of integrin, proteoglycan and growth factor receptor. *J Endocrinol,* 209**,** 139-51.

KIM, Y. M., KIM, T. H., CHUNG, H. T., TALANIAN, R. V., YIN, X. M. & BILLIAR, T. R. 2000. Nitric oxide prevents tumor necrosis factor alpha-induced rat hepatocyte apoptosis by the interruption of mitochondrial apoptotic signaling through S-nitrosylation of caspase-8. *Hepatology,* 32**,** 770-8.

KIM, Y. M., TALANIAN, R. V. & BILLIAR, T. R. 1997. Nitric oxide inhibits apoptosis by preventing increases in caspase-3-like activity via two distinct mechanisms. *J Biol Chem,* 272**,** 31138-48.

KIRSCHMANN, D. A., SEFTOR, E. A., NIEVA, D. R., MARIANO, E. A. & HENDRIX, M. J. 1999. Differentially expressed genes associated with the metastatic phenotype in breast cancer. *Breast cancer research and treatment,* 55**,** 125-134.

KISS, A. L. & BOTOS, E. 2009. Endocytosis via caveolae: alternative pathway with distinct cellular compartments to avoid lysosomal degradation? *Journal of cellular and molecular medicine,* 13**,** 1228-1237.

KNOTT, A. B. & BOSSY-WETZEL, E. 2009. Nitric oxide in health and disease of the nervous system. *Antioxidants & redox signaling,* 11**,** 541-554.

KOIVUSALO, M., WELCH, C., HAYASHI, H., SCOTT, C. C., KIM, M., ALEXANDER, T., TOURET, N., HAHN, K. M. & GRINSTEIN, S. 2010. Amiloride inhibits macropinocytosis by lowering submembranous pH and preventing Rac1 and Cdc42 signaling. *The Journal of cell biology,* 188**,** 547-563.

KRAMPE, S. & BOLES, E. 2002. Starvation-induced degradation of yeast hexose transporter Hxt7p is dependent on endocytosis, autophagy and the terminal sequences of the permease. *FEBS Lett,* 513**,** 193-6.

KUMAR, C. C. 1998. Signaling by integrin receptors. *Oncogene,* 17**,** 1365-73.

KURISU, S. & TAKENAWA, T. 2009. The WASP and WAVE family proteins. *Genome biology,* 10**,** 226-226.

KURONITA, T., ESKELINEN, E.-L., FUJITA, H., SAFTIG, P., HIMENO, M. & TANAKA, Y. 2002. A role for the lysosomal membrane protein LGP85 in the biogenesis and maintenance of endosomal and lysosomal morphology. *Journal of Cell Science,* 115**,** 4117-4131.

KUROSAKA, S. & KASHINA, A. 2008. Cell biology of embryonic migration. *Birth Defects Res C Embryo Today,* 84**,** 102-22.

LACHANCE, V., DEGRANDMAISON, J., MAROIS, S., ROBITAILLE, M., GÉNIER, S., NADEAU, S., ANGERS, S. & PARENT, J.-L. 2014. Ubiquitylation and activation of a Rab GTPase is promoted by a β₂AR–HACE1 complex. *Journal of Cell Science,* 127**,** 111-123.

LAL, H., S GULERIA, R., FOSTER, D., LU, G., WATSON, L., SANGHI, S., SMITH, M. & DOSTAL, D. 2007. *Integrins: novel therapeutic targets for cardiovascular diseases*.

LAMAZE, C., FUJIMOTO, L. M., YIN, H. L. & SCHMID, S. L. 1997. The Actin Cytoskeleton Is Required for Receptor-mediated Endocytosis in Mammalian Cells.

LANG, M. J., MARTINEZ-MARQUEZ, J. Y., PROSSER, D. C., GANSER, L. R., BUELTO, D., WENDLAND, B. & DUNCAN, M. C. 2014. Glucose starvation inhibits autophagy via vacuolar hydrolysis and induces plasma membrane internalization by down-regulating recycling. *J Biol Chem,* 289**,** 16736-47.

LAWSON, C., LIM, S. T., URYU, S., CHEN, X. L., CALDERWOOD, D. A. & SCHLAEPFER, D. D. 2012. FAK promotes recruitment of talin to nascent adhesions to control cell motility. *J Cell Biol,* 196**,** 223-32.

LE ROY, C. & WRANA, J. L. 2005. Clathrin- and non-clathrin-mediated endocytic regulation of cell signalling. *Nat Rev Mol Cell Biol,* 6**,** 112-126.

LEE, E. & DE CAMILLI, P. 2002. Dynamin at actin tails. *Proc Natl Acad Sci U S A,* 99**,** 161-6.

LEE, J. O., RIEU, P., ARNAOUT, M. A. & LIDDINGTON, R. 1995. Crystal structure of the A domain from the alpha subunit of integrin CR3 (CD11b/CD18). *Cell,* 80**,** 631-8.

LEE, M.-T. G., MISHRA, A. & LAMBRIGHT, D. G. 2009. Structural mechanisms for regulation of membrane traffic by rab GTPases. *Traffic (Copenhagen, Denmark),* 10**,** 1377-1389.

LEE, S. J., KIM, K. M., NAMKOONG, S., KIM, C. K., KANG, Y. C., LEE, H., HA, K. S., HAN, J. A., CHUNG, H. T., KWON, Y. G. & KIM, Y. M. 2005. Nitric oxide inhibition of homocysteine-induced human endothelial cell apoptosis by down-regulation of p53-dependent Noxa expression through the formation of S-nitrosohomocysteine. *J Biol Chem,* 280**,** 5781-8.

LEGATE, K. R. & FÄSSLER, R. 2009. Mechanisms that regulate adaptor binding to β-integrin cytoplasmic tails. *Journal of Cell Science,* 122**,** 187-198.

LENG, Q., WOODLE, M. C. & MIXSON, A. J. 2017. Targeted Delivery of siRNA Therapeutics to Malignant Tumors. *Journal of drug delivery,* 2017**,** 6971297-6971297.

LEON-BOLLOTTE, L., SUBRAMANIAM, S., CAUVARD, O., PLENCHETTE-COLAS, S., PAUL, C., GODARD, C., MARTINEZ-RUIZ, A., LEGEMBRE, P., JEANNIN, J. F. & BETTAIEB, A. 2011. S-nitrosylation of the death receptor fas promotes fas ligand-mediated apoptosis in cancer cells. *Gastroenterology,* 140**,** 2009-18, 2018.e1-4.

LETAI, A. 2017. Apoptosis and Cancer. *Annual Review of Cancer Biology,* 1**,** 275-294.

LEVIN, V. A., PANCHABHAI, S. C., SHEN, L., KORNBLAU, S. M., QIU, Y. & BAGGERLY, K. A. 2010. Different changes in protein and phosphoprotein levels result from serum starvation of high-grade glioma and adenocarcinoma cell lines. *Journal of proteome research,* 9**,** 179-191.

LI, J., MAO, X., DONG, L. Q., LIU, F. & TONG, L. 2007. Crystal structures of the BAR-PH and PTB domains of human APPL1. *Structure,* 15**,** 525-33.

LI, L., HE, Y., ZHAO, M. & JIANG, J. 2015a. Collective cell migration: Implications for wound healing and cancer invasion. *Burns & trauma,* 1**,** 21-26.

LI, L., WAN, T., WAN, M., LIU, B., CHENG, R. & ZHANG, R. 2015b. The effect of the size of fluorescent dextran on its endocytic pathway. *Cell Biol Int,* 39**,** 531-9.

LIANG, W., CURRAN, P. K., HOANG, Q., MORELAND, R. T. & FISHMAN, P. H. 2004. Differences in endosomal targeting of human β₁- and β₂-adrenergic receptors following clathrin-mediated endocytosis. *Journal of Cell Science,* 117**,** 723-734.

LIBERALI, P., KAKKONEN, E., TURACCHIO, G., VALENTE, C., SPAAR, A., PERINETTI, G., BÖCKMANN, R. A., CORDA, D., COLANZI, A., MARJOMAKI, V. & LUINI, A. 2008. The closure of Pak1-dependent macropinosomes requires the phosphorylation of CtBP1/BARS. *The EMBO journal,* 27**,** 970-981.

LIM, J. P. & GLEESON, P. A. 2011. Macropinocytosis: an endocytic pathway for internalising large gulps. *Immunol Cell Biol,* 89**,** 836-43.

LOBERT, V. H., BRECH, A., PEDERSEN, N. M., WESCHE, J., OPPELT, A., MALERØD, L. & STENMARK, H. 2010. Ubiquitination of α5β1 Integrin Controls Fibroblast Migration through Lysosomal Degradation of Fibronectin-Integrin Complexes. *Developmental Cell,* 19**,** 148-159.

LUKER, K. E., STEELE, J. M., MIHALKO, L. A., RAY, P. & LUKER, G. D. 2010. Constitutive and chemokine-dependent internalization and recycling of CXCR7 in breast cancer cells to degrade chemokine ligands. *Oncogene,* 29**,** 4599-610.

LUZIO, J. P., ROUS, B. A., BRIGHT, N. A., PRYOR, P. R., MULLOCK, B. M. & PIPER, R. C. 2000. Lysosome-endosome fusion and lysosome biogenesis. *J Cell Sci,* 113 (Pt 9)**,** 1515-24.

MACHESKY, L. M. & GOULD, K. L. 1999. The Arp2/3 complex: a multifunctional actin organizer. *Curr Opin Cell Biol,* 11**,** 117-21.

MACIA, E., EHRLICH, M., MASSOL, R., BOUCROT, E., BRUNNER, C. & KIRCHHAUSEN, T. 2006. Dynasore, a Cell-Permeable Inhibitor of Dynamin. *Developmental Cell,* 10**,** 839-850.

MADRI, J. A. & GRAESSER, D. 2000. Cell migration in the immune system: the evolving inter-related roles of adhesion molecules and proteinases. *Dev Immunol,* 7**,** 103-16.

MARITZEN, T., SCHACHTNER, H. & LEGLER, D. F. 2015. On the move: endocytic trafficking in cell migration. *Cell Mol Life Sci,* 72**,** 2119-34.

MÁRQUEZ, M. G., BRANDÁN, Y. R., GUAYTIMA, E. D. V., PAVÁN, C. H., FAVALE, N. O. & STERIN-SPEZIALE, N. B. 2014. Physiologically induced restructuring of focal adhesions causes mobilization of vinculin by a vesicular endocytic recycling pathway. *Biochimica et Biophysica Acta (BBA) - Molecular Cell Research,* 1843**,** 2991-3003.

MARTEL, V., VIGNOUD, L., DUPE, S., FRACHET, P., BLOCK, M. R. & ALBIGES-RIZO, C. 2000. Talin controls the exit of the integrin alpha 5 beta 1 from an early compartment of the secretory pathway. *Journal of Cell Science,* 113**,** 1951-1961.

MARTIN, K. H., SLACK, J. K., BOERNER, S. A., MARTIN, C. C. & PARSONS, J. T. 2002. Integrin connections map: to infinity and beyond. *Science,* 296**,** 1652-3.

MASSI, D., FRANCHI, A., SARDI, I., MAGNELLI, L., PAGLIERANI, M., BORGOGNONI, L., MARIA REALI, U. & SANTUCCI, M. 2001. Inducible nitric oxide synthase expression in benign and malignant cutaneous melanocytic lesions. *J Pathol,* 194**,** 194-200.

MATEUS, A. M., GORFINKIEL, N., SCHAMBERG, S. & MARTINEZ ARIAS, A. 2011. Endocytic and Recycling Endosomes Modulate Cell Shape Changes and Tissue Behaviour during Morphogenesis in Drosophila. *PLoS ONE,* 6**,** e18729.

MATSUSHITA, K., MORRELL, C. N., CAMBIEN, B., YANG, S. X., YAMAKUCHI, M., BAO, C., HARA, M. R., QUICK, R. A., CAO, W., O'ROURKE, B., LOWENSTEIN, J. M., PEVSNER, J., WAGNER, D. D. & LOWENSTEIN, C. J. 2003. Nitric oxide regulates exocytosis by S-nitrosylation of N-ethylmaleimide-sensitive factor. *Cell,* 115**,** 139-150.

MAUTHE, M., ORHON, I., ROCCHI, C., ZHOU, X., LUHR, M., HIJLKEMA, K.-J., COPPES, R. P., ENGEDAL, N., MARI, M. & REGGIORI, F. 2018. Chloroquine inhibits autophagic flux by decreasing autophagosome-lysosome fusion. *Autophagy,* 14**,** 1435-1455.

MAXFIELD, F. R. & MCGRAW, T. E. 2004. Endocytic recycling. *Nat Rev Mol Cell Biol,* 5**,** 121-32.

MAY, R. C., CARON, E., HALL, A. & MACHESKY, L. M. 2000. Involvement of the Arp2/3 complex in phagocytosis mediated by FcγR or CR3. *Nature Cell Biology,* 2**,** 246.

MAYLE, K. M., LE, A. M. & KAMEI, D. T. 2012. The intracellular trafficking pathway of transferrin. *Biochimica et biophysica acta,* 1820**,** 264-281.

MAYOR, S. & PAGANO, R. E. 2007. Pathways of clathrin-independent endocytosis. *Nat Rev Mol Cell Biol,* 8**,** 603-12.

MCBRIDE, H. M., RYBIN, V., MURPHY, C., GINER, A., TEASDALE, R. & ZERIAL, M. 1999. Oligomeric complexes link Rab5 effectors with NSF and drive membrane fusion via interactions between EEA1 and syntaxin 13. *Cell,* 98**,** 377-86.

MCCLELLAND, A., KUHN, L. C. & RUDDLE, F. H. 1984. The human transferrin receptor gene: genomic organization, and the complete primary structure of the receptor deduced from a cDNA sequence. *Cell,* 39**,** 267-74.

MCGUFFIN, L. J., ATKINS, J. D., SALEHE, B. R., SHUID, A. N. & ROCHE, D. B. 2015. IntFOLD: an integrated server for modelling protein structures and functions from amino acid sequences. *Nucleic Acids Res,* 43**,** W169-73.

MCGUFFIN, L. J., SHUID, A. N., KEMPSTER, R., MAGHRABI, A. H. A., NEALON, J. O., SALEHE, B. R., ATKINS, J. D. & ROCHE, D. B. 2018. Accurate template-based modeling in CASP12 using the IntFOLD4-TS, ModFOLD6, and ReFOLD methods. *Proteins,* 86 Suppl 1**,** 335-344.

MCLAUCHLAN, H., NEWELL, J., MORRICE, N., OSBORNE, A., WEST, M. & SMYTHE, E. 1998. A novel role for Rab5–GDI in ligand sequestration into clathrin-coated pits. *Current Biology,* 8**,** 34-45.

MCMAHON, H. T. & BOUCROT, E. 2011. Molecular mechanism and physiological functions of clathrin-mediated endocytosis. *Nature Reviews Molecular Cell Biology,* 12**,** 517.

MCNIVEN, M. A., KIM, L., KRUEGER, E. W., ORTH, J. D., CAO, H. & WONG, T. W. 2000. Regulated interactions between dynamin and the actin-binding protein cortactin modulate cell shape. *J Cell Biol,* 151**,** 187-98.

MEIER, O., GASTALDELLI, M., BOUCKE, K., HEMMI, S. & GREBER, U. F. 2005. Early Steps of Clathrin-Mediated Endocytosis Involved in Phagosomal Escape of Fcγ Receptor-Targeted Adenovirus. *Journal of Virology,* 79**,** 2604-2613.

MEIGHAN, C. M. & SCHWARZBAUER, J. E. 2008. Temporal and spatial regulation of integrins during development. *Current opinion in cell biology,* 20**,** 520-524.

MELLMAN, I. 1996. Endocytosis and molecular sorting. *Annu Rev Cell Dev Biol,* 12**,** 575-625.

MÉNARD, L., PARKER, P. J. & KERMORGANT, S. 2014. Receptor tyrosine kinase c-Met controls the cytoskeleton from different endosomes via different pathways. *Nature Communications,* 5**,** 3907.

MENDOZA, P. A., SILVA, P., DIAZ, J., ARRIAGADA, C., CANALES, J. & CERDA, O. 2018. Calpain2 mediates Rab5-driven focal adhesion disassembly and cell migration. 12**,** 185-194.

MERITHEW, E., STONE, C., EATHIRAJ, S. & LAMBRIGHT, D. G. 2003. Determinants of Rab5 interaction with the N terminus of early endosome antigen 1. *J Biol Chem,* 278**,** 8494-500.

MERRIFIELD, C. J., MOSS, S. E., BALLESTREM, C., IMHOF, B. A., GIESE, G., WUNDERLICH, I. & ALMERS, W. 1999. Endocytic vesicles move at the tips of actin tails in cultured mast cells. *Nat Cell Biol,* 1**,** 72-4.

METTLEN, M., PUCADYIL, T., RAMACHANDRAN, R. & SCHMID, S. L. 2009. Dissecting dynamin's role in clathrin-mediated endocytosis. *Biochemical Society transactions,* 37**,** 1022-1026.

MILLER, M. & MILLER, L. 2012. RAS Mutations and Oncogenesis: Not all RAS Mutations are Created Equally. *Frontiers in Genetics,* 2.

MISHRA, A., EATHIRAJ, S., CORVERA, S. & LAMBRIGHT, D. G. 2010. Structural basis for Rab GTPase recognition and endosome tethering by the C₂H₂ zinc finger of Early Endosomal Autoantigen 1 (EEA1). *Proceedings of the National Academy of Sciences,* 107**,** 10866-10871.

MITSUUCHI, Y., JOHNSON, S. W., SONODA, G., TANNO, S., GOLEMIS, E. A. & TESTA, J. R. 1999. Identification of a chromosome 3p14.3-21.1 gene, APPL, encoding an adaptor molecule that interacts with the oncoprotein-serine/threonine kinase AKT2. *Oncogene,* 18**,** 4891-8.

MIYA FUJIMOTO, L., ROTH, R., E. HEUSER, J. & SCHMID, S. 2000. *Actin Assembly Plays a Variable, but not Obligatory Role in Receptor-Mediated Endocytosis*.

MORBIDELLI, L., CHANG, C. H., DOUGLAS, J. G., GRANGER, H. J., LEDDA, F. & ZICHE, M. 1996. Nitric oxide mediates mitogenic effect of VEGF on coronary venular endothelium. *Am J Physiol,* 270**,** H411-5.

MORENO-BUENO, G., PORTILLO, F. & CANO, A. 2008. Transcriptional regulation of cell polarity in EMT and cancer. *Oncogene,* 27**,** 6958-69.

MORISCO, C., MARRONE, C., GALEOTTI, J., SHAO, D., VATNER, D. E., VATNER, S. F. & SADOSHIMA, J. 2008. Endocytosis machinery is required for beta1-adrenergic receptor-induced hypertrophy in neonatal rat cardiac myocytes. *Cardiovasc Res,* 78**,** 36-44.

MOSER, M., LEGATE, K. R., ZENT, R. & FASSLER, R. 2009. The tail of integrins, talin, and kindlins. *Science,* 324**,** 895-9.

MOSESSON, Y., MILLS, G. B. & YARDEN, Y. 2008. Derailed endocytosis: an emerging feature of cancer. *Nat Rev Cancer,* 8**,** 835-50.

MURPHY, J. E., PADILLA, B. E., HASDEMIR, B., COTTRELL, G. S. & BUNNETT, N. W. 2009. Endosomes: A legitimate platform for the signaling train. *Proceedings of the National Academy of Sciences,* 106**,** 17615-17622.

MURPHY, J. E., PLEASURE, I. T., PUSZKIN, S., PRASAD, K. & KEEN, J. H. 1991. Clathrin assembly protein AP-3. The identity of the 155K protein, AP 180, and NP185 and demonstration of a clathrin binding domain. *J Biol Chem,* 266**,** 4401-8.

MURRAY, D. H., JAHNEL, M., LAUER, J., AVELLANEDA, M. J., BROUILLY, N., CEZANNE, A., MORALES-NAVARRETE, H., PERINI, E. D., FERGUSON, C., LUPAS, A. N., KALAIDZIDIS, Y., PARTON, R. G., GRILL, S. W. & ZERIAL, M. 2016. An endosomal tether undergoes an entropic collapse to bring vesicles together. *Nature,* 537**,** 107-111.

MUSACCHIO, A., SMITH, C. J., ROSEMAN, A. M., HARRISON, S. C., KIRCHHAUSEN, T. & PEARSE, B. M. F. 1999. Functional Organization of Clathrin in Coats: Combining Electron Cryomicroscopy and X-Ray Crystallography. *Molecular Cell,* 3**,** 761-770.

NABI, I. R. & LE, P. U. 2003. Caveolae/raft-dependent endocytosis. *The Journal of cell biology,* 161**,** 673-677.

NADER, G. P., EZRATTY, E. J. & GUNDERSEN, G. G. 2016. FAK, talin and PIPKIgamma regulate endocytosed integrin activation to polarize focal adhesion assembly. *Nat Cell Biol,* 18**,** 491-503.

NAGANO, M., HOSHINO, D., SAKAMOTO, T., AKIZAWA, T., KOSHIKAWA, N. & SEIKI, M. 2011. *ZF21 is a new regulator of focal adhesion disassembly and a potential member of the spreading initiation center*.

NAKAMURA, T. & LIPTON, S. A. 2016. Protein S-Nitrosylation as a Therapeutic Target for Neurodegenerative Diseases. *Trends in pharmacological sciences,* 37**,** 73-84.

NAZAREWICZ, R. R., SALAZAR, G., PATRUSHEV, N., SAN MARTIN, A., HILENSKI, L., XIONG, S. & ALEXANDER, R. W. 2011. Early endosomal antigen 1 (EEA1) is an obligate scaffold for angiotensin II-induced, PKC-alpha-dependent Akt activation in endosomes. *The Journal of biological chemistry,* 286**,** 2886-2895.

NOBES, C. D. & HALL, A. 1999. Rho GTPases control polarity, protrusion, and adhesion during cell movement. *J Cell Biol,* 144**,** 1235-44.

NOIRI, E., HU, Y., BAHOU, W. F., KEESE, C. R., GIAEVER, I. & GOLIGORSKY, M. S. 1997. Permissive role of nitric oxide in endothelin-induced migration of endothelial cells. *J Biol Chem,* 272**,** 1747-52.

OHASHI, E., TANABE, K., HENMI, Y., MESAKI, K., KOBAYASHI, Y. & TAKEI, K. 2011. Receptor sorting within endosomal trafficking pathway is facilitated by dynamic actin filaments. *PloS one,* 6**,** e19942-e19942.

OKAYAMA, H., SAITO, M., OUE, N., WEISS, J. M., STAUFFER, J., TAKENOSHITA, S., WILTROUT, R. H., HUSSAIN, S. P. & HARRIS, C. C. 2013. NOS2 enhances KRAS-induced lung carcinogenesis, inflammation and microRNA-21 expression. *International journal of cancer,* 132**,** 9-18.

OLIVEIRA, C. J., CURCIO, M. F., MORAES, M. S., TSUJITA, M., TRAVASSOS, L. R., STERN, A. & MONTEIRO, H. P. 2008. The low molecular weight S-nitrosothiol, S-nitroso-N-acetylpenicillamine, promotes cell cycle progression in rabbit aortic endothelial cells. *Nitric Oxide,* 18**,** 241-55.

ORLOWSKI, J. & GRINSTEIN, S. 1997. Na+/H+ exchangers of mammalian cells. *J Biol Chem,* 272**,** 22373-6.

OZAWA, K., WHALEN, E. J., NELSON, C. D., MU, Y., HESS, D. T., LEFKOWITZ, R. J. & STAMLER, J. S. 2008. S-nitrosylation of beta-arrestin regulates beta-adrenergic receptor trafficking. *Molecular cell,* 31**,** 395-405.

PAAVILAINEN, V. O., BERTLING, E., FALCK, S. & LAPPALAINEN, P. 2004. Regulation of cytoskeletal dynamics by actin-monomer-binding proteins. *Trends Cell Biol,* 14**,** 386-94.

PALADE, G. E. 1953. Fine structure of blood capillaries. *J Appl phys,* 24**,** 1424-1436.

PALAMIDESSI, A., FRITTOLI, E., GARRE, M., FARETTA, M., MIONE, M., TESTA, I., DIASPRO, A., LANZETTI, L., SCITA, G. & DI FIORE, P. P. 2008. Endocytic trafficking of Rac is required for the spatial restriction of signaling in cell migration. *Cell,* 134**,** 135-47.

PARSONS, J. T. 2003. Focal adhesion kinase: the first ten years. *J Cell Sci,* 116**,** 1409-16.

PARSONS, J. T., HORWITZ, A. R. & SCHWARTZ, M. A. 2010. Cell adhesion: integrating cytoskeletal dynamics and cellular tension. *Nature reviews. Molecular cell biology,* 11**,** 633-643.

PARSONS, J. T., MARTIN, K. H., SLACK, J. K., TAYLOR, J. M. & WEED, S. A. 2000. Focal adhesion kinase: a regulator of focal adhesion dynamics and cell movement. *Oncogene,* 19**,** 5606-13.

PARTON, R. G. & COLLINS, B. M. 2016. Unraveling the architecture of caveolae. *Proceedings of the National Academy of Sciences,* 113**,** 14170-14172.

PAUL, N. R., JACQUEMET, G. & CASWELL, P. T. 2015. Endocytic Trafficking of Integrins in Cell Migration. *Curr Biol,* 25**,** R1092-105.

PEARSE, B. M. 1975. Coated vesicles from pig brain: purification and biochemical characterization. *J Mol Biol,* 97**,** 93-8.

PELLEGRINI, P., STRAMBI, A., ZIPOLI, C., HAGG-OLOFSSON, M., BUONCERVELLO, M., LINDER, S. & DE MILITO, A. 2014. Acidic extracellular pH neutralizes the autophagy-inhibiting activity of chloroquine: implications for cancer therapies. *Autophagy,* 10**,** 562-71.

PELLINEN, T., ARJONEN, A., VUORILUOTO, K., KALLIO, K., FRANSEN, J. A. & IVASKA, J. 2006. Small GTPase Rab21 regulates cell adhesion and controls endosomal traffic of beta1-integrins. *J Cell Biol,* 173**,** 767-80.

PERCIPALLE, P. 2013. Co-transcriptional nuclear actin dynamics. *Nucleus,* 4**,** 43-52.

PIERINI, L. M., LAWSON, M. A., EDDY, R. J., HENDEY, B. & MAXFIELD, F. R. 2000. Oriented endocytic recycling of alpha5beta1 in motile neutrophils. *Blood,* 95**,** 2471-80.

PIRKMAJER, S. & CHIBALIN, A. V. 2011. Serum starvation: caveat emptor. *American Journal of Physiology-Cell Physiology,* 301**,** C272-C279.

PLATTA, H. W. & STENMARK, H. 2011. Endocytosis and signaling. *Current Opinion in Cell Biology,* 23**,** 393-403.

POLLARD, T. D. & BORISY, G. G. 2003. Cellular motility driven by assembly and disassembly of actin filaments. *Cell,* 112**,** 453-65.

PORAT-SHLIOM, N., KLOOG, Y. & DONALDSON, J. G. 2008. A unique platform for H-Ras signaling involving clathrin-independent endocytosis. *Mol Biol Cell,* 19**,** 765-75.

QUALMANN, B., KESSELS, M. M. & KELLY, R. B. 2000. Molecular Links between Endocytosis and the Actin Cytoskeleton. *The Journal of Cell Biology,* 150**,** 111-116.

RAPPOPORT, J. Z. & SIMON, S. M. 2003. Real-time analysis of clathrin-mediated endocytosis during cell migration. *Journal of Cell Science,* 116**,** 847-855.

RATH, G., DESSY, C. & FERON, O. 2009. Caveolae, caveolin and control of vascular tone: nitric oxide (NO) and endothelium derived hyperpolarizing factor (EDHF) regulation. *J Physiol Pharmacol,* 60 Suppl 4**,** 105-9.

RAUCHENBERGER, R., HACKER, U., MURPHY, J., NIEWOHNER, J. & MANIAK, M. 1997. Coronin and vacuolin identify consecutive stages of a late, actin-coated endocytic compartment in Dictyostelium. *Curr Biol,* 7**,** 215-8.

RAYMENT, I., HOLDEN, H. M., WHITTAKER, M., YOHN, C. B., LORENZ, M., HOLMES, K. C. & MILLIGAN, R. A. 1993. Structure of the actin-myosin complex and its implications for muscle contraction. *Science,* 261**,** 58-65.

RHOADS, J. M., CHEN, W., GOOKIN, J., WU, G. Y., FU, Q., BLIKSLAGER, A. T., RIPPE, R. A., ARGENZIO, R. A., CANCE, W. G., WEAVER, E. M. & ROMER, L. H. 2004. Arginine stimulates intestinal cell migration through a focal adhesion kinase dependent mechanism. *Gut,* 53**,** 514-522.

RIDLEY, ANNE J. 2011. Life at the Leading Edge. *Cell,* 145**,** 1012-1022.

RINK, J., GHIGO, E., KALAIDZIDIS, Y. & ZERIAL, M. 2005. Rab Conversion as a Mechanism of Progression from Early to Late Endosomes. *Cell,* 122**,** 735-749.

RINNERTHALER, G., GEIGER, B. & SMALL, J. 1988. Contact formation during fibroblast locomotion: involvement of membrane ruffles and microtubules. *The Journal of cell biology,* 106**,** 747-760.

ROBERTS, M., BARRY, S., WOODS, A., VAN DER SLUIJS, P. & NORMAN, J. 2001a. PDGF-regulated rab4-dependent recycling of alphavbeta3 integrin from early endosomes is necessary for cell adhesion and spreading. *Curr Biol,* 11**,** 1392-402.

ROBERTS, M., BARRY, S., WOODS, A., VAN DER SLUIJS, P. & NORMAN, J. 2001b. PDGF-regulated rab4-dependent recycling of αvβ3 integrin from early endosomes is necessary for cell adhesion and spreading. *Current Biology,* 11**,** 1392-1402.

ROSALES, C. & URIBE-QUEROL, E. 2017. Phagocytosis: A Fundamental Process in Immunity. 2017**,** 9042851.

ROSENTHAL, J. A., CHEN, H., SLEPNEV, V. I., PELLEGRINI, L., SALCINI, A. E., DI FIORE, P. P. & DE CAMILLI, P. 1999. The epsins define a family of proteins that interact with components of the clathrin coat and contain a new protein module. *J Biol Chem,* 274**,** 33959-65.

RUBINO, M., MIACZYNSKA, M., LIPPE, R. & ZERIAL, M. 2000. Selective membrane recruitment of EEA1 suggests a role in directional transport of clathrin-coated vesicles to early endosomes. *J Biol Chem,* 275**,** 3745-8.

SABHARANJAK, S., SHARMA, P., PARTON, R. G. & MAYOR, S. 2002. GPI-anchored proteins are delivered to recycling endosomes via a distinct cdc42-regulated, clathrin-independent pinocytic pathway. *Dev Cell,* 2**,** 411-23.

SAKAI, K., NAKAMURA, T., SUZUKI, Y., IMIZU, T. & MATSUMOTO, K. 2011. 3-D collagen-dependent cell surface expression of MT1-MMP and MMP-2 activation regardless of integrin beta1 function and matrix stiffness. *Biochem Biophys Res Commun,* 412**,** 98-103.

SALIMIAN RIZI, B., ACHREJA, A. & NAGRATH, D. 2017. Nitric Oxide: The Forgotten Child of Tumor Metabolism. *Trends in cancer,* 3**,** 659-672.

SAMANIEGO, R., SÁNCHEZ-MARTÍN, L., ESTECHA, A. & SÁNCHEZ-MATEOS, P. 2007. Rho/ROCK and myosin II control the polarized distribution of endocytic clathrin structures at the uropod of moving T lymphocytes. *Journal of Cell Science,* 120**,** 3534.

SAMATOV, T. R., TONEVITSKY, A. G. & SCHUMACHER, U. 2013a. Epithelial-mesenchymal transition: focus on metastatic cascade, alternative splicing, non-coding RNAs and modulating compounds. *Molecular cancer,* 12**,** 107-107.

SAMATOV, T. R., TONEVITSKY, A. G. & SCHUMACHER, U. 2013b. Epithelial-mesenchymal transition: focus on metastatic cascade, alternative splicing, non-coding RNAs and modulating compounds. *Molecular Cancer,* 12**,** 107.

SANDILANDS, E., CANS, C., FINCHAM, V. J., BRUNTON, V. G., MELLOR, H., PRENDERGAST, G. C., NORMAN, J. C., SUPERTI-FURGA, G. & FRAME, M. C. 2004. RhoB and actin polymerization coordinate Src activation with endosome-mediated delivery to the membrane. *Dev Cell,* 7**,** 855-69.

SANDILANDS, E. & FRAME, M. C. 2008. Endosomal trafficking of Src tyrosine kinase. *Trends Cell Biol,* 18**,** 322-9.

SANUPHAN, A., CHUNHACHA, P., PONGRAKHANANON, V. & CHANVORACHOTE, P. 2013. Long-term nitric oxide exposure enhances lung cancer cell migration. *Biomed Res Int,* 2013**,** 186972.

SATO, K., WATANABE, T., WANG, S., KAKENO, M., MATSUZAWA, K., MATSUI, T., YOKOI, K., MURASE, K., SUGIYAMA, I., OZAWA, M. & KAIBUCHI, K. 2011. Numb controls E-cadherin endocytosis through p120 catenin with aPKC. *Mol Biol Cell,* 22**,** 3103-19.

SCHAFFER, M. R., TANTRY, U., GROSS, S. S., WASSERBURG, H. L. & BARBUL, A. 1996. Nitric oxide regulates wound healing. *J Surg Res,* 63**,** 237-40.

SCHALLER, M. D., HILDEBRAND, J. D., SHANNON, J. D., FOX, J. W., VINES, R. R. & PARSONS, J. T. 1994a. Autophosphorylation of the focal adhesion kinase, pp125FAK, directs SH2-dependent binding of pp60src. *Molecular and Cellular Biology,* 14**,** 1680-1688.

SCHALLER, M. D., HILDEBRAND, J. D., SHANNON, J. D., FOX, J. W., VINES, R. R. & PARSONS, J. T. 1994b. Autophosphorylation of the focal adhesion kinase, pp125FAK, directs SH2-dependent binding of pp60src. *Mol Cell Biol,* 14**,** 1680-8.

SCHIEFERMEIER, N., SCHEFFLER, J. M., DE ARAUJO, M. E. G., STASYK, T., YORDANOV, T., EBNER, H. L., OFFTERDINGER, M., MUNCK, S., HESS, M. W., WICKSTRÖM, S. A., LANGE, A., WUNDERLICH, W., FÄSSLER, R., TEIS, D. & HUBER, L. A. 2014. The late endosomal p14–MP1 (LAMTOR2/3) complex regulates focal adhesion dynamics during cell migration. *The Journal of Cell Biology,* 205**,** 525-540.

SCHIEFERMEIER, N., TEIS, D. & HUBER, L. A. 2011. Endosomal signaling and cell migration. *Current opinion in cell biology,* 23**,** 615-620.

SCHLESINGER, M. 2018. Role of platelets and platelet receptors in cancer metastasis. *Journal of Hematology & Oncology,* 11**,** 125.

SCHLUNCK, G., DAMKE, H., KIOSSES, W. B., RUSK, N., SYMONS, M. H., WATERMAN-STORER, C. M., SCHMID, S. L. & SCHWARTZ, M. A. 2004. Modulation of Rac localization and function by dynamin. *Mol Biol Cell,* 15**,** 256-67.

SCHMID, E. M. & MCMAHON, H. T. 2007. Integrating molecular and network biology to decode endocytosis. *Nature,* 448**,** 883.

SCHOENFELD, J. D., SIBENALLER, Z. A., MAPUSKAR, K. A., WAGNER, B. A., CRAMER-MORALES, K. L., FURQAN, M., SANDHU, S., CARLISLE, T. L., SMITH, M. C., ABU HEJLEH, T., BERG, D. J., ZHANG, J., KEECH, J., PAREKH, K. R., BHATIA, S., MONGA, V., BODEKER, K. L., AHMANN, L., VOLLSTEDT, S., BROWN, H., SHANAHAN KAUFFMAN, E. P., SCHALL, M. E., HOHL, R. J., CLAMON, G. H., GREENLEE, J. D., HOWARD, M. A., SCHULTZ, M. K., SMITH, B. J., RILEY, D. P., DOMANN, F. E., CULLEN, J. J., BUETTNER, G. R., BUATTI, J. M., SPITZ, D. R. & ALLEN, B. G. 2017. O2(-) and H2O2-Mediated Disruption of Fe Metabolism Causes the Differential Susceptibility of NSCLC and GBM Cancer Cells to Pharmacological Ascorbate. *Cancer Cell,* 31**,** 487-500.e8.

SCHUH, A. & DREAU, H. 2018. Clinically actionable mutation profiles in patients with cancer identified by whole-genome sequencing. 4.

SCHWARTZ, M. A. & ASSOIAN, R. K. 2001. Integrins and cell proliferation. *regulation of cyclin-dependent kinases via cytoplasmic signaling pathways,* 114**,** 2553-2560.

SCHWARTZ, S. L., CAO, C., PYLYPENKO, O., RAK, A. & WANDINGER-NESS, A. 2007. Rab GTPases at a glance. *Journal of cell science,* 120**,** 3905-3910.

SETH, D., HESS, D. T., HAUSLADEN, A., WANG, L., WANG, Y. J. & STAMLER, J. S. 2018. A Multiplex Enzymatic Machinery for Cellular Protein S-nitrosylation. *Mol Cell,* 69**,** 451-464.e6.

SEYFRIED, T. N. & HUYSENTRUYT, L. C. 2013. On the origin of cancer metastasis. *Critical reviews in oncogenesis,* 18**,** 43-73.

SHANG, Z. J., LI, Z. B. & LI, J. R. 2006. In vitro effects of nitric oxide synthase inhibitor L-NAME on oral squamous cell carcinoma: a preliminary study. *Int J Oral Maxillofac Surg,* 35**,** 539-43.

SHARIFI, M. N., MOWERS, E. E., DRAKE, L. E., COLLIER, C., CHEN, H., ZAMORA, M., MUI, S. & MACLEOD, K. F. 2016. Autophagy Promotes Focal Adhesion Disassembly and Cell Motility of Metastatic Tumor Cells through the Direct Interaction of Paxillin with LC3. *Cell Rep,* 15**,** 1660-72.

SHAUL, P. W. 2003. Endothelial nitric oxide synthase, caveolae and the development of atherosclerosis. *The Journal of physiology,* 547**,** 21-33.

SHI, Y. 2002. Mechanisms of caspase activation and inhibition during apoptosis. *Mol Cell,* 9**,** 459-70.

SHI, Y. 2004. Caspase activation, inhibition, and reactivation: a mechanistic view. *Protein science : a publication of the Protein Society,* 13**,** 1979-1987.

SHPETNER, H. S. & VALLEE, R. B. 1989. Identification of dynamin, a novel mechanochemical enzyme that mediates interactions between microtubules. *Cell,* 59**,** 421-32.

SIEG, D. J., HAUCK, C. R., ILIC, D., KLINGBEIL, C. K., SCHAEFER, E., DAMSKY, C. H. & SCHLAEPFER, D. D. 2000. FAK integrates growth-factor and integrin signals to promote cell migration. *Nat Cell Biol,* 2**,** 249-56.

SIGISMUND, S., CONFALONIERI, S., CILIBERTO, A., POLO, S., SCITA, G. & DI FIORE, P. P. 2012. Endocytosis and signaling: cell logistics shape the eukaryotic cell plan. *Physiol Rev,* 92**,** 273-366.

SIMONS, K. & SAMPAIO, J. L. 2011. Membrane organization and lipid rafts. *Cold Spring Harb Perspect Biol,* 3**,** a004697.

SIMONSEN, A., LIPPE, R., CHRISTOFORIDIS, S., GAULLIER, J.-M., BRECH, A., CALLAGHAN, J., TOH, B.-H., MURPHY, C., ZERIAL, M. & STENMARK, H. 1998. EEA1 links PI(3)K function to Rab5 regulation of endosome fusion. *Nature,* 394**,** 494.

SINGH, M., MUGLER, K., HAILOO, D. W., BURKE, S., NEMESURE, B., TORKKO, K. & SHROYER, K. R. 2011. Differential expression of transferrin receptor (TfR) in a spectrum of normal to malignant breast tissues: implications for in situ and invasive carcinoma. *Appl Immunohistochem Mol Morphol,* 19**,** 417-23.

SKALSKI, M., SHARMA, N., WILLIAMS, K., KRUSPE, A. & COPPOLINO, M. G. 2011. SNARE-mediated membrane traffic is required for focal adhesion kinase signaling and Src-regulated focal adhesion turnover. *Biochimica et Biophysica Acta (BBA) - Molecular Cell Research,* 1813**,** 148-158.

SLEPNEV, V. I., OCHOA, G. C., BUTLER, M. H. & DE CAMILLI, P. 2000. Tandem arrangement of the clathrin and AP-2 binding domains in amphiphysin 1 and disruption of clathrin coat function by amphiphysin fragments comprising these sites. *J Biol Chem,* 275**,** 17583-9.

SMITH, B. C. & MARLETTA, M. A. 2012. Mechanisms of S-nitrosothiol formation and selectivity in nitric oxide signaling. *Curr Opin Chem Biol,* 16**,** 498-506.

SMITH, E. W., LIMA, W. C., CHARETTE, S. J. & COSSON, P. 2010. Effect of starvation on the endocytic pathway in Dictyostelium cells. *Eukaryotic cell,* 9**,** 387-392.

SOLINGER, J. A. & SPANG, A. 2013. Tethering complexes in the endocytic pathway: CORVET and HOPS. *Febs j,* 280**,** 2743-57.

SOMSEL RODMAN, J. & WANDINGER-NESS, A. 2000. Rab GTPases coordinate endocytosis. *J Cell Sci,* 113 Pt 2**,** 183-92.

SORLIE, T., TIBSHIRANI, R., PARKER, J., HASTIE, T., MARRON, J. S., NOBEL, A., DENG, S., JOHNSEN, H., PESICH, R., GEISLER, S., DEMETER, J., PEROU, C. M., LONNING, P. E., BROWN, P. O., BORRESEN-DALE, A. L. & BOTSTEIN, D. 2003. Repeated observation of breast tumor subtypes in independent gene expression data sets. *Proc Natl Acad Sci U S A,* 100**,** 8418-23.

SOUSA, R. & LAFER, E. M. 2015. The role of molecular chaperones in clathrin mediated vesicular trafficking. *Frontiers in molecular biosciences,* 2**,** 26-26.

SPAARGAREN, M. & BOS, J. L. 1999. Rab5 induces Rac-independent lamellipodia formation and cell migration. *Molecular biology of the cell,* 10**,** 3239-3250.

STAHLSCHMIDT, W., ROBERTSON, M. J., ROBINSON, P. J., MCCLUSKEY, A. & HAUCKE, V. 2014. Clathrin terminal domain-ligand interactions regulate sorting of mannose 6-phosphate receptors mediated by AP-1 and GGA adaptors. *The Journal of biological chemistry,* 289**,** 4906-4918.

STENMARK, H., AASLAND, R., TOH, B. H. & D'ARRIGO, A. 1996. Endosomal localization of the autoantigen EEA1 is mediated by a zinc-binding FYVE finger. *J Biol Chem,* 271**,** 24048-54.

STOWELL, M. H., MARKS, B., WIGGE, P. & MCMAHON, H. T. 1999. Nucleotide-dependent conformational changes in dynamin: evidence for a mechanochemical molecular spring. *Nat Cell Biol,* 1**,** 27-32.

SUKSAWAT, M., TECHASEN, A., NAMWAT, N., BOONSONG, T., TITAPUN, A., UNGARREEVITTAYA, P., YONGVANIT, P. & LOILOME, W. 2018. Inhibition of endothelial nitric oxide synthase in cholangiocarcinoma cell lines - a new strategy for therapy. *FEBS open bio,* 8**,** 513-522.

SUN, M., WANG, G., PACIGA, J. E., FELDMAN, R. I., YUAN, Z. Q., MA, X. L., SHELLEY, S. A., JOVE, R., TSICHLIS, P. N., NICOSIA, S. V. & CHENG, J. Q. 2001. AKT1/PKBalpha kinase is frequently elevated in human cancers and its constitutive activation is required for oncogenic transformation in NIH3T3 cells. *Am J Pathol,* 159**,** 431-7.

SWANEY, K. F. & LI, R. 2016. Function and regulation of the Arp2/3 complex during cell migration in diverse environments. *Current Opinion in Cell Biology,* 42**,** 63-72.

SWANSON, J. A. & WATTS, C. 1995. Macropinocytosis. *Trends Cell Biol,* 5**,** 424-8.

SWEITZER, S. M. & HINSHAW, J. E. 1998. Dynamin Undergoes a GTP-Dependent Conformational Change Causing Vesiculation. *Cell,* 93**,** 1021-1029.

TAN, Y., YOU, H., WU, C., ALTOMARE, D. A. & TESTA, J. R. 2010. Appl1 is dispensable for mouse development, and loss of Appl1 has growth factor-selective effects on Akt signaling in murine embryonic fibroblasts. *J Biol Chem,* 285**,** 6377-89.

TANESE, K., GRIMM, E. A. & EKMEKCIOGLU, S. 2012. The role of melanoma tumor-derived nitric oxide in the tumor inflammatory microenvironment: its impact on the chemokine expression profile, including suppression of CXCL10. *Int J Cancer,* 131**,** 891-901.

TANG, A., ELLER, M. S., HARA, M., YAAR, M., HIROHASHI, S. & GILCHREST, B. A. 1994. E-cadherin is the major mediator of human melanocyte adhesion to keratinocytes in vitro. *J Cell Sci,* 107 (Pt 4)**,** 983-92.

TARANGELO, A. & DIXON, S. J. 2016. Nanomedicine: An iron age for cancer therapy. *Nat Nanotechnol,* 11**,** 921-922.

TEESALU, T., SUGAHARA, K. N. & RUOSLAHTI, E. 2013. Tumor-penetrating peptides. *Front Oncol,* 3**,** 216.

THEODOSIOU, M., WIDMAIER, M., BOTTCHER, R. T., ROGNONI, E., VEELDERS, M., BHARADWAJ, M., LAMBACHER, A., AUSTEN, K.,

MULLER, D. J., ZENT, R. & FASSLER, R. 2016. Kindlin-2 cooperates with talin to activate integrins and induces cell spreading by directly binding paxillin. *Elife,* 5**,** e10130.

THIERY, J. P. 2002. Epithelial-mesenchymal transitions in tumour progression. *Nat Rev Cancer,* 2**,** 442-454.

THOMPSON, P. M., RAMACHANDRAN, S., CASE, L. B., TOLBERT, C. E., TANDON, A., PERSHAD, M., DOKHOLYAN, N. V., WATERMAN, C. M. & CAMPBELL, S. L. 2017. A Structural Model for Vinculin Insertion into PIP2-Containing Membranes and the Effect of Insertion on Vinculin Activation and Localization. *Structure,* 25**,** 264-275.

THOMSEN, L. L., MILES, D. W., HAPPERFIELD, L., BOBROW, L. G., KNOWLES, R. G. & MONCADA, S. 1995. Nitric oxide synthase activity in human breast cancer. *Br J Cancer,* 72**,** 41-4.

TJELLE, T. E., BRECH, A., JUVET, L. K., GRIFFITHS, G. & BERG, T. 1996. Isolation and characterization of early endosomes, late endosomes and terminal lysosomes: their role in protein degradation. *J Cell Sci,* 109 (Pt 12)**,** 2905-14.

TOMAS, A., FUTTER, C. E. & EDEN, E. R. 2014. EGF receptor trafficking: consequences for signaling and cancer. *Trends in cell biology,* 24**,** 26-34.

TONG, X. & LI, H. 2004. eNOS protects prostate cancer cells from TRAIL-induced apoptosis. *Cancer Lett,* 210**,** 63-71.

TOOZE, S. A., ABADA, A. & ELAZAR, Z. Endocytosis and autophagy: exploitation or cooperation? *Cold Spring Harbor perspectives in biology,* 6**,** a018358-a018358.

TRAUB, L. M. 2009a. Tickets to ride: selecting cargo for clathrin-regulated internalization. *Nat Rev Mol Cell Biol,* 10**,** 583-596.

TRAUB, L. M. 2009b. Tickets to ride: selecting cargo for clathrin-regulated internalization. *Nat Rev Mol Cell Biol,* 10**,** 583-96.

TU, C., ORTEGA-CAVA, C. F., WINOGRAD, P., STANTON, M. J., REDDI, A. L., DODGE, I., ARYA, R., DIMRI, M., CLUBB, R. J., NARAMURA, M., WAGNER, K.-U., BAND, V. & BAND, H. 2010. Endosomal-sorting complexes required for transport (ESCRT) pathway-dependent endosomal traffic regulates the localization of active Src at focal adhesions. *Proceedings of the National Academy of Sciences of the United States of America,* 107**,** 16107-16112.

TU, Y. T., TAO, J., LIU, Y. Q., LI, Y., HUANG, C. Z., ZHANG, X. B. & LIN, Y. 2006. Expression of endothelial nitric oxide synthase and vascular endothelial growth factor in human malignant melanoma and their relation to angiogenesis. *Clin Exp Dermatol,* 31**,** 413-8.

VACCA, A., RIA, R., PRESTA, M., RIBATTI, D., IURLARO, M., MERCHIONNE, F., TANGHETTI, E. & DAMMACCO, F. 2001. αvβ3 integrin engagement modulates cell adhesion, proliferation, and protease secretion in human lymphoid tumor cells. *Experimental hematology,* 29**,** 993-1003.

VAN ZANTEN, T. S. & MAYOR, S. 2015. Current approaches to studying membrane organization. *F1000Res,* 4.

VASSILOPOULOS, S., GENTIL, C., LAINE, J., BUCLEZ, P. O., FRANCK, A., FERRY, A., PRECIGOUT, G., ROTH, R., HEUSER, J. E., BRODSKY, F. M.,

GARCIA, L., BONNE, G., VOIT, T., PIETRI-ROUXEL, F. & BITOUN, M. 2014. Actin scaffolding by clathrin heavy chain is required for skeletal muscle sarcomere organization. *J Cell Biol,* 205**,** 377-93.

VERBAANDERD, C., MAES, H., SCHAAF, M. B., SUKHATME, V. P., PANTZIARKA, P., SUKHATME, V., AGOSTINIS, P. & BOUCHE, G. 2017. Repurposing Drugs in Oncology (ReDO)-chloroquine and hydroxychloroquine as anti-cancer agents. *Ecancermedicalscience,* 11**,** 781-781.

VON KLEIST, L., STAHLSCHMIDT, W., BULUT, H., GROMOVA, K., PUCHKOV, D., ROBERTSON, MARK J., MACGREGOR, KYLIE A., TOMILIN, N., PECHSTEIN, A., CHAU, N., CHIRCOP, M., SAKOFF, J., VON KRIES, JENS P., SAENGER, W., KRÄUSSLICH, H.-G., SHUPLIAKOV, O., ROBINSON, PHILLIP J., MCCLUSKEY, A. & HAUCKE, V. 2011. Role of the Clathrin Terminal Domain in Regulating Coated Pit Dynamics Revealed by Small Molecule Inhibition. *Cell,* 146**,** 471-484.

WANG, G., MONIRI, N. H., OZAWA, K., STAMLER, J. S. & DAAKA, Y. 2006. Nitric oxide regulates endocytosis by S-nitrosylation of dynamin. *Proceedings of the National Academy of Sciences of the United States of America,* 103**,** 1295-1300.

WANG, J. T., KERR, M. C., KARUNARATNE, S., JEANES, A., YAP, A. S. & TEASDALE, R. D. 2010. The SNX-PX-BAR family in macropinocytosis: the regulation of macropinosome formation by SNX-PX-BAR proteins. *PLoS One,* 5**,** e13763.

WANG, L., SHI, G. G., YAO, J. C., GONG, W., WEI, D., WU, T. T., AJANI, J. A., HUANG, S. & XIE, K. 2005. Expression of endothelial nitric oxide synthase correlates with the angiogenic phenotype of and predicts poor prognosis in human gastric cancer. *Gastric Cancer,* 8**,** 18-28.

WANG, S. & BASSON, M. D. 2011. Akt directly regulates focal adhesion kinase through association and serine phosphorylation: implication for pressure-induced colon cancer metastasis. *American journal of physiology. Cell physiology,* 300**,** C657-C670.

WANG, Y., CAO, H., CHEN, J. & MCNIVEN, M. A. 2011. A direct interaction between the large GTPase dynamin-2 and FAK regulates focal adhesion dynamics in response to active Src. *Mol Biol Cell,* 22**,** 1529-38.

WANG, Y. & GILMORE, T. D. 2003. Zyxin and paxillin proteins: focal adhesion plaque LIM domain proteins go nuclear. *Biochim Biophys Acta,* 1593**,** 115-20.

WAY, M. & PARTON, R. G. 1995. M-caveolin, a muscle-specific caveolin-related protein. *FEBS Lett,* 376**,** 108-12.

WEBB, D. J., PARSONS, J. T. & HORWITZ, A. F. 2002. Adhesion assembly, disassembly and turnover in migrating cells–over and over and over again. *Nature cell biology,* 4**,** E97.

WELCH, M. D. & MULLINS, R. D. 2002. Cellular control of actin nucleation. *Annu Rev Cell Dev Biol,* 18**,** 247-88.

WEST, M. A., BRETSCHER, M. S. & WATTS, C. 1989. Distinct endocytotic pathways in epidermal growth factor-stimulated human carcinoma A431 cells. *J Cell Biol,* 109**,** 2731-9.

WILBUR, J. D., CHEN, C. Y., MANALO, V., HWANG, P. K., FLETTERICK, R. J. & BRODSKY, F. M. 2008. Actin binding by Hip1 (huntingtin-interacting protein 1) and Hip1R (Hip1-related protein) is regulated by clathrin light chain. *J Biol Chem,* 283**,** 32870-9.

WILSON, J. M., DE HOOP, M., ZORZI, N., TOH, B. H., DOTTI, C. G. & PARTON, R. G. 2000. EEA1, a tethering protein of the early sorting endosome, shows a polarized distribution in hippocampal neurons, epithelial cells, and fibroblasts. *Molecular biology of the cell,* 11**,** 2657-2671.

WITTRUP, A., AI, A., LIU, X., HAMAR, P., TRIFONOVA, R., CHARISSE, K., MANOHARAN, M., KIRCHHAUSEN, T. & LIEBERMAN, J. 2015. Visualizing lipid-formulated siRNA release from endosomes and target gene knockdown. *Nature biotechnology,* 33**,** 870-876.

WOZNIAK, M. A., MODZELEWSKA, K., KWONG, L. & KEELY, P. J. 2004. Focal adhesion regulation of cell behavior. *Biochimica et Biophysica Acta (BBA) - Molecular Cell Research,* 1692**,** 103-119.

XING, Y., BOCKING, T., WOLF, M., GRIGORIEFF, N., KIRCHHAUSEN, T. & HARRISON, S. C. 2010. Structure of clathrin coat with bound Hsc70 and auxilin: mechanism of Hsc70-facilitated disassembly. *Embo j,* 29**,** 655-65.

XU, W., LIU, L. Z., LOIZIDOU, M., AHMED, M. & CHARLES, I. G. 2002. The role of nitric oxide in cancer. *Cell Res,* 12**,** 311-20.

XUE, Y., LIU, Z., GAO, X., JIN, C., WEN, L., YAO, X. & REN, J. 2010. GPS-SNO: Computational Prediction of Protein S-Nitrosylation Sites with a Modified GPS Algorithm. *PLOS ONE,* 5**,** e11290.

YAO, J., SCHOECKLMANN, H. O., PROLS, F., GAUER, S. & STERZEL, R. B. 1998. Exogenous nitric oxide inhibits mesangial cell adhesion to extracellular matrix components. *Kidney Int,* 53**,** 598-608.

YOSHIDA, A., SAKAI, N., UEKUSA, Y., IMAOKA, Y., ITAGAKI, Y., SUZUKI, Y. & YOSHIMURA, S. H. 2018. Morphological changes of plasma membrane and protein assembly during clathrin-mediated endocytosis. 16**,** e2004786.

YOUN, J.-Y., WANG, T. & CAI, H. 2009. An ezrin/calpain/PI3K/AMPK/eNOSs1179 signaling cascade mediating VEGF-dependent endothelial nitric oxide production. *Circulation research,* 104**,** 50-59.

ZHAN, R., YANG, S., HE, W., WANG, F., TAN, J., ZHOU, J., YANG, S., YAO, Z., WU, J. & LUO, G. 2015. Nitric oxide enhances keratinocyte cell migration by regulating Rho GTPase via cGMP-PKG signalling. *PLoS One,* 10**,** e0121551.

ZHANG, Y. & XU, W. 2008. Progress on kinesin spindle protein inhibitors as anti-cancer agents. *Anticancer Agents Med Chem,* 8**,** 698-704.

ZHU, G., ZHAI, P., LIU, J., TERZYAN, S., LI, G. & ZHANG, X. C. 2004. Structural basis of Rab5-Rabaptin5 interaction in endocytosis. *Nat Struct Mol Biol,* 11**,** 975-83.

ZIDOVETZKI, R. & LEVITAN, I. 2007. Use of cyclodextrins to manipulate plasma membrane cholesterol content: evidence, misconceptions and control strategies. *Biochimica et biophysica acta,* 1768**,** 1311-1324.

ZIMERMAN, B., VOLBERG, T. & GEIGER, B. 2004. Early molecular events in the assembly of the focal adhesion-stress fiber complex during fibroblast spreading. *Cell Motil Cytoskeleton,* 58**,** 143-59.

ZONCU, R., PERERA, R. M., BALKIN, D. M., PIRRUCCELLO, M., TOOMRE, D. & DE CAMILLI, P. 2009. A phosphoinositide switch controls the maturation and signaling properties of APPL endosomes. *Cell,* 136**,** 1110-1121.